Title

Characterization of Trichomonas vaginalis rhomboid proteases and surface proteins that contribute to host: parasite interactions

Author

Riestra, Angelica Montenegro

Publication Date

2015

Peer reviewed|Thesis/dissertation

UNIVERSITY OF CALIFORNIA

Los Angeles

Characterization of *Trichomonas vaginalis* rhomboid proteases and surface proteins that contribute to host: parasite interactions

A dissertation submitted in partial satisfaction of

the requirements for the degree Doctor of Philosophy

in Microbiology, Immunology, and Molecular Genetics

by

Angelica Montenegro Riestra

2015

ASBTRACT OF THE DISSERTATION

Characterization of *Trichomonas vaginalis* rhomboid proteases and surface proteins that contribute to host: parasite interactions

by

Angelica Montenegro Riestra

Doctor of Philosophy in

Microbiology, Immunology, and Molecular Genetics

University of California, Los Angeles, 2015

Professor Patricia J. Johnson, Chair

Trichomonas vaginalis is a flagellated, protozoan parasite that causes trichomoniasis, the most common non-viral sexually transmitted infection in the world. While *T. vaginalis* infection is usually asymptomatic, long-term effects include associations with adverse pregnancy outcomes, cervical cancer and aggressive prostate cancer, and increased risk of HIV infection. Therefore, the public health threat posed by this parasite is high, yet little is known about its pathogenic mechanisms. As an obligate, extracellular parasite, *T. vaginalis* needs to attach to epithelial cells in order to gain a foothold in its host and maintain infection. However, only a few specific molecular players that contribute to these interactions have been reported. Given the roles of rhomboid proteases in cell signaling, modification of the cell surface, and contribution to pathogenesis in other protozoan parasites, we were interested in studying whether *T. vaginalis* also has functionally active rhomboid proteases. In this study, we demonstrate that two *T. vaginalis* rhomboids are proteolytically active and named them TvROM1 and TvROM3.

We also report that TvROM1 has a role in promoting *T. vaginalis* attachment to host cells and lysis of host cells. Furthermore, we have begun to unravel the mechanism of action for TvROM1 by the identification of two substrates also located at the cell surface. In our desire to discover additional factors that contribute to pathogenesis, we characterized various proteins that had been previously identified in the *T. vaginalis* cell surface proteome. We found that one protein, called TSP6, plays a sensory role based on striking relocalization of the protein upon contact with host cells, and a role in promoting parasite migration. We also identified another protein, TVAG_393390, which can increase both attachment to host cells and cytolysis of host cells and may function as a cadherin-like protein. Overall, the results from these studies have allowed us to gain insight about the contribution of rhomboid proteases and several surface proteins to host: parasite interactions-opening up a larger window of potential targets for therapeutic intervention to combat this widespread human pathogen.

The dissertation of Angelica Montenegro Riestra is approved.

David A. Campbell

Paul S. Bajaj

Patricia J. Johnson, Chair

University of California, Los Angeles

2015

Dedication Page

This work is dedicated to my parents, thank you for your love, your hard work and sacrifices to help me pursue an education and make this degree possible.

Table of Contents

Acknowledgements

I would first like to thank my advisor, Dr. Patricia Johnson, for allowing me to pursue these research projects and guiding my overall development as a scientist, providing invaluable knowledge, experience, and advice. I also thank my committee members for their helpful insight, advice, and support throughout my graduate studies. I also want to thank my fellow lab members, past and present, for their patience, advice, and friendship. I especially thank Dr. Natalia de Miguel, Dr. Gila Lustig, and Maria Delgadillo-Correa for taking me under their wings when I joined the laboratory and being additional science mentors.

The work presented in this dissertation was funded by support from a UCLA Eugene V. Cota-Robles Fellowship and a Howard Hughes Medical Institute Gilliam Fellowship for Advanced Study. I would especially like to thank the HHMI team for their support and the knowledge they provided to aid my professional development throughout my graduate studies.

The work presented in Chapter 2 was performed as a main collaboration with Dr. Sinisa Urban and Shiv Gandhi in the Department of Molecular Biology and Genetics at Johns Hopkins University School of Medicine. Shiv Gandhi performed the heterologous cell cleavage assays, mapped the substrate cleavage sites, and co-analyzed substrate features. We also collaborated with Dr. Sonja Hess, Dr. Michael J. Sweredoski, and Dr. Annie Moradian, at the Proteome Exploration Laboratory, Division of Biology and Biological Engineering, Beckman Institute at the California Institute of Technology. Dr. Sweredoski, Dr. Moradian, and Dr. Hess advised on the preparation of mass spectrometry samples and performed the mass spectrometry data analysis. I would also like to thank Dr. Frances Mercer for help processing the flow cytometry samples and Grant Stevens for DNA extractions. Chapter 2 is a manuscript in preparation.

The work presented in Chapter 3 was the main work of Dr. Natalia de Miguel and Dr. Patricia Johnson was the PI. Chapter 3 is reprinted with permission from the Journal of Cellular Microbiology (DOI: 10.1111/cmi.12003) 2012©Blackwell Publishing Ltd. I cloned the TSP6 protein with a C-terminal tail truncation and transfected it in parallel with the TSP6 protein that had been cloned and localized by Dr. de Miguel. I performed the initial observations of the cellular redistribution of TSP6 in contact with vaginal ectocervical cells, and the lack of flagellar targeting with the TSP6 C-terminal tail mutant, which is reported in Figures 3 and 4 of the manuscript. I also performed pilot studies investigating the migration of transfectants through transwells coated with Matrigel®.

Chapter 4 discusses unpublished work. I would like to thank my undergraduate student, Allison Guia for help in further characterizing the increased parasite attachment to host cell phenotype displayed by GFP-TVAG_393390 transfectants. I also want to thank Emma Goodwin for helping to clone a potential calcium binding site mutant of TVAG_393390 that will be used to further characterize this protein.

The work done in Chapter 5 is unpublished work. I would like to thank Dr. Jennifer Gordon and Dr. Clea Mantini who performed the initial FKBP-destabilization domain analysis and established an effect at the protein level. I also thank Grant Stevens for DNA extractions.

I thank Dr. Peter Bradley, Dr. Kent Hill, and their lab members for use and assistance with their fluorescence microscopes, which allowed me to capture all the fluorescence images shown in this thesis.

On a personal level, I would like to thank my parents Amanda Montenegro and Alberto Riestra. Gracias Padres! Your personal sacrifices to support me in the pursuit of an education have been my driving force to come this far. Your hard work ethic has taught me to push myself

to the maximum like you do to do your best job. Your loving and kind nature, have showed me how to lend a helping hand and help those in need. To my brothers, thanks for always encouraging me along the way, and helping me in every way that you could. I would also like to acknowledge my whole family, all the small gifts of food, words of encouragement, and prayers helped me to smile at life while in graduate school.

I would also like to thank all the mentors I have had along the way. Dr. Park Trefts, thanks for opening up the world of scientific research to me by allowing me to participate in the C.H.U.M. program in middle school, and mentoring me until this day. Equally important, thanks for teaching me how to go above and beyond to help bring opportunities to those most in need. Together, yours and Glenda's work have placed many of us in the science pipeline and higher education. I also want to thank all my mentors from Gompers Secondary, including Dolores Garcia, Dr. Stefan Bauer, and Christina Rodriguez. Your personal investment in all aspects of my life and education allowed me the confidence and the strength to pursue my dreams in the face of adversity. You taught me the importance of helping others and how to be a strong leader.

Dr. Mark Lawson, thanks for allowing me to conduct research in your laboratory as a high school student and inspiring me to become a scientist, you will always be my positive role model and successful scientist to emulate. Similarly, thanks to Dr. Sherie L. Morrison, Leticia Williams, Dr. Kileen Mershon, Dr. Anthony Baugh, and Dr. Williams Jacobs Jr. who believed in my scientific potential and guided me through my undergraduate research experiences. Thank you Dr. Elma Gonzales for allowing me to participate in the MARC program and providing critical training that has continued to be helpful throughout my scientific career.

I also want to acknowledge Dr. Edwin Paz, you have been a source of strength and inspiration in all aspects of my life. Thank you for being the trail blazer and accompanying me

through this journey-gently pushing me along at times of great difficulty, while also pausing to embrace the beautiful moments in our lives.

Thanks to all my friends whose love and support helped me to keep pursuing my education so that together we can accomplish our mission of helping others to pursue their dreams. I am especially grateful to Ayda Camacho, Alexandra Valdez, and Carolina Mendez for providing extra encouragement, smiles, and support during the completion of my thesis. I would also like to thank Dr. Shewit Tekeste and Dr. Miguel Nava. We started our graduate school journey together and were there for each other at every step of the way. Dr. Tekeste, your selfless ways and desire to help others continues to give me hope that good people like you can help change the world.

Lastly, I would like to thank the SACNAS at UCLA Chapter for constantly reminding me of why I am pursuing a higher education. Together we have outreached to thousands of students each year and helped to spark an interest in the sciences in the next generation. You were my home away from home.

Vita/Biographical Sketch

University of California, Los Angeles, B.S. in Microbiology, Immunology, and Molecular Genetics, College Honors and CUM LAUDE Latin Honors — 2008

Experience:

University of California, Los Angeles, Research with Dr. Patricia Johnson in the Department of Microbiology, Immunology, and Molecular Genetics on *Trichomonas vaginalis* rhomboid proteases and membrane proteins — 2008-present

University of California Los Angeles Teaching Assistant, "Molecular Parasitology" — 2009 and 2010

University of California, Los Angeles, Research with Dr. Sherie L. Morrison in the Department of Microbiology, Immunology, and Molecular Genetics on recombinant antibodies against *Cryptococcus neoformans*
NIH/Minority Access to Research Careers (MARC) Trainee — 2005-2008

Albert Einstein College of Medicine of Yeshiva University with Dr. William R. Jacobs Jr. in the Department of Microbiology and Immunology, on mechanisms of *Mycobacteria smegmatis* drug resistance
HHMI EXROP Student — 2006

Publications:

Saada EA, Kabututu ZP, Lopez M, Shimogawa MM, Langousis G, Oberholzer M**, Riestra A**, Jonsson ZO, Wohlschlegel JA, Hill KL. *Insect stage-specific receptor adenylate cyclases are localized to distinct subdomains of the Trypanosoma brucei flagellar membrane.* Eukaryotic Cell. 2014 Aug; 13(8):1046-76. Selected as **Spotlight: Article of Significant Interest** by Editors.

de Miguel N, **Riestra A.**, Johnson PJ. *Reversible association of tetraspanin with Trichomonas vaginalis flagella upon adherence to host cells*. Cell Microbiol. 2012 Dec; 14 (12): 1797-807. Selected as **Editor's Choice** paper.

Baughn AD, Deng J, Vilchèze C, **Riestra A**, Welch JT, Jacobs WR Jr, Zimhony O. *Mutually exclusive genotypes for pyrazinamide and 5-chloropyrazinamide resistance reveal a potential resistance-proofing strategy.* Antimicrob Agents Chemother. 2010 Dec; 54 (12): 5323-8.

Awards and Honors:

Best Oral Presentation, Southern California Eukaryotic Pathogen Symposium, 2014

SACNAS Outstanding Oral Presentation Award, Microbiology Category, 2014

UCLA Vice-Provost Service Award, 2011

Howard Hughes Medical Institute Gilliam Fellowship, 2009-2014

University of California Eugene V. Cota-Robles Fellowship, 2008

UCLA Science Poster Day Dean's Prize Winner, 2008

SACNAS Outstanding Poster Presentation Award, Health/Medicine Category, 2005

UCLA Alumni Scholarship, 2003-2007

Chapter 1:

Introduction

Trichomonas vaginalis is a unicellular, flagellated protozoan that is the causative agent of Trichomoniasis, the most common non-viral sexually transmitted infection in the world [1]. The World Health Organization estimates that there were 276.4 million new cases of *T. vaginalis* infection in 2008, which surpasses the total number of *Chlamydia trachomatis* (105.7 million), *Neisseria gonorrhea* (106.1), and syphilis (10.6) infections combined [1]. Moreover, in the United States *T. vaginalis* is one of the most common parasitic infections [2], with an estimated 3.7 million people currently infected [3], and 1.1 million people predicted to be newly infected each year [4]. Just as many parasitic diseases affect the world's poorest populations [5], *T. vaginalis* has also been found to disproportionally affect minorities and people from low socio-economic backgrounds in the U.S. [6, 7]. The public health threat posed by this parasite and its understudied nature has caused it to be recently recognized as one of the U.S.'s own neglected parasitic infections [6, 8, 9].

T. vaginalis colonizes the genitourinary tract of men and women, with the lower genital tract being the major sites of infection in women and the urethra in males [3]. Although, infection is usually asymptomatic, clinical manifestations include inflammation of the vagina, urethra, and the prostate, discharge, pruritus (itching), dysuria (painful urination), and hemorrhagic lesions [10]. Graver complications associated with *T. vaginalis* infections include adverse pregnancy outcomes such as giving birth prematurely and giving birth to low birth weight infants (1.3-fold increased risk for each, and 1.4-fold for both) [11], associations with increased risk of cervical cancer (2.1-3.3-fold) [12, 13] and aggressive prostate cancer (2.69-fold) [14, 15], and increased risk of acquiring (2.6 fold) [16] and potentially transmitting the human immunodeficiency virus (HIV) to a sexual partner [17]. Recently, a study of U.S. HIV^+ women found that co-infection with *T. vaginalis* was associated with 4.07-fold higher HIV-RNA

vaginal shedding [18]. Co-infection with HIV, *T. vaginalis,* and bacterial vaginosis led to a dramatic 18.63-fold increase in HIV shedding. Alarmingly, 43% of the HIV^+ women they surveyed had co-occurring *T. vaginalis* and bacterial vaginosis infections, highlighting the high prevalence of a sub-population that could contribute to increased HIV transmission [18]. These studies have suggested that preventative modalities controlling *T. vaginalis* infections could help prevent increased transmission and control of HIV and other sexually transmitted infections [16, 18].

The only treatment strategy for *T. vaginalis* infections is the use of one class of 5-nitoimidazole drugs. The two commercially available drugs for *T. vaginalis* are called metronidazole and tinidazole. It is recommended that upon diagnosis of infection, a patient's sexual partner should also receive treatment to prevent re-infection [19]. Re-infection is thought to be an important contributing factor to the epidemiology of *T. vaginalis* infection since the rates of re-infection have been reported to be ~ 8% in a general population of women [19] and as high as 36% in HIV^+ women [20]. Alarmingly, low-level *in vitro* resistance was observed in 4.3% of *T. vaginalis* strains isolated from patients attending 6 different STD clinics in the U.S. [21], pointing to the need of developing new therapeutics for *T. vaginalis* infection.

Understanding the molecular mechanisms utilized by *T. vaginalis* for successful colonization and persistence within the human host is imperative in order to identify targetable processes that may help combat *T. vaginalis* infection. The parasite mainly infects the squamous epithelium of the urogenital tract [22]. The epithelial mucosa provides the first line of defense against microbes that infect the urogenital tract [23]. Therefore, it has been proposed that *T. vaginalis* has evolved multiple factors that contribute to successful mucosal parasitism [24-26]. Microbes, including *T. vaginalis*, need to bore through the mucin layer and extracellular matrix

(ECM) of host cells in order to contact epithelial cells [27]. As an extracellular parasite, *T. vaginalis* then attaches to host cells and lyses host cells for nutrient uptake [28]. Proteins that are part of tight, adherens, and desmosomal junctions between epithelial cells which help form a tight protective barrier, are found 3 to 4 cell layers below the luminal surface of the ectocervix and vagina [23]. Therefore, the topmost layer may be potentially penetrated by *T. vaginalis.* The degree of penetrance is unknown but *T. vaginalis* does not enter the bloodstream. It has been shown that *T. vaginalis* can interact with and perturb junctional complexes of human Caco-2 cells [29]. *T. vaginalis* can also bind and degrade components of the extracellular and basement membrane *in vitro* [30-33].

T. vaginalis infection, results in an innate and adaptive immune response, but the effectiveness of these processes in controlling infection is largely unknown, especially due to the observation that up to 85% of women [7] and 77% of men [34] are asymptomatic and re-infection is predicted to be common [22]. An inflammatory response is mainly mounted against the parasite [24]. *T. vaginalis*-infected pregnant women, have been found to have increased levels of cervical neutrophil-released antimicrobial peptides called alpha-defensins and IL-8 [35]. IL-8 is an important activator and chemoattractant of neutrophils. Similarly, in another study, women with bacterial vaginosis and *T. vaginalis* co-infection had increased levels of vaginal IL-8, IL-1β (pro-inflammatory cytokine), and neutrophils compared to women that only had bacterial vaginosis [36]. *T. vaginalis* is coated with a sugar polysaccharide recently renamed as *T. vaginalis* lipoglycan (TvLG) [37-39]. Purified TvLG has also been found to increase IL-8 and macrophage inflammatory protein3α (chemoattractant) production from cervical and vaginal epithelial cells [40]. An adaptive immune response against *T. vaginalis* is also generated since circulating and mucosal antibodies against the parasite can be detected [14, 30, 41-43].

However, *T. vaginalis* cysteine proteases have the ability to degrade antibodies [44, 45] and thus the parasite may potentially be able to circumvent part of the humoral immune response.

In the urogenital tract *T. vaginalis* may also interact with a myriad of cell types that may also provide a nutrient source or aid its modulation of the immune response. *In vitro*, *T. vaginalis* can bind to and phagocytose white blood cells [28], red blood cells [28], yeast [46], bacteria [28, 47], and sperm [48]. However, the molecular players contributing to these heterotypic interactions are also largely unknown. Recently, a soluble factor released by *T. vaginalis* called Migration Inhibitory Factor (TvMIF) was shown to inhibit the migration of human monocytes through a chamber [43], highlighting the ability of *T. vaginalis* to influence immune cells. *T. vaginalis* may also contribute to modulation of the urogenital tract mirobiome and this is a heightened area of interest since such changes may also have an effect on the inflammatory response [49-51] and metabolites available for *T. vaginalis* consumption.

Molecular mechanisms of *T. vaginalis* pathogenesis

Although the general processes that contribute to *T. vaginalis* parasitism have been deduced to include degradation of mucin and ECM, adherence to and lysis of host cells, degradation of immune factors, and interactions with multiple host cell types, we have only began to decipher the molecular "interactome" that might mediate these processes. Mouse models of infection have been established [52, 53], however, their limited use and issues of reproducibility have contributed to a lack of their widespread implementation in the field. Therefore, *in vitro* studies using vaginal endocervical and ectocervical cells [54, 55] serve as the main models to study pathogenesis-associated factors.

Since *T. vaginalis* remains extracellular, attachment to host cells and cytolysis of host cells are considered two of the more important phases of infection. The most comprehensive

study of 26 *T. vaginalis* strains found a correlation between attachment and cytolysis in strains that display low-adherence and cytolytic capabilities but found no correlation in the more virulent strains [56]. It has therefore been proposed that a threshold of attachment must be reached to trigger cytolysis [56]. What triggers and regulates both processes still remains to be investigated. Identification of molecular factors that mediate parasite attachment to and cytolysis of host cells and those with differential contributions may allow these functions to be dissected further.

T. vaginalis has a dense glycocalyx, consisting of about ~$3X10^6$ molecules of *T. vaginalis* lipoglycan (TvLG) [38]. Purified TvLG can inhibit parasite attachment to ectocervical cells [57]. Chemical mutagenesis of *T. vaginalis* and subsequent selection for inability to bind to lectins, led to the identification of two mutants with defective TvLG [57] and TvLG purified from these mutants could not inhibit parasite attachment to ectocervical cells [57]. Together, these observations demonstrated a role of this abundant surface molecule in host: parasite interactions [57].

Small vesicles, called exosomes, released by *T. vaginalis* may also contribute to promote *T. vaginalis* attachment to host cells [58]. Extracellular vesicles (EVs) are released from bacteria, fungi, many mammalian cells types, and other protozoan parasites such as *Leishmania* spp., *Trypanosoma cruzi,* and helminths [59]. Extracellular vesicle/exosome release by pathogens has gained attention since these may be utilized to modulate the host immune response [59]. In *T. vaginalis*, exosomes from highly adherent strains could promote attachment of lowly adherent strains to ectocervical cells. Furthermore, cargo-specific properties of exosomes may be transferred between *T. vaginalis* strains as exosomes enriched from strains that have higher ability to adhere to a male prostate cell line could transfer this property to *T. vaginalis* strains that

normally have low binding to prostate cells [58]. One of the exosome cargo proteins, TvMIF, has been functionally characterized [43]. In addition to its ability of decreasing human monocyte migration mentioned previously, it has also been found to bind the human CD74 receptor and activate downstream signaling via activation of the Erk1/2 and Akt pathways [43].

Further identification of host cell receptors may also aid in highlighting properties of the *T. vaginalis* proteins that are bound and contribute to host: parasite interactions. Only one host protein has been identified to bind *T. vaginalis,* this protein binds the galactose sugar and is thus called galectin-1 [60]. The contribution of *T. vaginalis'* glycocalyx to binding galectin-1 on host ectocervical cells was demonstrated by the ability of purified TvLG to compete and inhibit *T. vaginalis* attachment to ectocervical cells [60]. Knockdown of galectin-1 also caused reduced *T. vaginalis* attachment to host cells. Future studies identifying additional host factors will shed light on whether predominant sets of proteins are utilized by *T. vaginalis* to attach to host cells and/or whether a combinatorial set of proteins and other chemical factors such as polysaccharides contribute to host colonization.

Molecular mechanisms of *T. vaginalis* pathogenesis-role of proteases

T. vaginalis encodes ~310 [26]-447 [61] peptidases (see Fig. 1-1), highlighting that *T. vaginalis* has one of the largest predicted degradomes amongst eukaryotic protists [61]. For comparison, humans have ~566 predicted proteases [62]. Cysteine proteases are one of the most studied families of proteins predicted to contribute to *T. vaginalis* pathogenesis. Proteases can be divided into 5 catalytic classes that describe the residue that performs nucleophilic attack of the peptide bond, or activates a water molecule to serve as the nucleophile [63]. The most recent analysis of the sequenced *T. vaginalis* genome predicts the presence of 156 cysteine proteases

(CPs) [26] while the more liberal annotation of the genome predicts 220 CPs [61] (see Fig. 1-1). Both estimates list CPs as the largest mechanistic class of proteases found in *T. vaginalis*.

In studies with the most physiologically relevant cell lines, it was first found that *T. vaginalis'* ability to attach to and lyse HeLa cells and vaginal epithelial cells is decreased upon treatment of parasites with the CP inhibitors TLCK and leupeptin [64]. Follow up studies identified specific groups of CPs that contribute to these processes. They were initially mainly named by their observed molecular weights on two-dimensional (2-D) substrate electrophoresis (zymograms) or SDS-PAGE; they include CP30, CP39, CP62, and CP65 [30, 45, 53, 65]; these CPs are mainly of the papain-like clan CA and legumain-like clan CD families [66].

Antibodies against CPs can be readily detected in patient sera from *T. vaginalis*-infected individuals [30, 31, 45, 66, 67], and CP activity is also present in vaginal washes (discussed below) [30]. These observations likely demonstrate the active presence of CPs at their predicted site of action. Furthermore, antibodies raised against CPs can specifically inhibit attachment to HeLa cells and ectocervical cells [53, 68] as we all cytotoxicity [31]. An additional contribution to host cell destruction, was revealed in a study which found that the purified CP30 fraction of CPs can cause apoptosis of ectocervical cells-detected by AnnexinV staining, caspase-3 activation, and nucleosomal DNA fragmentation [69]. Induction of apoptosis by *T. vaginalis* can be reduced by treatment of the parasite with the E64 CP inhibitor [69]. A role for CPs in lysis of red blood cells has also been identified, with an antibody against a specific CP called CP4 causing decreased red blood cell lysis [70]. *In vivo* support for the contribution of CPs in *T. vaginalis* pathogenesis stems from a study that found that passive antibody transfer of an anti-CP62 antibody before challenge with *T. vaginalis* infection by the intraperitoneal route caused a reduction in *T. vaginalis*-induced lesions [53]. Mechanistic insight into how CPs contribute to

attachment, cytolysis, and induction of apoptosis still remains to be uncovered, and will be aided by the identification of their *T. vaginalis* and human host substrates.

CPs may also contribute to *T. vaginalis* evasion of the immune response since *T. vaginalis* can degrade the complement protein C3 [71] and human antibodies (IgG, IgM, and IgA) [44, 45]; both activities are decreased by addition of CP inhibitors. *In vivo* support for *T. vaginalis* proteinase activity on immunoglobulins stems from the fact that vaginal washes collected from *T. vaginalis*-infected women have higher ability to degrade human IgG than uninfected women [44]. CPs, including CP30 and CP65, can also degrade additional vaginal proteins such as fibronectin, collagen IV, and hemoglobin [30, 31]. This is an important property that may have adverse effects on host cells, since changes in the extracellular matrix can cause metabolic reprogramming and promotion of tumorigenesis [72]

Much still remains to be investigated about the roles of other proteases in *T. vaginalis* and their potential contribution to pathogenesis. The second largest class of proteases in *T. vaginalis* are metallopeptidases. Activity for four metalloproteases has been reported [73-76], with activity that may point to a role in pathogenesis detected for two of these proteins [73, 75]. The human prostate contains higher concentrations of zinc than the female urogenital tract, and thus the authors of two studies were interested in identifying proteases that may play a role in male trichomoniasis. They compared the *T. vaginalis* degradome in the absence or presence of 1.6 mM Zn^{2+}, in order to identify proteases that were found at higher levels upon increased Zn^{2+} concentrations. Both studies identified a 50 kDa protease, annotated as aminopeptidase P-like metalloproteinase of the MG clan (which may be the same peptidase). The metalloprotease identified in the first study was shown to have proteolytic activity on HeLa cells and a prostate cell line (DU-145) [73]. The aminopeptidase identified in the second study was called TvMP50,

and could be detected only by sera from *T. vaginalis*-infected male patients and not from female-infected patients [75]. Further investigations of these metallopeptidases is therefore of interest, since strains that have preferential binding to male prostate cells over ectocervical cells have been identified, and we do not know the specific factors that may contribute to differential binding [56, 58].

There are also 43 predicted GP63 metalloprotease family members in *T. vaginalis* [77]. GP63 proteases are zinc metallopeptidases and they have been found to contribute to various parasite pathogenic processes in *Leishmania*, *Trypanosoma cruzi*, and *Trypanosoma brucei* [78]. Of particular interest is their contribution to promoting parasite attachment to host cells and contributions to degradation of complement for immune evasion [79]. By EST analysis TVAG_367130 was one of the most highly expressed GP63 family members and thus an antibody was generated against this protease and used for indirect immunofluorescence assays. The GP63 protein localized to the cell surface [77]. A wide spectrum metalloprotease inhibitor, 1,10-phenantroline, did not have an effect on *T. vaginalis* attachment to HeLa cells but it did cause a decrease in *T. vaginalis* ability to lyse cells [77]. Therefore, further characterization of *T. vaginalis* metalloproteases is of interest.

Serine proteases may also contribute to host-parasite interactions. *T. vaginalis* are predicted to encode 33 subtilases, making this the largest serine protease family in the parasite [80]. One *T. vaginalis* subtilase protein called SUB1 (TVAG_090450) has been characterized to date, the authors generated sera against SUB1 and found that the endogenous protein localized to the cell surface and cytosolic vesicles [80]. Further characterization of subtilases is of interest, due to their roles in cleavage of adhesive proteins in the parasite *Toxoplasma gondii* [81, 82].

One particular family of serine proteases which is a primary focus of this dissertation and also merits study due to their important contribution to pathogenesis in other parasitic protists are the rhomboid proteases [83, 84]. Rhomboid proteases belong to a group of membrane-embedded proteases that cleave their substrates within their transmembrane domain (TM), referred to as intramembrane cleaving proteases (I-CLiPs) [85, 86]. The role of I-CLiPs has never been previously studied in *T. vaginalis*. Three mechanistic classes of I-CLiPs exist: 1) site 2 (S2P) proteases 2) rhomboid proteases and 3) GxGD-type aspartyl proteases which include presenilin-dependent γ-secretase, signal-peptide peptidase, and signal-peptide peptidase-like proteases [87]. Rhomboids are serine proteases, presenilins which form the catalytic subunit of the γ-secretase complex and signal-peptide peptidases are aspartyl proteases, and the site-2 proteases are metalloproteases [86]. The most liberal [61] and conservative analysis [26] of predicted proteases in *T. vaginalis* reveals that there are 4 presenilin-like proteases. Based on our bioinfomatic analysis, there are also 4 predicted active rhomboid proteases. Therefore, we predict that *T. vaginalis* encodes for 8-I-CLiPs (see Fig. 1-1). For comparison, we estimate that there are 13 I-CLiPs in humans, 5 of which are predicted active rhomboid proteases [88-90].

Regulated intramembrane proteolysis (RiP) by I-CLiPs has important roles such as regulation of cell signaling and basic cell homeostasis [91]. One of the best studied I-CLiPs is the γ-secretase complex which performs the second cleavage of the amyloid precursor protein (APP) leading to the generation of the amyloid-beta peptide (Aβ) that forms protein aggregates/senile plaques contributing to Alzheimer's Disease [92]. The minimal components of the γ-secretase complex are presenilin, nicastrin, anterior pharynx-defective 1 (APH-1), and presenilin enhancer protein 2 (Pen-2) [93]. After β-secretase cleaves the APP protein, nicastrin binds the C-terminal fragment of the cleaved protein, called C99, and transports it to the

presenilin catalytic subunit which first cleaves C99 at the interface between the cytosol and TM domain releasing a small intracellular domain (ICD) into the cell [93]. Then presenilin performs carboxypeptidase-like processive/successive cleavage of the TM domain stub [93] yielding different sized peptides, one of which ($A\beta_{42}$) is more prone to aggregation [92]. *T. vaginalis* contains two proteins annotated as nicastrin-like and one of them (TVAG_267320) has been localized to the cell surface [94], highlighting the potential formation of active γ-secretase-complexes in the parasite. Of particular interest would be the discovery of a transcriptional regulatory role for the *T. vaginalis* γ-secretase-generated small ICD cleavage fragment released into the cytosol where it could activate a transcriptional response similar to ICD-mediated signaling generated by other proteases [95]. To our knowledge there are no reports of γ-secretase/presenilin studies in parasitic protists.

The second group of I-CLiPs identified in *T. vaginalis* are the rhomboid family of proteases which are also important candidates for contributing to pathogenesis-associated functions [61, 94]. Rhomboid proteases compose the largest family of I-CLiPs [96]. Rhomboids were first described in *Drosophila melanogaster*, where the founding member of the rhomboid family-*D. melanogaster* Rhomboid 1-was discovered to process the Spitz protein, leading to its release from the cell surface and binding to the Epidermal growth factor receptor on receiving cells where it initiates MAPK signaling [97, 98]. Unlike the γ-secretase proteases described above, rhomboid proteases do not require their substrates to undergo prior proteolytic processing and they do not require association with other proteins/co-factors [99]. This property has allowed for a very powerful reconstitution assay where rhomboid protease activity can be tested on various model/surrogate substrates that have been shown to be cleaved by rhomboid proteases [99]. This assay greatly aids the first phases of exploring whether predicted rhomboid proteases

are active, since substrate identification of rhomboids and I-CLiPs in general is still a bottleneck in the field [85].

A variety of biological functions mediated by rhomboid cleavage have been identified. The bacterial *Providencia stuartii* rhomboid AarA cleaves the twin-arginine translocase protein TatA, and this cleavage is required for proper homo-oligomerization of TatA necessary for proper export of a yet-unidentified protein that contributes to quorum sensing [100, 101]. A role for rhomboid proteases in regulation of mitochondrial fusion has best been described in yeast [102, 103]. Rhomboid proteases have an important role in cleaving adhesins in both intracellular parasites like *Toxoplasma* [104-106] and *Plasmodium* [107, 108] as well as the extracellular parasite *Entamoeba histolytica* [109]. In *E. histolytica*, rhomboid proteases also play an important role in phagocytosis of host cells [109, 110]. Since cell signaling, phagocytosis of host cells, and adhesion to host cells are important processes for *T. vaginalis* host cell colonization and nutrient acquisition [28, 111], the study of rhomboid proteases in *T. vaginalis* is greatly warranted.

The goals of the investigations presented in this dissertation are to determine whether various *T. vaginalis* surface proteins have a role in pathogenesis with emphasis on the characterization of rhomboid proteases. In Chapter 2, a study of *T. vaginalis* rhomboid proteases and their putative *T. vaginalis* substrates is presented. Chapter 3 focuses on the study of a tetraspanin protein, TSP6, and its role in host cell sensory reception and aspects of the TSP6 protein contributing to its flagellar targeting. Chapter 4 focuses on the characterization of a cadherin-like protein of interest. Chapter 5 focuses on efforts made to try to develop molecular tools to aid the study of pathogenesis-associated proteins, using rhomboid 1 and various proteins

identified in the *T. vaginalis* cell surface proteome [94]. Together, these studies shed light on multiple surface proteins that may contribute to host: parasite interactions.

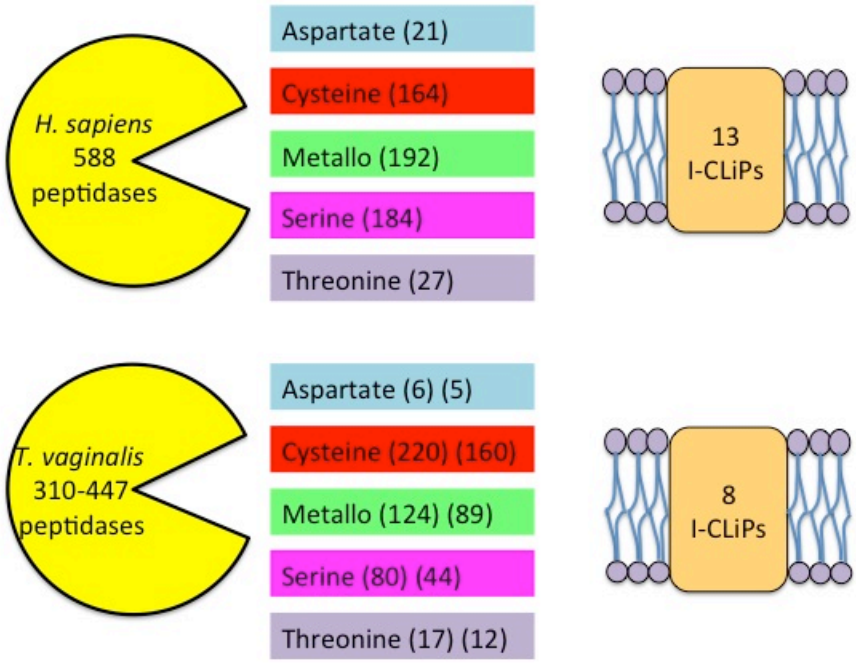

Figure 1-1: Comparison of predicted peptidases and Intramembrane-Cleaving Proteases in *Homo sapiens* versus *Trichomonas vaginalis.*
Figure was adapted from [112] to show the estimated number of peptidases in humans [62] *vs.* those in *T. vaginalis,* and their class distribution (numbers in colored boxes). Annotation of the *T. vaginalis* genome by Carlton *et al.* predicts the presence of 447 proteases [61]. The most recent MEROPS database analysis by Hirt *et al.* predicts 310 proteases [26]. The middle panel shows the catalytic class distribution, the number of each class predicted by Carlton *et al.* is shown in parenthesis on the left and that of Hirt *et al*. is shown on the right. Predicted number of I-CLiPs is shown in the membrane cartoon diagram on the right. Estimate for the number of I-CLiPs in humans is based on the bioinformatic estimates presented in [88-90] and those for *T. vaginalis* are based on the protease annotations in [14, 61] and adjusted based on our Pfam analysis of *T. vaginalis* rhomboid-like proteins. Metalloproteases and serine proteases make up the largest protease families in humans versus cysteine proteases and metalloproteases in *T. vaginalis*. Note the large number of peptidases in the single-celled *T. vaginalis* (310-447) *vs.* the 588 in the more complex multicellular organism, *H. sapiens*, highlighting the large degradome of *T. vaginalis*.

References:

1. WHO *Dept. of Reproductive Health and Research. Global incidence and prevalence of selected curable sexually transmitted infections-2008*. 2012.

2. Secor, W.E., et al., *Neglected parasitic infections in the United States: trichomoniasis.* Am J Trop Med Hyg, 2014. **90**(5): p. 800-4.

3. *Division of STD Prevention, National Center for HIV/AIDS, Viral Hepatitis, STD, and TB Prevention, Centers for Disease Control and Prevention. Trichomoniasis - CDC Fact Sheet*. 2015.

4. CDC, *Incidence, Prevalence, and Cost of Sexually Transmitted Infections in the United States*. 2013.

5. Feasey, N., et al., *Neglected tropical diseases.* Br Med Bull, 2010. **93**: p. 179-200.

6. Hotez, P.J., *America's most distressed areas and their neglected infections: the United States Gulf Coast and the District of Columbia.* PLoS Negl Trop Dis, 2011. **5**(3): p. e843.

7. Sutton, M., et al., *The prevalence of Trichomonas vaginalis infection among reproductive-age women in the United States, 2001-2004.* Clin Infect Dis, 2007. **45**(10): p. 1319-26.

8. Parise, M.E., P.J. Hotez, and L. Slutsker, *Neglected parasitic infections in the United States: needs and opportunities.* Am J Trop Med Hyg, 2014. **90**(5): p. 783-5.

9. CDC, *Neglected Parasitic Infections (NPIs) in the United States. 2014.*

10. Petrin, D., et al., *Clinical and microbiological aspects of Trichomonas vaginalis.* Clin Microbiol Rev, 1998. **11**(2): p. 300-17.

11. Cotch, M.F., et al., *Trichomonas vaginalis associated with low birth weight and preterm delivery. The Vaginal Infections and Prematurity Study Group.* Sex Transm Dis, 1997. **24**(6): p. 353-60.

12. Gram, I.T., et al., *Trichomonas Vaginalis (TV) and Human Papillomavirus (HPV) Infection and the Incidence of Cervical Intraepithelial Neoplasia (CIN) Grade III.* Cancer Causes & Control, 1992. **3**(3): p. 231-236.

13. Zhang, Z.F., et al., *Trichomonas vaginalis and cervical cancer. A prospective study in China.* Ann Epidemiol, 1995. **5**(4): p. 325-32.

14. Sutcliffe, S., et al., *Plasma antibodies against Trichomonas vaginalis and subsequent risk of prostate cancer.* Cancer Epidemiol Biomarkers Prev, 2006. **15**(5): p. 939-45.

15. Stark, J.R., et al., *Prospective study of Trichomonas vaginalis infection and prostate cancer incidence and mortality: Physicians' Health Study.* J Natl Cancer Inst, 2009. **101**(20): p. 1406-11.

16. Mavedzenge, S.N., et al., *Epidemiological synergy of Trichomonas vaginalis and HIV in Zimbabwean and South African women.* Sex Transm Dis, 2010. **37**(7): p. 460-6.

17. Shafir, S.C., F.J. Sorvillo, and L. Smith, *Current issues and considerations regarding trichomoniasis and human immunodeficiency virus in African-Americans.* Clin Microbiol Rev, 2009. **22**(1): p. 37-45, Table of Contents.

18. Fastring, D.R., et al., *Co-occurrence of Trichomonas vaginalis and bacterial vaginosis and vaginal shedding of HIV-1 RNA.* Sex Transm Dis, 2014. **41**(3): p. 173-9.

19. Kissinger, P., et al., *Patient-delivered partner treatment for Trichomonas vaginalis infection: a randomized controlled trial.* Sex Transm Dis, 2006. **33**(7): p. 445-50.

20. Niccolai, L.M., et al., *Incidence and predictors of reinfection with Trichomonas vaginalis in HIV-infected women.* Sex Transm Dis, 2000. **27**(5): p. 284-8.

21. Kirkcaldy, R.D., et al., *Trichomonas vaginalis antimicrobial drug resistance in 6 US cities, STD Surveillance Network, 2009-2010.* Emerg Infect Dis, 2012. **18**(6): p. 939-43.

22. Kissinger, P., *Epidemiology and treatment of trichomoniasis.* Curr Infect Dis Rep, 2015. **17**(6): p. 484.

23. Blaskewicz, C.D., J. Pudney, and D.J. Anderson, *Structure and Function of Intercellular Junctions in Human Cervical and Vaginal Mucosal Epithelia.* Biology of Reproduction, 2011. **85**(1): p. 97-104.

24. Fichorova, R.N., *Impact of T. vaginalis infection on innate immune responses and reproductive outcome.* J Reprod Immunol, 2009. **83**(1-2): p. 185-9.

25. Nakjang, S., et al., *A novel extracellular metallopeptidase domain shared by animal host-associated mutualistic and pathogenic microbes.* PLoS One, 2012. **7**(1): p. e30287.

26. Hirt, R.P., et al., *Trichomonas vaginalis pathobiology new insights from the genome sequence.* Adv Parasitol, 2011. **77**: p. 87-140.

27. Linden, S.K., et al., *Mucins in the mucosal barrier to infection.* Mucosal Immunol, 2008. **1**(3): p. 183-97.

28. Rendon-Maldonado, J.G., et al., *Trichomonas vaginalis: in vitro phagocytosis of lactobacilli, vaginal epithelial cells, leukocytes, and erythrocytes.* Exp Parasitol, 1998. **89**(2): p. 241-50.

29. da Costa, R.F., et al., *Trichomonas vaginalis perturbs the junctional complex in epithelial cells.* Cell Res, 2005. **15**(9): p. 704-16.

30. Mendoza-Lopez, M.R., et al., *CP30, a cysteine proteinase involved in Trichomonas vaginalis cytoadherence.* Infect Immun, 2000. **68**(9): p. 4907-12.

31. Alvarez-Sanchez, M.E., et al., *A novel cysteine proteinase (CP65) of Trichomonas vaginalis involved in cytotoxicity.* Microb Pathog, 2000. **28**(4): p. 193-202.

32. Hernandez, H.M., R. Marcet, and J. Sarracent, *Biological roles of cysteine proteinases in the pathogenesis of Trichomonas vaginalis.* Parasite, 2014. **21**: p. 54.

33. de Miguel, N., A. Riestra, and P.J. Johnson, *Reversible association of tetraspanin with Trichomonas vaginalis flagella upon adherence to host cells.* Cell Microbiol, 2012. **14**(12): p. 1797-807.

34. Sena, A.C., et al., *Trichomonas vaginalis infection in male sexual partners: implications for diagnosis, treatment, and prevention.* Clin Infect Dis, 2007. **44**(1): p. 13-22.

35. Simhan, H.N., et al., *Host immune consequences of asymptomatic Trichomonas vaginalis infection in pregnancy.* Am J Obstet Gynecol, 2007. **196**(1): p. 59 e1-5.

36. Cauci, S. and J.F. Culhane, *Modulation of vaginal immune response among pregnant women with bacterial vaginosis by Trichomonas vaginalis, Chlamydia trachomatis, Neisseria gonorrhoeae, and yeast.* Am J Obstet Gynecol, 2007. **196**(2): p. 133 e1-7.

37. Ryan, C.M., et al., *Chemical structure of Trichomonas vaginalis surface lipoglycan: a role for short galactose (beta1-4/3) N-acetylglucosamine repeats in host cell interaction.* J Biol Chem, 2011. **286**(47): p. 40494-508.

38. Singh, B.N., et al., *Identification of the lipid moiety and further characterization of the novel lipophosphoglycan-like glycoconjugates of Trichomonas vaginalis and Trichomonas foetus.* Arch Biochem Biophys, 1994. **309**(2): p. 273-80.

39. Singh, B.N., *Lipophosphoglycan-like glycoconjugate of Tritrichomonas foetus and Trichomonas vaginalis.* Mol Biochem Parasitol, 1993. **57**(2): p. 281-94.

40. Fichorova, R.N., et al., *Trichomonas vaginalis lipophosphoglycan triggers a selective upregulation of cytokines by human female reproductive tract epithelial cells.* Infect Immun, 2006. **74**(10): p. 5773-9.

41. Ton Nu, P.A., et al., *Kinetics of circulating antibody response to Trichomonas vaginalis: clinical and diagnostic implications.* Sex Transm Infect, 2015.

42. Kaur, S., et al., *Antitrichomonas IgG, IgM, IgA, and IgG subclass responses in human intravaginal trichomoniasis.* Parasitol Res, 2008. **103**(2): p. 305-12.

43. Twu, O., et al., *Trichomonas vaginalis homolog of macrophage migration inhibitory factor induces prostate cell growth, invasiveness, and inflammatory responses.* Proc Natl Acad Sci U S A, 2014. **111**(22): p. 8179-84.

44. Provenzano, D. and J.F. Alderete, *Analysis of human immunoglobulin-degrading cysteine proteinases of Trichomonas vaginalis.* Infect Immun, 1995. **63**(9): p. 3388-95.

45. Hernandez-Gutierrez, R., et al., *Trichomonas vaginalis: characterization of a 39-kDa cysteine proteinase found in patient vaginal secretions.* Exp Parasitol, 2004. **107**(3-4): p. 125-35.

46. Pereira-Neves, A. and M. Benchimol, *Phagocytosis by Trichomonas vaginalis: new insights.* Biol Cell, 2007. **99**(2): p. 87-101.

47. Juliano, C., P. Cappuccinelli, and A. Mattana, *In vitro phagocytic interaction between Trichomonas vaginalis isolates and bacteria.* Eur J Clin Microbiol Infect Dis, 1991. **10**(6): p. 497-502.

48. Benchimol, M., et al., *Trichomonas adhere and phagocytose sperm cells: adhesion seems to be a prominent stage during interaction.* Parasitol Res, 2008. **102**(4): p. 597-604.

49. Fettweis, J.M., et al., *An emerging mycoplasma associated with trichomoniasis, vaginal infection and disease.* PLoS One, 2014. **9**(10): p. e110943.

50. Hirt, R.P. and J. Sherrard, *Trichomonas vaginalis origins, molecular pathobiology and clinical considerations.* Curr Opin Infect Dis, 2015. **28**(1): p. 72-9.

51. Fiori, P.L., et al., *Association of Trichomonas vaginalis with its symbiont Mycoplasma hominis synergistically upregulates the in vitro proinflammatory response of human monocytes.* Sex Transm Infect, 2013. **89**(6): p. 449-54.

52. Cobo, E.R., L. Eckmann, and L.B. Corbeil, *Murine models of vaginal trichomonad infections.* Am J Trop Med Hyg, 2011. **85**(4): p. 667-73.

53. Hernandez, H., et al., *Monoclonal antibodies against a 62 kDa proteinase of Trichomonas vaginalis decrease parasite cytoadherence to epithelial cells and confer protection in mice.* Parasite Immunol, 2004. **26**(3): p. 119-25.

54. Fichorova, R.N., J.G. Rheinwald, and D.J. Anderson, *Generation of papillomavirus-immortalized cell lines from normal human ectocervical, endocervical, and vaginal epithelium that maintain expression of tissue-specific differentiation proteins.* Biol Reprod, 1997. **57**(4): p. 847-55.

55. Gilbert, R.O., et al., *Cytopathogenic effect of Trichomonas vaginalis on human vaginal epithelial cells cultured in vitro.* Infect Immun, 2000. **68**(7): p. 4200-6.

56. Lustig, G., et al., *Trichomonas vaginalis contact-dependent cytolysis of epithelial cells.* Infect Immun, 2013. **81**(5): p. 1411-9.

57. Bastida-Corcuera, F.D., et al., *Trichomonas vaginalis lipophosphoglycan mutants have reduced adherence and cytotoxicity to human ectocervical cells.* Eukaryot Cell, 2005. **4**(11): p. 1951-8.

58. Twu, O., et al., *Trichomonas vaginalis exosomes deliver cargo to host cells and mediate hostratioparasite interactions.* PLoS Pathog, 2013. **9**(7): p. e1003482.

59. Twu, O. and P.J. Johnson, *Parasite extracellular vesicles: mediators of intercellular communication.* PLoS Pathog, 2014. **10**(8): p. e1004289.

60. Okumura, C.Y., L.G. Baum, and P.J. Johnson, *Galectin-1 on cervical epithelial cells is a receptor for the sexually transmitted human parasite Trichomonas vaginalis.* Cell Microbiol, 2008. **10**(10): p. 2078-90.

61. Carlton, J.M., et al., *Draft Genome Sequence of the Sexually Transmitted Pathogen Trichomonas vaginalis.* Science, 2007. **315**(5809): p. 207-212.

62. Overall, C.M. and C.P. Blobel, *In search of partners: linking extracellular proteases to substrates.* Nat Rev Mol Cell Biol, 2007. **8**(3): p. 245-57.

63. Neitzel, J.J., *Enzyme Catalysis: The Serine Proteases.* Nature Education, 2010. **3**(9): p. 21.

64. Arroyo, R. and J.F. Alderete, *Trichomonas vaginalis surface proteinase activity is necessary for parasite adherence to epithelial cells.* Infection and Immunity, 1989. **57**(10): p. 2991-2997.

65. Arroyo, R. and J.F. Alderete, *Two Trichomonas vaginalis surface proteinases bind to host epithelial cells and are related to levels of cytoadherence and cytotoxicity.* Arch Med Res, 1995. **26**(3): p. 279-85.

66. Ramon-Luing, L.A., et al., *Immunoproteomics of the active degradome to identify biomarkers for Trichomonas vaginalis.* Proteomics, 2010. **10**(3): p. 435-44.

67. Yadav, M., et al., *Cysteine proteinase 30 (CP30) and antibody response to CP30 in serum and vaginal washes of symptomatic and asymptomatic Trichomonas vaginalis-infected women.* Parasite Immunol, 2007. **29**(7): p. 359-65.

68. Rendon-Gandarilla, F.J., et al., *The TvLEGU-1, a legumain-like cysteine proteinase, plays a key role in Trichomonas vaginalis cytoadherence.* Biomed Res Int, 2013. **2013**: p. 561979.

69. Sommer, U., et al., *Identification of Trichomonas vaginalis cysteine proteases that induce apoptosis in human vaginal epithelial cells.* J Biol Chem, 2005. **280**(25): p. 23853-60.

70. Cardenas-Guerra, R.E., et al., *The iron-induced cysteine proteinase TvCP4 plays a key role in Trichomonas vaginalis haemolysis.* Microbes Infect, 2013. **15**(13): p. 958-68.

71. Alderete, J.F., D. Provenzano, and M.W. Lehker, *Iron mediates Trichomonas vaginalis resistance to complement lysis.* Microb Pathog, 1995. **19**(2): p. 93-103.

72. Harisi, R. and A. Jeney, *Extracellular matrix as target for antitumor therapy.* Onco Targets Ther, 2015. **8**: p. 1387-98.

73. Vazquez-Carrillo L. I., Q.-G.L.I., Arroyo R., Mendoza-Hernández G., González-Robles A., Carvajal-Gamez B. I., Alvarez-Sánchez M. E, *The effect of Zn2+ on prostatic cell cytotoxicity caused by Trichomonas vaginalis.* Journal of Integrated OMICS. **1**(2): p. 198-210.

74. Brown, M.T., et al., *A functionally divergent hydrogenosomal peptidase with protomitochondrial ancestry.* Mol Microbiol, 2007. **64**(5): p. 1154-63.

75. Quintas-Granados, L.I., et al., *TvMP50 is an immunogenic metalloproteinase during male trichomoniasis.* Mol Cell Proteomics, 2013. **12**(7): p. 1953-64.

76. Bozner, P. and P. Demes, *Proteinases in Trichomonas vaginalis and Tritrichomonas mobilensis are not exclusively of cysteine type.* Parasitology, 1991. **102 Pt 1**: p. 113-5.

77. Ma, L., et al., *Involvement of the GP63 protease in infection of Trichomonas vaginalis.* Parasitol Res, 2011. **109**(1): p. 71-9.

78. Santos, A.L., M.H. Branquinha, and C.M. D'Avila-Levy, *The ubiquitous gp63-like metalloprotease from lower trypanosomatids: in the search for a function.* An Acad Bras Cienc, 2006. **78**(4): p. 687-714.

79. Yao, C., J.E. Donelson, and M.E. Wilson, *The major surface protease (MSP or GP63) of Leishmania sp. Biosynthesis, regulation of expression, and function.* Mol Biochem Parasitol, 2003. **132**(1): p. 1-16.

80. Hernandez-Romano, P., et al., *Identification and characterization of a surface-associated, subtilisin-like serine protease in Trichomonas vaginalis.* Parasitology, 2010. **137**(11): p. 1621-35.

81. Carruthers, V.B., G.D. Sherman, and L.D. Sibley, *The Toxoplasma adhesive protein MIC2 is proteolytically processed at multiple sites by two parasite-derived proteases.* J Biol Chem, 2000. **275**(19): p. 14346-53.

82. Lagal, V., et al., *Toxoplasma gondii protease TgSUB1 is required for cell surface processing of micronemal adhesive complexes and efficient adhesion of tachyzoites.* Cell Microbiol, 2010. **12**(12): p. 1792-808.

83. M. Santos, J., A. Graindorge, and D. Soldati-Favre, *New insights into parasite rhomboid proteases.* Molecular and Biochemical Parasitology, 2012. **182**(1–2): p. 27-36.

84. Sibley, L.D., *The roles of intramembrane proteases in protozoan parasites.* Biochimica et Biophysica Acta (BBA) - Biomembranes, 2013. **1828**(12): p. 2908-2915.

85. Wolfe, M.S., *Intramembrane-cleaving proteases.* J Biol Chem, 2009. **284**(21): p. 13969-73.

86. Hooper, N.M. and U. Lendeckel, *Intramembrane-cleaving proteases (I-CLiPs)*, in *Proteases in biology and disease v 6*. 2007, Springer,: Dordrect, Netherlands. p. ix, 142 p.

87. Lemberg, M.K., *Sampling the membrane: function of rhomboid-family proteins.* Trends Cell Biol, 2013. **23**(5): p. 210-7.

88. Martoglio, B. and T.E. Golde, *Intramembrane-cleaving aspartic proteases and disease: presenilins, signal peptide peptidase and their homologs.* Hum Mol Genet, 2003. **12 Spec No 2**: p. R201-6.

89. Rawson, R.B., *The site-2 protease.* Biochim Biophys Acta, 2013. **1828**(12): p. 2801-7.

90. Lemberg, M.K. and M. Freeman, *Functional and evolutionary implications of enhanced genomic analysis of rhomboid intramembrane proteases.* Genome Res, 2007. **17**(11): p. 1634-46.

91. Beel, A.J. and C.R. Sanders, *Substrate specificity of gamma-secretase and other intramembrane proteases.* Cell Mol Life Sci, 2008. **65**(9): p. 1311-34.

92. De Strooper, B., R. Vassar, and T. Golde, *The secretases: enzymes with therapeutic potential in Alzheimer disease.* Nat Rev Neurol, 2010. **6**(2): p. 99-107.

93. Tomita, T., *Molecular mechanism of intramembrane proteolysis by gamma-secretase.* J Biochem, 2014. **156**(4): p. 195-201.

94. de Miguel, N., et al., *Proteome analysis of the surface of Trichomonas vaginalis reveals novel proteins and strain-dependent differential expression.* Mol Cell Proteomics, 2010. **9**(7): p. 1554-66.

95. Beckett, C., et al., *Nuclear signalling by membrane protein intracellular domains: the AICD enigma.* Cell Signal, 2012. **24**(2): p. 402-9.

96. Urban, S., *Taking the plunge: integrating structural, enzymatic and computational insights into a unified model for membrane-immersed rhomboid proteolysis.* Biochem J, 2010. **425**(3): p. 501-12.

97. Urban, S., J.R. Lee, and M. Freeman, *Drosophila rhomboid-1 defines a family of putative intramembrane serine proteases.* Cell, 2001. **107**(2): p. 173-82.

98. Wasserman, J.D., S. Urban, and M. Freeman, *A family of rhomboid-like genes: Drosophila rhomboid-1 and roughoid/rhomboid-3 cooperate to activate EGF receptor signaling.* Genes Dev, 2000. **14**(13): p. 1651-63.

99. Urban, S. and M.S. Wolfe, *Reconstitution of intramembrane proteolysis in vitro reveals that pure rhomboid is sufficient for catalysis and specificity.* Proc Natl Acad Sci U S A, 2005. **102**(6): p. 1883-8.

100. Gallio, M., et al., *A conserved mechanism for extracellular signaling in eukaryotes and prokaryotes.* Proc Natl Acad Sci U S A, 2002. **99**(19): p. 12208-13.

101. Stevenson, L.G., et al., *Rhomboid protease AarA mediates quorum-sensing in Providencia stuartii by activating TatA of the twin-arginine translocase.* Proc Natl Acad Sci U S A, 2007. **104**(3): p. 1003-8.

102. Ishihara, N., et al., *Regulation of mitochondrial morphology through proteolytic cleavage of OPA1.* EMBO J, 2006. **25**(13): p. 2966-77.

103. Chan, E.Y. and G.A. McQuibban, *The mitochondrial rhomboid protease: its rise from obscurity to the pinnacle of disease-relevant genes.* Biochim Biophys Acta, 2013. **1828**(12): p. 2916-25.

104. Brossier, F., et al., *A spatially localized rhomboid protease cleaves cell surface adhesins essential for invasion by Toxoplasma.* Proc Natl Acad Sci U S A, 2005. **102**(11): p. 4146-51.

105. Dowse, T.J., et al., *Apicomplexan rhomboids have a potential role in microneme protein cleavage during host cell invasion.* Int J Parasitol, 2005. **35**(7): p. 747-56.

106. Opitz, C., et al., *Intramembrane cleavage of microneme proteins at the surface of the apicomplexan parasite Toxoplasma gondii.* EMBO J, 2002. **21**(7): p. 1577-85.

107. Baker, R.P., R. Wijetilaka, and S. Urban, *Two Plasmodium rhomboid proteases preferentially cleave different adhesins implicated in all invasive stages of malaria.* PLoS Pathog, 2006. **2**(10): p. e113.

108. Ejigiri, I., et al., *Shedding of TRAP by a Rhomboid Protease from the Malaria Sporozoite Surface Is Essential for Gliding Motility and Sporozoite Infectivity.* PLoS Pathogens, 2012. **8**(7): p. e1002725.

109. Baxt, L.A., et al., *Downregulation of an Entamoeba histolytica rhomboid protease reveals roles in regulating parasite adhesion and phagocytosis.* Eukaryot Cell, 2010. **9**(8): p. 1283-93.

110. Baxt, L.A., et al., *An Entamoeba histolytica rhomboid protease with atypical specificity cleaves a surface lectin involved in phagocytosis and immune evasion.* Genes Dev, 2008. **22**(12): p. 1636-46.

111. Ryan, C.M., N. de Miguel, and P.J. Johnson, *Trichomonas vaginalis: current understanding of host-parasite interactions.* Essays Biochem, 2011. **51**: p. 161-75.

112. Overall, C.M. and C.P. Blobel, *In search of partners: linking extracellular proteases to substrates.* Nat Rev Mol Cell Biol, 2007. **8**(3): p. 245-257.

Chapter 2:

Rhomboid intramembrane proteolysis contributes to *Trichomonas vaginalis* attachment and cytotoxicity to human ectocervical cells

Abstract:

Trichomonas vaginalis is an extracellular eukaryotic parasite that causes trichomoniasis, the most common, non-viral sexually transmitted infection worldwide. Although the disease burden is high, molecular mechanisms underlying the parasite's ability to cause disease are poorly understood. Here, we identify four putative *T. vaginalis* rhomboid proteases and demonstrate catalytic activity for two, TvROM1 and TvROM3. These two membrane serine proteases were found to display different subcellular localization and substrate specificities. TvROM1 is found on vesicles and the cell surface membrane and cleaves atypical model rhomboid protease substrates, whereas TvROM3 appears to be localized in the Golgi apparatus and recognizes a canonical model substrate. As rhomboid proteases and their substrates are found in the same membrane, we interrogated the *T. vaginalis* surface proteome, using quantitative proteomics and bioinformatics, to identify putative TvROM1 substrates. Of the nine identified, TVAG_166850 and TVAG_280090, were shown to be cleaved by TvROM1. Comparison of amino acid residues surrounding the predicted cleavage sites in biochemically confirmed TvROM substrates revealed a preference for small amino acids in the transmembrane domain. Over-expression of TvROM1 results in increased attachment to and cytolysis of host ectocervical cells. Similarly, mutations that block the cleavage of a TvROM1 substrate lead to an accumulation of the substrate on the cell surface and increased attachment of the parasite to host cells. Together, these data indicate a role for TvROM1 in host: parasite interactions by modulating attachment to and lysis of host cells, key processes contributing to *T. vaginalis* pathogenesis.

Importance: *Trichomonas vaginalis*, a common pathogen, causes a sexually transmitted infection and exacerbates other diseases. Only one class of drug is available to treat *T. vaginalis*

infection, making discovery of parasite factors contributing to host colonization critical for the development of new therapeutics. Here we report the first characterization of *T. vaginalis* intramembrane rhomboid proteases. One protease, TvROM1, is shown to increase the parasite's association with and destruction of host cells. To identify TvROM1 substrates, we developed and used an approach that can be applied to other biological systems; an important step forward, as identification of substrates has been a major challenge for understanding the cellular processes regulated by rhomboid proteases and other intramembrane proteases. We identified two TvROM1 substrates, one of which is involved in modulating host: parasite interactions. This study highlights the involvement of rhomboid proteases in *T. vaginalis* pathogenic processes, and provides further support for targeting parasite surface proteases for therapeutic intervention.

Introduction:

Trichomonas vaginalis is an extracellular, eukaryotic parasite that is the causative agent of trichomoniasis, the most common non-viral sexually transmitted infection in the world [1]. Approximately 276 million people become newly infected each year worldwide [1], and in the United States, an estimated 3.7 million people are currently infected [2]. Symptoms and outcomes of infection include vaginitis, urethritis, prostatitis, infertility, and adverse pregnancy outcomes (reviewed in Petrin *et al.* 1998) [3]. *T. vaginalis* infection is associated with an increased risk of HIV acquisition [4] and potentially transmission [5] due to HIV target cells being recruited to the site of infection [6] and increased viral shedding upon *T. vaginalis* co-infection [7, 8]. *T. vaginalis* is also associated with cervical cancer [9, 10] and aggressive prostate cancer [11, 12]. Due to the high burden, threat of illness, and understudied nature of *T. vaginalis* infection, trichomoniasis has been recently recognized as one of the United States' neglected parasitic infections [13-15].

Although the magnitude of parasite infection is high, little is known about how *T. vaginalis* colonizes the human host and causes disease [3, 16]. As an extracellular organism that thrives in the changing and physiologically diverse environment of the urogenital tract of men and women, *T. vaginalis* likely utilizes multiple mechanisms to establish an infection and persist. The parasite attaches to multiple host cell types such as vaginal and prostate epithelial cells [17], and red blood cells [18] and is capable of acquiring nutrients from them through cell lysis. *T. vaginalis* can also bind together to form clusters [19]. Cell aggregates are also observed when growing the parasite axenically and when placed on monolayers of host cells. However, only a few of the molecular players thought to mediate and regulate these host: parasite or parasite: parasite interactions have been identified [16, 19, 20].

Recent genomic, transcriptomic, and proteomic studies of *T. vaginalis* have aided the identification of protein families that may play important roles in *T. vaginalis* cell biology and pathogenesis [21-24]. In studies analyzing the surface proteome of six different *T. vaginalis* strains, we identified a rhomboid-like protein [23]. Rhomboids are polytopic serine proteases that are localized to membranes where they encounter and cleave their substrates. Rhomboid proteases belong to the intramembrane-cleaving protease family called I-CLiPs [25], however they differ from most I-CLiPs in that their cleavage products are often released to the outside of the cell. Rhomboid proteases were first described in *Drosophila melanogaster*, where their extracellularly-released cleavage fragments were found to bind other cells and initiate cell signaling [26-28]. Interestingly, rhomboid proteases from evolutionarily divergent organisms are capable of recognizing and cleaving a common set of substrates [26, 29-33] referred to as model substrates, a property that has been critical in the characterization of rhomboids from diverse organisms.

Rhomboid proteases are among the most conserved families of polytopic membrane proteins [34] and have been suggested to be one of the most ancient regulatory enzymes [25]. In addition to activating cell signaling pathways, rhomboid proteases have been reported to play roles in quorum sensing [29, 35], regulation of mitochondrial morphology [36], phagocytosis [37], and cleavage of adhesins in both intracellular parasites like *Toxoplasma* [30, 38-41] and *Plasmodium* [32, 42-45] as well as the extracellular parasite *Entamoeba histolytica* [31]. One of the greatest challenges in uncovering the biological functions of rhomboid proteases has been the identification of their substrates. For example, the substrate for the best studied bacterial rhomboid, *E. coli* GlpG, is still unknown [46].

Rhomboid proteases and other I-CLiPs evolved separately from soluble proteases [25], hence the mechanism(s) they use for substrate recognition and cleavage is also predicted to be different, as recent studies have began to reveal [47-49]. Selection of a specific rhomboid substrate is dictated by the TM segment dynamics of the substrate [49]. In particular, helix-destabilizing residues in the TM domain appear to be required for the substrate to exit the membrane and reside in the enzyme's active site [49]. There is also a preference for certain amino acids to surround the cleavage site. Cleavage of the substrate typically occurs after a small amino acid at the P1 position [33, 50], and in the case of eukaryotic rhomboid proteases an adjacent small amino acid in the P1' site is also preferred [51]. Strisovsky *et al.* published a consensus motif of amino acids surrounding the cleavage site that promote or block cleavage by the eubacterial AarA rhomboid [33]. However, it has been shown that *Drosophila* Rhomboid-1 can cleave its natural substrate Spitz with mutations that are disallowed by the Strisovsky *et al.* motif [49]. This suggests eukaryotic and eubacterial rhomboid proteases have different substrate specificity. The discovery of additional substrates will aid in defining specific substrate features

that promote rhomboid protease cleavage and how these may differ between different classes of rhomboid proteases.

In this study, we report the identification and characterization of two active *T. vaginalis* rhomboid proteases (TvROM1 & TvROM3). Exogenous expression of TvROM1 leads to increased attachment to and cytolysis of host ectocervical cells, two phenotypes implicated in pathogenesis. Using quantitative proteomics and bioinformatics, we identified two putative substrates that can be cleaved by TvROM1, neither of which is cleaved by TvROM3. Hence the two enzymes have different natural substrates, consistent with their specificity for different model substrates and different subcellular localizations. The *T. vaginalis* substrates identified for TvROM1 belong to a family of putative adhesins previously implicated in pathogenesis [20, 23]. Together, our observations indicate a role for TvROM1 in modulating parasite attachment and cytolysis of host cells.

Results:

Identification of active rhomboid proteases in *T. vaginalis*

The *T. vaginalis* genome (http://trichdb.org/trichdb) contains 9 genes annotated as "rhomboid-like". Bioinformatic analysis of these genes revealed that only 4 encode for proteins that contain both a serine (Ser) and a histidine (His) at the top of TMs 4 and 6, which are predicted to form the catalytic dyad required for substrate cleavage by rhomboid proteases (see schematic in Fig. 2-1). The proteins encoded by these 4 genes also have the Gly-X-Ser-X, (X = amino acid) that surrounds and identifies the catalytic Ser [52]. The other 5 genes (TrichDB accession numbers TVAG_282180, TVAG_378960, TVAG_233140, TVAG_183030, TVAG_037580) lack catalytic residues and are likely proteolytically inactive. TVAG_233140, which lacks a catalytic His was detected in the surface proteome of *T. vaginalis* [23]. We focused

our attention on the rhomboid proteins predicted to be active proteases. Table 2-S1 summarizes additional features found in the 4 predicted active *T. vaginalis* rhomboid proteases, which we named TvROM1-4 (TrichDB accession numbers TVAG_112900, TVAG_359500, TVAG_476950, TVAG_161010).

Localization of TvROMs in *T. vaginalis*

The genes encoding the predicted active rhomboids were cloned under the control of the strong α-SCS promoter with N-terminal hemagglutinin (HA) tags. The cellular localization of the proteins was determined in transfectants using indirect immunofluorescence assays (IFA) with an anti-HA antibody. HA-TvROM1 was located on the cell surface and vesicle-like structures (Fig. 2-1 B and C). To confirm the cell surface localization of TvROM1, transfectants were labeled using membrane-impermeable biotin as described previously [23]. We observed co-localization of the 3XHA-TvROM1 signal with the biotinylated cell surface (Fig. 2-1 D-F). No background staining was observed in non-biotinylated parasites used as a negative control (data not shown).

In contrast to the cell surface localization of TvROM1, TvROM2 and TvROM3 were located in a line structure next to the nucleus (Fig. 2-1 G-H, and I-J, respectively), which is likely the Golgi apparatus. Most rhomboids have been localized in the Golgi, including the founding member of the rhomboid family, *Drosophila* Rhomboid-1 (DmRho1) [26] and the *Toxoplasma gondii* TgROM2 [53]. Prior to mitosis, the *T. vaginalis* Golgi apparatus elongates and then divides through medial fission of each cisternae in a process called Golgikinesis, forming 2 Golgi ribbons [54]. We observed a similar structure adjacent to the nucleus in dividing cells to which TvROM2 (Fig. 2-1 G-H) and TvROM3 (data not shown) localize, providing additional

support for a Golgi localization of these proteins. We were unable to detect expression of HA-TvROM4 in transfectants and therefore did not continue to analyze this protein.

TvROM1 and TvROM3 are active proteases

We tested the proteolytic activities of TvROM1-3 using a heterologous cell cleavage assay previously described [32]. HA-tagged proteins were co-expressed in HEK293 cells with known rhomboid protease substrates tagged at the N-terminus with GFP or doubly tagged with an N-terminal GFP tag and a C-terminal FLAG tag. Rhomboid proteases known to cleave the substrate being tested were co-transfected as positive controls. Cells transfected without a rhomboid or co-transfected with catalytically inactive rhomboid mutants served as negative controls.

We first tested whether TvROMs cleave the *D. melanogaster* rhomboid substrate Spitz [26], as this canonical rhomboid substrate is cleaved by rhomboid proteases from several organisms [30-32, 51, 55]. TvROM3 was the only TvROM of the three *T. vaginalis* ROMs tested that could cleave Spitz, although weakly (data not shown). Cleavage was more efficient with APP+Spi7, which is a chimeric substrate in which the first 7 residues of the amyloid precursor protein (APP) transmembrane segment were replaced with those from Spitz (Fig. 2-2 A-lane 5). The positive control DmRho1 cleaved Spitz (Fig. 2-2 A-lane 2) releasing the cleaved fragment into the media. Cleavage by TvROM3 was specific as no cleavage product was detected with the TvROM3 His181Ala catalytic mutant (Fig. 2-2 A-lane 6).

Since TvROM1 could not cleave Spitz, we tested its ability to cleave *Plasmodium* adhesins. *Plasmodium falciparum* rhomboid 4 (PfROM4) cannot process Spitz, but can cleave other *Plasmodium* adhesins and this property was termed “atypical substrate specificity” [32] since many rhomboid proteases can cleave Spitz. PfROM4 served as the positive control for

testing cleavage of the erythrocyte-binding antigen 175 (EBA-175) protein (Fig. 2-2 B-lane 2) and the BA erythrocyte binding ligand (BAEBL/EBA140) protein (data not shown). TvROM1 can cleave EBA-175 (Fig. 2-2 B-lane 3) and BAEBL (data not shown). Conversely, the TvROM1 His316Ala catalytic mutant does not cleave these two proteins (Fig. 2-2 B-lane 4, and data not shown). Therefore, in addition to PfROM4 and *Entamoeba histolytica* rhomboid 1 (EhROM1), TvROM1 is the third parasite rhomboid protease that displays atypical substrate specificity [31, 32] suggesting this may be a common feature of eukaryotic parasite rhomboid proteases. Since TvROM1 displayed similar substrate specificity as PfROM4, we determined whether TvROM1 also cleaves EBA-175 at the same location as PfROM4. The FLAG-tagged C-terminal cleavage product produced by TvROM1 and PfROM4 co-transfectants was immunoprecipitated and the cleavage site was determined by MALDI-TOF analysis. We found that TvROM1 cleaves EBA-175 between Ala and Gly (Fig. 2-2 C) as previously found for PfROM4 [44]. Therefore, TvROM1 also cleaves its substrate between two small amino acids.

TvROM1 can also cleave human EphrinB3 (Fig. 2-2 D-lane 3), and bacterial TatA (Fig. 2-2 E-lane 3), substrates of the human RHBDL2 [56] and the bacterial AarA [35] rhomboid proteases, respectively. DmRho1 served as a positive control in the EphrinB3 and TatA cleavage assays (Fig. 2-2 D-lane 2 and Fig. 2-2 E-lane 2, respectively). Interestingly, although DmRho1 cleaves Spitz and these additional substrates, TvROM1 can cleave EphrinB3 and TatA, but not Spitz. Cleavage of EphrinB3 and TatA by TvROM1 was specific, since the TvROM1 His316Ala catalytic mutant did not produce cleavage fragments (Fig. 2-2 D-lane 4 and Fig. 2-2 E-lane 4). Conversely, TvROM3 did not specifically cleave EBA-175 (Fig. 2-2 B, lanes 5 & 6), EphrinB3 (Fig. 2-2 D, lanes 5 & 6), or TatA (Fig. 2-2 E, lanes 5 & 6). Taken together, these results demonstrate different substrate specificities for TvROM1 and TvROM3.

TvROM2 produced cleavage fragments of Spitz, however, the fragments are also produced by the TvROM2 His270Ala catalytic mutant (data not shown). As metalloproteases have been shown to cleave and release rhomboid substrates in the heterologous cell cleavage assay [26, 30, 32], we added 10 μM batimastat, a wide spectrum metalloprotease inhibitor, in assays testing whether TvROM2 cleaves EphrinB3. The inhibitor abolished the appearance of the predicted EphrinB3 cleavage fragment produced by TvROM2 (data not shown) but not by TvROM1 used as a positive control, therefore the cleavage products observed with the other substrates in the TvROM2 co-transfectants are also likely due to metalloprotease activity and not rhomboid protease activity (data not shown).

Serine protease activity and TvROM1 contributes to *T. vaginalis* attachment to and cytolysis of host ectocervical cells

To investigate the biological role of TvROMs and their possible contribution to parasite-host interactions, we tested the effect of the serine protease inhibitor 3,4-dichloroisocoumarin (3,4-DCI) on parasite attachment to and lysis of host cells. The contribution of specific cysteine proteases modulating these processes is well documented [57-63] whereas no biological role has been reported for the only *T. vaginalis* serine protease studied to date [64]. 3,4-DCI has been shown to inhibit the activity of rhomboid proteases from multiple organisms [30, 37, 42, 65]. We tested the effect of 3,4-DCI on parasite attachment to host cells, by exposing *T. vaginalis* to ectocervical cell monolayers for 30 min in the presence of increasing concentrations of 3,4-DCI. Unattached parasites were then washed away and the number of attached parasites was quantified (as previously described in [17]). A dose-response effect was observed with 10 and 15 μM 3,4-DCI decreasing attachment to host cells 40% and 64%, respectively, compared to vehicle-treated parasites (Fig. 2-3 A). To test cytolysis of host cells, we exposed *T. vaginalis* to

ectocervical cell monolayers for 3 hours in the presence of different 3,4-DCI concentrations and then assessed host cell lysis by measuring LDH released from damaged cells as described [17]. Similar to the observed reduction in attachment, cytolysis of host cells was reduced by 25%, 61%, and 73% in the presence of 5, 10, and 15 μM 3,4-DCI, respectively (Fig. 2-3 B). No effect on the viability of the parasites or host cells was observed at the concentrations used for both the attachment and cytolysis assays (data not shown). These results indicate that serine proteases likely play a role in two critical processes that contribute to *T. vaginalis* destruction of host cells.

To test the role of individual TvROMs specifically, we compared the ability of parasites exogenously expressing HA-tagged TvROMs to attach to and lyse host cells. Parasites expressing additional exogenous TvROM1 had a 1.6 fold increased ability to attach to host cells compared to empty vector control transfectants (p-value<0.01) (Fig. 2-3 C). Additionally, exogenous expression of TvROM1 resulted in a 4.2-fold increased ability to lyse host cells (p-value<0.01) (Fig. 2-3 D). The involvement of TvROMs in these processes was limited to TvROM1, as exogenous expression of TvROM2 and TvROM3 did not lead to increased attachment to or lysis of host cells (data not shown).

Use of quantitative proteomics identifies a putative TvROM1 substrate

Having demonstrated that TvROM1 is an active protease that modulates attachment to and lysis of host cells, we sought to identify its substrates using a quantitative proteomics approach. Given the cell surface localization of TvROM1, we identified proteins that are differentially released into the media by TvROM1 transfectants treated with the serine protease inhibitor 3,4-DCI compared to DMSO vehicle control (see flow chart in Fig 2-4 A). Proteins released into the media were collected and differentially labeled using stable isotope dimethyl labeling [66] to allow quantitative comparisons of protein abundance. We predicted that the

inhibition of TvROM1 activity by 50 μM 3,4-DCI would reduce the release of its plasma membrane substrates into the media. Table 2-S2 lists and Fig. 2-4 B shows the distribution of all the proteins identified in a combined analysis of two independent mass spectrometry experiments. Of the proteins identified, 17 protein groups decreased by more than 50% with 3,4-DCI *vs.* vehicle control treatment, with a statistically significant decrease observed for 7 protein groups. Five proteins of the 7 protein groups have a predicted TM domain and type 1 topology (N-terminus outside cell-TM domain-C-terminus inside cell), the minimal features of rhomboid protease substrates. Two proteins cannot be differentiated by the peptides obtained (TVAG_245580 and TVAG_425470), and since one amino acid difference is present in their predicted TM domains (Fig. 2-4 C), both proteins were considered individually in further analysis. The abundance of the 5 proteins in the media was reduced between 60-67% in the presence of 50 μM 3,4-DCI (Fig. 2-4 C).

The ability of TvROM1 to cleave the TM domains of the 5 candidate substrates was tested using the HEK293 heterologous cell cleavage assay. Initial attempts to express the full-length *T. vaginalis* substrates resulted in retention of these large proteins in the ER. Therefore, to assess cleavage at the cell surface, a chimeric protein of GFP-EBA-175 with its TM domain replaced with the putative substrate's TM domains was constructed and co-expressed with either TvROM1 or a TvROM1 His316Ala catalytic mutant. Only the TM domain of TVAG_166850 can be specifically cleaved by TvROM1 (Fig. 2-4 D, bottom panel, lane 2, and data not shown). Specificity of cleavage was demonstrated as no cleavage fragment was detected using the TvROM1 His316Ala catalytic mutant (Fig. 2-4 D, bottom panel, lane 3). We observed release of TVAG_573910 into the media; however cleavage was not dependent on co-transfection with TvROM1 (data not shown). We also tested whether any of the putative substrates could be

cleaved by TvROM3, the other active rhomboid protease identified, and found that none of the putative substrates were cleaved by TvROM3 (data not shown). Inspection of the amino acids in the TM domain of the 5 putative substrates (Fig. 2-4 C) reveals that the 4 proteins that were not cleaved by TvROM1 (TVAG_573910, TVAG_245580, TVAG_425470, and TVAG_393390) contain residues in the top of the TM domain that fit the previously published Strisovsky *et al.* motif [33], thus, the substrate specificity of both TvROM1 and TvROM3 appear to differ from the bacterial-like rhomboid specificity defined by the Strisovsky *et al.* motif. Instead, the TM domain of the substrate which is processed by TvROM1, TVAG_166850, has a predominant presence of the small amino acid alanine, and the helix relaxing residue glycine [67, 68] (Fig. 2-4 C), which led us to further investigate possible substrate determinants that might aid in identification of additional *T. vaginalis* rhomboid substrates.

Screening the *T. vaginalis* surface proteome for TM domains similar to TMs in parasite rhomboid protease substrates identifies an additional TvROM1 substrate and reveals features of *T. vaginalis* substrate specificity

Rhomboid proteases cleave near or at the external face of the TM domain of the substrate. Although the substrate's overall TM dynamics has been found to be the governing feature defining a rhomboid substrate [49], a subset of amino acids surrounding the P1-P1' cleavage site may impart a specific conformation that promotes cleavage [51]. Thus, we compiled and compared established and predicted cleavage sites for rhomboid substrates from other eukaryotic parasites: *Toxoplasma gondii*, *Plasmodium falciparum*, and *Entamoeba histolytica* [30-32, 38-40, 43, 44, 51, 53] (Table 2S-3). The resulting comparison revealed a predominance of specific residues in the predicted P4-P3' sites (Fig. 2-5 A) from which we created a consensus called the "parasite search motif" (Fig. 2-5 A). It is notable that this motif

has little overlap with the consensus motif of the P4-P2' sites preferred by bacterial rhomboid proteases [33].

Using the parasite search motif, we screened the *T. vaginalis* surface proteome [23] to identify putative TvROM1 substrates (see flowchart in Fig. 2-5 B). Out of 314 proteins searched, 7 proteins had the motif positioned in the top of the TM domain by at least 2 of 3 TM prediction programs and 5 of these were type 1, single TM proteins, typical of rhomboid protease substrates (list of proteins screened is shown in Table 2-S4). The predicted TM domains of the five putative substrates is shown in Fig. 2-5 C. Interestingly, TVAG_166850, the only substrate identified via our quantitative proteomics approach that can be cleaved by TvROM1 (Fig. 2-4 D) is also 1 of the 5 candidate substrates identified by this bioinformatics approach.

After confirming that the 5 candidate substrates are localized to the plasma membrane (Chapter 5 Fig. 5-10 B, 5-11 A, and data not shown) we performed heterologous cell cleavage assays to test whether TvROM1 could cleave the TM domain of the putative substrates. In addition to the TM domain of TVAG_166850, we found that the TM domain of TVAG_280090 is also cleaved by TvROM1 (Fig. 2-5 D, bottom panel, lane 2). It is notable that the TVAG_280090 protein has overall 55% identity and 69% similarity to TVAG_166850. The TvROM1 His316Ala catalytic mutant could not cleave TVAG_280090's TM domain (Fig. 2-5 D, bottom panel, lane 3), demonstrating specific cleavage. DmRho1 can also process the TM domain of TVAG_280090 (data not shown), providing further support that this protein is a rhomboid protease substrate. Similar to that observed for TVAG_166850, TvROM3 could not cleave TVAG_280090 (data not shown). The remaining candidate substrates were not cleaved by TvROM1 or TvROM3 (data not shown).

Comparison of the TMs of putative *T. vaginalis* substrates not cleaved by TvROM1 reveals that 7 of the 8 have Ile at the predicted P2, P3, or both positions (Fig. 2-S5) whereas the 2 cleaved have a predicted Ala (P2) or Ala or Leu (P1). Taking this into account, we searched the *T. vaginalis* genome (55,581 genes) with the parasite search motif, requiring proteins to have 1 TM domain, with the motif located in the top of the TM domain (20 genes), and excluding Ile at the P2 or P3 positions led to 5 proteins that meet these criteria. Of these, 2 were TVAG_166850 and TVAG_280090, the confirmed TvROM1 substrates (Fig. 2-4 D and Fig. 2-5 D). The remaining three proteins (TVAG_493860, TVAG_493930, and TVAG_206210) are annotated as leishmanolysin-like metallopeptidases (Fig. 2-S1 A). We found that TvROM1 could not cleave the TM domain of two of these metallopeptidases (Fig. 2-S1 B) and based on their similarity, it would not be predicted to cleave the third protein. The three metallopeptidases contain a stretch of seven small amino acids consisting of Ala, Gly, and Val surrounding the predicted cleavage site (Fig. 2-S1 A), similar to TVAG_166850 and TVAG_280090, underscoring the difficulty in predicting rhomboid protease substrates based solely on primary amino acid sequence analysis.

Mutation of predicted rhomboid cleavage site in the putative substrate TVAG_166850 increases its presence at the cell surface and leads to greater parasite attachment

We have previously reported that the TvROM1 substrate identified in this study, TVAG_166850, increases parasite attachment to host cells when exogenously expressed in a low adherent *T. vaginalis* strain [23]. To address whether cleavage by TvROM1 influences TVAG_166850's ability to mediate host cell attachment we introduced mutations at the predicted rhomboid cleavage site. The predicted P1-P1' site Ala672-Gly673 residues were mutated to Phe-Phe residues, since mutation of small amino acids at the predicted cleavage site to bulky Phe has been shown to significantly decrease rhomboid cleavage of the *T. gondii* AMA1

substrate [41]. Fig. 2-6 A shows a graphical representation of GFP-TVAG_166850 and the predicted rhomboid cleavage site. N-terminally tagged GFP-TVAG_166850^{WT} or the GFP-TVAG_166850$^{AG/FF}$ mutant were exogenously expressed in the poorly adherent *T. vaginalis* strain G3 and the levels of wild type and mutant proteins on the surface of transfectants was measured using flow cytometry. The percent of cells expressing the GFP-tagged proteins were similar in the GFP-TVAG_166850^{WT} and GFP-TVAG_166850$^{AG/FF}$ mutant populations (Fig. 2-6 B top panel). However, the mean fluorescence intensity (MFI) of the GFP-TVAG_166850$^{AG/FF}$ mutant population was consistently at least 3-fold higher than the wild type population in three independent experiments (a representative experiment is shown in Fig. 2-6 B, bottom panel). The increased MFI signal observed in the GFP-TVAG_166850$^{AG/FF}$ population continued to be observed after growing the parasites in culture for several days and after freeze-thaw of the population, providing evidence for a robust and stable phenotype. Higher surface staining of the rhomboid substrate MIC2 in *T. gondii* rhomboid knockout cells has also been reported by Shen *et al.* [69]. Therefore, we interpret the increased surface detection of the GFP-TVAG_166850$^{AG/FF}$ mutant protein to result from lack of cleavage by TvROM1, allowing for its greater accumulation at the cell surface.

To determine the phenotypic effect of mutating the predicted rhomboid cleavage site in GFP-TVAG_166850, we compared the attachment properties of the GFP-TVAG_166850^{WT} and GFP-TVAG_166850$^{AG/FF}$ mutant populations. Exogenous expression of GFP-TVAG_166850^{WT} led to a 1.3 fold increased ability to attach to host cells compared to empty vector transfectants (p-value<0.05), while exogenous expression of the GFP-TVAG_166850$^{AG/FF}$ mutant led to an even greater increase in attachment (1.7 fold) compared to empty vector (p-value<0.01) (Fig. 2-6 C). The change in attachment between the mutant and wild type was statistically significant (p-

value<0.01). These data indicate that reduced TvROM1 cleavage leads to the increased surface levels of the GFP-TVAG_166850$^{AG/FF}$ mutant protein (Fig. 2-6 B) which in turn leads to increased attachment to host cells (Fig. 2-6 C). Incubation of GFP-TVAG_166850^{WT} and GFP-TVAG_166850$^{AG/FF}$ mutant populations with ectocervical cells in a 4 hour cytolysis assay did not reveal a greater ability of the transfectants to lyse host cells (data not shown), indicating additional factors likely modulate *T. vaginalis* cytolysis of host cells. To verify that the mutations introduced into the GFP-TVAG_166850$^{AG/FF}$ mutant affect TvROM1 cleavage, the HEK293 heterologous cell cleavage assay was used to compare TvROM1 cleavage of the chimeric EBA-175 protein containing either the wild type or mutant TM domain of TVAG_166850. GFP-EBA-175-TVAG_166850TM$^{AG/FF}$ mutant chimeric protein was shown to be cleaved 90% less than the chimeric protein containing the wild type TM domain (Fig. 2-6 D, lane 4 *vs.* lane 9). Cleavage of the wild type and mutant TM domains, above background levels, was not observed using the His316Ala catalytic mutant of TvROM1 (Fig. 2-6 D, lanes 5 and 10). Similarly, TgROM5 cleaves the wild type TM domain of TVAG_166850 (Fig. 2-6 D-lane 3) and exhibits limited cleavage of the mutant TM domain (Fig. 2-6 D-lane 8).

Discussion:

We have characterized rhomboid proteases in the human-infective parasite *T. vaginalis*. Genome analyses identified 4 putative active rhomboid proteases, 2 of which, TvROM1 and TvROM3, were shown to be catalytically active using a heterologous cell cleavage assay. Activity of TvROM2 cannot be excluded, as it is possible that the TM domain features it recognizes are not present in the known rhomboid protease substrates tested. TvROM3 was found to cleave the canonical rhomboid substrate Spitz. TvROM1 displayed “atypical substrate specificity” being unable to cleave Spitz but capable of cleaving several *Plasmodium* adhesins

previously shown to be cleaved by eukaryotic parasite rhomboid proteases PfROM4 and EhROM1 [31, 32], which likewise do not cleave Spitz. In addition to having different substrate specificities, TvROM1 and TvROM3 are localized in different subcellular compartments in *T. vaginalis*; TvROM1 is present in cell surface and vesicle membranes whereas TvROM3 localizes to Golgi-like structures.

As a step towards defining the function of TvROMs, we identified putative *T. vaginalis* surface substrates using both quantitative proteomic and bioinformatic approaches. Five putative substrates were found using stable isotope, dimethyl labeling quantitative proteomics comparing the release of type I membrane proteins with 1 TM domain, the typical topology of a rhomboid protease substrate, in the presence and absence of the serine protease inhibitor 3,4-DCI. One of these (TVAG_166850) was also identified using a bioinformatics approach used to search the *T. vaginalis* surface proteome [23] and 4 other putative substrates, not identified using proteomics, were also found. Two of the 9 different proteins identified were shown to be TvROM1 substrates: TVAG_166850 and TVAG_280090. These proteins have a high degree of similarity and are members of a gene family consisting of over 150 members [20]. Interestingly, two other predicted substrates (TVAG_244130 and TVAG_335250) are paralogs of TVAG_166850 and TVAG_280090; however their TM domains are not cleaved by TvROM1. Whether these putative substrates are cleaved by other proteases, not examined in this study, remains to be determined. TvROM3 was not able to cleave any of the 9 putative *T. vaginalis* substrates identified. Thus TvROM1 and TvROM3, which have different subcellular localizations, also appear to have different substrate specificities.

Amino acids surrounding the predicted cleavage sites in substrates from other organisms cleaved by TvROM1 and the *T. vaginalis* substrates are similar. The predicted P1 and P1' site

residues are small amino acids, as previously noted for eukaryotic rhomboid protease substrates [41, 49, 51]. Additionally these substrates typically have small amino acids at the predicted P2' site. Notably, restriction of the P2' site in our parasite search motif to small amino acids was critical for identification of the two *T. vaginalis* substrates cleaved by TvROM1. Nevertheless, finding that only 2 of the 5 putative substrates identified using our parasite search motif are cleaved by the two active *T. vaginalis* rhomboid proteases tested underscore the difficulty in identifying substrates with search motifs alone.

Recently, crystal structures of *E. coli* GlpG with different inhibitors revealed a pocket in this protease that is predicted to be the S2' pocket that would bind the P2' residue of substrates [70]. This pocket in GlpG preferentially binds large hydrophobic groups [70]. TvROM1 and other parasite rhomboid proteases substrates may have smaller S2' pockets that accommodate small amino acids. Testing this prediction awaits crystal structure determination of parasite rhomboid proteases, to allow specific structural features of eukaryotic and bacterial proteases to be discerned.

TvROM1 putative biological function in *T. vaginalis*

Although the *T. vaginalis* genome contains an unusually large degradome of predicted proteases [21], only four proteins are anticipated to be active rhomboid proteases. This indicates a tight control of rhomboid protease function, with conserved roles in the majority of *T. vaginalis* strains. Moreover, finding that several predicted substrates are members of large protein families suggests these proteases may exhibit flexibility in the specific substrates they cleave in different strains. This is consistent with our observation that *T. vaginalis* surface proteomes contain a subset of proteins encoded by large multi-gene families, with different subsets expressed by different strains [23].

We found that overexpression of TvROM1 in *T. vaginalis* strain RU393 significantly increases attachment to and lysis of host cells, two properties critical for the pathogenesis of *T. vaginalis*. A role for TvROM1 in parasite adherence to host cells is consistent with its localization on the plasma membrane and our previous observation that overexpression of one of its substrates, TVAG_166850, increases parasite adherence [23]. The rhomboid protease of another luminal parasite, *Entamoeba histolytica*, also promotes attachment to host cells [37]. Overexpression of TvROM2 or TvROM3 did not promote parasite adherence or cytolysis, thus these proteases predicted to recognize substrates in the Golgi, are likely involved in other cellular processes.

In addition to an increase in attachment of parasites to host cells upon overexpression of TvROM1, exogenous expression of TvROM1 also increases parasite cytolysis. These data may be explained several ways. Signaling induced by cleavage of a substrate (TVAG_166850, TVAG_280090, or another yet to be identified) during the initial phase of parasite: host interactions may lead to an increase in adherent surface proteins. For example, DmRho1 cleaves epidermal growth factor receptor (EGFR) ligands that upon release bind EGFR receptors on receiving cells, activating MAPK/Ras signaling [26-28]. Increased MAPK/Ras signaling has in turn been found to increase DE-cadherin levels, and this upregulation required normal rhomboid levels [71].

In metazoans, cadherins play important roles in both promoting and regulating attachment to other cells and modulating cell motility [72], and their activity can be modulated by protease cleavage (reviewed in [73, 74]).

Similarly, structural analyses of TVAG_166850 and TVAG_280090 indicate these substrates may also be precursors of cadherin proteins that mediate cell-cell interactions.

Analysis using the Phyre2 program reveals that both TVAG_166850 and TVAG_280090 have cadherin-like predicted secondary structures and InterPro analysis identifies a cadherin-like domain in TVAG_166850. Exogenous expression of GFP-TVAG_166850 with the two small amino acids in the predicted P1-P1' rhomboid cleavage site mutated to bulky Phe residues that reduce TvROM1 cleavage led to an even greater increase in parasite attachment compared to exogenous expression of the wild type protein, consistent with a direct role for this substrate in adherence and possible regulation of its function by TvROM1 cleavage. The mutant substrate was also found to be increased on the surface using flow cytometry staining. These data imply that replacement of endogenous, cleavable TVAG_166850 by the non-cleavable mutant substrate directly leads to greater parasite attachment.

Our previous data, comparing the adherence and cytolysis of 26 strains of *T. vaginalis*, suggest that once a threshold of parasite attachment is reached, host cell cytolysis is triggered [17]. It is possible that TvROM1 plays a role at the junction of these processes as inhibition of serine protease activity by the 3,4-DCI inhibitor resulted in a dose-dependent inhibition on cytolysis and exogenous expression of TvROM1 led to a 4.2-fold increase in cytolysis. Interestingly, *E. histolytica* EhROM1 has also recently been reported to contribute to cytolysis of host cells [75].

Lastly, the proteins identified in supernatants of *T. vaginalis* are, to our knowledge, the most comprehensive set of secreted/released proteins reported so far. We identified cysteine proteases, considered to be established and secreted virulence factors of *T. vaginalis* (reviewed in [76]). This list also provides experimental evidence for the release of proteins previously predicted to be *T. vaginalis* secreted proteins, such as cysteine protease inhibitors called cystatins [20, 77] and pore-forming/saposin-like proteins hypothesized to help lyse host cells [20, 21, 78].

Other soluble factors uncovered in our proteomic studies may be candidates for contributing to *T. vaginalis* virulence.

In summary, we have identified two active *T. vaginalis* rhomboid proteases and provide evidence that one of these, TvROM1, plays a role in regulating attachment dynamics to host cells leading to cytolysis of host cells. These data are significant as few proteins have been shown to contribute to both *T. vaginalis* attachment and cytolysis of host cells (reviewed in [16]). The results of this study also expand the finding that rhomboid proteases contribute to pathogenesis-associated processes in parasites that pose important public health problems (reviewed in [79] and [80]). As both human and TvROM1 substrate specificities are better defined, it may be possible to selectively target *T. vaginalis* rhomboid proteases as a therapeutic agent.

Materials and Methods:

Growth of *T. vaginalis.*

The *T. vaginalis* strains G3 (ATCC PRA98) and RU393 (ATCC 50142) were grown in TYM medium supplemented with 10% horse serum, penicillin and streptomycin (Invitrogen), and iron as described previously [81]. Parasites were incubated at 37°C and passaged daily for less than two weeks.

Growth of ectocervical cells.

The human ectocervical cell line Ect1 E6/E7 (ATCC CRL-2614) was grown as described [82] in Keratinocyte-serum free media (K-SFM, GIBCO) completed with recombinant protein supplements provided by the company (human recombinant epidermal growth factor and bovine pituitary extract), and 0.4 mM filter-sterilized calcium chloride. Cells were grown at 37°C in a

5% CO_2 incubator. This cell line is also referred to as VECs (vaginal epithelial cells) in the *T. vaginalis* literature.

TvROMs plasmid construction and exogenous expression in *T. vaginalis.*

TvROMs were PCR amplified from G3 genomic DNA, using the following primer pairs in which SacII and BamHI restriction sites were encoded in the Fwd and Rev primers, respectively: TvROM1 (Fwd 5'-CCGCGGATGTCGAATATTACAACCTTCAATG-3', Rev 5'-GGATCCTTATTTCCTTGTAAAGATAATTGGAAG-3'), TvROM2 (Fwd 5'-CCGCGGATGAGCGACGAAGTTGATAATG-3', Rev 5'-GGATCCTTATCTAAATAACTTCTTGAAAAATTC-3'), TvROM3 (Fwd 5'-CCGCGGATGCTTGCGTGGCTAGATG-3', Rev 5'-GGATCCTTATTCAATAGTATGTGCAGTACCATG-3'). PCR fragments were cloned into the Nt-HA-MasterNeo plasmid [23] which contains an N-terminal hemagglutinin (HA) tag and drives expression from the strong alpha-succinyl CoA synthetase B (alpha-SCS) promoter [83]. To increase the detection of tagged TvROMs, 2 additional HA tags were inserted to generate 3X-HA-TvROMs by cutting the 1X-HA-TvROM plasmids with Nde1 and ligation with hybridized oligos encoding two HA-tags and the Nde1 restrictions sites (2HA-NdeFwd 5'-TATGTACCCATACGATGTTCCAGATTACGCTTACCCATACGATGTTCCAGATTACGCTCA-3', 2HA-NdeR 5'-TATGAGCGTAATCTGGAACATCGTATGGGTAAGCGTAATCTGGAACATCGTATGGGTACA-3'). The 3X-HA-TvROM-MasterNeo plasmid was then digested with ClaI to remove the fragment encoding the neomycin phosphotransferase (Neo) selectable marker and its flanking 5' and 3' beta-tubulin untranslated regions (UTRs) and ligated to close the vector. A fragment encoding the puromycin *N*-acetyltransferase (PAC) gene flanked with alpha-SCS 5' and 3' UTRs

previously described in [84] was cloned into the Master (-Neo) plasmid using the ApaI restriction site.

Electroporation of the G3 and RU393 strains was performed as previously described [83] using 50-100 μg of circular plasmid DNA. Four hours after transfection, transfectants were selected with 100 μg/ml G418 (GIBCO) or 60 μg/ml puromycin dihydrochloride (A.G. Scientific, Inc.) and maintained with drug selection.

TvROMs Indirect Immunofluorescence Assays.

The cellular localization of HA-TvROM1 in G3 transfectants was determined by binding parasites to glass coverslips and fixing with cold methanol for 10 min. Coverslips were washed three times with 1X PBS and then blocked by incubation with 3% bovine serum albumin (BSA)/2% horse serum/1X PBS for 30 min at room temperature. Afterwards, coverslips were incubated for 1 hour in a 1:1,000 dilution of mouse anti-HA antibody (Covance) diluted in the blocking solution. After three PBS washes, coverslips were incubated for 1 hour in a 1:5,000 goat anti-mouse Alexa Fluor®488-conjugated secondary antibody dilution (Molecular Probes) prepared in blocking solution. Three PBS washes were performed and coverslips were mounted onto glass microscope slides using ProLong Gold antifade reagent with 4'-6'-diamidino-2-phenylindole (DAPI) (Invitrogen). Cellular localization of 3X-HA-TvROM2 and 3X-HA-TvROM3 in G3 transfectants was tested as described above except that blocking was performed in 3% BSA/1X PBS and antibody solutions were made in 3% BSA/1X PBS.

To compare TvROM1's cellular localization relative to the cell surface, 3X-HA-TvROM1 RU393 transfectants were biotinylated as described [23] using the membrane impermeable EZ-Link-Sulfo-NHS-SS-biotin (Pierce), but with a smaller amount of parasites ($3.18X10^7$ cells in 30 ml). 3X-HA-TvROM1+Biotin or –Biotin treated cells were allowed to bind

to coverslips coated with 100 μg/ml poly-L-Lysine (SIGMA)+3% BSA and IFA was performed as described above except for the following changes. Parasites were fixed in 4% formaldehyde/1X PBS for 20 min and then permeabilized for 15 min in PBS+0.2% TritonX-100. 3% BSA/1X PBS was used for blocking and antibody dilutions. Parasites were co-stained with 1:1,000 dilutions of mouse anti-Biotin antibody (Jackson ImmunoResearch Laboratories, Inc.) and rabbit anti-HA antibody (SIGMA). 1:5,000 dilutions of goat anti-mouse-Alexa Fluor®-488 and goat anti-rabbit-Alexa Fluor®-594 secondary antibodies (Molecular Probes) were used. Coverslips were mounted using Mowiol (Calbiochem). Images were taken using an Axioskope 2 Epifluorescent microscope (Zeiss) equipped with an Axiocam camera, or an Axio Imager Z1 microscope equipped with an AxioCamMR3 camera. Image processing was performed using the AxioVision 3.2 program (Zeiss).

TvROMs Cytolysis and Attachment Assays.

T. vaginalis adherence and cytolysis assays were preformed as described [17] except RU393 or 3X-HA-TvROM1 RU393 transfectants were used. The RU393 strain was chosen because it displays medium levels of adherence and cytolysis [17] in the 3 hr incubation time necessary to test the effect of the 3,4-Dichloroisocoumarin (3,4-DCI, SIGMA) inhibitor on parasite cytolysis. To test the effect of 3,4-DCI on parasite adherence, 3,4-DCI or DMSO vehicle control was added to parasites resuspended in completed K-SFM media at the indicated concentrations and this mixture was added to ectocervical cell monolayers. Adherence to monolayers was allowed to proceed for 30 minutes. Cytolysis assays were incubated for 3 or 4 hrs for wt RU393 and RU393 3X-HA-TvROM1 transfectants, respectively. A shorter incubation was necessary for the wt RU393 strain to prevent full lysis of the monolayer by the vehicle control.

Stable isotope dimethyl labeling of cell supernatants and quantitative proteomics.

2.25X10^8 log-phase 3XHA-TvROM1 RU393 *T. vaginalis* transfectants were aliquoted, centrifuged at 3,200 rpm for 10 min, and washed once in PBS+5% sucrose. Parasites were resuspended in 225 ml PBS+5% sucrose to a final cell concentration of 1X10^6 cells/ml. 5 X10^6 cells were aliquoted into four 50 ml conical tubes. 3,4-DCI was added for a final concentration of 50 μM to 2 tubes and DMSO vehicle control was added to the other two. Parasites were incubated for 1 hr at 37°C, then pelleted at 3,200 rpm for 10 min and 40 ml of the supernatant was transferred to a new tube. Supernatants were filtered through a 0.22 μm Steriflip™ 50 ml filter (Millipore) and frozen at -80°C. Upon thawing, supernatants from the same treatment group were pooled and concentrated to ~300 μl using an Amicon® Ultra Centrifugal filter unit (3 kDa molecular weight cutoff) at 4°C and then lyophilized. The experiment was performed twice.

25 μg of each sample was reduced using DTT, alkylated using iodoacetamide and digested with Lys-C endopeptidase (Wako, Richmond, VA) for 4 hours and trypsin for 14 hours (Thermo Scientific) as previously described in [85]. Digested peptides were desalted by HPLC using a Michrom Bioresources Microtrap column (2-20 μg binding capacity). Stable isotope dimethyl labeling of peptides was performed as described [66], with the addition of an HPLC desalting step after peptide labeling followed by lyophilization of peptides. Peptides from the vehicle control were labeled with the "light label" and 3,4-DCI samples were labeled with the "intermediate label." Labeled peptides were reconstituted in 0.2% formic acid, and equal protein amounts were mixed. For mass spec analysis, 8 μl of a mixture containing 1 μg of each sample was separated on an analytical (75 μm ID) HPLC column packed in-house with ReproSil-Pur C_{18}AQ 3 μm resin (120 Å pore size, Ammerbuch, Germany) coupled to an LTQ-Orbitrap Classic mass spectrometer (Thermo Scientific, Bremen, Germany) essentially as previously described

[86] with the following modifications. The gradient of the nanoflow LC system, EASY nLC II, was as follows: 2–30% B (80 min), 30-100% B (1 min) and 100% B (8 min).

MS data analysis.

MaxQuant (v. 1.4.1.2) was used to search Thermo RAW files [87]. Spectra were searched against *T. vaginalis* (50623 entries) as well as a contaminant database (245 entries). MaxQuant generated decoy sequences (reversed peptide sequences) to estimate the false discovery rate. Search parameters included variable oxidation of methionine, variable protein N-terminal acetylation, fixed carboxyamidomethylation of cysteine and dimethyl labeling of peptide N-terminus and lysine. Trypsin was specified as the digestion enzyme with up to 2 missed cleavages. A 1% false discovery rate threshold was applied for protein and peptide identifications. Precursor mass tolerance was 7 ppm (or less for individual peptides). Fragment mass tolerance was 0.5 Da. Confidence intervals and p-values were calculated using a hierarchical model with bootstrap resampling and pooled variance estimates as described [88]. P-values were adjusted using the Benjamini and Hochberg method to correct for multiple hypothesis testing [89].

HEK293 Heterologous Cell Cleavage Assays and PfEBA-175 cleavage site determination.

Heterologous cell cleavage assays were performed in HEK293T cells as previously described in [32]. TvROMs did not express in HEK293T cells and were thus recoded for human expression (GeneArt). For cleavage site determination, HEK293T cells were transfected, lysed in RIPA buffer, subjected to anti-FLAG immunopurification (Sigma) and analyzed by MALDI-TOF mass spectrometry as previously described [90].

Site-directed mutagenesis, expression, and phenotypic analysis of GFP-TVAG_166850^{WT} and rhomboid cleavage-site mutant GFP-TVAG_166850$^{AG/FF}$.

The plasmid encoding for TVAG_166850 with an N-terminal enhanced green fluorescent protein (eGFP) tag was constructed as follows. EGFP was PCR amplified with flanking Nde1 and SacII restriction sites and cloned into the location of the HA-tag in the Nt-HA-MasterNeo construct using the Nde1 and SacII restriction sites, to generate Nt-eGFP-MasterNeo. The TVAG_166850 gene was PCR amplified with primers encoding SacII and BamH1 restriction sites in the forward and reverse primers, respectively (Fwd 5'-CCGCGGATGTTACCACTATTTTACACA-3', Rev 5'-GGATCCTTAAGCTGGGAAGATTCCTTCGAC-3') and cloned into the Nt-eGFP-MasterNeo construct using the SacII and BamH1 restriction sites. The TVAG_166850 AG/FF putative rhomboid cleavage site mutant was generated by site-directed mutagenesis of the GFP-TVAG_166850 construct using the QuikChange kit (Stratagene) and primers that encoded the Ala672Phe and Gly673Phe mutations (Fwd 5'-ATTATCGGCTTAGCTTTCTTCGGTGGTGTTGCCGCC-3', Rev 5'-GGCGGCAACACCACCGAAGAAAGCTAAGCCGATAAT-3'). Plasmids were transfected into the poorly adherent G3 strain for gain of function analysis, and selected with G418. Attachment to and cytolysis of host cells was assayed as described above except the cytolysis assayed were incubated for 18 hrs.

Flow cytometry analysis of surface GFP-TVAG_166850^{WT} and GFP-TVAG_166850$^{AG/FF}$ mutant proteins.

1X10^6 log-phase G3 transfectants were centrifuged at 3,5000 rpm for 10 min, washed twice with FACS buffer (5% fetal bovine serum/0.1% sodium azide/1X PBS), and 2X10^5 cells were aliquoted in triplicate. Parasites were stained with 1 μg/ml mouse-anti-GFP (Clontech) diluted in FACS buffer or in FACS buffer only. Empty vector transfectants not expressing GFP

were used as secondary (2°Ab) only control. Staining was detected with 1 μg/ml goat anti-mouse-Alexa Fluor®488 2°Ab antibody. All antibody incubations were performed on ice for 30 min, followed by parasite centrifugation at 4°C, and washing of parasites with 1 ml of FACS buffer. Samples were analyzed on a Becton Dickinson Fortessa flow cytometer in the FITC channel. Empty vector 2°Ab samples were used to set the GFP^+ population gates. The mean fluorescence values were calculated for each sample, done in triplicate, using the FlowJo 8.4 software. The experiment was performed three times and representative data from one experiment is shown.

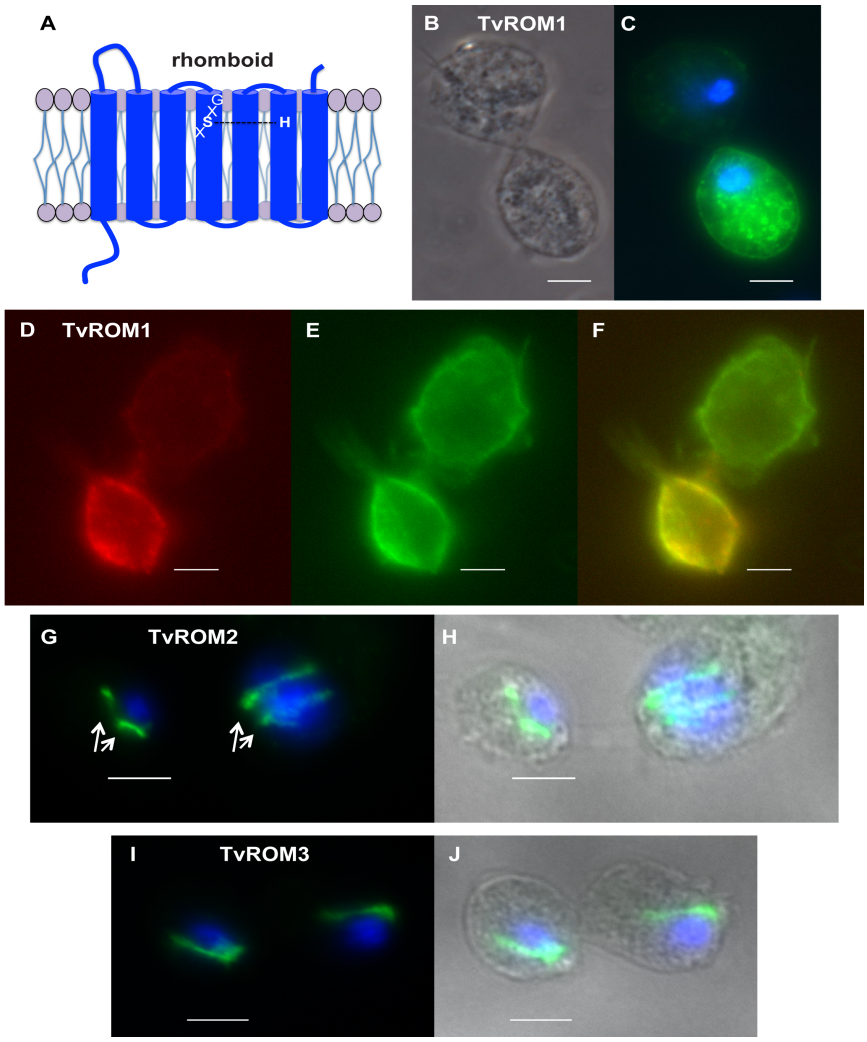

Fig. 2-1. Subcellular localization of HA-tagged TvROMs in *T. vaginalis* transfectants. **(A)** Predicted topology of TvROM1 and 2. TvROM3 has similar topology but contains only the first 6 transmembrane domains (TM) therefore the C-terminus is predicted to be intracellular. Active rhomboids contain two catalytic residues, serine (S) and Histidine (H), located near the top parts of TMs 4 and 6. A GxSx motif surrounds the catalytic serine. (**B-C** and **G-J**) Fluorescence microscopy images of indirect immunofluorescence assays (IFA) performed on *T. vaginalis* exogenously expressing N-terminal hemagglutinin (HA)-tagged rhomboids 1, 2, or 3 using a mouse anti-HA antibody (green) and nuclear staining using 4'-6'-diamidino-2-phenylindole (DAPI-blue). Phase images are shown on the right. (**B** and **C**) IFA images using methanol fixation show HA-TvROM1 is located at the cell surface and vesicle-like structures, scale bar=5.35 µm. (**D-F**) 3XHA-TvROM1 transfectants were reacted with membrane impermeable biotin (EZ-Link-Sulfo-NHS-SS-Biotin) and IFA was then performed using formaldehyde fixation and staining with an anti-HA (**D**-red) and anti-Biotin (**E**-green) antibodies. (**F**) merge shows co-localization of TvROM1 with the biotin-labeled *T. vaginalis* cell surface, scale bar=10 µm. IFA images of 3XHA-TvROM2 (**G-H**) and 3XHA-TvROM3 (**I-J**) show localization in a line structure adjacent to the nucleus, scale bar=5 µm. Two juxtanuclear structures of different sizes can be observed in early and late dividing cells in TvROM2 transfectants (**G**, see arrows).

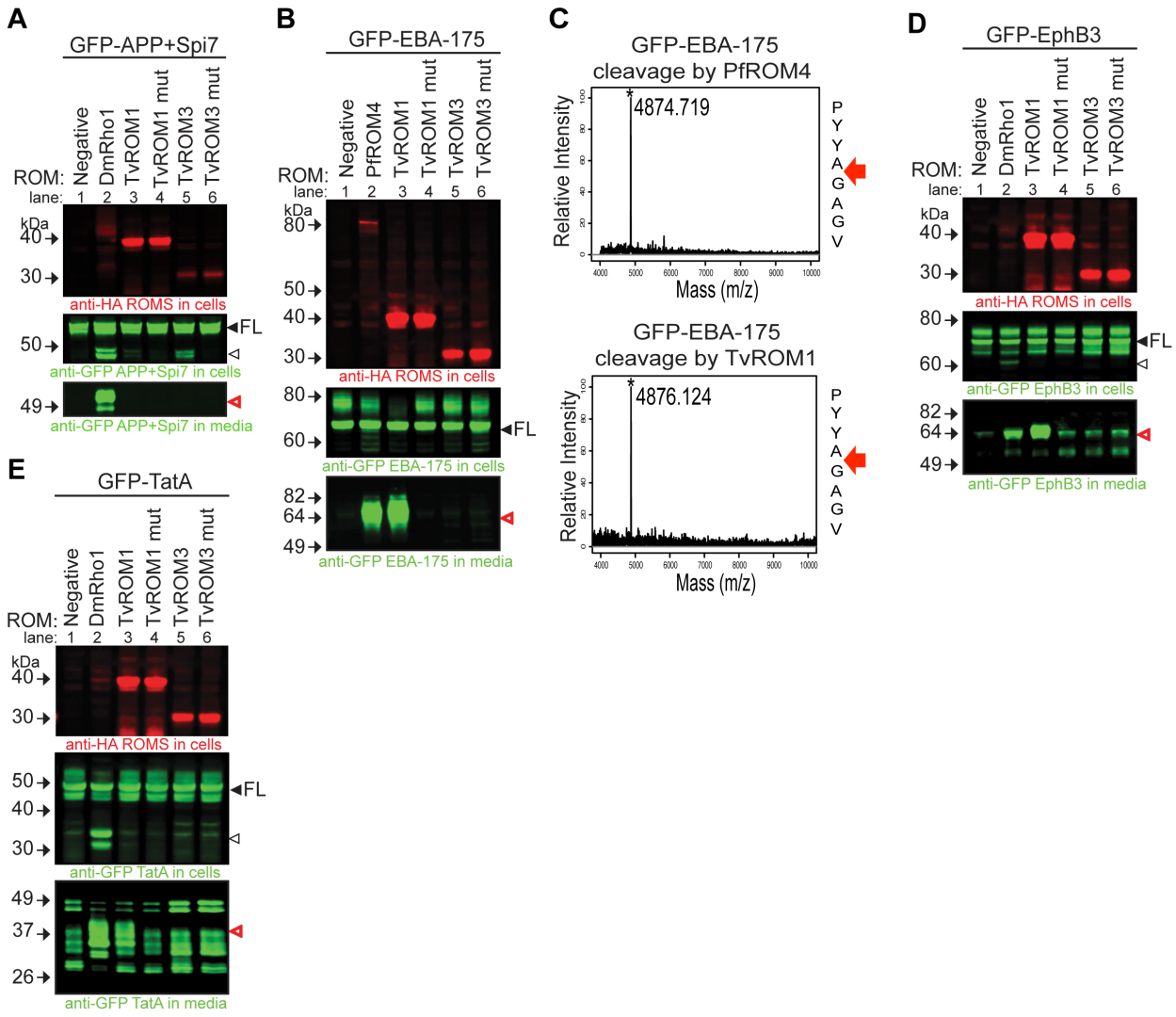

Fig. 2-2: TvROM Catalytic Activity Analyses

The activities of *T. vaginalis* rhomboid proteases were tested by co-transfecting the proteases with known rhomboid substrates in a heterologous cell cleavage assay using HEK293 cells. Proteases were HA tagged and substrates contained an N-terminal GFP tag to allow detection. (**A**, **B**, **D** & **E**) Whole cell lysates (WCL) and conditioned media (CM) were collected from co-transfectants and analyzed by Western blot analyses. Top panels: rhomboid protease detected in WCL using an anti-HA antibody; middle panels: full-length (filled arrowhead) and cleaved substrates (small arrowheads) detected in WCL using an anti-GFP antibody; bottom panels: cleaved substrate fragments detected in CM using an anti-GFP antibody (see red, open arrowheads). The substrates tested were **(A)** APP+7 residues of the *Drosophila* Spitz protein encompassing the rhomboid protease cleavage site (APP+Spi7), **(B)** *Plasmodium* EBA-175, **(D)** human EphB3 and **(E)** bacterial TatA. The positive control HA-tagged rhomboid protease (see lane 2) used for cleavage of APP+Spitz7 (A), human EphB3 (D) and bacterial TatA (E) was

DmRho1; the positive control protease for cleavage of EBA-175 (B) was HA-tagged PfROM4 (lane 2). Negative controls (Negative-lane 1) were only transfected with the substrate tested. TvROM1/TvROM3=wild type protease; TvROM1 mut/TvROM3 mut=protease with the catalytic histidine mutated to alanine. TvROM3 was found to cleave only Spitz (cleavage fragment detected in middle and bottom panels A-lane 5) whereas TvROM1 does not cleave Spitz (lower panel A-lane 3) but does cleave the other 3 substrates (bottom panels (B), (D) & (E), lane 3). **(C)** The location of EBA-175 cleavage by PfROM4 (control, top panel) and TvROM1 (bottom panel) determined by subjecting the immunoprecipitated cleavage fragment to MALDI-TOF analysis. Red arrows indicate cleavage of the substrate between Alanine (A) and Glycine (G) by both proteases.

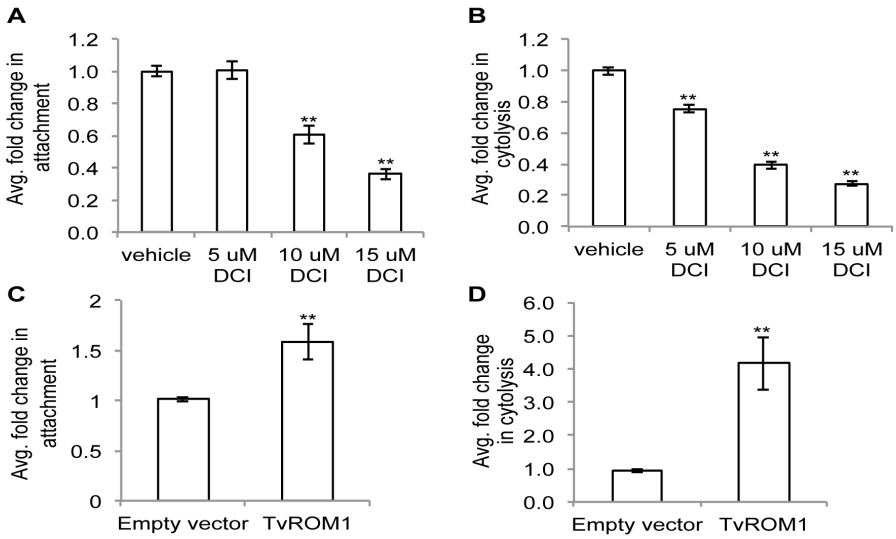

Fig. 2-3: Serine protease activity and TvROM1 contribute to *T. vaginalis* attachment and lysis of ectocervical cells.

(A) Treatment of fluorescently labeled *T. vaginalis* incubated with ectocervical cell monolayers in the presence of increasing concentrations of the serine protease inhibitor 3,4-dichloroisocoumarin (3,4-DCI) followed by quantification of adhered parasites. The average fold change in attachment compared to vehicle control for four experiments each performed in triplicate is shown. Error bars denote the standard error, **$p<0.01$. **(B)** Treatment of parasites incubated with ectocervical cell monolayers in the presence of increasing 3,4-DCI followed by assessment of ectocervical cell lysis. The average fold change in cytolysis compared to vehicle treatment for three experiments performed in triplicate is shown. Error bars denote the standard error, **$p<0.01$. **(C)** Average fold difference in attachment of 3XHA-TvROM1 transfectants compared to empty vector transfectants in four experiments each conducted in triplicate, with standard error shown as error bars, **$p<0.01$. **(D)** Average fold change in cytolysis of ectocervical cells by 3XHA-TvROM1 transfectants compared to empty vector transfectants, results are from four experiments performed in triplicate. Standard error is shown as error bars, **$p<0.01$.

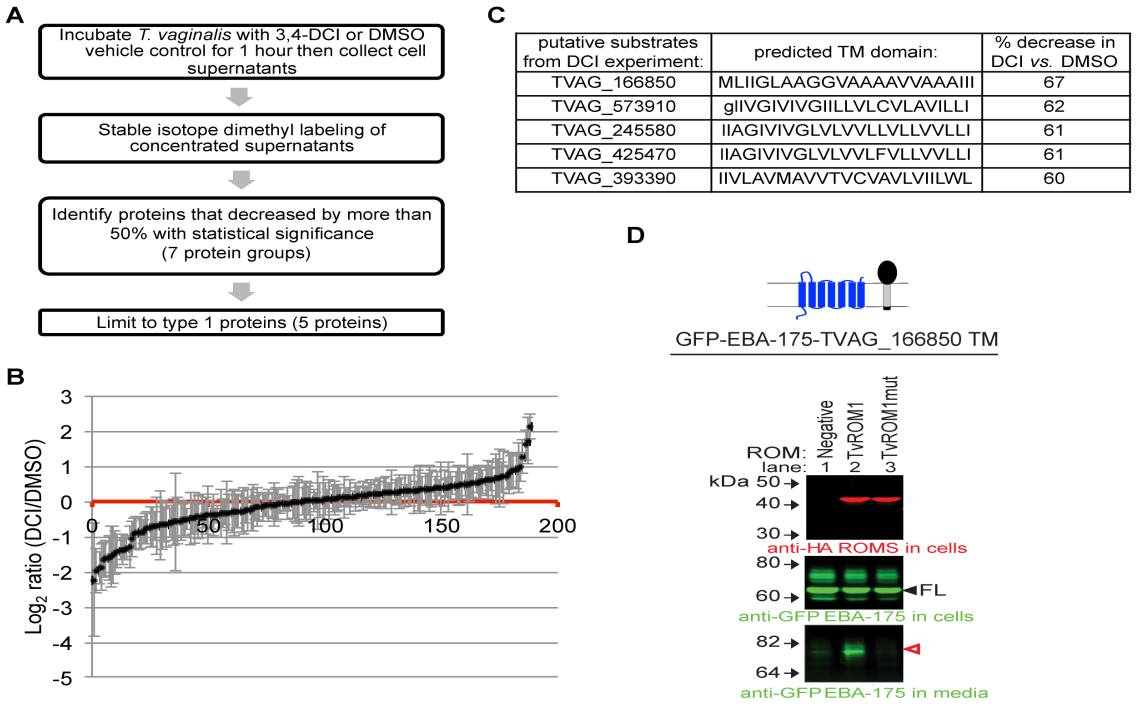

Fig. 2-4: Use of quantitative proteomics identifies a putative TvROM1 substrate. **(A)** Flow chart of the approach taken to identify putative substrates for TvROM1 using quantitative proteomics of cell supernatants from 3X-HA-TvROM1 *T. vaginalis* transfectants treated with vehicle or 50 µM 3,4-DCI serine protease inhibitor. **(B)** The profile of proteins identified in two independent mass spectrometry experiments and the magnitude of change on a $\log_2$ scale, errors bars denote the standard error. Proteins that decreased with 3,4-DCI treatment have $\log_2$(DCI/DMSO) ratios<0, and those that increased are >0. **(C)** The predicted transmembrane domains of the 5 putative substrates identified in **A**, and the percent decrease in protein levels with 3,4-DCI *vs.* DMSO vehicle treatment are shown. Capital letters indicate amino acids predicted to be part of the TM domain, lowercase letters denote amino acids found outside the predicted TM domain. **(D)** The TM domain of TVAG_166850 can be cleaved by TvROM1 in the HEK293 heterologous cell cleavage assay. A plasmid encoding a chimeric protein composed of GFP-*P. falciparum* EBA-175 with the TM domain replaced with that of TVAG_166850 (see cartoon) was co-transfected with a plasmid encoding HA-TvROM1 or a TvROM1 catalytic His to Ala mutant (mut). No TvROM1 was co-transfected as a negative control (negative). Western blot analysis of whole cell lysates and conditioned media from co-transfectants was performed with an anti-GFP antibody to test for the presence of a smaller GFP-EBA-175 fragment released into the media by TvROM1 cleavage. An anti-HA antibody was used to confirm expression of TvROM1 wt and mut proteins (top panel). Full-length chimeric substrate is annotated with a closed arrowhead (middle panel). TvROM1 can cleave the TM domain of TVAG_166850 as indicated by the presence of a GFP-tagged cleavage product in the media (red, open arrowhead, bottom panel) of TvROM1 co-transfectants (TvROM1) not present in TvROM1 catalytic His to Ala mutant (TvROM1 mut) co-transfectants. TvROM1 did not cleave the four remaining putative substrates and none of the proteins were cleaved by TvROM3 (data not shown).

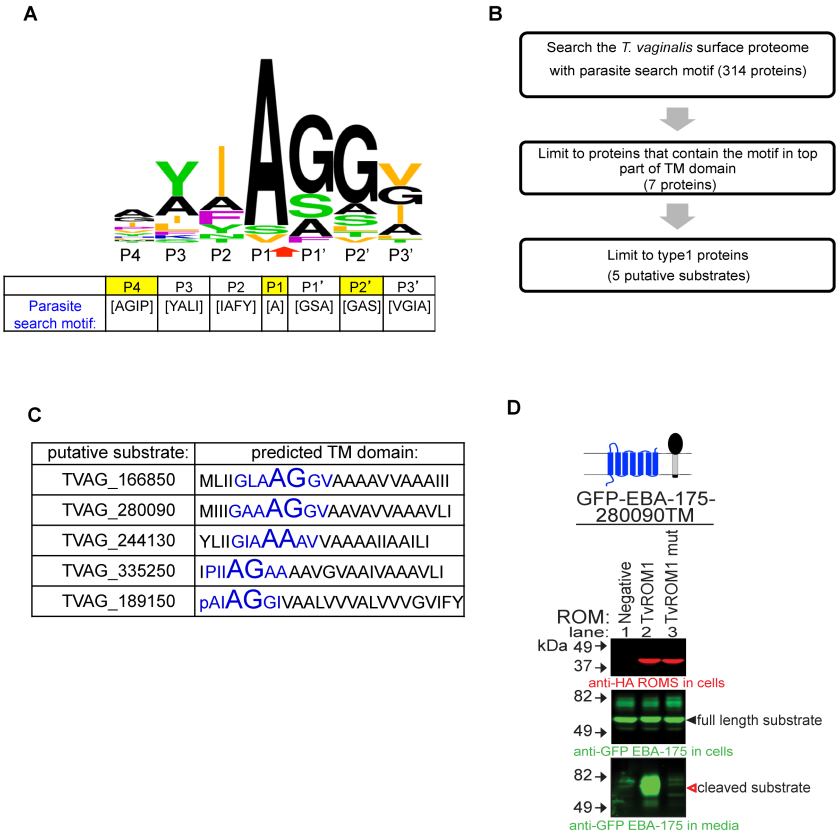

Fig. 2-5: Screening of the *T. vaginalis* surface proteome with a parasite search motif identifies an additional TvROM1 substrate.
(A) Graphical representation of the amino acids found in the predicted and established P4-P3' positions of 20 parasite proteins cleaved by rhomboid proteases and the canonical *Drosophila* rhomboid substrate Spitz. The height of an amino acid indicates its relative frequency. Residue colors indicate the properties of their side chains: small=black (A and G), basic=blue (K), aliphatic=orange (L, I, and V), green=uncharged, polar (Y, T, S, and N), nonpolar, nonaliphatic=purple (F and P). The most common amino acids in these proteins were used to generate a parasite search motif (shown in bottom panel). **(B)** Flow chart of the approach taken to identify putative TvROM1 substrates by searching the *T. vaginalis* surface proteome published by de Miguel *et al.* 2010 with the parasite search motif. Five type 1 proteins were identified as putative substrates. **(C)** The accession numbers and predicted TM domain of the 5 putative surface proteome substrates are shown. The parasite search motif is indicated by blue font and the P1-P1' residues predicative of the rhomboid cleavage site is shown in larger font. Capital letters indicate amino acids predicted to be part of the TM domain, lowercase letters denote amino acids found outside the predicted TM domain. **(D)** The TM domain of putative substrate TVAG_280090 is cleaved by TvROM1. A GFP-EBA-175 chimeric protein that has its TM domain replaced with that of TVAG_280090 (see cartoon) was co-expressed with TvROM1 or TvROM1 catalytic His to Ala mutant (mut) in the HEK293 heterologous cell cleavage assay. Negative control (Negative-lane 1) was transfected only with the chimeric substrate. Western blot analyses of whole cell lysates confirm expression of the TvROM1 wt and mut proteins (top panel) and the full-length substrate (closed arrowhead, middle panel). Analyses of conditioned

media from the co-transfectants show a GFP-tagged cleavage product in the media (red, open arrowhead, bottom panel) of TvROM1 co-transfectants (TvROM1) and not in the TvROM1 catalytic His to Ala mutant (TvROM1 mut). The remaining putative substrates were not cleaved by TvROM1 or TvROM3 (data not shown).

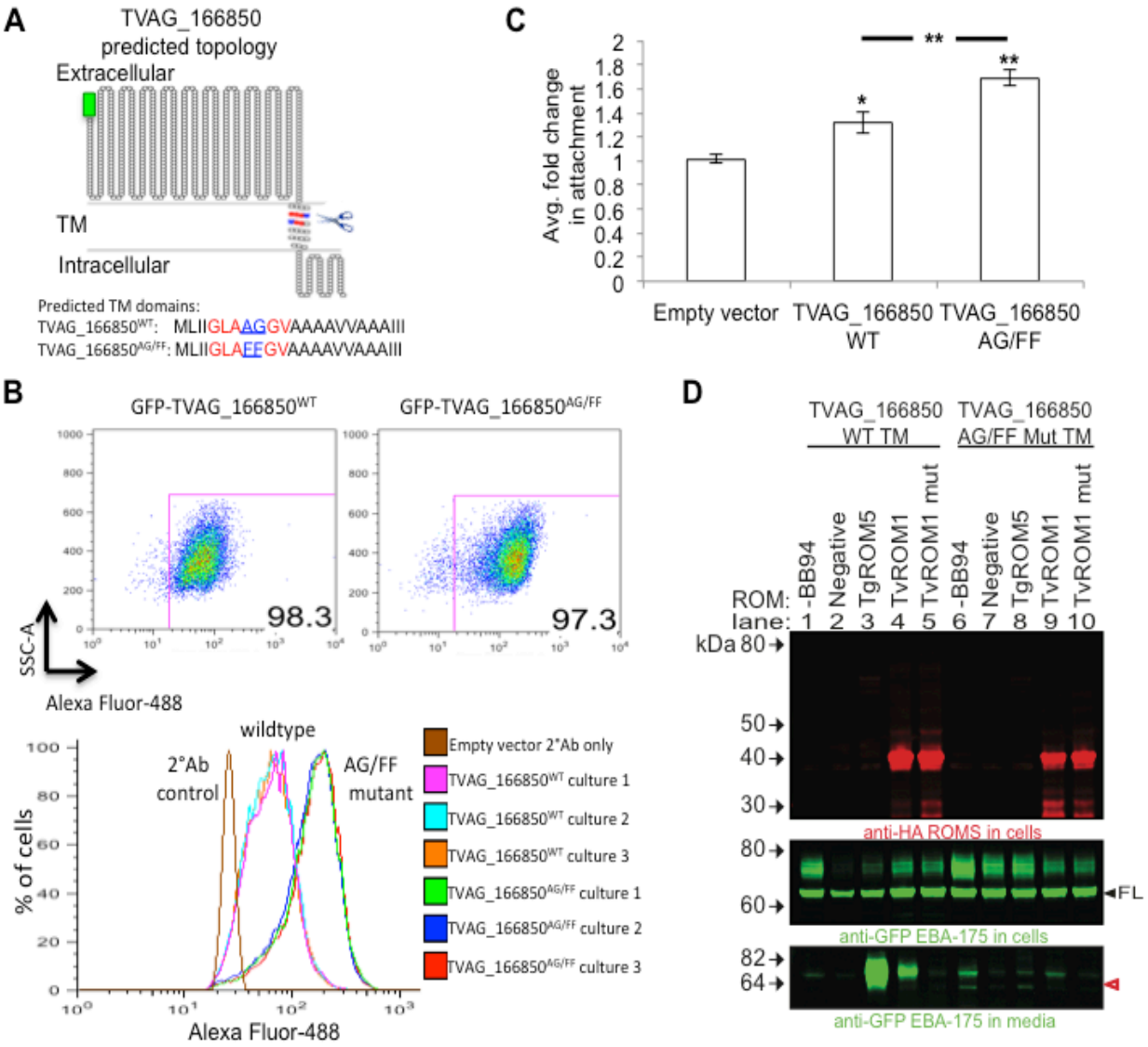

Fig. 2-6: Phenotypic analysis of predicted rhomboid cleavage site mutation in the putative substrate TVAG_166850.

(A) Predicted topology of the putative substrate TVAG_166850 using the Spoctopus TM prediction program and the TOPO2 graphical representation program. TVAG_166850^{WT} was tagged at the N-terminus with a GFP tag (green box). The majority of the protein is predicted to be extracellular. The predicted rhomboid cleavage site (scissors) and the predicted P1-P1' cleavage site residues are highlighted in blue. The surrounding parasite search motif residues are highlighted in red. The TM residues are shown below. A rhomboid cleavage site mutant was generated by mutating the predicted P1-P1' residues (underlined in sequence) consisting of the small amino acids Ala-Gly to bulky Phe-Phe residues to generate the GFP-TVAG_166850$^{AG/FF}$ mutant. **(B)** The GFP-TVAG_166850^{WT} and GFP-TVAG_166850$^{AG/FF}$ mutant proteins were exogenously expressed in *T. vaginalis*. Transfectants were stained without permeabilization at 4°C to detect surface levels of the fusion protein. An anti-GFP antibody used for staining was detected using an Alexa Fluor488-conjugated secondary antibody. Quantification of staining was

performed using flow cytometry. Empty vector transfectants treated only with the secondary antibody (2°Ab only) were used as a negative control to set the gates. Three independent cultures were analyzed for each experiment, and three independent experiments were performed. Representative results from one experiment are shown. Top panel shows a representative of the GFP^+ population, similar percentages of GFP^+ cells were detected for the GFP-$TVAG\_166850^{WT}$ and GFP-$TVAG\_166850^{AG/FF}$ mutant transfectants. The bottom histogram shows the fluorescence intensity distribution of the GFP^+ population. GFP-$TVAG\_166850^{AG/FF}$ mutant transfectants had at least three-fold higher mean fluorescence intensity (MFI) levels compared to wildtype transfectants. **(C)** GFP-$TVAG\_166850^{WT}$ and GFP-$TVAG\_166850^{AG/FF}$ mutant transfectants were assessed for their ability to attach to ectocervical cells compared to empty vector transfectants. Results show the average of three experiments, each conducted in triplicate, errors bar denote the standard error. Exogenous expression of GFP-$TVAG\_166850^{WT}$ leads to a statistically significant increase in attachment compared to empty vector transfectants (*$p<0.05$). Overexpression of the GFP-$TVAG\_166850^{AG/FF}$ mutant leads to an even greater increase in attachment compared to empty vector (**$p<0.01$) and wildtype GFP-$TVAG\_166850^{WT}$ transfectants (**$p<0.01$). Decreased rhomboid cleavage of the GFP-$TVAG\_166850^{AG/FF}$ mutant may lead to its increased detection at the cell surface and greater attachment to host cells. **(D)** Introduction of the AG/FF mutation at the predicted P1-P1' sites in the TM domain of TVAG_166850 causes a reduction in its processing by TvROM1. A chimeric GFP-EBA-175 protein containing the wildtype or AG/FF mutant TM domain of TVAG_166850 was assessed using the HEK293 heterologous cell cleavage assay. Expression of the GFP-EBA-175-$TVAG\_166850TM^{AG/FF}$ chimeric protein caused release of the protein into the media when no rhomboid was co-transfected likely due to metalloprotease activity (-BB-94), therefore the cleavage assay was performed in the presence of a metalloprotease inhibitor (BB-94, 10 uM) to monitor rhomboid-specific cleavage. The GFP-EBA-175 chimeric proteins were co-transfected with HA-tagged TvROM1, the TvROM1 catalytic mutant, or the positive control TgROM5. Western blot analyses of whole cell lysates confirmed expression of the HA-tagged rhomboids (top panel) and the full-length substrate (closed arrowhead, middle panel). Analysis of conditioned media from the co-transfectants (lower panel) shows a drastic reduction (~90%) in the rhomboid-specific cleavage product of the EBA-175-$TVAG\_166850TM^{AG/FF}$ mutant protein *vs*. the $TVAG\_166850TM^{WT}$ protein (red, open arrowhead, bottom panel) in TvROM1 (lane 9 vs. lane 4) and TgROM5 (lane 8 *vs.* lane 3) co-transfectants. No difference in rhomboid-specific cleavage of the wildtype or mutant chimeric protein was observed in the TvROM1 catalytic His to Ala co-transfectants (lane 10 *vs.* lane 5).

Supplemental Figures:

T. vaginalis rhomboid:	TrichDB accession number	TrichDB predicted # of TM domains	GxSx motif surrounding catalytic serine in TM4	Catalytic histidine in TM6	GxSxxxF motif surrounding catalytic serine found in secretase B-type rhomboids?	WR motif in L1 loop?	GxxxG dimerization motif in TM6 below catalytic histidine?
TvROM1	TVAG_112900	7	GASA Ser262	His316	yes	yes	yes
TvROM2	TVAG_359500	7	GSSN Ser216	His270	yes	yes	yes
TvROM3	TVAG_476950	6	GFSG Ser129	His181	yes	yes	yes
TvROM4	TVAG_161010	7	GTSG Ser299	His351	no	yes	yes

Table 2-S1: Summary of bioinformatic analysis for the main conserved rhomboid features found in the predicted active *T. vaginalis* rhomboids.
Active rhomboid proteases contain a catalytic Serine (S) and Histidine (H) located at the top parts of TMs 4 and 6, with a GxSx motif surrounding the catalytic Serine (x=any amino acid)[52]. Identification of the catalytic residues was performed using Pfam analysis and the TM predictions from TrichDB. Rhomboid proteases that are found in the secretory pathway have been classified into 2 types, type A and type B [52]. Parasitic rhomboids do not fall clearly into either subfamily, as they appear to either be functionally different or too divergent, and can display characteristics of both subfamilies [52]. Type A rhomboids contain a WR motif located in the L1 loop whereas type B rhomboids have only a conserved R in the L1 loop. The arginine that is part of the WR motif helps stabilize the L1 loop by donating several hydrogen bonds [91]. *T. vaginalis* rhomboids contain the conserved WR motif. Additionally, all the *T. vaginalis* rhomboids contain a GxxxG dimerization motif located beneath the predicted catalytic histidine in TM6, which is predicted to mediate dimerization with TM4 to bring the catalytic serine and histidine together [91].

Fasta headers	DCI/DMSO ratio	% decrease in DCI *vs.* DMSO	% increase in DCI vs DMSO	DCI/DMSO Std Error	adj p-value	Lower bound 95% confidence interval	Upper bound 95% confidence interval	Yellow or pink highlighting marks proteins/protein groups that decreased by more than 50% in abundance in presence of 3,4-DCI with statistical significance (p<0.05), presence or absence of TM domain and parasite search motif or Strisovsky *et al.* 2009 motif within top part of TM domain is indicated
>tr|Q8IEV2|Q8IEV2_TRIVA Thioredoxin peroxidase OS=Trichomonas vaginalis GN=trxp PE=2 SV=1	0.2136577	79		1.5988254	0.6281555	-5.360267	0.9070134	no TM
>sp|O96432|CBK_TRIVA Carbamate kinase OS=Trichomonas vaginalis GN=CBK PE=1 SV=1;>tr|A2DUA9|A2DUA9_TRIVA Carbamate kinase, putative OS=Trichomonas vaginalis GN=TVAG_261970 PE=4 SV=1;>tr|A2ED74|A2ED74_TRIVA Carbamate kinase, putative OS=Trichomonas vaginalis	0.2581513	74		0.6405329	0.043003	-3.2091325	-0.6982897	no TM
>tr|A2E8J5|A2E8J5_TRIVA Putative uncharacterized protein OS=Trichomonas vaginalis GN=TVAG_410350 PE=4 SV=1	0.2718652	73		0.4582002	0.0019342	-2.7770923	-0.9809804	no TM
>tr|Q6S4N6|Q6S4N6_TRIVA Ferredoxin 2 OS=Trichomonas vaginalis GN=TVAG_399860 PE=4 SV=1	0.2749561	73		0.6642018	0.0789616	-3.1645387	-0.5609154	no TM
>tr|A2GH90|A2GH90_TRIVA Putative uncharacterized protein (Fragment) OS=Trichomonas vaginalis GN=TVAG_529190 PE=4 SV=1	0.3202572	68		0.4668995	0.0116642	-2.5578033	-0.727591	no TM
>tr|A2DE92|A2DE92_TRIVA Putative uncharacterized protein OS=Trichomonas vaginalis GN=TVAG_166850 PE=4 SV=1	0.3255583	67		0.5235884	0.043003	-2.6452266	-0.5927977	has TM-has parasite search motif in TM domain-possible substrate
>tr|A2FD35|A2FD35_TRIVA Clan CA, family C1, cathepsin L-like cysteine peptidase OS=Trichomonas vaginalis GN=TVAG_355480 PE=3 SV=1	0.3288051	67		0.6252071	0.1206521	-2.8300786	-0.3793119	no TM
>sp|P21149|FER_TRIVA Ferredoxin OS=Trichomonas vaginalis PE=1 SV=1;>tr|A2E5A4|A2E5A4_TRIVA Ferredoxin 1 OS=Trichomonas vaginalis GN=TVAG_003900 PE=4 SV=1	0.3378225	66		0.8775706	0.4157582	-3.2856695	0.1543439	no TM
>tr|A2EP01|A2EP01_TRIVA Enolase family protein OS=Trichomonas vaginalis GN=TVAG_263740 PE=3 SV=1;>tr|A2ELB9|A2ELB9_TRIVA Enolase OS=Trichomonas vaginalis GN=TVAG_358110 PE=3 SV=1;>tr|A2E9S4|A2E9S4_TRIVA Enolase OS=Trichomonas vaginalis GN=TVAG_282090 PE=3	0.3490732	65		0.8043932	0.3782872	-3.0949802	0.0581833	no TM, no TM, no TM
>tr|A2F0E3|A2F0E3_TRIVA Ferredoxin 4 OS=Trichomonas vaginalis GN=TVAG_292710 PE=4 SV=1	0.361881	64		0.609144	0.1777097	-2.6603132	-0.2725124	no TM
>tr|A2GBF6|A2GBF6_TRIVA Putative uncharacterized protein (Fragment) OS=Trichomonas vaginalis GN=TVAG_293660 PE=4 SV=1	0.3774614	62		0.4733232	0.0509565	-2.3332953	-0.4779025	no TM
>tr|A2GCR8|A2GCR8_TRIVA Putative uncharacterized protein OS=Trichomonas vaginalis GN=TVAG_573910 PE=4 SV=1	0.3841085	62		0.2645321	1.697E-05	-1.8988875	-0.8619407	has TM-has Strisovsky *et al.* 2009 motif in TM domain-possible substrate
>tr|O15556|O15556_TRIVA Glyceraldehyde-3-phosphate dehydrogenase (Fragment) OS=Trichomonas vaginalis GN=gap2 PE=3 SV=1	0.3874885	61		0.4438987	0.043003	-2.2378	-0.4977492	no TM
>tr|A2G7A4|A2G7A4_TRIVA Putative uncharacterized protein OS=Trichomonas vaginalis GN=TVAG_245580 PE=4 SV=1;>tr|A2G2L3|A2G2L3_TRIVA Putative uncharacterized protein OS=Trichomonas vaginalis GN=TVAG_425470 PE=4 SV=1	0.3889002	61		0.2851095	0.0001104	-1.9213324	-0.8037238	both proteins have a TM domain-both have Strisovsky *et al.* 2009 motif in TM domain-possible substrates
>tr|A2DYD5|A2DYD5_TRIVA Putative uncharacterized protein OS=Trichomonas vaginalis GN=TVAG_393390 PE=4 SV=1	0.3996181	60		0.3433216	0.0043617	-1.9962042	-0.6504083	has TM-has Strisovsky *et al.* 2009 motif in TM domain-possible substrate
>tr|A2EVN0|A2EVN0_TRIVA Putative uncharacterized protein OS=Trichomonas vaginalis GN=TVAG_193800 PE=3 SV=1;>tr|A2DA33|A2DA33_TRIVA Putative uncharacterized protein OS=Trichomonas vaginalis GN=TVAG_476100 PE=3 SV=1	0.4112546	59		0.5965343	0.3059424	-2.4510821	-0.1127108	no TM,no TM
>tr|A2GVU9|A2GVU9_TRIVA Putative uncharacterized protein (Fragment) OS=Trichomonas vaginalis GN=TVAG_405680 PE=4 SV=1;>tr|A2H566|A2H566_TRIVA Putative uncharacterized protein (Fragment) OS=Trichomonas vaginalis GN=TVAG_546190 PE=4 SV=1;>tr|A2GR04|A2GR04_TR	0.4763152	52		0.5042003	0.3059424	-2.0582259	-0.081797	no TM,no TM
>tr|A2GVA2|A2GVA2_TRIVA Putative uncharacterized protein OS=Trichomonas vaginalis GN=TVAG_369130 PE=4 SV=1	0.5282845	47		0.4346599	0.3059424	-1.7725306	-0.0686953	
>tr|A2FBF3|A2FBF3_TRIVA Glycosyl hydrolase family 14 protein OS=Trichomonas vaginalis GN=TVAG_080000 PE=3 SV=1;>tr|A2F5N5|A2F5N5_TRIVA Glycosyl hydrolase family 14 protein OS=Trichomonas vaginalis GN=TVAG_175670 PE=3 SV=1	0.5385126	46		0.4647566	0.3782872	-1.8038543	0.0179581	
>tr|A2FRU0|A2FRU0_TRIVA Actinin, putative OS=Trichomonas vaginalis GN=TVAG_156680 PE=4 SV=1	0.5396095	46		0.4805823	0.3883328	-1.8319364	0.0519116	
>tr|A2EM29|A2EM29_TRIVA Glyceraldehyde-3-phosphate dehydrogenase OS=Trichomonas vaginalis GN=TVAG_475220 PE=3 SV=1	0.5442832	46		0.4513206	0.3782872	-1.7621428	0.0070016	
>tr|A2FMK8|A2FMK8_TRIVA Clan MH, family M20, peptidase T-like metallopeptidase OS=Trichomonas vaginalis GN=TVAG_224980 PE=4 SV=1	0.5493214	45		0.3310095	0.1183369	-1.5130443	-0.2155109	
>tr|A2DKH4|A2DKH4_TRIVA Surface antigen BspA-like OS=Trichomonas vaginalis GN=TVAG_190460 PE=4 SV=1	0.587805	41		0.4503808	0.4608702	-1.6493206	0.1161398	
>tr|A2DWE3|A2DWE3_TRIVA Putative uncharacterized protein OS=Trichomonas vaginalis GN=TVAG_394260 PE=4 SV=1	0.597644	40		0.4568147	0.4769444	-1.637982	0.1526988	
>tr|A2FXT2|A2FXT2_TRIVA Clan IH, family I25, phytocystatin-like peptidase inhibitor OS=Trichomonas vaginalis GN=TVAG_272260 PE=4 SV=1	0.6001585	40		0.5755755	0.6985181	-1.8646917	0.3915229	
>tr|A2E0V9|A2E0V9_TRIVA Actin-like protein 3, putative OS=Trichomonas vaginalis GN=TVAG_371880 PE=3 SV=1	0.612261	39		0.569077	0.7170755	-1.8231518	0.4075893	
>tr|A2EC21|A2EC21_TRIVA Peptidyl-prolyl cis-trans isomerase OS=Trichomonas vaginalis GN=TVAG_137880 PE=3 SV=1	0.6210196	38		0.4083693	0.4608702	-1.4876783	0.1130999	
>tr|A2F8B9|A2F8B9_TRIVA CAMK family protein kinase OS=Trichomonas vaginalis GN=TVAG_409590 PE=4 SV=1	0.6219657	38		0.8170861	0.8436018	-2.2865524	0.9163662	
>tr|A2G129|A2G129_TRIVA Putative uncharacterized protein OS=Trichomonas vaginalis GN=TVAG_442350 PE=4 SV=1	0.6278431	37		0.9793583	0.8684254	-2.5910311	1.2479828	
>tr|A2F6N7|A2F6N7_TRIVA Putative uncharacterized protein OS=Trichomonas vaginalis GN=TVAG_408360 PE=4 SV=1	0.6305809	37		0.694098	0.8146335	-2.0256538	0.6951606	
>sp|P53401|SUCA3_TRIVA Succinyl-CoA ligase [GDP-forming] subunit alpha-3, mitochondrial OS=Trichomonas vaginalis GN=ALPHA-SCS3 PE=3 SV=1;>sp|P53399|SUCA1_TRIVA Succinyl-CoA ligase [GDP-forming] subunit alpha-1, mitochondrial OS=Trichomonas vaginalis GN=ALP	0.633959	37		0.4856816	0.6609523	-1.609457	0.2943798	
>tr|A2E1I9|A2E1I9_TRIVA Family T1, proteasome alpha subunit, threonine peptidase OS=Trichomonas vaginalis GN=TVAG_206040 PE=4 SV=1	0.6341311	37		0.634316	0.7838697	-1.9003835	0.5860896	
>tr|A2EM51|A2EM51_TRIVA Clan CA, family C1, cathepsin L-like cysteine peptidase OS=Trichomonas vaginalis GN=TVAG_034140 PE=3 SV=1	0.6539713	35		0.3938452	0.5236977	-1.3846232	0.1592215	
>tr|Q4JHB2|Q4JHB2_TRIVA Saposin-like protein 2 (Fragment) OS=Trichomonas vaginalis PE=2 SV=1;>tr|A2FFY3|A2FFY3_TRIVA Surfactant B protein, putative OS=Trichomonas vaginalis GN=TVAG_000220 PE=4 SV=1	0.6570938	34		0.5166238	0.7394676	-1.618393	0.4067352	
>tr|A2DRE4|A2DRE4_TRIVA Putative uncharacterized protein OS=Trichomonas vaginalis GN=TVAG_297490 PE=4 SV=1	0.6713698	33		0.6605895	0.8436018	-1.8695521	0.7199113	
>tr|D5MC19|D5MC19_TRIVA Translation initiation factor 5A 1 OS=Trichomonas vaginalis GN=eIF-5A1 PE=2 SV=1;>tr|D5I1Q2|D5I1Q2_TRIVA Translation initiation factor 5A 2 OS=Trichomonas vaginalis GN=eIF-5A2 PE=2 SV=1;>tr|A2GG34|A2GG34_TRIVA Translation initiation	0.6714978	33		1.3918222	0.871854	-3.3024669	2.1533758	
>tr|O15566|O15566_TRIVA Adhesin protein AP51-2 (Fragment) OS=Trichomonas vaginalis GN=ap51-2 PE=2 SV=1;>tr|A2FVK7|A2FVK7_TRIVA Adhesin protein AP51-2, putative OS=Trichomonas vaginalis GN=TVAG_144730 PE=3 SV=1	0.6831534	32		0.6646651	0.8436018	-1.8524382	0.7530009	
>tr|A2DKE2|A2DKE2_TRIVA 60S ribosomal protein L22-1, putative OS=Trichomonas vaginalis GN=TVAG_121380 PE=4 SV=1;>tr|A2DNV5|A2DNV5_TRIVA 60S ribosomal protein L22-1, putative OS=Trichomonas vaginalis GN=TVAG_057020 PE=4 SV=1	0.6864105	31		0.5559415	0.8146335	-1.6324818	0.5467688	
>tr|A2GA05|A2GA05_TRIVA Glyceraldehyde-3-phosphate dehydrogenase OS=Trichomonas vaginalis GN=TVAG_412780 PE=3 SV=1;>tr|A2FNQ3|A2FNQ3_TRIVA Glyceraldehyde-3-phosphate dehydrogenase OS=Trichomonas vaginalis GN=TVAG_347410 PE=3 SV=1	0.6961318	30		0.4505433	0.7394676	-1.4056163	0.3604811	
>tr|A2DCQ3|A2DCQ3_TRIVA Beige/BEACH domain containing protein OS=Trichomonas vaginalis GN=TVAG_237030 PE=4 SV=1	0.705478	29		0.476275	0.7838697	-1.436809	0.4301549	
>tr|A2D968|A2D968_TRIVA Aminotransferase, class V family protein OS=Trichomonas vaginalis GN=TVAG_183300 PE=3 SV=1;>tr|A2FXW5|A2FXW5_TRIVA Aminotransferase, class V family protein OS=Trichomonas vaginalis GN=TVAG_099570 PE=3 SV=1;>tr|A2DW27|A2DW27_TRIVA Am	0.7088637	29		0.3040287	0.4769444	-1.0923051	0.0994656	
>tr|A2DW42|A2DW42_TRIVA Putative uncharacterized protein OS=Trichomonas vaginalis GN=TVAG_224190 PE=4 SV=1	0.7118971	29		0.7351167	0.8684254	-1.9310617	0.9505429	
>tr|A2FVM1|A2FVM1_TRIVA Ribosomal protein L10, putative OS=Trichomonas vaginalis GN=TVAG_344700 PE=3 SV=1;>tr|A2EES5|A2EES5_TRIVA Ribosomal protein L10, putative OS=Trichomonas vaginalis GN=TVAG_051160 PE=3 SV=1;>tr|A2DHM5|A2DHM5_TRIVA Ribosomal protein L1	0.7187734	28		0.4564387	0.7838697	-1.3709945	0.4182124	
>tr|A2FJ33|A2FJ33_TRIVA Thioredoxin OS=Trichomonas vaginalis GN=TVAG_204390 PE=3 SV=1	0.7263319	27		0.72279	0.8684254	-1.8779415	0.9553432	
>tr|Q6EHZ7|Q6EHZ7_TRIVA Legumain-like cysteine proteinase 1 OS=Trichomonas vaginalis GN=legu-1 PE=2 SV=1;>tr|A2DYT2|A2DYT2_TRIVA Clan CD, family C13, asparaginyl endopeptidase-like cysteine peptidase OS=Trichomonas vaginalis GN=TVAG_426660 PE=4 SV=1	0.7370142	26		0.41877	0.7838697	-1.2610097	0.3805384	
>tr|A2GL34|A2GL34_TRIVA Clathrin and VPS domain-containing protein (Fragment) OS=Trichomonas vaginalis GN=TVAG_532880 PE=4 SV=1	0.7396426	26		0.6174698	0.8684254	-1.6453183	0.775119	
>tr|O15567|O15567_TRIVA Adhesin protein AP51-3 (Fragment) OS=Trichomonas vaginalis GN=ap51-3 PE=2 SV=1;>tr|A2D987|A2D987_TRIVA Adhesin protein AP51-3, putative OS=Trichomonas vaginalis GN=TVAG_183500 PE=3 SV=1	0.7491905	25		0.6219007	0.8684254	-1.6354983	0.8023075	
>tr|A2FYE4|A2FYE4_TRIVA Polyadenylate-binding protein, putative OS=Trichomonas vaginalis GN=TVAG_371220 PE=4 SV=1;>tr|A2FYE5|A2FYE5_TRIVA Embryonic poly, putative OS=Trichomonas vaginalis GN=TVAG_371230 PE=4 SV=1	0.7562413	24		0.3597804	0.7479067	-1.108238	0.3020753	
>tr|A2GTQ6|A2GTQ6_TRIVA Putative uncharacterized protein OS=Trichomonas vaginalis GN=TVAG_525700 PE=4 SV=1;>tr|A2GME7|A2GME7_TRIVA Putative uncharacterized protein (Fragment) OS=Trichomonas vaginalis GN=TVAG_522470 PE=4 SV=1;>tr|A2HBN2|A2HBN2_TRIVA Putativ	0.7567979	24		0.531391	0.8619682	-1.4435272	0.6394872	
>tr|A2F259|A2F259_TRIVA 4-alpha-glucanotransferase family protein OS=Trichomonas vaginalis GN=TVAG_154680 PE=4 SV=1;>tr|A2E3F9|A2E3F9_TRIVA 4-alpha-glucanotransferase family protein OS=Trichomonas vaginalis GN=TVAG_222040 PE=4 SV=1	0.7621215	24		0.8159576	0.8693111	-1.9911547	1.2073404	
>tr|A2HXI6|A2HXI6_TRIVA Putative uncharacterized protein (Fragment) OS=Trichomonas vaginalis GN=TVAG_539120 PE=4 SV=1	0.7681122	23		0.3972346	0.8146335	-1.1591766	0.3979545	
>tr|A2FH22|A2FH22_TRIVA Actin family protein OS=Trichomonas vaginalis GN=TVAG_354020 PE=3 SV=1	0.7689427	23		0.5986226	0.8684254	-1.5523307	0.7942266	
>tr|A2ECS2|A2ECS2_TRIVA Putative uncharacterized protein OS=Trichomonas vaginalis GN=TVAG_276410 PE=4 SV=1	0.7692743	23		0.1815211	0.3169518	-0.7342049	-0.0226551	
>tr|A2FKG4|A2FKG4_TRIVA Alcohol dehydrogensae, putative OS=Trichomonas vaginalis GN=TVAG_422780 PE=4 SV=1	0.7738068	23		0.2595902	0.6281555	-0.8787422	0.1388328	
>tr|A2FHH0|A2FHH0_TRIVA Putative uncharacterized protein OS=Trichomonas vaginalis GN=TVAG_045340 PE=4 SV=1	0.791146	21		0.6864845	0.8693111	-1.6834692	1.0075008	
>tr|A2G9W5|A2G9W5_TRIVA GDP dissociation inhibitor family protein OS=Trichomonas vaginalis GN=TVAG_126970 PE=4 SV=1	0.7957637	20		0.4035127	0.8436018	-1.1204583	0.4612824	
>tr|A2F422|A2F422_TRIVA Adenylyl cyclase-associated protein OS=Trichomonas vaginalis GN=TVAG_407250 PE=3 SV=1	0.7983908	20		0.3474431	0.8314036	-1.005809	0.356143	
>tr|A2FKH3|A2FKH3_TRIVA Dynein light chain 1, cytoplasmic, putative OS=Trichomonas vaginalis GN=TVAG_134920 PE=4 SV=1;>tr|A2ED60|A2ED60_TRIVA Dynein light chain 1, cytoplasmic, putative OS=Trichomonas vaginalis GN=TVAG_312170 PE=4 SV=1	0.8050352	19		0.8978524	0.8997853	-2.0726344	1.4468821	
>tr|A2EZN7|A2EZN7_TRIVA Clan CA, family C1, cathepsin L-like cysteine peptidase OS=Trichomonas vaginalis GN=TVAG_090100 PE=3 SV=1;>tr|Q27108|Q27108_TRIVA Cysteine proteinase, putative (Fragment) OS=Trichomonas vaginalis GN=CP3 PE=2 SV=1	0.8057041	19		0.5059992	0.8693111	-1.3034183	0.6800621	
>tr|A2GSG4|A2GSG4_TRIVA Putative uncharacterized protein (Fragment) OS=Trichomonas vaginalis GN=TVAG_509310 PE=4 SV=1;>tr|A2GNG7|A2GNG7_TRIVA Putative uncharacterized protein (Fragment) OS=Trichomonas vaginalis GN=TVAG_535840 PE=4 SV=1	0.8075089	19		0.5897103	0.8693111	-1.4642608	0.847361	
>tr|A2DJ14|A2DJ14_TRIVA Malic enzyme OS=Trichomonas vaginalis GN=TVAG_228520 PE=3 SV=1	0.8103262	19		0.6715442	0.871854	-1.6196278	1.0127771	
>tr|Q27820|Q27820_TRIVA Glyceraldehyde-3-phosphate dehydrogenase (Fragment) OS=Trichomonas vaginalis PE=2 SV=1;>tr|A2DHT2|A2DHT2_TRIVA Putative uncharacterized protein OS=Trichomonas vaginalis GN=TVAG_146910 PE=4 SV=1	0.8111462	19		0.4513988	0.8684254	-1.1866916	0.5827593	
>tr|A2F3X4|A2F3X4_TRIVA Family T1, proteasome beta subunit, threonine peptidase OS=Trichomonas vaginalis GN=TVAG_290960 PE=4 SV=1	0.8296581	17		0.4722652	0.8693111	-1.1950341	0.6562116	
>tr|A2DNP0|A2DNP0_TRIVA Putative uncharacterized protein OS=Trichomonas vaginalis GN=TVAG_113870 PE=4 SV=1;>tr|A2FS74|A2FS74_TRIVA Putative uncharacterized protein OS=Trichomonas vaginalis GN=TVAG_164890 PE=4 SV=1	0.8297292	17		0.5902304	0.871854	-1.4261178	0.8875429	
>tr|A2HF76|A2HF76_TRIVA Surface immunogen P270-related protein (Fragment) OS=Trichomonas vaginalis GN=TVAG_133500 PE=4 SV=1	0.8304759	17		0.6519431	0.871854	-1.5457747	1.0097952	
>tr|A2D9B6|A2D9B6_TRIVA AP65-3 adhesin OS=Trichomonas vaginalis GN=TVAG_183790 PE=3 SV=1;>tr|Q27102|Q27102_TRIVA AP65-3 adhesin OS=Trichomonas vaginalis PE=2 SV=1	0.8403696	16		0.3659531	0.8684254	-0.9681591	0.4663509	
>tr|Q8IEV4|Q8IEV4_TRIVA Thioredoxin OS=Trichomonas vaginalis GN=trx PE=1 SV=1	0.8417787	16		0.5924219	0.871854	-1.4096126	0.9126386	
>tr|A2EMJ7|A2EMJ7_TRIVA Malate dehydrogenase:SUBUNIT=A, putative OS=Trichomonas vaginalis GN=TVAG_068130 PE=4 SV=1	0.8441144	16		0.5961369	0.871854	-1.4128963	0.9239173	
>tr|Q27090|Q27090_TRIVA Hydrogenosomal malic enzyme subunit B proprotein OS=Trichomonas vaginalis GN=maeB PE=3 SV=1	0.8775837	12		0.6631328	0.9279166	-1.4881077	1.111325	
>tr|A2F347|A2F347_TRIVA Threonyl-tRNA synthetase family protein OS=Trichomonas vaginalis GN=TVAG_208470 PE=3 SV=1	0.8917694	11		0.3381416	0.8693111	-0.8280026	0.4974879	
>tr|A2ENN9|A2ENN9_TRIVA Profilin A, putative OS=Trichomonas vaginalis GN=TVAG_100620 PE=4 SV=1	0.8971853	10		0.5531083	0.9279166	-1.2405946	0.9275503	
>tr|A2FUZ1|A2FUZ1_TRIVA 14-3-3 protein OS=Trichomonas vaginalis GN=TVAG_251260 PE=4 SV=1	0.8995095	10		0.3897946	0.8770098	-0.9167729	0.6111937	
>tr|A2FYS8|A2FYS8_TRIVA Actin family protein OS=Trichomonas vaginalis GN=TVAG_434970 PE=3 SV=1	0.9011151	10		0.4291453	0.8997853	-0.991326	0.6908926	
>tr|A2F1M8|A2F1M8_TRIVA Malate dehydrogenase:SUBUNIT=A, putative OS=Trichomonas vaginalis GN=TVAG_412220 PE=3 SV=1;>tr|A2GMN0|A2GMN0_TRIVA Malate dehydrogenase:SUBUNIT=A, putative (Fragment) OS=Trichomonas vaginalis GN=TVAG_416100 PE=3 SV=1	0.9173185	8		0.316244	0.8770098	-0.7443323	0.4953216	
>tr|A2DYM3|A2DYM3_TRIVA Putative uncharacterized protein OS=Trichomonas vaginalis GN=TVAG_388910 PE=4 SV=1;>tr|A2DD62|A2DD62_TRIVA Putative uncharacterized protein OS=Trichomonas vaginalis GN=TVAG_013060 PE=4 SV=1;>tr|A2D873|A2D873_TRIVA Putative uncharact	0.9208878	8		0.3143107	0.8838635	-0.7349404	0.497135	
>tr|A2FXM6|A2FXM6_TRIVA Clan CD, family C13, asparaginyl endopeptidase-like cysteine peptidase OS=Trichomonas vaginalis GN=TVAG_385340 PE=4 SV=1	0.9251628	7		0.46148	0.9317753	-1.016705	0.7922633	
>tr|A2DPX6|A2DPX6_TRIVA Ribosomal protein L5 OS=Trichomonas vaginalis GN=TVAG_064640 PE=3 SV=1;>tr|A2DNM5|A2DNM5_TRIVA Ribosomal protein L5 OS=Trichomonas vaginalis GN=TVAG_113720 PE=3 SV=1;>tr|Q76KT0|Q76KT0_TRIVA Ribosomal protein L5 OS=Trichomonas vagina	0.9255364	7		0.3777268	0.9279166	-0.8519693	0.6286925	
>tr|Q5EFD8|Q5EFD8_TRIVA Enolase OS=Trichomonas vaginalis GN=Eno PE=2 SV=1;>tr|Q9NDF8|Q9NDF8_TRIVA Enolase (Fragment) OS=Trichomonas vaginalis PE=3 SV=1	0.9389068	6		0.6210388	0.971413	-1.3081599	1.1262675	
>tr|Q27106|Q27106_TRIVA Clan CA, family C1, cathepsin L-like cysteine peptidase OS=Trichomonas vaginalis GN=CP1 PE=2 SV=1	0.9420847	6		0.4898214	0.9629563	-1.0461036	0.8739611	
>tr|Q8IEV3|Q8IEV3_TRIVA Thioredoxin reductase OS=Trichomonas vaginalis GN=trxr PE=2 SV=1	0.9521755	5		0.4289063	0.9639456	-0.9113414	0.7699404	
>tr|Q86S09|Q86S09_TRIVA Alcohol dehydrogenase OS=Trichomonas vaginalis GN=Adh PE=4 SV=1;>tr|A2FRL9|A2FRL9_TRIVA Alcohol dehydrogenase OS=Trichomonas vaginalis GN=TVAG_327470 PE=4 SV=1;>tr|Q9XYL4|Q9XYL4_TRIVA Putative NADPH-dependent butanol dehydrogenase O	0.9543366	5		0.2655968	0.9279166	-0.5879901	0.4531303	
>tr|A2DLF4|A2DLF4_TRIVA Phosphoglycerate kinase OS=Trichomonas vaginalis GN=TVAG_268050 PE=3 SV=1	0.9591516	4		0.1848399	0.9092205	-0.4224487	0.3021103	
>tr|A2EEC2|A2EEC2_TRIVA Pyruvate, phosphate dikinase family protein OS=Trichomonas vaginalis GN=TVAG_073860 PE=4 SV=1	0.96078	4		0.2123613	0.9279166	-0.4739423	0.3584985	
>tr|Q8WQT4|Q8WQT4_TRIVA Glycogen phosphorylase OS=Trichomonas vaginalis PE=2 SV=1;>tr|Q6Y2E4|Q6Y2E4_TRIVA Glycogen phosphorylase OS=Trichomonas vaginalis PE=3 SV=1;>tr|A2DSX4|A2DSX4_TRIVA Glycogen phosphorylase OS=Trichomonas vaginalis GN=TVAG_348330 PE=3	0.9651271	3		0.4572483	0.9786503	-0.9473993	0.8449811	
>tr|Q27093|Q27093_TRIVA AP65-1 adhesin OS=Trichomonas vaginalis GN=AP65-1 PE=2 SV=1;>tr|A2EKE3|A2EKE3_TRIVA Adhesin AP65-1 OS=Trichomonas vaginalis GN=TVAG_340290 PE=3 SV=1	0.9686898	3		0.2194159	0.9519477	-0.4759406	0.3841538	
>tr|A2DED9|A2DED9_TRIVA Nucleoside diphosphate kinase OS=Trichomonas vaginalis GN=TVAG_167320 PE=3 SV=1	0.9843927	2		0.4669595	0.9954371	-0.9379178	0.8925296	
>tr|B6CAS9|B6CAS9_TRIVA Cytotoxic cysteine proteinase OS=Trichomonas vaginalis GN=cp39 PE=3 SV=1;>tr|A2ET02|A2ET02_TRIVA Clan CA, family C1, cathepsin L-like cysteine peptidase OS=Trichomonas vaginalis GN=TVAG_298080 PE=3 SV=1	0.9947104	1		0.551691	0.9954371	-1.088946	1.073643	
>tr|A2E7L8|A2E7L8_TRIVA 60S ribosomal protein L11, putative OS=Trichomonas vaginalis GN=TVAG_044560 PE=3 SV=1;>tr|A2EA92|A2EA92_TRIVA 60S ribosomal protein L11, putative OS=Trichomonas vaginalis GN=TVAG_271230 PE=3 SV=1	0.997572	0		0.6132785	0.9954371	-1.205511	1.1984966	
>tr|A2DNM4|A2DNM4_TRIVA Phosphoglycerate mutase, putative OS=Trichomonas vaginalis GN=TVAG_113710 PE=3 SV=1;>tr|A2E2R4|A2E2R4_TRIVA Phosphoglycerate mutase, putative OS=Trichomonas vaginalis GN=TVAG_212740 PE=3 SV=1;>tr|A2DVE4|A2DVE4_TRIVA Phosphoglycerate	1.0037202		100	0.7183247	0.9954371	-1.4025335	1.4132477	
>tr|A2G0N8|A2G0N8_TRIVA Coronin OS=Trichomonas vaginalis GN=TVAG_222320 PE=3 SV=1;>tr|Q9NFT4|Q9NFT4_TRIVA Coronin OS=Trichomonas vaginalis GN=cor1 PE=3 SV=1;>tr|A2G3C8|A2G3C8_TRIVA Coronin OS=Trichomonas vaginalis GN=TVAG_177180 PE=3 SV=1	1.0042544		100	0.3884919	0.9954371	-0.7553055	0.7675549	
>tr|A2EFR4|A2EFR4_TRIVA Thioredoxin OS=Trichomonas vaginalis GN=TVAG_145440 PE=3 SV=1	1.0068066		101	0.5150925	0.9954371	-0.9997762	1.0193495	
>tr|A2FJR3|A2FJR3_TRIVA Chloroplastic iron superoxide dismutase, putative OS=Trichomonas vaginalis GN=TVAG_049140 PE=3 SV=1	1.0081127		101	0.5744161	0.9954371	-1.1141781	1.1374919	
>tr|A2DUA7|A2DUA7_TRIVA QXW lectin repeat family protein OS=Trichomonas vaginalis GN=TVAG_261950 PE=4 SV=1	1.0139578		101	0.4221922	0.9954371	-0.8074839	0.8474792	
>tr|A2F3X9|A2F3X9_TRIVA Ribosomal protein, putative OS=Trichomonas vaginalis GN=TVAG_291010 PE=4 SV=1;>tr|A2DFF0|A2DFF0_TRIVA Ribosomal protein, putative OS=Trichomonas vaginalis GN=TVAG_437020 PE=4 SV=1	1.01459		101	0.5260819	0.9954371	-1.0102047	1.0519984	
>tr|Q4KXQ3|Q4KXQ3_TRIVA 14-3-3 protein OS=Trichomonas vaginalis GN=TVAG_462940 PE=2 SV=1	1.0166651		102	0.3279483	0.9954371	-0.6189223	0.6666113	
>tr|A2EK40|A2EK40_TRIVA Putative uncharacterized protein OS=Trichomonas vaginalis GN=TVAG_099730 PE=4 SV=1	1.0187773		102	0.2400481	0.9786503	-0.4436469	0.4973242	
>tr|A2F0H0|A2F0H0_TRIVA Transaldolase OS=Trichomonas vaginalis GN=TVAG_272910 PE=3 SV=1	1.0228647		102	0.8233695	0.9954371	-1.5811592	1.64639	
>tr|A2EJJ9|A2EJJ9_TRIVA Endoribonuclease L-PSP family protein OS=Trichomonas vaginalis GN=TVAG_197820 PE=4 SV=1	1.0237155		102	0.4875014	0.9954371	-0.9216702	0.9893	
>tr|A2ER97|A2ER97_TRIVA Putative uncharacterized protein OS=Trichomonas vaginalis GN=TVAG_226630 PE=4 SV=1;>tr|A2DYS0|A2DYS0_TRIVA Putative uncharacterized protein OS=Trichomonas vaginalis GN=TVAG_111510 PE=4 SV=1	1.0315591		103	0.6817462	0.9954371	-1.2913714	1.3810245	
>tr|A2FS39|A2FS39_TRIVA Ribosomal protein L14, putative OS=Trichomonas vaginalis GN=TVAG_262730 PE=4 SV=1	1.0434219		104	0.4524167	0.9751749	-0.8253977	0.948043	
>tr|A2EPR1|A2EPR1_TRIVA Heat shock protein, putative OS=Trichomonas vaginalis GN=TVAG_153560 PE=3 SV=1;>tr|Q5KTX0|Q5KTX0_TRIVA Cytosolic-type hsp90 (Fragment) OS=Trichomonas vaginalis PE=2 SV=1	1.0482007		105	0.2602622	0.9279166	-0.4421897	0.5780195	
>tr|A2FIS4|A2FIS4_TRIVA Putative uncharacterized protein OS=Trichomonas vaginalis GN=TVAG_032440 PE=4 SV=1;>tr|A2FBZ4|A2FBZ4_TRIVA GP63-like OS=Trichomonas vaginalis GN=TVAG_064340 PE=4 SV=1	1.0498884		105	0.5729515	0.9786503	-1.0527284	1.1932003	
>tr|A2E9V0|A2E9V0_TRIVA Polyubiquitin, putative OS=Trichomonas vaginalis GN=TVAG_174190 PE=4 SV=1;>tr|Q27100|Q27100_TRIVA Ubiquitin (Fragment) OS=Trichomonas vaginalis GN=Ub2B PE=4 SV=1;>tr|A2DC67|A2DC67_TRIVA Polyubiquitin, putative OS=Trichomonas vaginal	1.0501542		105	0.3709535	0.9558232	-0.6564543	0.7976566	
>tr|A2EKU1|A2EKU1_TRIVA Phosphoenol pyruvate carboxykinase, putative OS=Trichomonas vaginalis GN=TVAG_310250 PE=3 SV=1;>tr|A2ETS2|A2ETS2_TRIVA Phosphoenol pyruvate carboxykinase, putative OS=Trichomonas vaginalis GN=TVAG_314830 PE=4 SV=1	1.0551971		106	0.4797779	0.9639456	-0.8628348	1.01786	
>tr|A2G583|A2G583_TRIVA Profilin, putative OS=Trichomonas vaginalis GN=TVAG_492250 PE=4 SV=1;>tr|A2GCC3|A2GCC3_TRIVA Profilin 1, putative OS=Trichomonas vaginalis GN=TVAG_159160 PE=4 SV=1	1.0567127		106	0.3832181	0.9519477	-0.6715105	0.8306769	
>tr|A2EIJ3|A2EIJ3_TRIVA Coronin OS=Trichomonas vaginalis GN=TVAG_124870 PE=3 SV=1;>tr|Q9NFT3|Q9NFT3_TRIVA Coronin (Fragment) OS=Trichomonas vaginalis GN=cor2 PE=3 SV=1	1.0723246		107	0.3634471	0.9279166	-0.6116016	0.813085	
>tr|A2E4A4|A2E4A4_TRIVA Phosphoenol pyruvate carboxykinase, putative OS=Trichomonas vaginalis GN=TVAG_139300 PE=3 SV=1;>tr|A2EYV2|A2EYV2_TRIVA Phosphoenol pyruvate carboxykinase, putative OS=Trichomonas vaginalis GN=TVAG_213710 PE=3 SV=1;>tr|A2ED62|A2ED62_	1.0833834		108	0.2689346	0.871854	-0.4115582	0.642646	
>tr|A2E0R3|A2E0R3_TRIVA Dihydroorotate dehydrogenase family protein OS=Trichomonas vaginalis GN=TVAG_468240 PE=4 SV=1;>tr|A2ELU8|A2ELU8_TRIVA Dihydroorotate dehydrogenase family protein OS=Trichomonas vaginalis GN=TVAG_151830 PE=4 SV=1	1.0848328		108	0.5866874	0.952798	-1.0324135	1.2673588	
>tr|Q27107|Q27107_TRIVA Clan CA, family C1, cathepsin L-like cysteine peptidase OS=Trichomonas vaginalis GN=CP2 PE=2 SV=1	1.0896006		109	0.2516932	0.8693111	-0.3695102	0.6171089	
>tr|A2DZL5|A2DZL5_TRIVA Fimbrin, putative OS=Trichomonas vaginalis GN=TVAG_351310 PE=4 SV=1	1.0905183		109	0.2772349	0.871854	-0.4183565	0.6683844	
>tr|A2F093|A2F093_TRIVA Phosphoglycerate kinase OS=Trichomonas vaginalis GN=TVAG_383940 PE=3 SV=1	1.0925976		109	0.4918714	0.9279166	-0.8362881	1.0918124	
>tr|A2DKH3|A2DKH3_TRIVA Alpha-actinin, putative OS=Trichomonas vaginalis GN=TVAG_190450 PE=4 SV=1;>tr|O96524|O96524_TRIVA Alpha-actinin OS=Trichomonas vaginalis GN=AACTI PE=2 SV=1;>tr|O77068|O77068_TRIVA Alpha actinin (Fragment) OS=Trichomonas vaginalis GN	1.1013096		110	0.1429272	0.8146335	-0.1409121	0.4193523	
>tr|O76307|O76307_TRIVA Endoplasmic reticulum heat shock protein 70 (Fragment) OS=Trichomonas vaginalis GN=HSP70 PE=3 SV=1;>tr|A2F7C5|A2F7C5_TRIVA Endoplasmic reticulum heat shock protein 70, putative OS=Trichomonas vaginalis GN=TVAG_092490 PE=3 SV=1	1.1014364		110	0.4081932	0.9003711	-0.6606577	0.9394302	
>tr|A2G3U5|A2G3U5_TRIVA Ornithine carbamoyltransferase family protein OS=Trichomonas vaginalis GN=TVAG_041310 PE=3 SV=1;>tr|A2EUY0|A2EUY0_TRIVA Ornithine carbamoyltransferase family protein OS=Trichomonas vaginalis GN=TVAG_368740 PE=3 SV=1	1.1092024		111	0.2330634	0.8684254	-0.3072731	0.6063186	
>tr|Q2PCA5|Q2PCA5_TRIVA A-type flavoprotein (Fragment) OS=Trichomonas vaginalis GN=fprA PE=2 SV=1;>tr|A2EVX8|A2EVX8_TRIVA Pyridine nucleotide-disulphide oxidoreductase family protein OS=Trichomonas vaginalis GN=TVAG_049830 PE=4 SV=1	1.1152881		112	0.3034077	0.8693111	-0.4372519	0.7520846	
>tr|A2ET60|A2ET60_TRIVA Ribosomal protein L7Ae, putative OS=Trichomonas vaginalis GN=TVAG_009840 PE=4 SV=1;>tr|A2EB73|A2EB73_TRIVA Ribosomal protein L7Ae, putative OS=Trichomonas vaginalis GN=TVAG_274830 PE=4 SV=1;>tr|A2DDW2|A2DDW2_TRIVA Ribosomal protein	1.129693		113	0.4168654	0.871854	-0.6411104	0.9929718	
>tr|A2DLF1|A2DLF1_TRIVA Aspartate aminotransferase OS=Trichomonas vaginalis GN=TVAG_268020 PE=3 SV=1;>tr|A2F7X5|A2F7X5_TRIVA Aminotransferase, classes I and II family protein OS=Trichomonas vaginalis GN=TVAG_431780 PE=4 SV=1	1.1312706		113	0.2696802	0.8684254	-0.3506194	0.7065075	
>tr|A2DGG1|A2DGG1_TRIVA Actinin, putative OS=Trichomonas vaginalis GN=TVAG_239310 PE=4 SV=1	1.1353147		114	0.1992777	0.8314036	-0.207485	0.5736694	
>tr|A2DAL5|A2DAL5_TRIVA Inhibitor of the eukaryotic translation initiation 5A OS=Trichomonas vaginalis GN=TVAG_035410 PE=2 SV=1	1.1475475		115	0.3451374	0.8693111	-0.477903	0.8750109	
>tr|A2EXE5|A2EXE5_TRIVA Ubiquitin-conjugating enzyme family protein OS=Trichomonas vaginalis GN=TVAG_406710 PE=4 SV=1	1.1593339		116	0.3920261	0.8693111	-0.5550609	0.9816532	
>tr|A2DDM9|A2DDM9_TRIVA 14-3-3 protein OS=Trichomonas vaginalis GN=TVAG_198430 PE=4 SV=1	1.1650559		117	0.4021504	0.8693111	-0.5678011	1.0085994	
>tr|A2FT29|A2FT29_TRIVA Triosephosphate isomerase OS=Trichomonas vaginalis GN=TVAG_096350 PE=1 SV=1;>tr|A2EGX9|A2EGX9_TRIVA Triosephosphate isomerase OS=Trichomonas vaginalis GN=TVAG_497370 PE=1 SV=1	1.1657967		117	0.2697069	0.8436018	-0.3072996	0.749932	
>tr|O97108|O97108_TRIVA Elongation factor 1-alpha (Fragment) OS=Trichomonas vaginalis GN=tef1 PE=2 SV=1;>tr|A2DSF6|A2DSF6_TRIVA Elongation factor 1-alpha OS=Trichomonas vaginalis GN=TVAG_067400 PE=3 SV=1;>tr|F8QX91|F8QX91_TRIVA Elongation factor 1-alpha (F	1.1687192		117	0.3716326	0.8693111	-0.5034581	0.9533148	
>tr|A2E264|A2E264_TRIVA Ribosomal protein S14, putative OS=Trichomonas vaginalis GN=TVAG_464120 PE=3 SV=1	1.1701668		117	0.4349363	0.8693111	-0.6257452	1.0791736	
>tr|A2EF58|A2EF58_TRIVA Pyrophosphate-dependent fructose 6-phosphate 1-phosphotransferase, putative OS=Trichomonas vaginalis GN=TVAG_079260 PE=4 SV=1	1.1794992		118	0.4456322	0.8693111	-0.6352486	1.1115974	
>tr|Q6UJG4|Q6UJG4_TRIVA Thioredoxin peroxidase OS=Trichomonas vaginalis GN=TPx PE=2 SV=1	1.189923		119	0.4643489	0.8693111	-0.6592388	1.1609753	
>tr|A2EIF8|A2EIF8_TRIVA Transketolase family protein OS=Trichomonas vaginalis GN=TVAG_212020 PE=4 SV=1	1.192419		119	0.2812326	0.8405953	-0.2973146	0.8050971	
>tr|A2FBC9|A2FBC9_TRIVA 4-alpha-glucanotransferase family protein OS=Trichomonas vaginalis GN=TVAG_157940 PE=4 SV=1	1.1927906		119	0.2631926	0.8146335	-0.2615073	0.7701888	
>tr|A2EUZ5|A2EUZ5_TRIVA Cysteine synthase OS=Trichomonas vaginalis GN=TVAG_368890 PE=3 SV=1;>tr|A2FS16|A2FS16_TRIVA Cysteine synthase OS=Trichomonas vaginalis GN=TVAG_337280 PE=3 SV=1;>tr|A2FS17|A2FS17_TRIVA Cysteine synthase OS=Trichomonas vaginalis GN=TV	1.1968731		120	0.6260215	0.871854	-0.9677094	1.4862498	
>tr|A2EZH8|A2EZH8_TRIVA Putative uncharacterized protein OS=Trichomonas vaginalis GN=TVAG_047990 PE=3 SV=1	1.2048318		120	0.3374242	0.8436018	-0.3925076	0.930171	
>tr|A2DUP2|A2DUP2_TRIVA Thiol peroxidase, putative OS=Trichomonas vaginalis GN=TVAG_165610 PE=3 SV=1	1.2059375		121	0.3665336	0.8668481	-0.4482375	0.9885477	
>tr|A2FS11|A2FS11_TRIVA Iron superoxide dismutase, putative OS=Trichomonas vaginalis GN=TVAG_337230 PE=3 SV=1;>tr|A2D7H9|A2D7H9_TRIVA Iron superoxide dismutase, putative OS=Trichomonas vaginalis GN=TVAG_120340 PE=3 SV=1;>tr|Q95053|Q95053_TRIVA Iron superox	1.2070851		121	0.4797849	0.8693111	-0.6688338	1.2118886	
>tr|Q717I9|Q717I9_TRIVA Malic enzyme OS=Trichomonas vaginalis PE=3 SV=1;>tr|A2G150|A2G150_TRIVA Malic enzyme OS=Trichomonas vaginalis GN=TVAG_009460 PE=3 SV=1	1.2218203		122	0.3633067	0.8436018	-0.4230359	1.0011001	
>tr|A2EFN8|A2EFN8_TRIVA Enolase OS=Trichomonas vaginalis GN=TVAG_487600 PE=3 SV=1	1.223358		122	0.4462505	0.8684254	-0.5837882	1.1654816	
>tr|A2E9H3|A2E9H3_TRIVA Pyrophosphate-dependent fructose 6-phosphate 1-phosphotransferase, putative OS=Trichomonas vaginalis GN=TVAG_364620 PE=4 SV=1	1.2373763		124	0.1697033	0.4123372	-0.0253281	0.6398967	
>tr|O15565|O15565_TRIVA Methionine gamma-lyase OS=Trichomonas vaginalis GN=mgl2 PE=1 SV=1;>tr|O15564|O15564_TRIVA Methionine gamma-lyase OS=Trichomonas vaginalis GN=mgl1 PE=1 SV=1;>tr|A2FEV4|A2FEV4_TRIVA Chain A, Methionine Gamma-Lyase OS=Trichomonas vagin	1.2375034		124	0.4441871	0.8684254	-0.5631582	1.1780233	
>tr|A2E0R0|A2E0R0_TRIVA Putative uncharacterized protein OS=Trichomonas vaginalis GN=TVAG_468210 PE=3 SV=1;>tr|A2DYC4|A2DYC4_TRIVA Putative uncharacterized protein OS=Trichomonas vaginalis GN=TVAG_393280 PE=3 SV=1	1.2397172		124	0.4409868	0.8684254	-0.5543072	1.1743294	
>tr|A2E269|A2E269_TRIVA Enolase 4, putative OS=Trichomonas vaginalis GN=TVAG_464170 PE=3 SV=1;>tr|Q9NDF7|Q9NDF7_TRIVA Enolase (Fragment) OS=Trichomonas vaginalis PE=3 SV=1	1.2415726		124	0.6546831	0.8693111	-0.9709866	1.5953239	
>tr|A2E7V8|A2E7V8_TRIVA Glucose-6-phosphate isomerase OS=Trichomonas vaginalis GN=TVAG_061930 PE=3 SV=1;>tr|Q8WRQ8|Q8WRQ8_TRIVA Glucose-6-phosphate isomerase (Fragment) OS=Trichomonas vaginalis GN=GPI PE=2 SV=1	1.2447895		124	0.2532562	0.7170755	-0.1804712	0.8122747	
>tr|A2G527|A2G527_TRIVA Adseverin, putative OS=Trichomonas vaginalis GN=TVAG_244120 PE=4 SV=1	1.2459519		125	0.5844837	0.8693111	-0.8283185	1.4628153	
>tr|A2E3Y1|A2E3Y1_TRIVA O-Glycosyl hydrolase family 30 protein OS=Trichomonas vaginalis GN=TVAG_074640 PE=4 SV=1	1.2661043		127	0.6688179	0.8693111	-0.9704627	1.6512552	
>tr|A2FNW2|A2FNW2_TRIVA Actin-binding protein, putative OS=Trichomonas vaginalis GN=TVAG_376130 PE=4 SV=1;>tr|A2DCW9|A2DCW9_TRIVA Actin-binding protein, putative OS=Trichomonas vaginalis GN=TVAG_237690 PE=4 SV=1	1.266346		127	0.3868026	0.8436018	-0.4174475	1.0987909	
>tr|A2F6T1|A2F6T1_TRIVA Fructose-1,6-bisphosphate aldolase OS=Trichomonas vaginalis GN=TVAG_043170 PE=4 SV=1;>tr|A2F6S0|A2F6S0_TRIVA Fructose-1,6-bisphosphate aldolase OS=Trichomonas vaginalis GN=TVAG_043060 PE=4 SV=1	1.2722262		127	0.4512183	0.8555142	-0.5370165	1.2317268	
>tr|A2EU51|A2EU51_TRIVA 14-3-3 protein OS=Trichomonas vaginalis GN=TVAG_454380 PE=4 SV=1	1.280531		128	0.4580471	0.8539863	-0.5410137	1.2544981	
>tr|A2FH97|A2FH97_TRIVA Aldose 1-epimerase OS=Trichomonas vaginalis GN=TVAG_123260 PE=3 SV=1	1.2923294		129	0.6490362	0.8693111	-0.9021138	1.6420614	
>tr|A2E7Y6|A2E7Y6_TRIVA Purine nucleoside phosphorylase, putative OS=Trichomonas vaginalis GN=TVAG_127180 PE=1 SV=1	1.2936384		129	0.5251244	0.8684254	-0.6577906	1.4006593	
>tr|A2F8R8|A2F8R8_TRIVA WD repeat protein, putative OS=Trichomonas vaginalis GN=TVAG_333620 PE=4 SV=1	1.2976581		130	0.3279769	0.7394676	-0.2669126	1.0187333	
>sp|P51540|SAHH_TRIVA Adenosylhomocysteinase OS=Trichomonas vaginalis PE=3 SV=1;>tr|A2E342|A2E342_TRIVA Adenosylhomocysteinase OS=Trichomonas vaginalis GN=TVAG_405240 PE=3 SV=1;>tr|A2DVT9|A2DVT9_TRIVA Adenosylhomocysteinase OS=Trichomonas vaginalis GN=TVAG	1.298889		130	0.4655187	0.8436018	-0.5351217	1.289678	
>tr|A2EAJ8|A2EAJ8_TRIVA Malic enzyme OS=Trichomonas vaginalis GN=TVAG_491670 PE=3 SV=1	1.3009523		130	0.2316284	0.4769444	-0.0744153	0.8335513	
>tr|A2DEJ9|A2DEJ9_TRIVA 40S ribosomal protein S6 OS=Trichomonas vaginalis GN=TVAG_033590 PE=3 SV=1	1.3050167		131	0.756156	0.8693111	-1.0979702	1.8661068	
>tr|A2EU62|A2EU62_TRIVA Purine nucleoside phosphorylase, putative OS=Trichomonas vaginalis GN=TVAG_454490 PE=3 SV=1	1.3075246		131	0.5167171	0.8622757	-0.6259087	1.3995849	
>tr|A2FW50|A2FW50_TRIVA Phosphoglucomutase/phosphomannomutase, alpha/beta/alpha domain I family protein OS=Trichomonas vaginalis GN=TVAG_205910 PE=3 SV=1	1.313983		131	0.2652536	0.5744396	-0.1259408	0.9138341	
>tr|A2FLK9|A2FLK9_TRIVA Fructose-1,6-bisphosphate aldolase, putative OS=Trichomonas vaginalis GN=TVAG_360700 PE=4 SV=1	1.3261881		133	0.6990883	0.8693111	-0.9629025	1.7774733	
>tr|A2GB88|A2GB88_TRIVA Putative uncharacterized protein OS=Trichomonas vaginalis GN=TVAG_259540 PE=3 SV=1;>tr|A2F6E3|A2F6E3_TRIVA Putative uncharacterized protein OS=Trichomonas vaginalis GN=TVAG_139990 PE=3 SV=1;>tr|A2EWU2|A2EWU2_TRIVA Putative uncharact	1.3564496		136	0.4062609	0.7712614	-0.3564212	1.2360921	
>sp|Q9GTW9|GLK1_TRIVA Glucokinase 1 OS=Trichomonas vaginalis GN=GK1 PE=1 SV=1;>tr|A2FTT2|A2FTT2_TRIVA Putative uncharacterized protein OS=Trichomonas vaginalis GN=TVAG_092750 PE=4 SV=1	1.3649651		136	0.2522698	0.4157582	-0.0455756	0.9433038	
>tr|A2HV24|A2HV24_TRIVA Glucosylceramidase, putative (Fragment) OS=Trichomonas vaginalis GN=TVAG_593180 PE=4 SV=1;>tr|A2HQ10|A2HQ10_TRIVA Glucosylceramidase, putative OS=Trichomonas vaginalis GN=TVAG_508090 PE=4 SV=1;>tr|A2HAT7|A2HAT7_TRIVA Glucosylceramid	1.3659534		137	0.3911513	0.7394676	-0.3167342	1.2165508	
>tr|A2G4P3|A2G4P3_TRIVA Nucleoside diphosphate kinase OS=Trichomonas vaginalis GN=TVAG_293370 PE=3 SV=1;>tr|A2DTU7|A2DTU7_TRIVA Nucleoside diphosphate kinase OS=Trichomonas vaginalis GN=TVAG_341380 PE=3 SV=1	1.367075		137	0.5600389	0.8436018	-0.6465637	1.5487484	
>tr|A2EDB3|A2EDB3_TRIVA Putative uncharacterized protein OS=Trichomonas vaginalis GN=TVAG_417930 PE=4 SV=1	1.3780585		138	0.5528898	0.8436018	-0.6210069	1.5462811	
>tr|A2DJ40|A2DJ40_TRIVA Alcohol dehydrogenase 1, putative OS=Trichomonas vaginalis GN=TVAG_228780 PE=3 SV=1;>tr|Q8MV15|Q8MV15_TRIVA Alcohol dehydrogenase 1 (Fragment) OS=Trichomonas vaginalis PE=3 SV=1	1.3842103		138	0.3973271	0.7394676	-0.3096838	1.24781	
>tr|A2EL72|A2EL72_TRIVA Clan MH, family M20, peptidase T-like metallopeptidase OS=Trichomonas vaginalis GN=TVAG_056190 PE=4 SV=1	1.4001214		140	0.3189281	0.5464669	-0.1395357	1.1106395	
>tr|A2FZ05|A2FZ05_TRIVA 60S ribosomal protein L6, putative OS=Trichomonas vaginalis GN=TVAG_303050 PE=4 SV=1;>tr|A2D7E3|A2D7E3_TRIVA Putative uncharacterized protein OS=Trichomonas vaginalis GN=TVAG_119970 PE=4 SV=1;>tr|A2FXW1|A2FXW1_TRIVA 60S ribosomal pr	1.4019637		140	0.8600052	0.8693111	-1.1981301	2.1730282	
>tr|A2EBB4|A2EBB4_TRIVA Enolase 2, putative OS=Trichomonas vaginalis GN=TVAG_329460 PE=3 SV=1	1.4043652		140	0.4890349	0.8146335	-0.4685726	1.4484089	
>tr|A2EZN6|A2EZN6_TRIVA Clan MH, family M20, peptidase T-like metallopeptidase OS=Trichomonas vaginalis GN=TVAG_090090 PE=4 SV=1	1.4229122		142	0.3864132	0.6747868	-0.2485094	1.2662026	
>tr|A2F397|A2F397_TRIVA Putative uncharacterized protein OS=Trichomonas vaginalis GN=TVAG_180840 PE=4 SV=1	1.4252154		143	0.4174094	0.7279476	-0.3069274	1.3292875	
>tr|Q9BKK1|Q9BKK1_TRIVA Actin type 6 OS=Trichomonas vaginalis PE=3 SV=1;>tr|P90623|P90623_TRIVA Actin OS=Trichomonas vaginalis GN=TVAG_337240 PE=3 SV=1;>tr|A2G1K5|A2G1K5_TRIVA Actin OS=Trichomonas vaginalis GN=TVAG_054030 PE=3 SV=1;>tr|A2FA04|A2FA04_TRIVA	1.4384		144	0.2755505	0.3782872	-0.0156041	1.0645339	
>tr|A2DAU3|A2DAU3_TRIVA NAC domain containing protein OS=Trichomonas vaginalis GN=TVAG_036210 PE=4 SV=1	1.4511279		145	0.4760054	0.7479067	-0.3957788	1.4701282	
>tr|A2EKG5|A2EKG5_TRIVA Putative uncharacterized protein OS=Trichomonas vaginalis GN=TVAG_340510 PE=4 SV=1	1.4807467		148	0.4857056	0.7394676	-0.3856406	1.5182904	
>tr|A2FJ30|A2FJ30_TRIVA Malate dehydrogenase, putative OS=Trichomonas vaginalis GN=TVAG_204360 PE=4 SV=1	1.4868457		149	0.3408335	0.4608702	-0.0957664	1.2402763	
>tr|Q6IV59|Q6IV59_TRIVA Thioredoxin OS=Trichomonas vaginalis GN=Trx1 PE=3 SV=1	1.524728		152	0.4311807	0.6281555	-0.2365468	1.4536505	
>tr|A2EIR1|A2EIR1_TRIVA Putative uncharacterized protein OS=Trichomonas vaginalis GN=TVAG_499760 PE=3 SV=1;>tr|A2DXP9|A2DXP9_TRIVA Putative uncharacterized protein OS=Trichomonas vaginalis GN=TVAG_411440 PE=3 SV=1;>tr|A2DQV0|A2DQV0_TRIVA Putative uncharact	1.5251615		153	0.5532874	0.7605859	-0.4754614	1.6933854	
>tr|Q27819|Q27819_TRIVA Cytosolic malate dehydrogenase OS=Trichomonas vaginalis PE=4 SV=1;>tr|A2DMN2|A2DMN2_TRIVA Malate dehydrogenase OS=Trichomonas vaginalis GN=TVAG_253650 PE=4 SV=1	1.5542326		155	0.322736	0.3782872	0.0036516	1.2687533	
>tr|A2DPV5|A2DPV5_TRIVA Putative uncharacterized protein OS=Trichomonas vaginalis GN=TVAG_453790 PE=4 SV=1	1.5583175		156	0.4885817	0.6747868	-0.3176134	1.5975918	
>tr|A2FWR9|A2FWR9_TRIVA Ribosomal protein S3Ae, putative OS=Trichomonas vaginalis GN=TVAG_142060 PE=4 SV=1;>tr|A2FDS0|A2FDS0_TRIVA Ribosomal protein S3Ae, putative OS=Trichomonas vaginalis GN=TVAG_414510 PE=4 SV=1;>tr|A2DSV0|A2DSV0_TRIVA Ribosomal protein	1.5645983		156	0.7252938	0.8436018	-0.7757574	2.0673421	
>tr|A2E6S8|A2E6S8_TRIVA RNA-binding protein, putative OS=Trichomonas vaginalis GN=TVAG_158990 PE=4 SV=1;>tr|Q9UAB6|Q9UAB6_TRIVA RNA-binding protein OS=Trichomonas vaginalis GN=rbp1 PE=2 SV=1	1.5712674		157	0.5481075	0.7394676	-0.4223422	1.7261996	
>tr|A2ENX0|A2ENX0_TRIVA Flavodoxin family protein OS=Trichomonas vaginalis GN=TVAG_216360 PE=4 SV=1	1.5811978		158	0.825488	0.8436018	-0.9569089	2.2789446	
>tr|A2FAF3|A2FAF3_TRIVA Fructose-1,6-bisphosphate aldolase, putative OS=Trichomonas vaginalis GN=TVAG_300000 PE=4 SV=1	1.6176457		162	0.4454756	0.5236977	-0.1792204	1.5670117	
>tr|A2FSC5|A2FSC5_TRIVA Clan MG, familly M24, aminopeptidase P-like metallopeptidase OS=Trichomonas vaginalis GN=TVAG_386080 PE=3 SV=1;>tr|A2FCF5|A2FCF5_TRIVA Clan MG, familly M24, aminopeptidase P-like metallopeptidase OS=Trichomonas vaginalis GN=TVAG_437	1.6214418		162	0.7547799	0.8314036	-0.7820643	2.1766187	
>tr|A2ELE4|A2ELE4_TRIVA Putative uncharacterized protein OS=Trichomonas vaginalis GN=TVAG_358360 PE=4 SV=1;>tr|A2F0E1|A2F0E1_TRIVA Putative uncharacterized protein OS=Trichomonas vaginalis GN=TVAG_292690 PE=4 SV=1	1.6233441		162	0.3525139	0.3782872	0.0080543	1.3898834	
>tr|A2FHW2|A2FHW2_TRIVA Phosphoglucomutase/phosphomannomutase, alpha/beta/alpha domain I family protein OS=Trichomonas vaginalis GN=TVAG_054830 PE=3 SV=1	1.7433918		174	0.5744644	0.6281555	-0.3240328	1.9278265	
>tr|E5FCB6|E5FCB6_TRIVA Putative actin depolymerizing factor (Fragment) OS=Trichomonas vaginalis GN=ADF PE=4 SV=1;>tr|E5FCB5|E5FCB5_TRIVA Putative actin depolymerizing factor (Fragment) OS=Trichomonas vaginalis GN=ADF PE=4 SV=1;>tr|E5FCB4|E5FCB4_TRIVA Puta	1.7969574		180	0.4502146	0.3782872	-0.0368481	1.7279606	
>tr|O61068|O61068_TRIVA Pyrophosphate-dependent fructose 6-phosphate 1-phosphotransferase OS=Trichomonas vaginalis GN=Pfk1 PE=4 SV=1	1.8390307		184	0.462522	0.3782872	-0.0275809	1.7854719	
>tr|A2E4D0|A2E4D0_TRIVA Ribosomal protein, putative OS=Trichomonas vaginalis GN=TVAG_128790 PE=4 SV=1;>tr|A2E1Z6|A2E1Z6_TRIVA Ribosomal protein, putative OS=Trichomonas vaginalis GN=TVAG_164550 PE=4 SV=1;>tr|A2DAA4|A2DAA4_TRIVA Ribosomal protein, putative	1.8402456		184	0.516245	0.4608702	-0.1319234	1.89172	
>tr|A2F8Y2|A2F8Y2_TRIVA Clan MG aminopeptidase P-like metallopeptidase OS=Trichomonas vaginalis GN=mp50 PE=2 SV=1	1.9495192		195	0.7223071	0.6723885	-0.4525775	2.3788143	
>tr|A2EAY1|A2EAY1_TRIVA EF hand family protein OS=Trichomonas vaginalis GN=TVAG_118780 PE=4 SV=1	1.9759311		198	0.417313	0.1937585	0.1646141	1.8004512	
>tr|A2G4E1|A2G4E1_TRIVA Ribosomal protein L13e, putative OS=Trichomonas vaginalis GN=TVAG_112230 PE=4 SV=1;>tr|A2DTH0|A2DTH0_TRIVA Ribosomal protein L13e, putative OS=Trichomonas vaginalis GN=TVAG_423320 PE=4 SV=1;>tr|A2DKF7|A2DKF7_TRIVA Ribosomal protein	2.4124446		241	0.4749457	0.1080591	0.3396194	2.2013723	
>tr|A2FC75|A2FC75_TRIVA 40S ribosomal protein S4-C, putative OS=Trichomonas vaginalis GN=TVAG_335480 PE=3 SV=1;>tr|A2DBB7|A2DBB7_TRIVA 40S ribosomal protein S4-C, putative OS=Trichomonas vaginalis GN=TVAG_131210 PE=3 SV=1;>tr|A2ECC6|A2ECC6_TRIVA 40S riboso	3.051863		305	0.4298493	0.0056573	0.7672011	2.4521793	
>tr|A2FFS8|A2FFS8_TRIVA 40S ribosomal protein S21 OS=Trichomonas vaginalis GN=TVAG_022100 PE=3 SV=1;>tr|A2GYE6|A2GYE6_TRIVA 40S ribosomal protein S21 OS=Trichomonas vaginalis GN=TVAG_459980 PE=3 SV=1	3.2930712		329	0.6624341	0.1183369	0.4210867	3.0177807	
>tr|A2DXL4|A2DXL4_TRIVA TolA, putative OS=Trichomonas vaginalis GN=TVAG_411090 PE=4 SV=1	4.4166183		442	0.3614639	5.747E-07	1.4344859	2.8513984	

Table 2-S2: Total list of proteins identified in stable isotope dimethyl labeling quantitative proteomics experiments.

188 total proteins were identified. 17 protein groups were decreased by more than 50%, 7 protein groups were statistically significantly decreased (adj p-val <0.05) upon 3,4-DCI treatment *vs*. DMSO (yellow or pink highlighting). 5 proteins were significantly decreased and had a TM domain (pink highlighting)-2 proteins belong to the same protein group-both counted individually as a putative substrate.

Rhomboid Substrate:	P4	P3	P2	P1	P1'	P2'	P3'
Dm Spitz	L	E	K	A	S	I	A
Pf AMA-1	I	I	I	A	S	S	A
Pf EBA-175	P	Y	Y	A	G	A	G
Pf BAEBL	P	Y	F	A	A	G	G
Pf JESEBL	H	Y	I	A	G	G	G
Pf MAEBL	V	Y	F	A	G	A	G
Pf Rh1	M	Y	F	A	S	G	I
Pf Rh2a	I	Y	T	A	G	S	V
Pf Rh2b	V	Y	N	A	G	G	V
Pf Rh4	I	F	Y	A	G	G	I
Pf TRAP	Y	K	I	A	G	G	I
Pf CTRP	A	L	A	A	G	V	I
Pf MTRAP	L	Y	I	A	S	G	V
Pf PFF0800c	Y	A	A	S	F	T	L
EHI_044650	A	A	I	A	A	G	T
Tg MIC2	G	A	I	A	G	G	V
TgMIC6	G	A	I	A	G	G	V
Tg MIC12	A	A	I	A	G	G	V
Tg MIC 8	G	I	I	A	G	G	I
Tg MIC16	T	Y	A	V	A	G	G
TgAMA1	A	L	I	A	G	L	A
parasite search motif	[AGIP]	[YALI]	[IAFY]	[A]	[GSA]	[GAS]	[VGIA]

Table 2-S3: Amino acid comparison used to generate a parasite rhomboid substrate search motif.

Table shows the predicted and established (Spitz, PfAMA1, EBA-175, TgMIC2, TgMIC6, TgAMA1), P4-P3'amino acids of parasite proteins that can be cleaved by rhomboids and the canonical rhomboid substrate Spitz. To generate the table, the predicted TM and rhomboid cleavage sites found in [30-32, 39, 43, 44, 51, 92] were compiled and aligned around the small P1-P1' residues where cleavage occurs or is predicted to take place. The cleavage site of the following substrates has been mapped as listed, Spitz by [49], PfAMA1 by [43], EBA-175 by [44], TgMIC2 by [40], TgMIC6 by [39], and TgAMA1 by [41]. Strisovsky *et al*. 2009 found that the P4, P1, and P2' sites (highlighted in yellow) in the bacterial TatA rhomboid substrate were the most sensitive to mutations [33]. We generated a parasite search motif based on the most commonly appearing amino acids (shown graphically in Fig. 2-5A)

1	2	3	4	5	6	7	8	9	10	11	12	13	14	15
[Gene]	[Product Description]	[# TM Domains]	[SignalP Peptide]	[Predicted GO Function]	[Predicted GO Process]	[Predicted GO Component]	candidate substrate?	TM predicted by TrichDB	predicted Trich DB orientation	TM predicted by Spoctopus	predicted Spoctopus orientation	TM predicted by Phobius	predicted Phobius orientation	comments
TVAG_166850	conserved hypothetical protein	1	null	calcium ion binding	homophilic cell adhesion	membrane	yes	MLII**GLAAGGV**AAAAVVAAAIII	outside-TM-inside	II**GLAAGGV**AAAAVVAAAIII	inside-TM-outside	MLII**GLAAGGV**AAAAVVAAAIII	outside-TM-inside	previously shown to increase adherence of *T. vaginalis* to ectocervical cells in de Miguel *et al.* Mol Cell Proteomics 2010
TVAG_122850	hypothetical protein	8	NN: MSIPGGDLAGVLGNAGVAGAAGAAAG	null	null	null	no-motif is not in the right location and orientation based on predicted topology (motif starts from the middle to the top of TM1)	(1)AGVAGAA**GAAAGSG**VVSAVGAQF (2)IFYAWAIVSMVFFIFWLI (3)GTIWNLWVYGLVTAITLLYLPSI (4)WIHFAVAMVHFLFIGLYLPFQVY (5)WSAYKVITMVVKMLLIIPLIPLF (6)ACVSLAIVTVYALCSIISSPFIL (7)WIDLSARITAVCTIVLQICVI (8)LSVVNFANLGIMIIIFLSNLQFV	inside-TM1-o-TM2-i-TM3-o-TM4-i-TM5-o-TM6-i-TM7-o-TM8-inside	(1)VWQFVMGITELQIFYAWAIVSMVFFIFWLI (2)WNLWVYGLVTAITLLYLPSIT (3)WIHFAVAMVHFLFIGLYLPFQ (4)GWSAYKVITMVVKMLLIIPLIP (5)ALAPACVSLAIVTVYALCSII (6)LSARITAVCTIVLQICVIKDV (7)LSVVNFANLGIMIIIFLSNLQ	outside-TM1-i-TM2-o-TM3-i-TM4-o-TM5-i-TM6-o-TM7-inside	(1)LFHKFMDFVSLVWQFVMGI (2)FYAWAIVSMVFFIFWLIQ (3)LWVYGLVTAITLLYLPSITSGFKV I(4)WIHFAVAMVHFLFIGLYLPFQVYLTI (5)VITMVVKMLLIIPLIPLFTAALA (6)LAIVTVYALCSIISSPFIL (7)ITAVCTIVLQICVIKDVLYP (8)FANLGIMIIIFLSNLQFVKVFF	inside-TM1-o-TM2-i-TM3-o-TM4-i-TM5-o-TM6-i-TM7-o-TM8-inside	
TVAG_465250	Clan SB, family S8, subtilisin-like serine peptidase	1	null	subtilase activity	proteolysis	null	no-missing last residue in motif (green font)	I**ALIASG**SVVFVCIVCLVVIL	outside-TM-inside	(1)a**IIASG**SVVFVCIVCLVVILCVK	outside-TM-inside	I**ALIASG**SVVFVCIVCLVVILCV	outside-TM1-inside	
TVAG_460770	conserved hypothetical protein	4	NN: MALNGKCLRWVIIIINILIVIAAVIAC	null	null	integral to membrane	possible multiple TM substrate? motif is present in top part of TM4 by TrichDb, Spoctopus, and Phobius TM predictions	(1)IIIINILIVIAAVIACAVVYTRI (2)YPFFAILAVCAAVCIIGVFLICC (3)IFYVVCLFLVLIVEIIILICMFL (4)MY**GLAAAAI**VIIVFELALIVISC	inside-TM1-o-TM2-i-TM3-o-TM4-inside	(1)VIIIINILIVIAAVIACAVVY (2)PFFAILAVCAAVCIIGVFLIC (3)AIFYVVCLFLVLIVEIIILIC (4)**gLAAAAI**VIIVFELALIVISCM	outside-TM1-i-TM2-o-TM3-i-TM4-outside	(1)CLRWVIIIINILIVIAAVIACAVVYT (2)ALYPFFAILAVCAAVCIIGVFLIC (3)AIFYVVCLFLVLIVEIIILICMFLL (4)**gLAAAAIV**IIVFELALIVISCMYAC	inside-TM1-o-TM2-i-TM3-outside	
TVAG_399430	conserved hypothetical protein	6	NN: MRKITVIPTVTALLVLLLGVAY	null	null	null	no-motif is not in the right location for rhomboid cleavage based on predicted topology (motif is at bottom of TM4 opposite of where rhomboid cleavage should occur in the top of TM)	(1)TVIPTVTALLVLLLGVAYFRIPT (2)MIPGIIGLVFMIVVISLMLGRYF (3)FYRYAIIVISFFLEAVLIYGYFA (4)LVIIFNLILSTIGCSL**GIAAGSV** (5)LIMVILFAISDCLFFFSFGIHLA (6)MMITQFAGSILLVILTILGIPAI	inside-TM1-o-TM2-i-TM3-o-TM4-i-TM5-o-TM6-inside	(1)VIPTVTALLVLLLGVAYFRIP (2)YIMIPGIIGLVFMIVVISLML (3)FYRYAIIVISFFLEAVLIYGY (4)RMLVIIFNLILSTIGCSLGIAA (5)SPVLIMVILFAISDCLFFFSF (6)MITQFAGSILLVILTILGIPA		(1)IMYIMIPGIIGLVFMIVVISLMLGRYF (2)FYRYAIIVISFFLEAVLIYGYF (3)IFRMLVIIFNLILSTIGCSLGI (4)LIMVILFAISDCLFFFSFGIHLA (5)LYMMMITQFAGSILLVILTILGI	outside-TM1-i-TM2-o-TM3-i-TM4-o-TM5-inside	
TVAG_127290	conserved hypothetical protein	6	NN: MKTRSMTNSLFILLFAFIGSYLVYEGYAK	null	null	null	no-no motif found in TM domains	(1)TNSLFILLFAFIGSYLVY (2)LVNIILCAAVGLLFTFIFLIVLS (3)GCLLIFAFILEFLLIYSFFV (4)IRMLVVILALGSCTIACTFGIAA (5)WPVWIMVIMSIILFPFIWASFAF (6)TLSQCVASLFLIFICSTGIGSIL	inside-TM1-o-TM2-i-TM3-o-TM4-i-TM5-o-TM6-inside	(1)NIILCAAVGLLFTFIFLIVLS (2)RGCLLIFAFILEFLLIYSFFV (3)RGCLLIFAFILEFLLIYSFFV (4)IRMLVVILALGSCTIACTFGI (5)PVWIMVIMSIILFPFIWASFA	outside-TM1-i-TM2-o-TM3-i-TM4-o-TM5-inside	(1)LVNIILCAAVGLLFTFIFLIVLSCKFCC (2)SRGCLLIFAFILEFLLIYSFF (3)IRMLVVILALGSCTIACTFGIAA (4)WPVWIMVIMSIILFPFIWASFAFHF	outside-TM1-i-TM2-o-TM3-i-TM4-o-TM5-inside	
TVAG_498870	conserved hypothetical protein	1	null	null	null	null	no-motif is not in the right location for rhomboid cleavage based on predicted TrichDB and Phobius topology (motif is at bottom of TM opposite of where rhomboid cleavage should occur in the top of TM)	WIYIGAGIAVGVAA**IAAAAI**IAY	outside-TM-inside	IGAGIAVGVAA**IAAAAI**IAYE	inside-TM-outside	WIYIGAGIAVGVAA**IAAAAI**IAY	outside-TM-inside	
TVAG_034240	ctl transporter, putative	10	null	null	null	null	possible multiple TM substrate? by TrichDB and Phobius has 10 TMs-motif is in the top part of TM 10, by Spoctopus prediction has 12 TMs-motif is in top part of TM12	(1)CFCAIVFLILFGCMIALLVIGVL (2)WQILACSAASLIVGLVWIML (3)CIVYFVVMLVPIALIGFGVWLFM (4)SQITAVIVWVIAFMVILIIIFLW (5)FMVIFVPIITMIFAFLLWAALLV (6)VLQYMLIYNFVYLVFISVHMYFV (7)YFTGQEGKTCCGCTCFYGFWLAW (8)LGTITISSLIMTPLYLFIIF (9)ISFFILFLSKVVVSIITTLGFMI (10) IAGS**ILAAAAV**FFLSYIVSSFLL	inside-TM1-o-TM2-i-TM3-o-TM4-i-TM5-o-TM6-i-TM7-o-TM8-i-TM9-o-TM10-inside	(1)CFCAIVFLILFGCMIALLVIG (2)QILACSAASLIVGLVWIMLLR (3)ITGCIVYFVVMLVPIALIGFG (4)ITAVIVWVIAFMVILIIIFLW (5)NFMVIFVPIITMIFA (6)LLWAALLVSSVTLYT (7)LQYMLIYNFVYLVFI (8)VHMYFVNYYASSVTL (9)WTKGLGTITISSLIMTPLYLF (10)QFLIKCLKCCLWCFTKIVQYL (11)ISFFILFLSKVVVSIITTLGF (12)S**ILAAAAV**FFLSYIVSSFLLSAFDNIIDIVF	inside-TM1-o-TM2-i-TM3-o-TM4-i-TM5-o-TM6-i-TM7-o-TM8-i-TM9-o-TM10-i-TM11-o-TM12-inside	(1)CFCAIVFLILFGCMIALLVIGVL (2)WQILACSAASLIVGLVWIMLL (3)IVYFVVMLVPIALIGFGVWLFM (4)SQITAVIVWVIAFMVILIIIFLW (5)FMVIFVPIITMIFAFLLWAAL (6)MLIYNFVYLVFISVHMYFV (7)WYFTGQEGKTCCGCTCFYGFW (8)GLGTITISSLIMTPLYLFIIF (9)FFILFLSKVVVSIITTLGFMIWVYY (10)IAGS**ILAAAAV**FFLSYIVSSFLL		
TVAG_453250	adenylate and guanylate cyclases, putative	13	null	phosphorus-oxygen lyase activity, signal transducer activity	cyclic nucleotide biosynthetic process, intracellular signaling cascade, signal transduction	null	no-motif is present in TM6 but is located at the bottom of TM domain based on Spoctopus predicted topology, by Phobius the motif is present in TM8 but also located at the bottom of TM domain based on predicted topology	(1)ILFDYVTTASPPYYFLHVIFSIW (2)ATPYFMLIFSCLFIVFYIFIII (3)VFFGTAGYILPPIACEMAAETIG (4)IIGIILVVFTVSVYVWLVAAIYS (5)IVPSVQVSVILVTLTLYTITGVA (6)LYPRVVFTLLGAVVYLSTLFATN (7)AIFASSISGIILLCICVIFELVN (8)EYVILAILALWIIIYFVCNFYLE (9)IVFILLFLICFLLPVVVLAAIIP (10)YIMIFGSAFIFIVYMIAAYFIVK (11)IVCVTFLMLTNIASICVLGSFII (12)YMMAAYMFEFSSVVAMNLAACHF (13)AIIGGAFAILFVGLIFEAVILGL	inside-TM1-o-TM2-i-TM3-o-TM4-i-TM5-o-TM6-i-TM7-o-TM8-i-TM9-o-TM10-i-TM11-o-TM12-i-TM13-outside	(1) YFLHVIFSIWRILQFFGPSFC (2)PYFMLIFSCLFIVFYIFIIIC (3)VPPILTVFFGTAGYILPPIAC (4)AMNIIGIILVVFTVSVYVWLV (5)YPRVVFTLLGAVVYLSTLFAT (6)KK**AIFASSI**SGIILLCICVIF (7)KEYVILAILALWIIIYFVCNF (8)ARIVFILLFLICFLLPVVVLA (9)TKYIMIFGSAFIFIVYMIAAY (10)ITIIVCVTFLMLTNIASICVL (11)IGGAFAILFVGLIFEAVILGLL	outside-TM1-i-TM2-o-TM3-i-TM4-o-TM5-i-TM6-o-TM7-i-TM8-o-TM9-i-TM10-o-TM11-inside	(1)YFLHVIFSIWRILQFFGPSFC (2)TMSTVNDVLSFFFSIVPASF (3)PYFMLIFSCLFIVFYIFIIICA (4)VVPPILTVFFGTAGYILPPIA (5)NAMNIIGIILVVFTVSVYVWLVAAIYSV (6)IVPSVQVSVILVTLTLYTIT (7)VVFTLLGAVVYLSTLFATNQY (8)**aIFASSI**SGIILLCICVIFELVN (9)YVILAILALWIIIYFVCNFYL (10)IVFILLFLICFLLPVVVLAAII (11)YIMIFGSAFIFIVYMIAAYFIV (12)ITIIVCVTFLMLTNIASICVLGSFII (13)YMFEFSSVVAMNLAACHFSGYGVA (14)AIIGGAFAILFVGLIFEAVILGLL	outside-TM1-i-TM2-o-TM3-i-TM4-o-TM5-i-TM6-o-Tm7-i-TM8-o-TM9-i-TM10-o-TM11-i-TM12-o-TM13-i-TM14-outside	
TVAG_189150	conserved hypothetical protein	1	null	null	null	null	yes	**pAIAGGI**VAALVVVALVVVGVIFY	outside-TM-inside	**paIAGGI**VAALVVVALVVVGVIF	outside-TM-inside	**pAIAGGI**VAALVVVALVVVGVIFY	outside-TM-inside	*T. gondii* MIC2 also has AIAGG, *P.falciparum* TRAP also has IAGGIV; annotated as Immuno-dominant variable surface antigen-like by NCBI [Trichomonas vaginalis G3]
TVAG_299950	adenylate cyclase, putative	13	null	phosphorus-oxygen lyase activity	cyclic nucleotide biosynthetic process, intracellular signaling cascade	null	no-by TichDB prediction has motif in top part of TM12, by Spoctopus and Phobius prediction the motif is at the bottom of TM11 (opposite of where rhomboid cleavage should occur in the top of TM)	(1)WFLAFVAFYIMLQILIIAFWVYT (2)MYRTLIVSLFAFFWVFFVIY (3)LLYITSLIVDILVPVFITPSAYV (4)TIIGEIIIGFISYGITLMNFSIT (5)SSIVVWTISTTLCCILSAILTYF (6)TQIIVIVIHAIISCYLCYRLLFI (7)ASVLAFAITSIVLDIYSILMQLI (8)YEYIPFILIGSLIISFIFASIFY (9)NLTILANSILVVCFSIFIAYYAY (10)FRYMSLALDKTYYASFVLTLEWA (11)LWTGIGGGIVLFVTFIPMIIIII (12)ISIF**IYFASAA**LITVLYCLSGLY (13)LVIELLISLFLFILPLFIRAVIW	inside-TM1-o-TM2-i-TM3-o-TM4-i-TM5-o-TM6-i-TM7-o-TM8-i-TM9-o-TM10-i-TM11-o-TM12-i-TM13-outside	(1)WFLAFVAFYIMLQILIIAFWV (2)NMYRTLIVSLFAFFWVFFVIY (3)LLYITSLIVDILVPVFITPSA (4)IIGEIIIGFISYGITLMNFSI (5)IVVWTISTTLCCILSAILTYF (6)TQIIVIVIHAIISCYLCYRLL (7)ASVLAFAITSIVLDIYSILMQ (8)EYIPFILIGSLIISFIFASIF (9)NLTILANSILVVCFSIFIAYY (10)WTGIGGGIVLFVTFIPMIIII (11)EISIF**IYFASAA**LITVLYCLS (12)LTIYLVIELLISLFLFILPLF	inside-TM1-o-TM2-i-TM3-o-TM4-i-TM5-o-TM6-i-TM7-o-TM8-i-TM9-o-TM10-i-TM11-o-TM12-inside	(1)WFLAFVAFYIMLQILIIAFWVY (2)MYRTLIVSLFAFFWVFFVIY (3)LLYITSLIVDILVPVFITPSAYV (4)IIIGFISYGITLMNFSITTTL (5)IVVWTISTTLCCILSAILTYF (6)IIVIVIHAIISCYLCYRLLF (7)VLAFAITSIVLDIYSILMQLIK (8)YIPFILIGSLIISFIFASIFY (9)LTILANSILVVCFSIFIAYYAY (10)VWLWTGIGGGIVLFVTFIPMIIIIINYY (11)IF**IYFASAA**LITVLYCLSGLYTYY (12)IYLVIELLISLFLFILPLFIRAVI	inside-TM1-o-TM2-i-TM3-o-TM4-i-TM5-o-TM6-i-TM7-o-TM8-i-TM9-o-TM10-i-TM11-o-TM12-inside	
TVAG_280090	conserved hypothetical protein	1	null	calcium ion binding	homophilic cell adhesion	membrane	yes	MIII**GAAAGGV**AAVAVVAAAVLI	outside-TM-inside	II**GAAAGGV**AAVAVVAAAVLI	inside-TM-outside	NKKKMIII**GAAAGGV**AAVAVVAAAVLI	outside-TM-inside	similar to TVAG_166850 and TVAG_244130
TVAG_244130	conserved hypothetical protein	1	null	null	null	null	yes	YLII**GIAAAAV**VAAAAIIAAILI	outside-TM-inside	II**GIAAAAV**VAAAAIIAAILI	inside-TM-outside	YLII**GIAAAAV**VAAAAIIAAILIA	outside-TM-inside	previously shown to increase adherence of *T. vaginalis* to ectocervical cells in de Miguel *et al.* Mol Cell Proteomics 2010
TVAG_335250	conserved hypothetical protein	1	null	null	null	null	yes	I**PIIAGAA**AAVGVAAIVAAAVLI	outside-TM-inside	**PIIAGAA**AAVGVAAIVAAAVL	inside-TM-outside	LI**PIIAGAA**AAVGVAAIVAAAVLI	outside-TM-inside	similar to TVAG_166850 and TVAG_244130

Table 2-S4: Results from surface proteome screen using the parasite search motif. Columns 1-7 show the hit results of searching the *T. vaginalis* surface proteome with the parasite search motif (using TrichDB, motif located anywhere in the protein, and protein contains at least 1 TM domain). To identify potential substrates visual inspection of the predicted transmembrane (TM) domains was performed (columns 8-15) to determine whether the motif was present in the top part of the TM domain, summary of analysis is presented in column 8. Predicted TM domain residues are shown as capital letters, if motif was found within TM it is indicated by blue bold letters. If motif was present but missing beginning residue-the amino acid before the TM domain was also checked and if it fit the parasite search motif it is shown as a lowercase letter in TM domain annotation. If one amino acid was missing from motif it was indicated by green font. For predicted topology of protein, i, TM, and o, indicate whether the predicted part of the protein is inside the cell (i), forms part of the transmembrane domain (TM), or is outside the cell (o). Pink highlighting indicates possible single TM substrates and yellow highlighting indicates possible multiple TM substrates.

	P4	P3	P2	P1	P1'	P2'	P3'		
Strisovsky *et al.* 2009 motif	[IMYF WLV]	[^WPD]	[^WF]	[AGCS]	[^P]	[FIMVA CLTW]			
parasite search motif:	[AGIP]	[YALI]	[IAFY]	[A]	[GSA]	[GSA]	[IVGA]	cleaved by TvROM1?	cleaved by TvROM3?
Substrate tested:									
PfEBA-175	P	Y	Y	A	G	A	G	yes	no
PfBAEBL	P	Y	F	A	A	G	G	yes	no
Hs EphrinB3	P	A	V	A	G	A	A	yes	no
PsTatA	I	A	T	A	A	F	G	yes	no
TV_166850	G	L	A	A	G	G	V	yes	no
TV_280090	G	A	A	A	G	G	V	yes	no
TV_244130	G	I	A	A	A	A	V	no	no
TV_335250	P	I	I	A	G	A	A	no	no
TV_189150	P	A	I	A	G	G	I	no	no
TV_573910	I	I	V	G	I	V	I	no	no
TV_245580	g	I	I	A	G	I	V	no	no
TV_425470	g	I	I	A	G	I	V	no	no
TV_393390	I	V	L	A	V	M	A	no	no
Spitz	L	E	K	A	S	I	A	no	yes

Identified in DCI experiment and surface proteome screen, contain parasite search motif

Identified in surface proteome screen, contain parasite search motif

Identified in DCI experiment, contain Strisovsky *et al.* 2009 motif

Table 2-S5: Comparison and summary of all rhomboid substrates and putative *T. vaginalis* rhomboid substrates tested.

Table shows the predicted and established (EBA-175, TatA, and Spitz) P4-P3' residues of all the substrates tested in this study, for comparison and prediction of substrate determinants that may promote or decrease processing by TvROM1 or TvROM3. The cleavage sites of EBA175, TatA, and Spitz have been mapped by [33, 44, 49], respectively. Substrates that could be cleaved by TvROM1 are highlighted in yellow and the only protein that could be cleaved by TvROM3, the *Drosophila* Spitz protein, is shown with blue highlighting. Rhomboid substrates from other organisms whose cleavage was tested in Fig. 2-2 and in data not shown are at the top. The putative *T. vaginalis* substrates identified by searching the *T. vaginalis* surface proteome (Fig. 2-5) and those identified in the DCI quantitative mass spectrometry experiments (Fig. 2-4) are denoted with brackets. Capital letters indicate amino acids predicted to be part of the TM domain, lowercase letters denote amino acids found outside the predicted TM domain. Note the presence of small amino acids at the predicted P1-P2' sites of cleaved substrates. The presence of I at the predicted P2, P3, or both sites is also found in substrates that are not cleaved by TvROM1.

A

TrichDB accession number	TrichDB annotation	TrichDB predicted TM	TM can be cleaved by TvROM1?
TVAG_166850	conserved hypothetical protein	MLIIGLA**AG**GVAAAAVVAAAIII	Yes
TVAG_280090	conserved hypothetical protein	MIIIGAA**AG**GVAAVAVVAAAVLI	Yes
TVAG_493860	Clan MA, family M8, leishmanolysin-like metallopeptidase	WIIIGAA**AG**GALLLIIIIVFTVIA	No
TVAG_493930	Clan MA, family M8, leishmanolysin-like metallopeptidase	WIIIGAA**AG**GALLLIIIIVSVIA	No
TVAG_206210	Clan MA, family M8, leishmanolysin-like metallopeptidase	IIIGAA**AA**GAVVLIIIIVVAVVV	Not tested

B

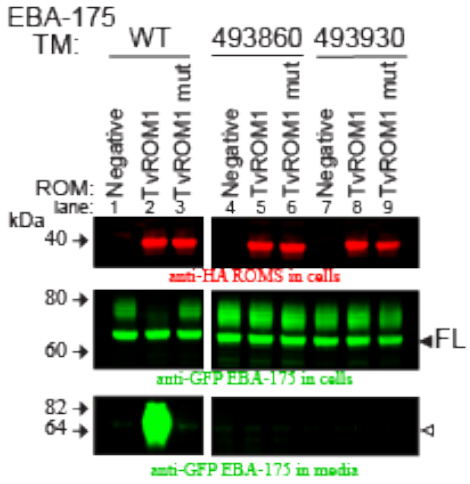

Fig. 2-S1: TvROM1 cleavage analysis of putative substrates identified by screening the *T. vaginalis* genome with the parasite search motif.
(A) Table shows the 5 putative substrates identified in the *T. vaginalis* genome search after additional restriction of no Ile located at the P2 or P3 sites predicted to be disfavored for TvROM1 cleavage (based on amino acid comparison shown in Table 2-S5). Table shows the accession numbers of the 5 putative substrates, the amino acids in their predicted TM domain, and the parasite search motif residues highlighted in blue bold font. The predicted P1-P1' residues (shown in large font) is where cleavage is predicted to occur. **(B)** The TM domain of TVAG_493860 and TVAG_493930 is not cleaved by TvROM1 in the HEK293 heterologous cell cleavage assay. A chimeric protein of GFP-EBA-175 containing the TM domain of the putative substrates (indicated above the blot) was co-transfected with TvROM1 or TvROM1 catalytic mutant (mut). Negative control (Negative-lane 1) was transfected with substrate alone. Western blot analyses of whole cell lysates confirmed expression of the HA-tagged rhomboids (top panel) and the full-length substrate (closed arrowhead, middle panel). Analyses of conditioned media from the co-transfectants (lower panel) did not reveal a cleavage product of the predicted size (lower panel, open arrowhead) indicating lack of processing by TvROM1. Note that although the residues surrounding the predicted rhomboid cleavage site in the TM domain of TVAG_493860 and TVAG_493930 are very similar to the two substrates that are

cleaved by TvROM1 (comparison shown in A), they are not processed by TvROM1. Therefore, the remaining bottom half TM residues may also contribute to features favored for TvROM1 cleavage as has been previously reported [49-51].

References:

1. WHO *Dept. of Reproductive Health and Research. Global incidence and prevalence of selected curable sexually transmitted infections-2008*. 2012.

2. CDC, *Incidence, Prevalence, and Cost of Sexually Transmitted Infections in the United States*. 2013.

3. Petrin, D., et al., *Clinical and microbiological aspects of Trichomonas vaginalis.* Clin Microbiol Rev, 1998. **11**(2): p. 300-17.

4. Mavedzenge, S.N., et al., *Epidemiological synergy of Trichomonas vaginalis and HIV in Zimbabwean and South African women.* Sex Transm Dis, 2010. **37**(7): p. 460-6.

5. Shafir, S.C., F.J. Sorvillo, and L. Smith, *Current issues and considerations regarding trichomoniasis and human immunodeficiency virus in African-Americans.* Clin Microbiol Rev, 2009. **22**(1): p. 37-45, Table of Contents.

6. Kiviat, N.B., et al., *Cytologic manifestations of cervical and vaginal infections. I. Epithelial and inflammatory cellular changes.* JAMA, 1985. **253**(7): p. 989-96.

7. Fastring, D.R., et al., *Co-occurrence of Trichomonas vaginalis and bacterial vaginosis and vaginal shedding of HIV-1 RNA.* Sex Transm Dis, 2014. **41**(3): p. 173-9.

8. Hobbs, M.M., et al., *Trichomonas vaginalis as a cause of urethritis in Malawian men.* Sex Transm Dis, 1999. **26**(7): p. 381-7.

9. Gram, I.T., et al., *Trichomonas Vaginalis (TV) and Human Papillomavirus (HPV) Infection and the Incidence of Cervical Intraepithelial Neoplasia (CIN) Grade III.* Cancer Causes & Control, 1992. **3**(3): p. 231-236.

10. Zhang, Z.F., et al., *Trichomonas vaginalis and cervical cancer. A prospective study in China.* Ann Epidemiol, 1995. **5**(4): p. 325-32.

11. Sutcliffe, S., et al., *Plasma antibodies against Trichomonas vaginalis and subsequent risk of prostate cancer.* Cancer Epidemiol Biomarkers Prev, 2006. **15**(5): p. 939-45.

12. Stark, J.R., et al., *Prospective study of Trichomonas vaginalis infection and prostate cancer incidence and mortality: Physicians' Health Study.* J Natl Cancer Inst, 2009. **101**(20): p. 1406-11.

13. Parise, M.E., P.J. Hotez, and L. Slutsker, *Neglected parasitic infections in the United States: needs and opportunities.* Am J Trop Med Hyg, 2014. **90**(5): p. 783-5.

14. CDC, *Neglected Parasitic Infections (NPIs) in the United States. 2014.*

15. Hotez, P.J., *America's most distressed areas and their neglected infections: the United States Gulf Coast and the District of Columbia.* PLoS Negl Trop Dis, 2011. **5**(3): p. e843.

16. Ryan, C.M., N. de Miguel, and P.J. Johnson, *Trichomonas vaginalis: current understanding of host-parasite interactions.* Essays Biochem, 2011. **51**: p. 161-75.

17. Lustig, G., et al., *Trichomonas vaginalis contact-dependent cytolysis of epithelial cells.* Infect Immun, 2013. **81**(5): p. 1411-9.

18. Krieger, J.N., M.A. Poisson, and M.F. Rein, *Beta-hemolytic activity of Trichomonas vaginalis correlates with virulence.* Infect Immun, 1983. **41**(3): p. 1291-5.

19. Coceres, V.M., et al., *The C-terminal tail of tetraspanin proteins regulates their intracellular distribution in the parasite Trichomonas vaginalis.* Cell Microbiol, 2015.

20. Hirt, R.P., et al., *Trichomonas vaginalis pathobiology new insights from the genome sequence.* Adv Parasitol, 2011. **77**: p. 87-140.

21. Carlton, J.M., et al., *Draft Genome Sequence of the Sexually Transmitted Pathogen Trichomonas vaginalis.* Science, 2007. **315**(5809): p. 207-212.

22. Noel, C.J., et al., *Trichomonas vaginalis vast BspA-like gene family: evidence for functional diversity from structural organisation and transcriptomics.* BMC Genomics, 2010. **11**: p. 99.

23. de Miguel, N., et al., *Proteome analysis of the surface of Trichomonas vaginalis reveals novel proteins and strain-dependent differential expression.* Mol Cell Proteomics, 2010. **9**(7): p. 1554-66.

24. Woehle, C., et al., *The parasite Trichomonas vaginalis expresses thousands of pseudogenes and long non-coding RNAs independently from functional neighbouring genes.* BMC Genomics, 2014. **15**: p. 906.

25. Hooper, N.M. and U. Lendeckel, *Intramembrane-cleaving proteases (I-CLiPs)*, in *Proteases in biology and disease v 6*. 2007, Springer,: Dordrect, Netherlands. p. ix, 142 p.

26. Urban, S., J.R. Lee, and M. Freeman, *Drosophila rhomboid-1 defines a family of putative intramembrane serine proteases.* Cell, 2001. **107**(2): p. 173-82.

27. Wasserman, J.D., S. Urban, and M. Freeman, *A family of rhomboid-like genes: Drosophila rhomboid-1 and roughoid/rhomboid-3 cooperate to activate EGF receptor signaling.* Genes Dev, 2000. **14**(13): p. 1651-63.

28. Guichard, A., et al., *brother of rhomboid, a rhomboid-related gene expressed during early Drosophila oogenesis, promotes EGF-R/MAPK signaling.* Dev Biol, 2000. **226**(2): p. 255-66.

29. Gallio, M., et al., *A conserved mechanism for extracellular signaling in eukaryotes and prokaryotes.* Proc Natl Acad Sci U S A, 2002. **99**(19): p. 12208-13.

30. Brossier, F., et al., *A spatially localized rhomboid protease cleaves cell surface adhesins essential for invasion by Toxoplasma.* Proc Natl Acad Sci U S A, 2005. **102**(11): p. 4146-51.

31. Baxt, L.A., et al., *An Entamoeba histolytica rhomboid protease with atypical specificity cleaves a surface lectin involved in phagocytosis and immune evasion.* Genes Dev, 2008. **22**(12): p. 1636-46.

32. Baker, R.P., R. Wijetilaka, and S. Urban, *Two Plasmodium rhomboid proteases preferentially cleave different adhesins implicated in all invasive stages of malaria.* PLoS Pathog, 2006. **2**(10): p. e113.

33. Strisovsky, K., H.J. Sharpe, and M. Freeman, *Sequence-specific intramembrane proteolysis: identification of a recognition motif in rhomboid substrates.* Mol Cell, 2009. **36**(6): p. 1048-59.

34. Koonin, E.V., et al., *The rhomboids: a nearly ubiquitous family of intramembrane serine proteases that probably evolved by multiple ancient horizontal gene transfers.* Genome Biology, 2003. **4**(3): p. R19-R19.

35. Stevenson, L.G., et al., *Rhomboid protease AarA mediates quorum-sensing in Providencia stuartii by activating TatA of the twin-arginine translocase.* Proc Natl Acad Sci U S A, 2007. **104**(3): p. 1003-8.

36. Ishihara, N., et al., *Regulation of mitochondrial morphology through proteolytic cleavage of OPA1.* EMBO J, 2006. **25**(13): p. 2966-77.

37. Baxt, L.A., et al., *Downregulation of an Entamoeba histolytica rhomboid protease reveals roles in regulating parasite adhesion and phagocytosis.* Eukaryot Cell, 2010. **9**(8): p. 1283-93.

38. Dowse, T.J., et al., *Apicomplexan rhomboids have a potential role in microneme protein cleavage during host cell invasion.* Int J Parasitol, 2005. **35**(7): p. 747-56.

39. Opitz, C., et al., *Intramembrane cleavage of microneme proteins at the surface of the apicomplexan parasite Toxoplasma gondii.* EMBO J, 2002. **21**(7): p. 1577-85.

40. Zhou, X.W., et al., *Proteomic analysis of cleavage events reveals a dynamic two-step mechanism for proteolysis of a key parasite adhesive complex.* Mol Cell Proteomics, 2004. **3**(6): p. 565-76.

41. Parussini, F., et al., *Intramembrane proteolysis of Toxoplasma apical membrane antigen 1 facilitates host-cell invasion but is dispensable for replication.* Proceedings of the National Academy of Sciences, 2012. **109**(19): p. 7463-7468.

42. Ejigiri, I., et al., *Shedding of TRAP by a Rhomboid Protease from the Malaria Sporozoite Surface Is Essential for Gliding Motility and Sporozoite Infectivity.* PLoS Pathogens, 2012. **8**(7): p. e1002725.

43. Howell, S.A., et al., *Distinct mechanisms govern proteolytic shedding of a key invasion protein in apicomplexan pathogens.* Mol Microbiol, 2005. **57**(5): p. 1342-56.

44. O'Donnell, R.A., et al., *Intramembrane proteolysis mediates shedding of a key adhesin during erythrocyte invasion by the malaria parasite.* J Cell Biol, 2006. **174**(7): p. 1023-33.

45. Vera, I.M., et al., *Plasmodium protease ROM1 is important for proper formation of the parasitophorous vacuole.* PLoS Pathog, 2011. **7**(9): p. e1002197.

46. Freeman, M., *The rhomboid-like superfamily: molecular mechanisms and biological roles.* Annu Rev Cell Dev Biol, 2014. **30**: p. 235-54.

47. Baker, R.P. and S. Urban, *Architectural and thermodynamic principles underlying intramembrane protease function.* Nat Chem Biol, 2012. **8**(9): p. 759-68.

48. Dickey, S.W., et al., *Proteolysis inside the membrane is a rate-governed reaction not driven by substrate affinity.* Cell, 2013. **155**(6): p. 1270-81.

49. Moin, S.M. and S. Urban, *Membrane immersion allows rhomboid proteases to achieve specificity by reading transmembrane segment dynamics.* Elife, 2012. **1**: p. e00173.

50. Akiyama, Y. and S. Maegawa, *Sequence features of substrates required for cleavage by GlpG, an Escherichia coli rhomboid protease.* Mol Microbiol, 2007. **64**(4): p. 1028-37.

51. Urban, S. and M. Freeman, *Substrate Specificity of Rhomboid Intramembrane Proteases Is Governed by Helix-Breaking Residues in the Substrate Transmembrane Domain.* Molecular Cell, 2003. **11**(6): p. 1425-1434.

52. Lemberg, M.K. and M. Freeman, *Functional and evolutionary implications of enhanced genomic analysis of rhomboid intramembrane proteases.* Genome Res, 2007. **17**(11): p. 1634-46.

53. Sheiner, L., T.J. Dowse, and D. Soldati-Favre, *Identification of trafficking determinants for polytopic rhomboid proteases in Toxoplasma gondii.* Traffic, 2008. **9**(5): p. 665-77.

54. Benchimol, M., et al., *Structure and division of the Golgi complex in Trichomonas vaginalis and Tritrichomonas foetus.* Eur J Cell Biol, 2001. **80**(9): p. 593-607.

55. Urban, S., D. Schlieper, and M. Freeman, *Conservation of intramembrane proteolytic activity and substrate specificity in prokaryotic and eukaryotic rhomboids.* Curr Biol, 2002. **12**(17): p. 1507-12.

56. Pascall, J.C. and K.D. Brown, *Intramembrane cleavage of ephrinB3 by the human rhomboid family protease, RHBDL2.* Biochem Biophys Res Commun, 2004. **317**(1): p. 244-52.

57. Arroyo, R. and J.F. Alderete, *Trichomonas vaginalis surface proteinase activity is necessary for parasite adherence to epithelial cells.* Infection and Immunity, 1989. **57**(10): p. 2991-2997.

58. Sommer, U., et al., *Identification of Trichomonas vaginalis cysteine proteases that induce apoptosis in human vaginal epithelial cells.* J Biol Chem, 2005. **280**(25): p. 23853-60.

59. Mendoza-Lopez, M.R., et al., *CP30, a cysteine proteinase involved in Trichomonas vaginalis cytoadherence.* Infect Immun, 2000. **68**(9): p. 4907-12.

60. Hernandez, H., et al., *Monoclonal antibodies against a 62 kDa proteinase of Trichomonas vaginalis decrease parasite cytoadherence to epithelial cells and confer protection in mice.* Parasite Immunol, 2004. **26**(3): p. 119-25.

61. Alvarez-Sanchez, M.E., et al., *A novel cysteine proteinase (CP65) of Trichomonas vaginalis involved in cytotoxicity.* Microb Pathog, 2000. **28**(4): p. 193-202.

62. Rendon-Gandarilla, F.J., et al., *The TvLEGU-1, a legumain-like cysteine proteinase, plays a key role in Trichomonas vaginalis cytoadherence.* Biomed Res Int, 2013. **2013**: p. 561979.

63. Cardenas-Guerra, R.E., et al., *The iron-induced cysteine proteinase TvCP4 plays a key role in Trichomonas vaginalis haemolysis.* Microbes Infect, 2013. **15**(13): p. 958-68.

64. Hernandez-Romano, P., et al., *Identification and characterization of a surface-associated, subtilisin-like serine protease in Trichomonas vaginalis.* Parasitology, 2010. **137**(11): p. 1621-35.

65. Urban, S. and M.S. Wolfe, *Reconstitution of intramembrane proteolysis in vitro reveals that pure rhomboid is sufficient for catalysis and specificity.* Proc Natl Acad Sci U S A, 2005. **102**(6): p. 1883-8.

66. Boersema, P.J., et al., *Multiplex peptide stable isotope dimethyl labeling for quantitative proteomics.* Nat Protoc, 2009. **4**(4): p. 484-94.

67. Monne, M., M. Hermansson, and G. von Heijne, *A turn propensity scale for transmembrane helices.* J Mol Biol, 1999. **288**(1): p. 141-5.

68. Monne, M., et al., *Turns in transmembrane helices: determination of the minimal length of a "helical hairpin" and derivation of a fine-grained turn propensity scale.* J Mol Biol, 1999. **293**(4): p. 807-14.

69. Shen, B., et al., *Functional analysis of rhomboid proteases during Toxoplasma invasion.* MBio, 2014. **5**(5): p. e01795-14.

70. Vinothkumar, K.R., et al., *Structure of rhomboid protease in complex with beta-lactam inhibitors defines the S2' cavity.* Structure, 2013. **21**(6): p. 1051-8.

71. O'Keefe, D.D., et al., *Egfr/Ras signaling regulates DE-cadherin/Shotgun localization to control vein morphogenesis in the Drosophila wing.* Dev Biol, 2007. **311**(1): p. 25-39.

72. Tepass, U., *Genetic analysis of cadherin function in animal morphogenesis.* Curr Opin Cell Biol, 1999. **11**(5): p. 540-8.

73. Marambaud, P., et al., *A presenilin-1/gamma-secretase cleavage releases the E-cadherin intracellular domain and regulates disassembly of adherens junctions.* EMBO J, 2002. **21**(8): p. 1948-56.

74. Reiss, K., A. Ludwig, and P. Saftig, *Breaking up the tie: disintegrin-like metalloproteinases as regulators of cell migration in inflammation and invasion.* Pharmacol Ther, 2006. **111**(3): p. 985-1006.

75. Rastew, E., L. Morf, and U. Singh, *Entamoeba histolytica rhomboid protease 1 has a role in migration and motility as validated by two independent genetic approaches.* Exp Parasitol, 2015. **154**: p. 33-42.

76. Hernandez, H.M., R. Marcet, and J. Sarracent, *Biological roles of cysteine proteinases in the pathogenesis of Trichomonas vaginalis.* Parasite, 2014. **21**: p. 54.

77. Puente-Rivera, J., et al., *Trichocystatin-2 (TC-2): an endogenous inhibitor of cysteine proteinases in Trichomonas vaginalis is associated with TvCP39.* Int J Biochem Cell Biol, 2014. **54**: p. 255-65.

78. Fiori, P.L., et al., *Trichomonas vaginalis haemolysis: Evidence of functional pores formation on red cell membranes*. Vol. 109. 1993. 13-18.

79. M. Santos, J., A. Graindorge, and D. Soldati-Favre, *New insights into parasite rhomboid proteases.* Molecular and Biochemical Parasitology, 2012. **182**(1–2): p. 27-36.

80. Sibley, L.D., *The roles of intramembrane proteases in protozoan parasites.* Biochimica et Biophysica Acta (BBA) - Biomembranes, 2013. **1828**(12): p. 2908-2915.

81. Clark, C.G. and L.S. Diamond, *Methods for cultivation of luminal parasitic protists of clinical importance.* Clin Microbiol Rev, 2002. **15**(3): p. 329-41.

82. Fichorova, R.N., J.G. Rheinwald, and D.J. Anderson, *Generation of papillomavirus-immortalized cell lines from normal human ectocervical, endocervical, and vaginal epithelium that maintain expression of tissue-specific differentiation proteins.* Biol Reprod, 1997. **57**(4): p. 847-55.

83. Delgadillo, M.G., et al., *Transient and selectable transformation of the parasitic protist Trichomonas vaginalis.* Proc Natl Acad Sci U S A, 1997. **94**(9): p. 4716-20.

84. Ortiz, D. and P.J. Johnson, *Tetracycline-inducible gene expression in Trichomonas vaginalis.* Mol Biochem Parasitol, 2003. **128**(1): p. 43-9.

85. Bell, C., et al., *Characterization of the Mycobacterium tuberculosis proteome by liquid chromatography mass spectrometry-based proteomics techniques: a comprehensive resource for tuberculosis research.* J Proteome Res, 2012. **11**(1): p. 119-30.

86. Kalli, A. and S. Hess, *Effect of mass spectrometric parameters on peptide and protein identification rates for shotgun proteomic experiments on an LTQ-orbitrap mass analyzer.* Proteomics, 2012. **12**(1): p. 21-31.

87. Cox, J. and M. Mann, *MaxQuant enables high peptide identification rates, individualized p.p.b.-range mass accuracies and proteome-wide protein quantification.* Nat Biotechnol, 2008. **26**(12): p. 1367-72.

88. Olma, M.H. and I. Dikic, *Cullins getting undressed by the protein exchange factor Cand1*. Cell, 2013. **153**(1): p. 14-6.

89. Benjamini, Y. and Y. Hochberg, *Controlling the false discovery rate: a practical and powerful approach to multiple testing.* Journal of the Royal Statistical Society Series B (Methodological), 1995. **57**: p. 289-300.

90. Baker, R.P., et al., *Enzymatic analysis of a rhomboid intramembrane protease implicates transmembrane helix 5 as the lateral substrate gate.* Proc Natl Acad Sci U S A, 2007. **104**(20): p. 8257-62.

91. Urban, S., *Taking the plunge: integrating structural, enzymatic and computational insights into a unified model for membrane-immersed rhomboid proteolysis.* Biochem J, 2010. **425**(3): p. 501-12.

92. Dowse, T.J. and D. Soldati, *Rhomboid-like proteins in Apicomplexa: phylogeny and nomenclature.* Trends Parasitol, 2005. **21**(6): p. 254-8.

Chapter 3:

Reversible association of tetraspanin with *Trichomonas vaginalis* flagella upon adherence to host cells

Reversible association of tetraspanin with *Trichomonas vaginalis* flagella upon adherence to host cells

Natalia de Miguel,[1,2] Angelica Riestra[1] and Patricia J. Johnson[1]*

[1]*Department of Microbiology, Immunology, and Molecular Genetics, University of California, Los Angeles, CA 90095-1489, USA.*

[2]*IIB-INTECH, CONICET-UNSAM, Camino de Circunvalación Laguna Km. 6, C.C 164, B7130IIWA Chascomús, Buenos Aires, Argentina.*

Summary

The parasite *Trichomonas vaginalis* is the causative agent of trichomoniasis, a prevalent sexually transmitted infection. Here, we report the cellular analyses of *T. vaginalis* tetraspanin 6 (TvTSP6). This family of membrane proteins has been implicated in cell adhesion, migration and proliferation in vertebrates. We observed that TvTSP6 expression is upregulated upon contact with vaginal ectocervical cells (VECs) and that parasite strains that are highly adherent to VECs express higher levels of TvTSP6 mRNA relative to poorly adherent strains. TvTSP6 is localized predominantly on the flagella of parasites cultured in the absence of host cells; however, adherence of the parasite to VECs initially results in a redistribution of the protein to intracellular vesicles and the plasma membrane of the main body of the cell. We found that a 16-amino-acid C-terminal intracellular tail of TvTSP6 is necessary and sufficient for flagellar localization and protein redistribution when the parasite is in contact with VECs. Additionally, deletion of the C-terminal tail reduced parasite migration through Matrigel, a mimic of the extracellular matrix. Together, our data support roles for TvTSP6 in parasite migration in the host and sensory reception during infection.

Received 19 April, 2012; revised 19 July, 2012; accepted 20 July, 2012. *For correspondence. E-mail johnsonp@ucla.edu; Tel. (+1) 310 825 4870; Fax (+1) 310 206 5231.

Introduction

Trichomonas vaginalis, an extracellular flagellated protozoan, is the cause of trichomoniasis, a sexually transmitted infection that affects over 248 million people annually worldwide (World Health Organization, 2005). Although asymptomatic infection by *T. vaginalis* is common, multiple symptoms and pathologies can arise in both men and women, including vaginitis, urethritis, prostatitis, low-birth-weight infants, preterm delivery, premature rupture of membranes and infertility (Swygard *et al.*, 2004; Fichorova, 2009). Additionally, infection by this parasite is associated with the development of cervical and prostate cancer (Gander *et al.*, 2009; Stark *et al.*, 2009; Sutcliffe *et al.*, 2009) and an increased susceptibility to human immunodeficiency virus (HIV) infection (McClelland *et al.*, 2007; Van Der Pol *et al.*, 2008). These severe complications and high incidence of infection underscore the need to identify new diagnostic methods and drug targets and to advance vaccine development. Understanding the mechanisms by which *T. vaginalis* colonizes the host is central to developing strategies to prevent infection. Despite the prevalence of trichomoniasis, the underlying biochemical processes that lead to pathogenesis are poorly defined (Fiori *et al.*, 1999; Hirt *et al.*, 2011; Ryan *et al.*, 2011). As an extracellular organism, surface proteins are likely to play important roles in the initial adherence to mucosal tissue as well as the long-term survival of the pathogen on mucosal surfaces. We have previously identified ~400 putative *T. vaginalis* surface proteins (de Miguel *et al.*, 2010); however, with the exception of two, their possible roles in pathogenesis remain undefined.

One class of proteins identified were the tetraspanins (TSPs). This family of cell surface proteins has a common structure that includes four hydrophobic transmembrane domains, two extracellular domains characterized by a high concentration of hydrophilic amino acids, and short intracellular amino and carboxyl tails (Hemler, 2005). TSPs modulate a variety of fundamental biological processes such as adhesion, migration, proliferation and fusion by functioning as organizers of multimolecular membrane complexes, termed

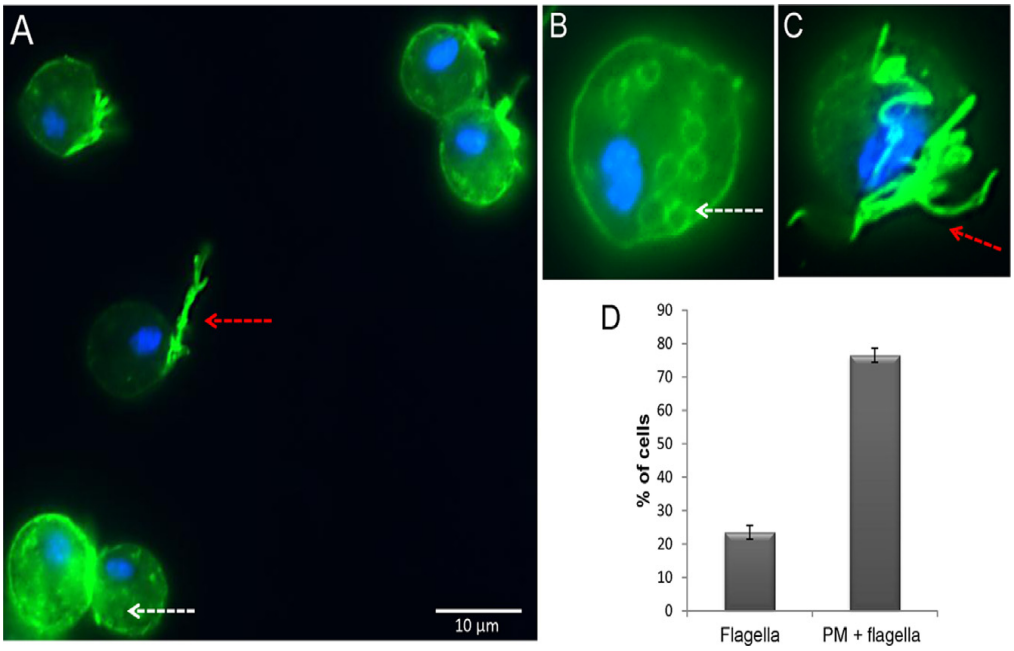

Fig. 1. Subcellular localization of TvTSP6 in *T. vaginalis* transfectants.
A–C. Cells exogenously expressing TvTSP6 with a C-terminal haemagglutinin (HA) tag stained for immunofluorescence microscopy using a mouse anti-HA antibody. The nucleus (blue) was also stained with 4′,6′-diamidino-2-phenylindole (DAPI). Red arrows indicate the flagella and white arrows indicate intracellular vesicles. Scale bar, 10 µm.
D. Percentage of cells with TSP6 detected on the flagella only (flagella) or flagella and plasma membrane (flagella + PM) ± the standard deviation of the mean is indicated. One hundred parasites were counted in triplicate in four independent experiments.

'tetraspanin-enriched microdomains' (Hemler, 2003; 2005; Pols and Klumperman, 2009). The extensive spectrum of biological functions in which TSP involvement has been implicated is compatible with their wide distribution in multiple cell types and organisms, and indicates their functional importance. As a number of these processes are likely critical for *T. vaginalis* to colonize its host, we hypothesize that TSPs could act as modulators of host : pathogen interactions. In mammalian cells, a 'transmembrane linker' model for TSPs has been proposed (Hemler, 1998). In this model, TSP extracellular domains link to integrins, whereas cytoplasmic domains link to intracellular signalling enzymes such as phosphatidylinositol 4-kinase and PKC (Hemler, 1998; Yauch and Hemler, 2000; Zhang *et al*., 2001). Here, we have examined a *T. vaginalis* TSP, called TvTSP6, that was identified in the plasma membrane surface proteome (de Miguel *et al*., 2010). Our data indicate roles for this protein in parasite migration and sensory reception during infection and provide support for a transmembrane linker model in which the C-terminal tail of a TSP links with intracellular pathways to mediate these activities.

Results

TvTSP6 *localizes to the flagellar membrane of parasites cultured in the absence of host cells*

We have previously determined the surface proteome of *T. vaginalis* to identify proteins on the surface of the parasite that might be involved in pathogenesis (de Miguel *et al*., 2010). Among others, these analyses revealed the presence of three members of the TSP family. As mammalian TSPs participate in adhesion and migration, which are processes *T. vaginalis* uses to colonize its host, we have examined one of these proteins called TvTSP6 (TVAG_460770). The gene encoding TvTSP6 was cloned and expressed under the control of the α-SCS promoter as a C-terminally haemagglutinin (HA)-tagged protein in *T. vaginalis* strain B7RC2. We then determined the localization of the tagged protein in transfected cells using immunofluorescence assays. As predicted, TvTSP6 was found to be present on the plasma membrane (Fig. 1A). The protein was also found to localize to intracellular vesicles (Fig. 1B). In addition to these locations, the protein is present on the flagellar membrane (Fig. 1A and C). On virtually all cells for which the flagella was in the

visible plane, the bulk of the TvTSP6 signal was found on the flagella membrane (see arrow, Fig. 1A), with lesser signal on the plasma membrane and/or intracellular vesicles. TvTSP6 was detectable only on the flagella in ~ 20% of the cells (Fig. 1D). The TvTSP6 signal is typically stronger on the flagellar membrane than on the plasma membrane or vesicles. This is likely due both to a greater abundance of the protein on flagellar membranes and to a fusion of multiple signals as the four anterior flagella tend to cluster.

TvTSP6 mRNA is more abundant in parasites that are highly adherent and cytolytic to vaginal ectocervical cells (VECs)

We compared TvTSP6 mRNA levels between six strains with different capacities to adhere to VECs. Three strains, T1, G3 and SD10 which are poorly adherent and are five- to 15-fold less adherent than strains B7268, B7RC2 and SD7 (de Miguel *et al*., 2010), were compared. As shown in Fig. 2A, qPCR analyses revealed that the expression level of TvTSP6 correlates with the adherence and cytotoxicity of the strains. TvTSP6 is five-, seven- and ten-fold more highly expressed in adherent strains B7268, B7RC2 and SD7, respectively, relative to the less adherent G3 strain (Fig. 2A). The greater abundance in mRNA expression observed in highly adherent versus less adherent parasites is consistent with an involvement of TvTSP6 in host : parasite interactions.

TvTSP6 is redistributed upon binding of the parasite to host cells

To evaluate a possible involvement of TvTSP6 in host–parasite interactions, parasites transfected with the TvTSP6–HA constructs described above were exposed to VECs for 0.5 to 6 h, immunostained with an anti-HA antibody and examined using fluorescence microscopy (Fig. 3). As shown in Fig. 1, in the absence of host cells, TvTSP6 is found preferentially on the flagellar membrane and present at lower levels on the plasma membrane and intracellular vesicles of parasites. Upon exposure to VECs we found that the TvTSP6 localization changes. Within 30 min of contact with host cells, the protein is found on the plasma membrane and flagella membrane (> 95%), whereas after 3 h ~ 15% of the parasites have TvTSP6 protein only on the flagella and after 6 h > 50% of the cells have flagellar-only TvTSP6 (Fig. 3).

We have also exposed untransformed parasites to VECs and have followed the expression of endogenous TvTSP6 by qPCR (Fig. 2B). In agreement with immunofluorescence data shown in Fig. 3, TvTSP6 was found to be upregulated upon contact with VECs, increasing ~ 14-fold after 30 min. Expression subsequently decreased between 30 min and 2 h and then increased again ~ 19-fold after 4 h of exposure to VECs (Fig. 2B). The observed bipartite upregulation of TvTSP6 over time suggests multiple functions for this protein. Since *in vitro* attachment of the parasites is mostly completed within ~ 20 min of exposure to the VECs (Okumura *et al*., 2008), the second wave of upregulation suggests TvTSP6 plays a role in events occurring downstream of adherence.

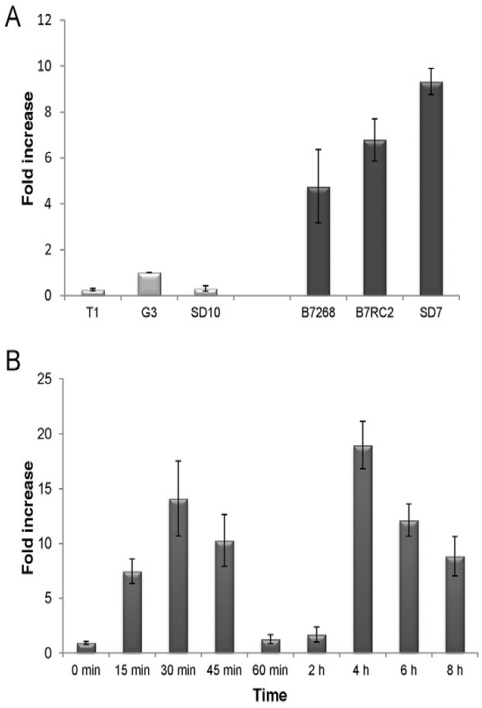

Fig. 2. Expression analysis of TvTSP6.
A. mRNA expression levels of TvTSP6 in previously described (de Miguel *et al*., 2010) strains with different adherence capacities were analysed by qPCR. Data are expressed as fold increase compared with the poorly adherent G3 strain ± the standard deviation of the mean. Every sample and points of the standard curve were carried out in duplicates in three independent experiments.
B. Endogenous TvTSP6 mRNA expression upon exposure to host cells. B7RC2 parasites were exposed to VECs and the kinetics of TSP6 expression was analysed by qPCR. Data are expressed as fold increase compared with time 0 min ± the standard deviation of the mean. TvTSP6 mRNA levels are upregulated in contact with VECs, increasing ~ 14-fold at 30 min. Levels subsequently decrease dramatically at 60 min and 2 h and then increased again ~ 19-fold after 4 h of exposure to VECs. Every sample and point on the standard curve were carried out in duplicates in three independent experiments.

The C-terminal tail of TvTSP6 is essential for flagellar targeting and protein redistribution upon parasite binding to VECs

As depicted in Fig. 4A, TSPs span the membrane four times, and have two external domains and short

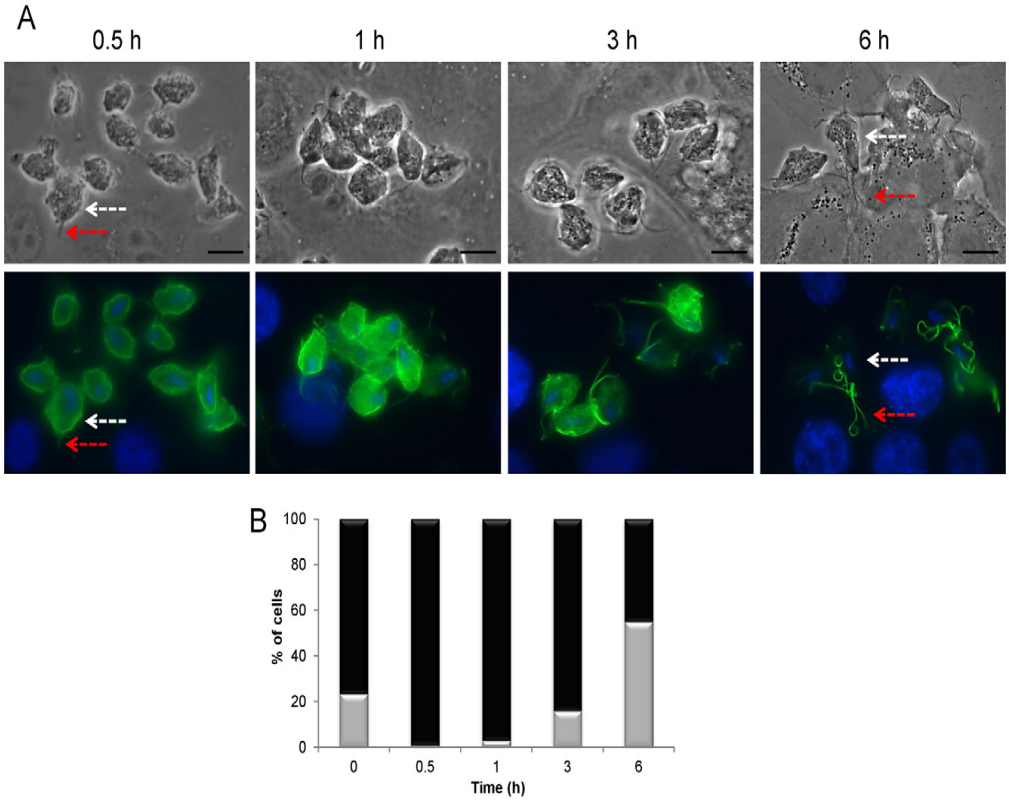

Fig. 3. Subcellular localization of *T. vaginalis* TvTSP6 of parasites bound to VECs.
A. Parasites expressing the TvTSP6–HA-tagged construct were bound to VECs for 0.5, 1, 3 and 6 h and TvTSP6 was localized using an anti-HA antibody. The localization changed from primarily flagella in the absence of host cells (Fig. 1) to primarily plasma membrane and intracellular vesicles, returning to its original flagellar localization at 6 h post host cell exposure. Red arrows indicate the flagella and white arrows indicate intracellular vesicles and the plasma membrane of the main body of the cell. Under these conditions, the host cells are still intact at 6 h. Scale bar, 10 μm.
B. Percentage of cells with TSP6 present predominantly on the flagella (grey columns) or flagella and plasma membrane (black columns) during exposure to VECs. One hundred parasites were counted in triplicate in four independent experiments.

N-terminal and C-terminal tails. The C-terminal cytoplasmic tail has been shown to play critical roles in determining the functional consequences of ligand binding for mammalian TSPs (Zhang *et al*., 2002; Latysheva *et al*., 2006). Therefore, we investigated whether the C-terminal tail of TvTSP6 contributes to the targeting of the protein to the flagellar membrane. An expression construct lacking the 16-amino-acid C-terminal tail (TvTSP6ΔCt) was transfected into parasites (Fig. 4A). Unlike full-length TvTSP6, TvTSP6ΔCt does not localize to the flagella (Fig. 4B). Hundreds of parasites with visual flagella were examined and no flagellar TvTSP6 was detected (data not shown). Instead, TvTSP6ΔCt localized exclusively to the plasma membrane and intracellular vesicles and its localization did not change when transfected parasites bound to VECs (Fig. 4C) in stark contrast to the redistribution observed for full-length TvTSP6 (Fig. 3A). These data demonstrate that the cytoplasmic tail is necessary for both flagellar targeting and cellular redistribution of the protein upon the binding of the parasite to host cells.

The C-terminal tail of TvTSP6 is sufficient for flagella targeting and protein redistribution upon the binding of parasites to VECs

The *T. vaginalis* genome encodes nine TSP genes (http://www.trichdb.org) and all are predicted to have a short C-terminal cytoplasmic tail following the fourth transmembrane domain (N. de Miguel and P.J. Johnson, unpubl. data). To further analyse the role of the C-terminal tail of TvTSP6 we prepared two HA-tagged, chimeric constructs replacing the C-terminal cytoplasmic tail of two different TSPs (TSP1 and TSP3) with the 16-amino-acid C-terminal tail of TvTSP6. Non-chimeric constructs expressing TSP1–HA and TSP3–HA were also prepared and transfected into parasites. As shown in Fig. 5,

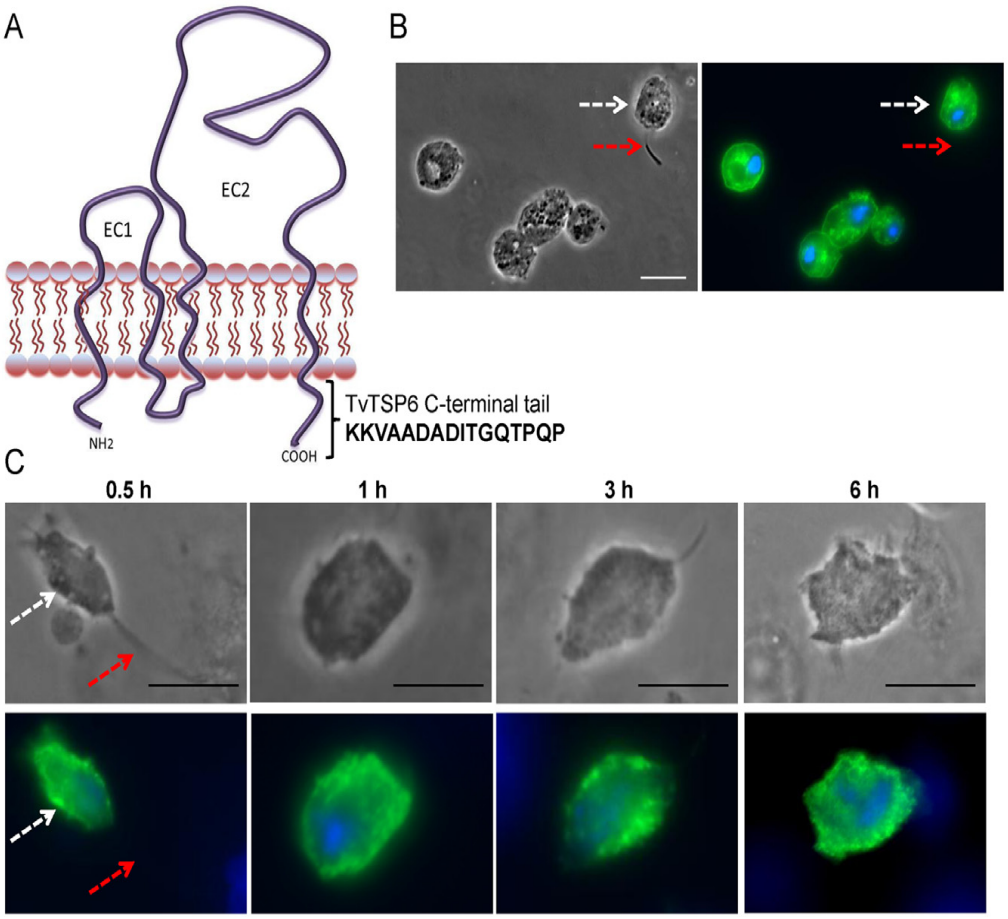

Fig. 4. Subcellular localization of TvTSP6ΔCt in absence and presence of host cells using immunofluorescence microscopy.
A. The predicted structure of TvTSP6 in the plasma membrane is shown. EC1 and EC2 = extracellular domains; cytoplasmic NH2 and C-terminal tails are depicted, and the 16 amino acids deleted from the C-terminal tail of TvTSP6ΔCt are shown.
B. Subcellular localization of TvTSP6ΔCt in the absence of host cells is detected using an anti-HA antibody. Flagella (red arrows) and the main body of the cell (white arrows) were indicated. Note the lack of signal in the flagella.
C. Subcellular localization of TSP6ΔCt in parasites bound to VECs. No change in localization is observed. One hundred parasites were counted in triplicate in four independent experiments. Scale bar, 10 μm.

TSP1–HA and TSP3–HA are detected primarily on the plasma membrane and intracellular vesicles, with a very faint signal found on the flagellar membrane. In contrast, localization of the chimeric proteins (TSP1CT6 and TSP3CT6) is similar to that of full-length TvTSP6, being detected predominantly on the flagella, with less signal on the plasma membrane and vesicles (Fig. 5).

To address whether the C-terminal tail of TvTSP6 is responsible for protein redistribution upon contact with host cells, TSP1CT6- and TSP3CT6-transfected parasites were allowed to bind to VECs. A change in localization of TSP1CT6 and TSP3CT6 that mirrors that observed for TvTSP6 was seen when transfected parasites bound VECs (Figs 6 and S1). These results indicate that the C-terminal tail of TvTSP6 is sufficient for protein redistribution upon VECs exposure.

As shown in Fig. 4A, there are two threonines (T) in the 16-amino-acid TvTSP6 tail. To assess whether phosphorylation of these threonines is required for the targeting and distribution of the protein, the two residues were mutated to alanine. The localization of the mutant protein was indistinguishable from that of the full-length wild-type protein (data not shown). Hence, the two threonine residues present in the C-terminal tail are not necessary for flagellar targeting or protein redistribution.

TvTSP6 plays a role in parasite migration

To adhere to epithelial cells of the host's urogenital tract, *T. vaginalis* must migrate through the extracellular matrix (ECM) that surrounds these cells. As mammalian TSPs are known to be involved in cellular migration (Hemler,

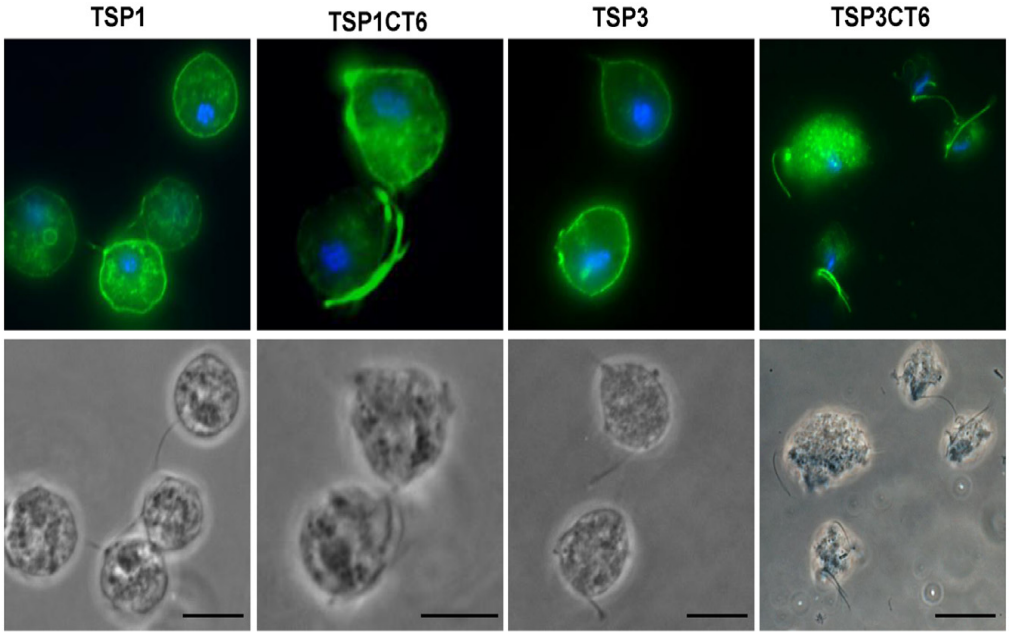

Fig. 5. Subcellular localization of TSP1, TSP1CT6, TSP3 and TSP3CT6 in absence of host cells. Cells expressing C-terminal HA-tagged versions of TSP3 (TVAG_280860), TSP3CT6 (chimera with the C-terminal tail of TSP3 replaced by the C-terminal tail of TvTSP6), TSP1 (TVAG_019180) and TSP1CT6 (chimera with the C-terminal tail of TSP1 replaced by the C-terminal tail of TvTSP6) were stained for immunofluorescence microscopy using an anti-HA antibody. The nucleus (blue) was also stained with DAPI. Scale bar, 10 μm. Note the intensity of flagella signal on the chimeric proteins TSP1CT6 and TSP3CT6 relative to wild-type TSP1 and TSP3 proteins.

1998; Yauch and Hemler, 2000; Zhang *et al*., 2001), we tested whether TvTSP6 facilitates parasite migration through the ECM. A commercial invasion system in which parasites are placed in a cell culture insert and assessed for their ability to pass through 8 μm diameter pores impregnated with ECM proteins (Matrigel™) was used. Parasites were transfected with either an episomal vector expressing TvTSP6 or TvTSP6ΔCt expressing the truncated C-terminal version of TvTSP6 (see Fig. 4A). At increasing times post inoculation, the number of parasites that migrated through the Matrigel and crossed into the bottom chamber was counted. After 3 h, 84% of the TvTSP6-transfected parasites had migrated into the lower chamber compared to 70% of TvTSP6ΔCt transfectants (Fig. 7). Six hours after inoculation the differences were even more pronounced, with 100% of the TvTSP6 transfectants having migrated through the Matrigel, compared to 70% for the TVTSP6ΔCt transfectants. Migration of parasites mock-transfected with an empty vector was similar to that observed for TvTSP6 transfectants (data not shown). These results indicate a role for TvTSP6 in migration wherein the C-terminal tail modulates migration as its deletion substantially reduces the percentage of migrating parasites.

Discussion

In this study we have identified a flagellar protein, TvTSP6, of the parasite *T. vaginalis* that is a member of the TSP family of integral membrane proteins. TSPs have primarily been studied in mammals and worms where they have been shown to reside in the plasma membrane and the membranes of intracellular vesicles (Hemler, 2003; 2005; Hong *et al*., 2005; Tran *et al*., 2006; Huang *et al*., 2007; Pearson *et al.,* 2012). Although TvTSP6 is predominantly in the flagellar membrane when the parasite is not in contact with host cells, we found that it redistributes to the plasma membrane of the cell body and intracellular vesicles upon initial binding to host cells (VECs). Interestingly, TvTSP6 then reappears primarily on the flagella within 3 h of exposure to VECs. As the flagella is known to function in sensory reception in addition to motility (Scholey, 2003), redistribution of TvTSP upon host cell exposure suggests a role for this protein in sensing external host-derived stimuli.

Interestingly, the only sequenced parasitic protist genomes that contain TSP genes are those of *T. vaginalis* and *Entamoeba histolytica* (N. de Miguel, our unpublished BLAST analyses) and the gene does not appear to have

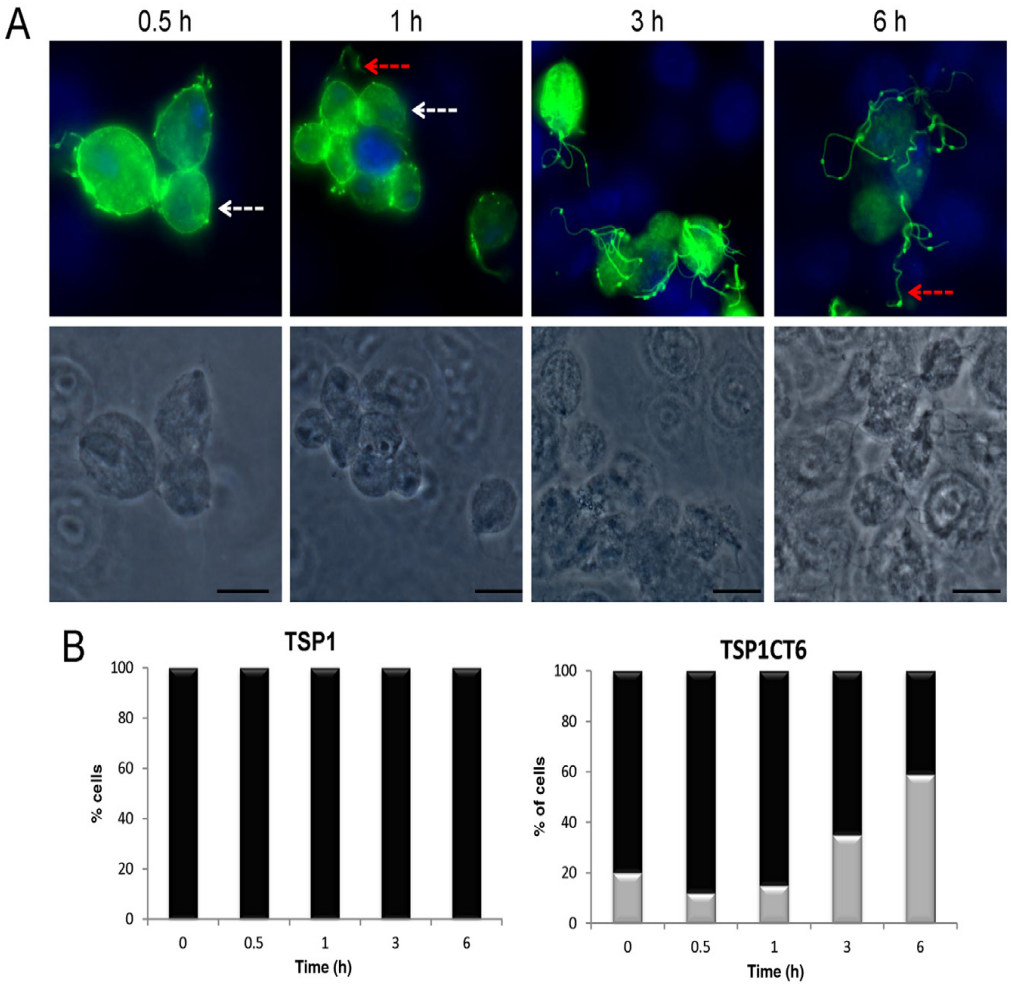

Fig. 6. Subcellular localization of the TvTSP1CT6 protein in parasites bound to VECs.
A. Parasites transfected with TvTSP1CT6 containing a C-terminal HA tag were bound to VECs for 0.5, 1, 3 and 6 h and the protein was localized using an anti-HA antibody. Note the change in localization from plasma membrane and intracellular vesicles to flagellar localization at 3 and 6 h post host cell exposure. Flagella (red arrows) and the main body of the cell (white arrows) were indicated. Scale bar, 10 μm.
B. Percentage of cells transfected with TvTSP1 and TvTSP1CT6 with the respective protein detected on the flagella only (grey columns) or flagella and plasma membrane (black columns) during exposure to VECs. One hundred parasites were counted in triplicate in four independent experiments.

been conserved in *Trypanosoma*, *Leishmania*, *Plasmodium* or *Toxoplasma*. This suggests that TSPs may be specifically involved in the pathogenesis of a subgroup of extracellular mucosal parasites. Consistent with this we found that expression levels of TvTSP6 correlate with the ability of different *T. vaginalis* strains to adhere to host VECs. Additionally, expression is upregulated upon adherence, consistent with a role for TvTSP6 in parasite : host cell interactions.

Tetraspanins are characterized by the presence of N-terminal and C-terminal intracellular tails that have been implicated in 'outside-in' signalling in mammalian cells (Zhang *et al.*, 2002; Latysheva *et al.*, 2006). Here we have demonstrated that the 16 amino acids composing the C-terminal tail of TvTSP6 are necessary and sufficient for TSP localization to the flagellar membrane. Using domain-swapping experiments the C-terminal tail of TvTSP6 was shown to be capable of redirecting and preferentially targeting *T. vaginalis* TSP1 and TSP3 to the flagellar membrane. We propose that this 16-amino-acid tail is recognized by a protein(s) involved in flagellar targeting, thus mediating the association of TvTSP6 with the flagellar membrane protein trafficking machinery (Tobin and Beales, 2009). Little is known about the mechanisms used for targeting membrane proteins to the flagella; however, for the parasite *Trypanosoma brucei*, lipid rafts

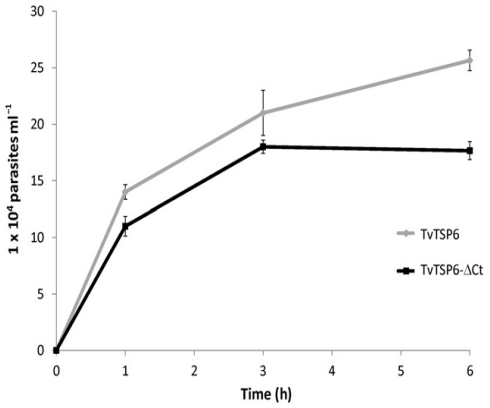

Fig. 7. Cell migration through Matrigel. Migration of parasites transfected with EpNEO, an empty episomal expression vector (black line), or TvTSP6ΔCt, a truncated C-terminal version of TvTSP6 (grey line), was determined over a 6 h period. Every sample in each point of the curve was carried out in triplicates. Error bars indicate standard deviations. A representative experiment of six independent experiments is shown. Note that after 6 h, 100% of the TvTSP6-transfected parasites had migrated into the lower chamber compared to 70% of TvTSP6ΔCt transfectants.

and palmitoylation appear to play crucial roles (Emmer *et al*., 2009; 2010). In this regard, it is notable that mammalian TSPs are known to reside in microdomains within the plasma membrane and to be palmitoylated (Hemler, 2005). We have also determined that TvTSP6 is palmitoylated (N. de Miguel *et al*., unpubl. data).

The pathobiology of *T. vaginalis* is multifaceted and involves the adhesion to and alteration of various mucosal landmarks: mucus, epithelial cell barrier, ECM, innate and adaptive immune cells, and bacterial microflora. These interactions are thought to be critical in initiating and maintaining infections (Fiori *et al*., 1999; Lehker and Alderete, 2000; Noel *et al*., 2010; Hirt *et al*., 2011; Ryan *et al*., 2011). Using an *in vitro* system that mimics the ECM, we demonstrated that TvTSP6 influences the migration of the parasite. When the C-terminal tail of this protein was deleted, the cell migration through Matrigel was reduced. We propose that the TvTSP6 C-terminal tail mutant (TvTSP6ΔCt) has a dominant negative effect on endogenous TvTSP6, similar to that observed upon the deletion of the C-terminal tail of the TSP protein CD151 (Zhang *et al*., 2002). This might be explained by the mutant TvTSP6ΔCt shifting the stoichiometric balance of endogenous wild-type TvTSP6 via the formation of oligomeric complexes between the two proteins. This in turn could disrupt critical TvTSP6 tail-dependent interactions involved in cellular migration, such as the interaction of the tail with proteases that degrade ECM. However, this is only one of several possible explanations; defining the mechanism underlying the observed reduction in migration awaits future studies. Although mammalian TSPs have been shown to be involved in cell migration (Liu *et al*., 2007; Powner *et al*., 2011) it also remains unclear which cellular processes are affected in this system.

The migration of *T. vaginalis* through Matrigel requires at least two activities: cell motility and degradation of ECM proteins. Mammalian TSPs are known to regulate cell motility (Maecker *et al*., 1997; Yanez-Mo *et al*., 1998; 2009) providing precedent for a possible role for TvTSP6 in promoting motility, a property of the parasite thought to be important for adhering to host cells. Alternatively, TvTSP6 may play a role in ECM degradation. Consistent with this, in mammalian cells, specific TSPs regulate proteolytic activity of metalloproteases (Sugiura and Berditchevski, 1999; Lafleur *et al*., 2009) and/or are involved in post-adhesion signalling (Hemler, 2003; 2005).

A transmembrane linker role has also been proposed for TSPs (Hemler, 1998) wherein extracellular domains of the protein link to external proteins while cytoplasmic domains link to intracellular enzymes to mediate, for example, 'outside-in' signalling (Hemler, 1998; Yauch and Hemler, 2000; Zhang *et al*., 2001). Similarly, intracellular TSP tail domains are thought to associate with signalling molecules such as PtdIns 4-K (Berditchevski *et al*., 1997; Yauch and Hemler, 2000) and PKC (Zhang *et al*., 2001). Our observations that the C-terminal cytoplasmic tail of TvTSP6 is involved in the redistribution of the protein upon exposure to host cells and parasite migration add further support for TSPs acting as transmembrane linkers. In conclusion, our results support a function for TvTSP6 in sensory reception and migration of *T. vaginalis*. Additional studies will be required to better define how these functions are mediated by TvTSP6, the first flagellar protein identified in this extracellular parasite.

Experimental procedures

Parasites, cell culture and media

The *T. vaginalis* strain B7RC2 (PA strain, ATCC 50167) was cultured in Diamond's Trypticase-yeast extract-maltose (TYM) medium supplemented with 10% horse serum, penicillin, streptomycin (Invitrogen) and iron as previously described (Clark and Diamond, 2002). Parasites were grown at 37°C and passaged daily. The human cervical ectocervical cell line Ect1 E6/E7 (ectocervical, ATCC CRL-2614), referred to as VECs, were grown as previously described (Fichorova *et al*., 1997) in keratinocyte-SFM complemented with provided recombinant protein supplements, penicillin, streptomycin and cultured at 37°C/5% CO_2.

Quantitative PCR (qPCR)

RNA was extracted from ~ 4×10^6 *T. vaginalis* from strains with different adherence capacities (de Miguel *et al*., 2010) using

TRIzol (Invitrogen) following the manufacturer's instructions. For exposure to host cells, ~ 10^7 B7RC2 parasites were incubated with vaginal epithelial cells (VECs) for various times, unattached parasites were removed and RNA was subsequently prepared from attached parasites and VECs scraped from the plate. Total RNA was treated with amplification grade DNase I (Invitrogen) and reverse transcribed using SuperScript III reverse transcriptase and oligo(dT) primers (Invitrogen). Real-time PCRs were performed using Brilliant SYBR Green qPCR Master Mix (Stratagene), a 150–450 nM concentration of each primer, and 200–500 ng of cDNA in a 20 μl reaction volume using an Eppendorf Mastercycler and realplex v.1.5 (Eppendorf). Parallel reactions performed without reverse transcriptase were included as negative controls. During the exponential phase of the qPCR, threshold cycle (CT) and base lines were set according to Eppendorf Mastercycler protocols. Data from different samples were interpolated from standard curves ran for each primer set and then normalized against the tubulin housekeeping gene. Every experimental and standard curve sample was tested in duplicate in three independent experiments. qPCR primer pair sequences were as follows: TUB-F, GTCTCG GCACACTCCTTCTC and TUB-R, AGACGTGGGAATGGAAC AAG; TvTSP6-qPCR-F, GCCAACTGTAAGCGAAAC; TvTSP6-qPCR-R, CGAAGACAATGATAACAATAGC.

Plasmid construction and exogenous protein expression in T. vaginalis

The TvTSP6, TvTSP6ΔCt, TSP1, TS1DCt, TSP3 and TSP3ΔCt constructs were generated using the following primer pairs:

TvTSP6-ATG-NdeI, AAACATATGATGGCGCTTAACGGAAAGT; TvTSP6-R-KpnI, TTTGGTACCTGGTTGTGGTGTTTGGCCTG; TvTSP6-ΔCt-KpnI, TTTGGTACCGTACATGCAGGAAATAACAAT; TSP1-ATG-NdeI, CATATGATGACCTGCTGTTCATGCA; Tsp1-R-Kpn1, GGTACCAACGTATGTGATGCCTTCCTT; TSP1DCT-R, TTTGGTACCTGGATCTTCGTAGCAGAAAGCGT; TSP3-ATG-NdeI, AAACATATGATGACTTGCTGTTCATGCA; TSP3-R-KpnI, AAAGGTACCAGAATATGAAGAACTAGAAT; TSP3-ΔCt-R, AAAGGTACCATGTGGTTTGTAGCAGCATCC.

NdeI and KpnI restriction sites were engineered into the 5′- and 3′-primers respectively. PCR fragments were generated using standard procedures and the resulting fragments were then cloned into the Master-Neo-$(HA)_2$ plasmid (Dyall *et al.*, 2000) to generate constructs to transfect into *T. vaginalis*. To generate the TSP1CT6 and TSP3CT6 constructs, two oligos of the C-terminal tail of TvTSP6: (TvTSP6C-F) GTACCAAGGTTGCT GCCGATGCTGATATCACAGGCCAAACACCACAACCAG and (TvTSP6CT-R) GTACCTGGTTGTGGTGTTTGGCCTGTGATAT CAGCATCGGCAGCAACCTTG, were annealed and cloned in frame into the TSP1ΔCT and TSP3ΔCt construct respectively. Electroporation of *T. vaginalis* strain B7RC2 was carried out as described previously (Delgadillo *et al.*, 1997) with 50 μg of circular plasmid DNA. Transfectants were selected with 100 μg ml^{-1} G418 (Sigma).

Immunolocalization experiments

Parasites in the absence of host cells were incubated at 37°C on glass coverslips as previously described (de Miguel *et al.*, 2010). To assess TSP6 localization in parasites attached to VECs, parasite were incubated at 37°C with VECs for 0.5, 1, 3 and 6 h, followed by 3× PBS washes to remove unbound parasites. All further incubations were carried out at room temperature. Cells were washed in PBS with 5% sucrose (PBS-S) and fixed in 4% formaldehyde for 20 min. After three washes, cells were permeabilized with 0.2% Triton X-100 in PBS for 15 min, blocked with 3% BSA in PBS (PBS-BSA) for 30 min, incubated with a 1:1000 dilution of anti-HA primary antibody (Covance, Emeryville, CA, USA) diluted in PBS–BSA, washed and then incubated with a 1:5000 dilution of Alexa Fluor-conjugated secondary antibody (Molecular Probes). The coverslips were mounted onto microscope slips using ProLong Gold antifade reagent with 4′,6′-diamidino-2-phenylindole (Invitrogen). Stained parasites were examined using an Axioscope 2 epifluorescence microscope (Zeiss), and images were recorded with an AxioCam camera and processed with the AxioVision 3.2 program (Zeiss).

Migration assays

Migration assays were performed on Matrigel invasion chambers (BD Biocoat, Beckton Dickinson Labware). Approximately 2.5×10^5 serum-starved transfected parasites were added to the upper chamber. In the bottom well, complete TYM media plus 20% v/v of VECs-conditioned media were added as a chemoattractant. The cells were incubated at 37°C over a time course to allow migration. The numbers of parasites that crossed the Matrigel and entered the bottom chamber were counted automatically using a Z1 coulter particles counter (Beckman). The number of cells in each of three wells per time point was counted and the standard error was calculated and plotted. As a control, the migration capacity of parasites transfected with an empty vector (EpNEO) was compared.

Acknowledgements

We thank Dr Clea Mantini for her contribution to the project, Drs Brian Janssen, Gil Lustig, Olivia Twu, Anh Vu and Yael Wexler-Cohen for critical comments on the manuscript and our colleagues in the lab for helpful discussions. This work was supported by the National Institute of Health R01 Grant AI069058 and ANPCyT (Agencia Nacional de Promocion Cientıfica y Tecnologica) Grant PICT-2011-0279. A. R. was supported by a UCLA Eugene V. Cota-Robles Fellowship and the Howard Hughes Medical Institute's Gilliam Fellowship for Advanced Study.

References

Berditchevski, F., Tolias, K.F., Wong, K., Carpenter, C.L., and Hemler, M.E. (1997) A novel link between integrins, transmembrane-4 superfamily proteins (CD63 and CD81), and phosphatidylinositol 4-kinase. *J Biol Chem* **272:** 2595–2598.

Clark, C.G., and Diamond, L.S. (2002) Methods for cultivation of luminal parasitic protists of clinical importance. *Clin Microbiol Rev* **15:** 329–341.

Delgadillo, M.G., Liston, D.R., Niazi, K., and Johnson, P.J. (1997) Transient and selectable transformation of the

parasitic protist *Trichomonas vaginalis*. *Proc Natl Acad Sci USA* **94:** 4716–4720.

Dyall, S.D., Koehler, C.M., Delgadillo-Correa, M.G., Bradley, P.J., Plumper, E., Leuenberger, D., *et al.* (2000) Presence of a member of the mitochondrial carrier family in hydrogenosomes: conservation of membrane-targeting pathways between hydrogenosomes and mitochondria. *Mol Cell Biol* **20:** 2488–2497.

Emmer, B.T., Souther, C., Toriello, K.M., Olson, C.L., Epting, C.L., and Engman, D.M. (2009) Identification of a palmitoyl acyltransferase required for protein sorting to the flagellar membrane. *J Cell Sci* **122:** 867–874.

Emmer, B.T., Maric, D., and Engman, D.M. (2010) Molecular mechanisms of protein and lipid targeting to ciliary membranes. *J Cell Sci* **123:** 529–536.

Fichorova, R.N. (2009) Impact of *T. vaginalis* infection on innate immune responses and reproductive outcome. *J Reprod Immunol* **83:** 185–189.

Fichorova, R.N., Rheinwald, J.G., and Anderson, D.J. (1997) Generation of papillomavirus-immortalized cell lines from normal human ectocervical, endocervical, and vaginal epithelium that maintain expression of tissue-specific differentiation proteins. *Biol Reprod* **57:** 847–855.

Fiori, P.L., Rappelli, P., and Addis, M.F. (1999) The flagellated parasite *Trichomonas vaginalis*: new insights into cytopathogenicity mechanisms. *Microbes Infect* **1:** 149–156.

Gander, S., Scholten, V., Osswald, I., Sutton, M., and van-Wylick, R. (2009) Cervical dysplasia and associated risk factors in a juvenile detainee population. *J Pediatr Adolesc Gynecol* **22:** 351–355.

Hemler, M.E. (1998) Integrin associated proteins. *Curr Opin Cell Biol* **10:** 578–585.

Hemler, M.E. (2003) Tetraspanin proteins mediate cellular penetration, invasion, and fusion events and define a novel type of membrane microdomain. *Annu Rev Cell Dev Biol* **19:** 397–422.

Hemler, M.E. (2005) Tetraspanin functions and associated microdomains. *Nat Rev Mol Cell Biol* **6:** 801–811.

Hirt, R.P., de Miguel, N., Nakjang, S., Dessi, D., Liu, Y.C., Diaz, N., *et al.* (2011) *Trichomonas vaginalis* pathobiology new insights from the genome sequence. *Adv Parasitol* **77:** 87–140.

Hong, I.K., Kim, Y.M., Jeoung, D.I., Kim, K.C., and Lee, H. (2005) Tetraspanin CD9 induces MMP-2 expression by activating p38 MAPK, JNK and c-Jun pathways in human melanoma cells. *Exp Mol Med* **37:** 230–239.

Huang, H., Sossey-Alaoui, K., Beachy, S.H., and Geradts, J. (2007) The tetraspanin superfamily member NET-6 is a new tumor suppressor gene. *J Cancer Res Clin Oncol* **133:** 761–769.

Lafleur, M.A., Xu, D., and Hemler, M.E. (2009) Tetraspanin proteins regulate membrane type-1 matrix metalloproteinase-dependent pericellular proteolysis. *Mol Biol Cell* **20:** 2030–2040.

Latysheva, N., Muratov, G., Rajesh, S., Padgett, M., Hotchin, N.A., Overduin, M., and Berditchevski, F. (2006) Syntenin-1 is a new component of tetraspanin-enriched microdomains: mechanisms and consequences of the interaction of syntenin-1 with CD63. *Mol Cell Biol* **26:** 7707–7718.

Lehker, M.W., and Alderete, J.F. (2000) Biology of trichomonosis. *Curr Opin Infect Dis* **13:** 37–45.

Liu, L., He, B., Liu, W.M., Zhou, D., Cox, J.V., and Zhang, X.A. (2007) Tetraspanin CD151 promotes cell migration by regulating integrin trafficking. *J Biol Chem* **282:** 31631–31642.

McClelland, R.S., Sangare, L., Hassan, W.M., Lavreys, L., Mandaliya, K., Kiarie, J., *et al.* (2007) Infection with *Trichomonas vaginalis* increases the risk of HIV-1 acquisition. *J Infect Dis* **195:** 698–702.

Maecker, H.T., Todd, S.C., and Levy, S. (1997) The tetraspanin superfamily: molecular facilitators. *FASEB J* **11:** 428–442.

de Miguel, N., Lustig, G., Twu, O., Chattopadhyay, A., Wohlschlegel, J.A., and Johnson, P.J. (2010) Proteome analysis of the surface of *Trichomonas vaginalis* reveals novel proteins and strain-dependent differential expression. *Mol Cell Proteomics* **9:** 1554–1566.

Noel, C.J., Diaz, N., Sicheritz-Ponten, T., Safarikova, L., Tachezy, J., Tang, P., *et al.* (2010) *Trichomonas vaginalis* vast BspA-like gene family: evidence for functional diversity from structural organisation and transcriptomics. *BMC Genomics* **11:** 99.

Okumura, C.Y., Baum, L.G., and Johnson, P.J. (2008) Galectin-1 on cervical epithelial cells is a receptor for the sexually transmitted human parasite *Trichomonas vaginalis*. *Cell Microbiol* **10:** 2078–2090.

Pearson, M.S., Pickering, D.A., McSorley, H.J., Bethony, J.M., Tribolet, L., Dougall, A.M., *et al.* (2012) Enhanced protective efficacy of a chimeric form of the schistosomiasis vaccine antigen Sm-TSP-2. *PLoS Negl Trop Dis* **6:** e1564.

Pols, M.S., and Klumperman, J. (2009) Trafficking and function of the tetraspanin CD63. *Exp Cell Res* **315:** 1584–1592.

Powner, D., Kopp, P.M., Monkley, S.J., Critchley, D.R., and Berditchevski, F. (2011) Tetraspanin CD9 in cell migration. *Biochem Soc Trans* **39:** 563–567.

Ryan, C.M., de Miguel, N., and Johnson, P.J. (2011) *Trichomonas vaginalis*: current understanding of host-parasite interactions. *Essays Biochem* **51:** 161–175.

Scholey, J.M. (2003) Intraflagellar transport. *Annu Rev Cell Dev Biol* **19:** 423–443.

Stark, J.R., Judson, G., Alderete, J.F., Mundodi, V., Kucknoor, A.S., Giovannucci, E.L., *et al.* (2009) Prospective study of *Trichomonas vaginalis* infection and prostate cancer incidence and mortality: Physicians' Health Study. *J Natl Cancer Inst* **101:** 1406–1411.

Sugiura, T., and Berditchevski, F. (1999) Function of alpha3beta1-tetraspanin protein complexes in tumor cell invasion. Evidence for the role of the complexes in production of matrix metalloproteinase 2 (MMP-2). *J Cell Biol* **146:** 1375–1389.

Sutcliffe, S., Alderete, J.F., Till, C., Goodman, P.J., Hsing, A.W., Zenilman, J.M., *et al.* (2009) Trichomonosis and subsequent risk of prostate cancer in the Prostate Cancer Prevention Trial. *Int J Cancer* **124:** 2082–2087.

Swygard, H., Sena, A.C., Hobbs, M.M., and Cohen, M.S. (2004) Trichomoniasis: clinical manifestations, diagnosis and management. *Sex Transm Infect* **80:** 91–95.

Tobin, J.L., and Beales, P.L. (2009) The nonmotile ciliopathies. *Genet Med* **11:** 386–402.

Tran, M.H., Pearson, M.S., Bethony, J.M., Smyth, D.J., Jones, M.K., Duke, M., *et al.* (2006) Tetraspanins on the surface of *Schistosoma mansoni* are protective antigens against schistosomiasis. *Nat Med* **12:** 835–840.

Van Der Pol, B., Kwok, C., Pierre-Louis, B., Rinaldi, A., Salata, R.A., Chen, P.L., *et al.* (2008) *Trichomonas vaginalis* infection and human immunodeficiency virus acquisition in African women. *J Infect Dis* **197:** 548–554.

World Health Organization (2005) Prevalence and incidence of selected sexually transmitted infections, *Chlamydia trachomatis*, *Neisseria gonorrhoeae*, syphilis and *Trichomonas vaginalis*: methods and results used by WHO to generate 2005 estimates. *WHO Library Cataloguing-in-Publication Data*, 1–36.

Yanez-Mo, M., Alfranca, A., Cabanas, C., Marazuela, M., Tejedor, R., Ursa, M.A., *et al.* (1998) Regulation of endothelial cell motility by complexes of tetraspan molecules CD81/TAPA-1 and CD151/PETA-3 with alpha3 beta1 integrin localized at endothelial lateral junctions. *J Cell Biol* **141:** 791–804.

Yanez-Mo, M., Barreiro, O., Gordon-Alonso, M., Sala-Valdes, M., and Sanchez-Madrid, F. (2009) Tetraspanin-enriched microdomains: a functional unit in cell plasma membranes. *Trends Cell Biol* **19:** 434–446.

Yauch, R.L., and Hemler, M.E. (2000) Specific interactions among transmembrane 4 superfamily (TM4SF) proteins and phosphoinositide 4-kinase. *Biochem J* **351** (Pt 3)**:** 629–637.

Zhang, X.A., Bontrager, A.L., and Hemler, M.E. (2001) Transmembrane-4 superfamily proteins associate with activated protein kinase C (PKC) and link PKC to specific beta(1) integrins. *J Biol Chem* **276:** 25005–25013.

Zhang, X.A., Kazarov, A.R., Yang, X., Bontrager, A.L., Stipp, C.S., and Hemler, M.E. (2002) Function of the tetraspanin CD151-alpha6beta1 integrin complex during cellular morphogenesis. *Mol Biol Cell* **13:** 1–11.

Supporting information

Additional Supporting Information may be found in the online version of this article:

Fig. S1. Subcellular localization of the TvTSP3CT6 protein in parasites bound to VECs. Parasites transfected with TvTSP3CT6 containing a C-terminal HA tag were bound to VECs for 0.5, 1, 3 and 6 h and the protein was localized using an anti-HA antibody. Note the change in localization from plasma membrane and intracellular vesicles to primarily a flagellar localization at 3 and 6 h post host cell exposure. The red arrow indicates the flagella and the white arrow indicates intracellular vesicles and the plasma membrane of the main body of the cell. Scale bar, 10 μm.

Chapter 4:

TVAG_393390, a potential adhesin and cytolytic factor of *Trichomonas vaginalis*

Abstract:

Cell to cell attachment is considered to be one of the critical processes that allowed the rise of multicellular metazoans. However, relics of these initial cell-to-cell interactions may be present in single celled eukaryotes. In this study we present initial characterization of a hypothetical protein, called TVAG_393390, with a predicted cadherin-like secondary structure. This feature is of interest since cadherins mediate cell-to-cell attachment in multicellular organisms. We report that exogenous expression of TVAG_393390 with an N-terminal GFP tag, leads to the increased ability of *T. vaginalis* to attach to and lyse host cells, thus further mechanistic dissection of this protein and its family members may reveal important *T. vaginalis* adhesins.

Introduction:

The flagellated, extracellular, protozoan parasite *Trichomonas vaginalis* successfully inhabits many human hosts worldwide, owing to its status of causing the most common non-viral sexually transmitted disease [1]. For *T. vaginalis* and other mucosal pathogens, adherence to host cells in the initial phase of infection is important in order to gain a foothold in its human host and prevent its mechanical clearance [2]. After attachment, *T. vaginalis* lyse host cells for nutrient acquisition [3]. Little is still known about parasite factors that mediate both of these processes [4].

The *T. vaginalis* genome encodes about 60,000 genes [5], making it the highest gene-coding protozoan parasite [5]. Bioinformatic analysis of the genome [4-6], transcriptomic studies [7, 8], and proteomic studies [9-11] have pointed to the presence of proteins/protein groups that may contribute to pathogenesis. However, many of these proteins are annotated as "hypothetical" proteins and lack identifiable domains to reveal functional aspects that may be

further studied. Therefore, at this point in time, mining the genome and surface proteome for potential virulence factors is still a challenging endeavor, but definitely one that is worth undertaking since such analyses of *T. vaginalis* may reveal important cellular aspects applicable to eukaryotes in general.

Single-celled protists, like *T. vaginalis*, do not contain cell junctions which mediate the strongest forms of cell-cell attachment [12], however, it has been hypothesized that protein precursors found in protozoans may have given rise to the complexes that allowed cell-cell interactions leading to multicellularity [13]. *T. vaginalis* cell-cell interactions are readily observed as groups of parasites are visible when growing the parasite axenically [14] and when attached to ectocervical cells and prostate cells [15, 16]. The ability of *T. vaginalis* to aggregate also appears to correlate with strains that have higher adherence and cytolytic properties [14], and a role for one protein, called tetraspanin 8 (TSP8), has been recently found to help mediate this process [14]. Tetraspanins are proteins with four transmembrane domains which function as molecular facilitators, bringing together other membrane proteins to increase the efficacy of their function [17]. Interestingly, after 30 minutes of attachment to host cells, the endogenous expression of another *T. vaginalis* tetraspanin called TSP6, increases by 14-fold [18], further demonstrating a potential involvement of TSPs in *T. vaginalis* attachment. In mammalian cells, integrin proteins are one of the predominant protein groups complexed by tetraspanins [17], however the *T. vaginalis* genome does not contain any proteins annotated as integrin-like (www.trichdb.org). Furthermore, there has been no successful identification of TSP6 partners (our unpublished results). Consequently, identification of adhesion-related proteins that may make contact with TSPs are of great interest to pursue.

A candidate family of proteins that may interact with and help TSPs promote parasite-parasite attachment and/or host-parasite interactions-are cadherin-like proteins. Interestingly, the human E-cadherin protein has been found to interact with a tetraspanin protein [19]. Cadherins are cell-adhesion proteins that form part of adherens junctions, mainly binding homophilically between two apposing cells [20]. Cadherin binding to Ca^{2+} ions is necessary to rigidify their extracellular domains and mediate cell-cell interactions [21]. Multiple mucosal microorganisms co-opt host proteins such as E-cadherin and exploit them for attachment and invasion [22]. One of the best examples of this phenomenon is highlighted by *Listeria monocytogenes*, a bacterium that causes a severe food-borne disease, which binds host cell E-cadherin [2]. Interestingly, E-cadherin is also expressed on the surface of endocervical and ectocervical cells where *T. vaginalis* may interact with it via cadherin-like proteins.

A study has demonstrated that *T. vaginalis* interacts with and perturbs human junctional complexes [23]. Incubation of *T. vaginalis* with a human intestinal cell line (Caco-2) caused a decrease in transepithelial electrical resistance indicating an effect on the integrity and permeability of the epithelial barrier [23]. Furthermore, *T. vaginalis* also caused a relocalization of the junctional complex proteins occludin, E-cadherin, and ZO-1 at sites where the parasite was attached [23]. This finding could indicate that *T. vaginalis* can make contact with tight junctions and adherens junctions [24]. *T. vaginalis* association with higher rates of human immunodeficiency virus (HIV) acquisition are predicted to occur in part due to *T. vaginalis* perturbation and damage of the epithelial barrier expanding human HIV's portal of entry [25]. Therefore, studies investigating the physical and molecular nature of *T. vaginalis* interaction with human host cells of the urogenital tract are necessary to better understand the course of *T. vaginalis* infection and potential mechanisms leading to exacerbation of other diseases.

A *T. vaginalis* surface protein, TVAG_166850, has a role in promoting parasite attachment to host cells [9] and it possesses a cadherin-like domain (Riestra *et al.* unpublished results), supporting the possibility of cadherin-like proteins having a potential role in host-parasite interactions. We have found another hypothetical *T. vaginalis* cell surface protein, TVAG_393390, that was previously identified in the *T. vaginalis* cell surface proteome [9], which contains a predicted cadherin-like secondary structure and its characterization is presented in this study.

Results:

Bioinformatic analysis reveals potential secondary structure similarity to cadherin proteins

TVAG_393390 is annotated in the TrichDB genome as a "conserved hypothetical protein" with no annotation of predicted domains. InterPro (http://www.ebi.ac.uk/interpro), Pfam (http://pfam.xfam.org), and NCBI protein BLAST analysis (http://blast.ncbi.nlm.nih.gov/blast/Blast.cgi?PROGRAM =blastp&PAGE_TYPE=BlastSearch&LINK_LOC=blasthome) did not identify any functional domains either. However, the secondary structure prediction program called Phyre2 (http://www.sbg.bio.ic.ac.uk/phyre2/html/page.cgi?id=index) did yield some insight into a predicted function for this protein. The Phyre2 program is used to predict a protein's structure based on a large database of known secondary structures [26].

Phyre2 analysis produced 20 predicted 3-D models with greater than 97% confidence for the TVAG_393390 protein. The most common modeling to a particular type of protein was to cadherin proteins. The 5 predicted models using cadherin proteins as templates yielded models with 97.9-98.6 % confidence (see Fig. 4-1 A). Fig. 4-1 B shows the predicted TVAG_393390 structure modeled on the mouse n-cadherin/cadherin 2 protein, which gave the highest

confidence model. The modeled region spans most of the TVAG_393390 protein-shown graphically in Fig. 4-1 C. TVAG_393390 has one predicted TM domain (aa 539-561) and a peculiarly small 2 amino acid C-terminal tail (Fig. 4-1 C).

Most cadherin proteins have 5 extracellular domains (EC) with Ca^{2+} ion binding sites at the regions between these ECs [27]. Similarly, TVAG_393390 also contains 5 predicted ECs with the classical β-sandwich domains and Greek-key folding of cadherin proteins [28] (see Fig. 4-1 B). Inspection of the TVAG_393390 protein sequence together with Phyre2 analysis reveals that there are also 5 predicted Ca^{2+} binding sites (Fig 4-2 A) at the interfaces of these ECs, another classical feature of cadherin proteins [21] (Fig. 4-2 B).

Interestingly, the C-terminus of TVAG_393390 did not show conservation and was not modeled on the cadherin templates (see Fig. 4-1 C). C-termini of cadherins interact with β- and α-catenin proteins that connect the cadherin C-termini with the cytoskeleton, but this feature is only found in metazoans [12]. There are also no proteins annotated as catenin-like in the *T. vaginalis* genome. Therefore TVAG_393390 may represent an early evolutionary form of cadherin-like proteins.

Exogenous expression of GFP-TVAG_393390 and investigation of its cellular location

Analysis of the proteins identified in the cell surface proteomes of six different strains by de Miguel *et al.* revealed that TVAG_393390 was present on the cell surface of all the strains surveyed [9]. This may indicate a highly conserved role in strains that display low and high adherence and cytolytic properties. To further examine the localization and function of TVAG_393390, we exogenously expressed the gene with an N-terminal GFP tag under the control of the strong α-SCS promoter. We confirmed expression of the tagged fusion protein by western blot (Fig. 4-3). The expected molecular weight of GFP-TVAG_393390 is 91 kDa, but

we observed it to migrate higher (~110 kDa) which is likely due to glycosylation of the protein, since it has at least 7 predicted glycosylation sites (TOPO2 program).

Next, we examined the localization of GFP-TVAG_393390 in *T. vaginalis*. The GFP tag is located on the extracellular portion of TVAG_393390, thus it should be accessible to binding with an anti-GFP antibody in the absence of permeabilization.

We performed indirect immunofluorescence assays using an anti-GFP antibody with both non-permeabilized and permeabilized transfectants. GFP-TVAG_393390 transfectants were indeed stained even in the absence of permeabilization (Fig. 4-4 A), and the signal was not too different from permeabilized cells (Fig. 4-4 E)-further supporting a cell-surface localization of TVAG_393390. It must be noted that this signal is not likely to stem from internal GFP fluorescence, since special aeration of cells for prolonged periods of time are necessary to detect fluorescent signal from the GFP protein without the use of an antibody (our unpublished studies). Interestingly, upon shorter exposure times (which reduced the strong cell surface signal) we could also view localization of GFP-TVAG_393390 on what appears to be the recurrent flagella/undulating membrane that is attached to the body of the parasite. This signal could be observed in non-permeabilized (Fig. 4-4 C-D) and permeabilized cells as well (Fig. 4-4 G-H).

Exogenous expression of TVAG_393390 in *T. vaginalis* increases its attachment to and cytolysis of ectocervical cells

Having confirmed expression of GFP-TVAG_393390 by western blot and fluorescence microscopy, we wanted to determine whether TVAG_393390 contributes to parasite attachment to host cells, since it exhibits similarity to cadherin proteins that have roles in cell-cell adhesion. We compared the ability of empty vector and GFP-TVAG_393390 transfectants to attach to ectocervical cells and found that exogenous expression of GFP-TVAG_393390 led to a 2.8-fold

increase in parasite attachment (Fig. 4-5 A). After *T. vaginalis* attach to host cells, they lyse the host cells [29]. However, not all proteins that promote attachment also promote cytolysis (our unpublished results).

Only a few proteins that promote cytolysis of host cells have been identified [3]. We tested whether exogenous expression of GFP-TVAG_393390 had an effect on *T. vaginalis* ability to lyse host cells and found that GFP-TVAG_393390 transfectants had a 7.4-fold increased ability to lyse host cells (Fig. 4-5 B). Therefore TVAG_393390 may participate in two important phases of *T. vaginalis* interaction with host cells. Current work investigating the contribution of one of the more highly conserved predicted Ca^{2+} binding sites (shown in Fig. 4-2) is underway. Functionally dissecting the properties of TVAG_393390 will help uncover how the protein helps to induce increased parasite adherence and cytolysis.

Discussion:

Elucidation of *T. vaginalis'* "interactome" by identification of proteins that contribute to parasite-parasite and parasite-host attachment will shed light on the mechanistic aspects utilized by *T. vaginalis* to successfully inhabit and thrive in the harsh environment of the urogenital tract. We have identified one surface protein, TVAG_393390, which may contribute to *T. vaginalis* interaction with host cells based on its ability to increase attachment to and lysis of host ectocervical cells. TVAG_393390 may be structurally analogous to cadherin proteins in metazoans which are one of the main families that mediate cell-cell adhesion [20].

While most cadherin proteins display homophilic binding, some also display heterophilic binding [20]. This latter property may give precedence to a potential cadherin-like protein on *T. vaginalis* binding a cadherin protein on the host cell. This notion is further strengthened by the ability of other microbes to bind E-cadherin for host cell entry [2]. A similar molecular mimicry strategy may also be utilized by *T. vaginalis*, since *T. vaginalis* is itself a eukaryotic cell that may

possess some early evolutionary forms of these proteins. Four main families mediate cellular attachment in mammalian cells, they are 1) Cadherin family 2) Immunoglobulin superfamily 3) Integrin superfamily and the 4) Selectin family [30]. To our knowledge, no previous reports of proteins resembling these adhesion proteins in *T. vaginalis* exist, but an exciting possibility is that TVAG_393390 and other family members may highlight the presence of cadherin-like proteins.

Further investigation is necessary to specifically determine the mechanism by which TVAG_393390 promotes attachment and cytolysis. Furthermore, testing whether anti-cadherin antibodies can block or reduce the interaction of *T. vaginalis* with host cells may be helpful to identify which/if any cadherin host proteins are bound by TVAG_393390. E-cadherin and N-cadherin are expressed in the human male and female urogenital and reproductive tracts [24, 31]. E- and N-cadherin are also found on spermatozoa [31], and *T. vaginalis* can also attach to and phagocytose sperm cells [32]. It would therefore be interesting to test whether GFP-TVAG_393390 transfectants also display higher attachment to sperm cells, as there is no current knowledge of the proteins that mediate these interactions. Interestingly, E-cadherin localizes to the cell surface and flagella in sperm [31] and we also observed localization of GFP-TVAG_393390 on the cell surface and what appears to be the recurrent flagellum in *T. vaginalis*. Future co-localization studies with the TSP6 protein which displays very strong flagellar targeting when exogenously expressed in *T. vaginalis* [18] will help to further confirm TVAG_393390's flagellar localization. Given the possible interactions between tetraspanin and cadherin proteins [19], it will also be of interest to determine whether these two family members can physically interact in *T. vaginalis.* We are now one protein closer to delineating the molecular links between *T. vaginalis* and host cells.

Materials and Methods:

Growth of *T. vaginalis.*

The *T. vaginalis* RU393 strain (ATCC 50142) was grown in TYM medium supplemented with 10% horse serum, penicillin and streptomycin (Invitrogen), and iron as described previously [33]. Parasites were incubated at 37°C and passaged daily for less than two weeks.

Growth of ectocervical cells.

The human ectocervical cell line Ect1 E6/E7 (ATCC CRL-2614) was grown as described [34] in Keratinocyte-serum free media (K-SFM, GIBCO) completed with recombinant protein supplements provided by the company (human recombinant epidermal growth factor and bovine pituitary extract), and 0.4 mM filter-sterilized calcium chloride. Cells were grown at 37°C in a 5% CO_2 incubator.

GFP-TVAG_393390 plasmid construction and exogenous expression in *T. vaginalis.*

TVAG_393390 was PCR amplified from G3 genomic DNA with flanking SacII and BamH1 restriction sites encoded in the forward and reverse primers, respectively (Fwd 5'-ccgcggATTTGGACTTTTTTATTGCAGGATGC, Rev 5'-ggatccTTACTTTCTAAGCCAAAGAATTATTACTAACACT) and cloned into the Nt-eGFP-MasterNeo construct using the SacII and BamH1 restriction sites. GFP-TVAG_393390 expression is driven from the strong alpha-succinyl CoA synthetase B (alpha-SCS) promoter [35]. Electroporation of the RU393 strain was performed as previously described [35] using 100 ug of circular plasmid DNA. Four hours after transfection, transfectants were selected with 100 µg/ml G418 (GIBCO) and maintained with drug selection.

Western blot detection of the GFP-TVAG_393390 protein:

$5X10^6$ cells of GFP-TVAG_393390 or Empty vector transfectants (negative control) were spun down at 3,200 rpm for 10 minutes. Cell pellets were washed with 1 ml of PBS+5% sucrose+HALT protease inhibitors (SIGMA). Cells were spun for 5 minutes at 3,500 rpm and cell pellets were resuspended in 250 ul of 2%SDS/50 mM Tris pH 7.5 lysis buffer+HALT protease inhibitors. Sonication of samples was performed 3 times with 10 sec bursts at the 3.8 setting. Afterwards, cells were spun down at 13,000 rpm for 10 min to remove insoluble material, and the supernatant was transferred to a new tube. A BCA assay (ThermoScientific) was performed to determine protein concentrations and equal protein samples were used for western bot analysis using an anti-GFP (Clontech) antibody and a donkey-anti-mouse-HRP conjugated secondary antibody (Jackson Laboratories).

Indirect Immunofluorescence Assays.

GFP-TVAG_393390 or Empty vector transfectants were allowed to bind to glass coverslips and afterwards fixed with 4% formaldehyde/1X PBS for 20 minutes. Coverslips were washed three times with 1X PBS and then half of the samples were permeabilized for 15 min in PBS+0.2% TritonX-100. All samples were then blocked in 3% BSA/1X PBS for 30 minutes at room temperature. Coverslips were incubated for 1 hour in a 1:1,000 dilution of mouse anti-GFP (Clontech) diluted in the blocking solution. After three PBS washes, coverslips were incubated for 1 hour in a 1:5,000 goat anti-mouse Alexa Fluor®488-conjugated secondary antibody dilution (Molecular Probes) also prepared in blocking solution. Three PBS washes were performed and coverslips were mounted onto glass microscope slides using ProLong Gold antifade reagent with 4'-6'-diamidino-2-phenylindole (DAPI) (Invitrogen). Images were taken using an Axio Imager Z1 microscope equipped with an AxioCamMR3 camera. Image processing was performed using the AxioVision 3.2 program (Zeiss).

Cytolysis and Attachment Assays.

T. vaginalis adherence and cytolysis of ectocervical cells was assayed as described in [29]. For attachment assays, $5X10^4$ parasites were added per well and incubated with ectocervical cells for 30 minutes. For cytolysis assays, $1X10^5$ parasites were added per well and incubated for 4 hours with ectocervical cells.

A

Template	amino-acid region aligned	% confidence	% identity
Xenopus laevis (frog) c-cadherin ectodomain	7-520	98.6	10
mouse e-cadherin ectododomain	7-520	98.6	10
Drosophila n-cadherin 1 ectodomain 1-3	225-515	98.3	7
mouse n-cadherin ectodomain	8-514	98	12
Drosophila n-cadherin ectodomain1-4	170-515	97.9	10

B

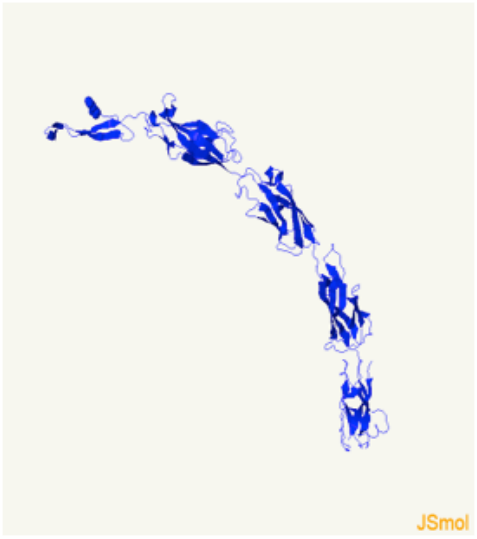

C

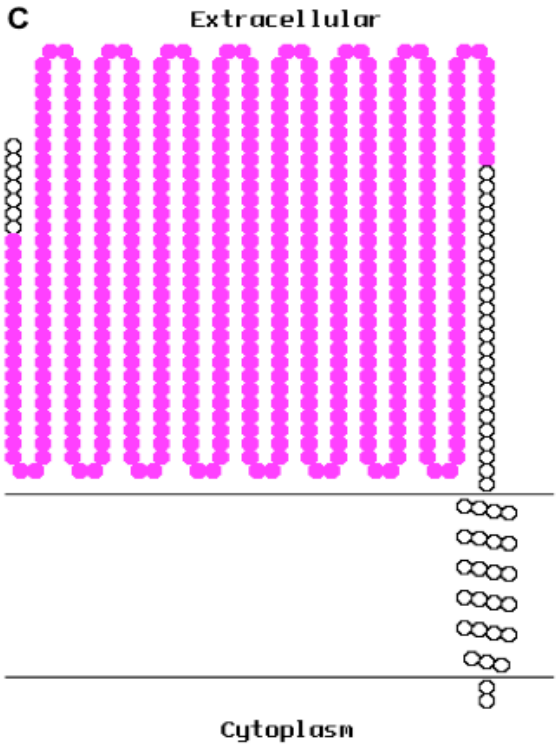

Figure 4-1: Cadherin-like Phyre2 secondary structure prediction of TVAG_393390. **(A)** The characteristics of the Phyre2 3-D models using cadherin proteins as templates for prediction of TVAG_393390's secondary structure are shown. **(B)** Predicted structure of TVAG_393390 in the highest confidence model using mouse n-cadherin as the template. **(C)** Predicted topology of TVAG_393390 generated with the TOPO2 program. Pink highlighting shows the region of TVAG_393390 aligned in the highest confidence model shown in B.

A

Predicted sequence of Ca^{2+} ion binding site	amino acid locations
DQD	112-114
DGED	171-174
DEYD	218-221
DPD	443-445

B

Figure 4-2: Predicted Ca^{2+} binding sites in TVAG_393390.
(A) Inspection of the TVAG_393390 protein sequence for potential Ca^{2+} binding sites (LDRE, DXD, DXXD, x=any amino acid [27]) reveals 4 predicted Ca^{2+} binding sites that are located between the predicted extracellular domains like in mammalian cadherins. The predicted amino acid location of the calcium binding sites is shown. **(B)** The location of one of the predicted Ca^{2+} ion binding sites between two extracellular domains and predicted by Phyre2 analysis to be highly sensitive to mutations (DPD) is shown by two red balls indicative of the D443 and D445 residues.

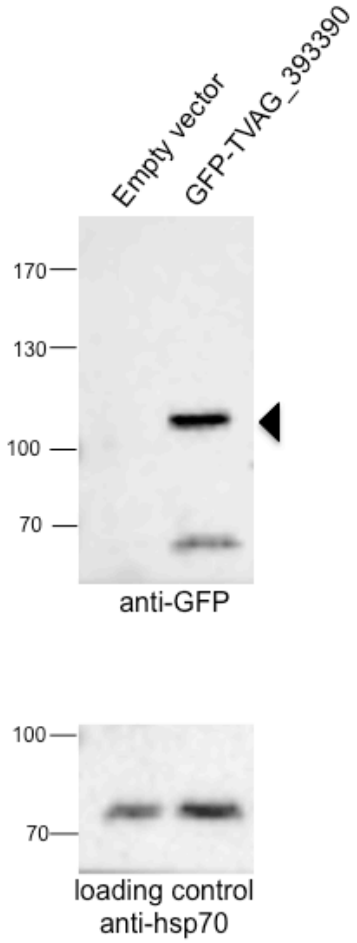

Figure 4-3: Exogenous expression of TVAG_393390 in the *T. vaginalis* RU393 strain.
The RU393 *T. vaginalis* strain was transfected with a construct encoding TVAG_393390 with an N-terminal GFP tag. As a negative control, *T. vaginalis* cells were transfected with an empty vector. Western blot of whole cell lysates was performed using an anti-GFP antibody (top panel) or an anti-hsp70 (bottom panel) for equal loading control. Expression of GFP-TVAG_393390 in transfectants (indicated by black arrow) was confirmed.

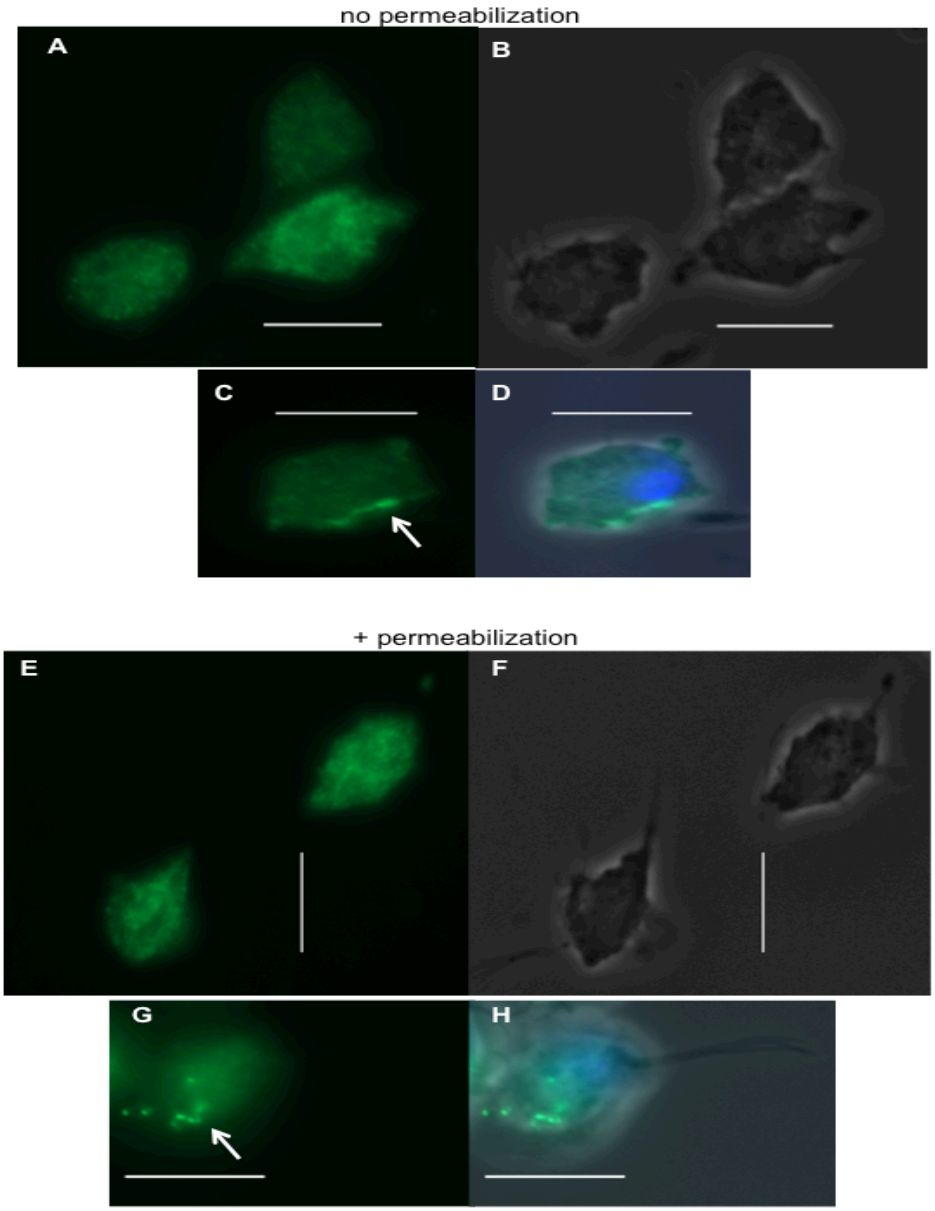

Figure 4-4: Subcellular localization of GFP-TVAG_393390 in *T. vaginalis*.
Indirect immunofluorescence assays of GFP-TVAG_393390 or Empty vector transfectants (not shown) was performed using an anti-GFP antibody (green) and 4% formaldehyde fixation without permeabilization (A-D) or with permeabilization (E-H). Nuclear staining in C-D and G-H was performed using 4'-6'-diamidino-2-phenylindole (DAPI-blue). Phase images are shown in B and F. Merge of phase+DAPI+anti-GFP images is shown in D and H. Scale bar=10μm. In addition to cell surface localization, white arrow also denotes possible presence on the recurrent flagellum.

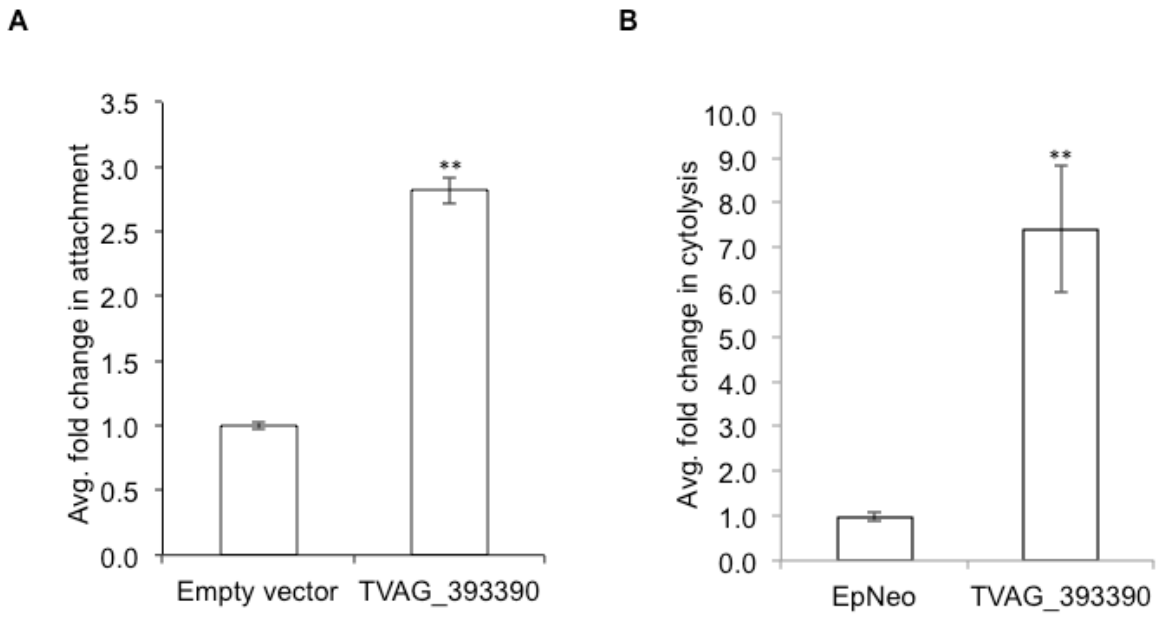

Figure 4-5: TVAG_393390 exogenous expression in *T. vaginalis* leads to an increased ability to attach to and lyse ectocervical cells.
(A) Empty vector and GFP-TVAG_393390 transfectants were fluorescently labeled and incubated with ectocervical cell monolayers for 30 min followed by quantification of adhered parasites. The average fold change in attachment compared to empty vector transfectants for two experiments each performed in triplicate is shown. Error bars denote the standard error, **p<0.01. **(B)** Empty vector and GFP-TVAG_393390 transfectants were incubated with ectocervical cell monolayers for 4 hours and ectocervical cell lysis was measured using the LDH release assay. The average fold change in cytolysis compared to empty vector transfectants for two experiments performed in triplicate is shown. Error bars denote the standard error, **p<0.01.

References:

1. WHO *Dept. of Reproductive Health and Research. Global incidence and prevalence of selected curable sexually transmitted infections-2008*. 2012.

2. Boyle, E.C. and B.B. Finlay, *Bacterial pathogenesis: exploiting cellular adherence.* Curr Opin Cell Biol, 2003. **15**(5): p. 633-9.

3. Ryan, C.M., N. de Miguel, and P.J. Johnson, *Trichomonas vaginalis: current understanding of host-parasite interactions.* Essays Biochem, 2011. **51**: p. 161-75.

4. Hirt, R.P., et al., *Trichomonas vaginalis pathobiology new insights from the genome sequence.* Adv Parasitol, 2011. **77**: p. 87-140.

5. Carlton, J.M., et al., *Draft Genome Sequence of the Sexually Transmitted Pathogen Trichomonas vaginalis.* Science, 2007. **315**(5809): p. 207-212.

6. Nakjang, S., et al., *A novel extracellular metallopeptidase domain shared by animal host-associated mutualistic and pathogenic microbes.* PLoS One, 2012. **7**(1): p. e30287.

7. Gould, S.B., et al., *Deep sequencing of Trichomonas vaginalis during the early infection of vaginal epithelial cells and amoeboid transition.* Int J Parasitol, 2013. **43**(9): p. 707-19.

8. Huang, K.Y., et al., *Comparative transcriptomic and proteomic analyses of Trichomonas vaginalis following adherence to fibronectin.* Infect Immun, 2012. **80**(11): p. 3900-11.

9. de Miguel, N., et al., *Proteome analysis of the surface of Trichomonas vaginalis reveals novel proteins and strain-dependent differential expression.* Mol Cell Proteomics, 2010. **9**(7): p. 1554-66.

10. Cuervo, P., et al., *Differential soluble protein expression between Trichomonas vaginalis isolates exhibiting low and high virulence phenotypes.* J Proteomics, 2008. **71**(1): p. 109-22.

11. Ramon-Luing, L.A., et al., *Immunoproteomics of the active degradome to identify biomarkers for Trichomonas vaginalis.* Proteomics, 2010. **10**(3): p. 435-44.

12. Miller, P.W., et al., *The evolutionary origin of epithelial cell-cell adhesion mechanisms.* Curr Top Membr, 2013. **72**: p. 267-311.

13. King, N., *The unicellular ancestry of animal development.* Dev Cell, 2004. **7**(3): p. 313-25.

14. Coceres, V.M., et al., *The C-terminal tail of tetraspanin proteins regulates their intracellular distribution in the parasite Trichomonas vaginalis.* Cell Microbiol, 2015.

15. Kusdian, G., et al., *The actin-based machinery of Trichomonas vaginalis mediates flagellate-amoeboid transition and migration across host tissue.* Cell Microbiol, 2013. **15**(10): p. 1707-21.

16. Vazquez-Carrillo L. I., Q.-G.L.I., Arroyo R., Mendoza-Hernández G., González-Robles A., Carvajal-Gamez B. I., Alvarez-Sánchez M. E, *The effect of Zn2+ on prostatic cell cytotoxicity caused by Trichomonas vaginalis.* Journal of Integrated OMICS, 2011. **1**(2): p. 198-210.

17. Hemler, M.E., *Tetraspanin functions and associated microdomains.* Nat Rev Mol Cell Biol, 2005. **6**(10): p. 801-11.

18. de Miguel, N., A. Riestra, and P.J. Johnson, *Reversible association of tetraspanin with Trichomonas vaginalis flagella upon adherence to host cells.* Cellular microbiology, 2012. **14**(12): p. 1797-1807.

19. Greco, C., et al., *E-cadherin/p120-catenin and tetraspanin Co-029 cooperate for cell motility control in human colon carcinoma.* Cancer Res, 2010. **70**(19): p. 7674-83.

20. Zaidel-Bar, R., *Cadherin adhesome at a glance.* J Cell Sci, 2013. **126**(Pt 2): p. 373-8.

21. Kim, S.A., et al., *Calcium-dependent dynamics of cadherin interactions at cell-cell junctions.* Proc Natl Acad Sci U S A, 2011. **108**(24): p. 9857-62.

22. Costa, A.M., et al., *Adherens junctions as targets of microorganisms: a focus on Helicobacter pylori.* FEBS Lett, 2013. **587**(3): p. 259-65.

23. da Costa, R.F., et al., *Trichomonas vaginalis perturbs the junctional complex in epithelial cells.* Cell Res, 2005. **15**(9): p. 704-16.

24. Blaskewicz, C.D., J. Pudney, and D.J. Anderson, *Structure and Function of Intercellular Junctions in Human Cervical and Vaginal Mucosal Epithelia.* Biology of Reproduction, 2011. **85**(1): p. 97-104.

25. Shafir, S.C., F.J. Sorvillo, and L. Smith, *Current issues and considerations regarding trichomoniasis and human immunodeficiency virus in African-Americans.* Clin Microbiol Rev, 2009. **22**(1): p. 37-45, Table of Contents.

26. Kelley, L.A., et al., *The Phyre2 web portal for protein modeling, prediction and analysis.* Nat Protoc, 2015. **10**(6): p. 845-58.

27. Nollet, F., P. Kools, and F. van Roy, *Phylogenetic analysis of the cadherin superfamily allows identification of six major subfamilies besides several solitary members.* J Mol Biol, 2000. **299**(3): p. 551-72.

28. Patel, S.D., et al., *Cadherin-mediated cell-cell adhesion: sticking together as a family.* Curr Opin Struct Biol, 2003. **13**(6): p. 690-8.

29. Lustig, G., et al., *Trichomonas vaginalis contact-dependent cytolysis of epithelial cells.* Infect Immun, 2013. **81**(5): p. 1411-9.

30. Juliano, R.L., *Signal transduction by cell adhesion receptors and the cytoskeleton: functions of integrins, cadherins, selectins, and immunoglobulin-superfamily members.* Annu Rev Pharmacol Toxicol, 2002. **42**: p. 283-323.

31. Vazquez-Levin, M.H., et al., *Epithelial and neural cadherin expression in the mammalian reproductive tract and gametes and their participation in fertilization-related events.* Dev Biol, 2015. **401**(1): p. 2-16.

32. Benchimol, M., et al., *Trichomonas adhere and phagocytose sperm cells: adhesion seems to be a prominent stage during interaction.* Parasitol Res, 2008. **102**(4): p. 597-604.

33. Clark, C.G. and L.S. Diamond, *Methods for cultivation of luminal parasitic protists of clinical importance.* Clin Microbiol Rev, 2002. **15**(3): p. 329-41.

34. Fichorova, R.N., J.G. Rheinwald, and D.J. Anderson, *Generation of papillomavirus-immortalized cell lines from normal human ectocervical, endocervical, and vaginal epithelium that maintain expression of tissue-specific differentiation proteins.* Biol Reprod, 1997. **57**(4): p. 847-55.

35. Delgadillo, M.G., et al., *Transient and selectable transformation of the parasitic protist Trichomonas vaginalis.* Proc Natl Acad Sci U S A, 1997. **94**(9): p. 4716-20.

Chapter 5:

Efforts towards development of *T. vaginalis* molecular tools and characterization of several *T. vaginalis* putative cell surface proteins

Abstract:

Elucidation of the *Trichomonas vaginalis*-human host interactome is an important endeavor as it may reveal unique parasite proteins that can be targeted to prevent disease. A limitation in identifying these proteins is the fact that a large majority of the parasite's proteins are classified as hypothetical proteins. At minimal, proteins of interest may be located at the cell surface and the *T. vaginalis* surface proteome conducted by de Miguel *et al.* [1] revealed such proteins. In this study we report on the characterization of 6 hypothetical proteins. We currently need a one by one protein approach to study the potential function of proteins with the limited molecular tools that we posses to manipulate the parasite. In this study, we explored the adaptation of the FKBP-destabilization domain system and antisense oligos containing locked nucleic acids as a way to help modulate protein levels and gain functional insight. Although we were able to successfully use the FKBP-destabilization domain to regulatably express a rhomboid 1 catalytic mutant protein, we could not conclude on the successful adaptation of antisense LNA-oligos. However, with the latter we did obtain modulation of host cell cytolysis when targeting a couple of proteins thus future optimization of this molecular tool may be warranted.

Introduction:

The surface of the extracellular parasite *Trichomonas vaginalis* is a vastly unchartered territory. This is an important interphase that helps the parasite bind to its human host for colonization of the urogenital tract. Therefore, it is imperative that we identify and characterize the factors that contribute to this key interaction. *T. vaginalis* adheres to the epithelia, which often leads to host cell lysis. However, we still do not have a clear understanding of the temporal and mechanistic details of these two processes. Questions such as the following exist. Does

adherence always lead to killing of host cells, and if not, how are both processes regulated? Is damage of host cells an additive process and a group effort by *T. vaginalis*? What factors, other than mechanical lysis, cause adverse effects on its human host such as alterations in host cell signaling? Furthermore, *T. vaginalis* exhibits contact-dependent and contact-independent mechanisms for host cell destruction [2], therefore do different molecular players may contribute to each process?

The best functionally characterized *T. vaginalis* surface molecule is a dense sugar structure recently renamed lipoglycan (previously referred to as lipophosphoglycan-LPG) [3-5]. It is estimated that about $3X10^6$ molecules of TvLG coat the cell surface of *T. vaginalis* [3]. The TvLG molecule contains terminal galactose and N-acetylglucosamine sugars which allow the parasite to bind the host galectin-1 protein to promote parasite attachment to host cells [6]. To date, there has been no other host proteins identified as receptors for *T. vaginalis*.

About 86% of the *T. vaginalis* genome is predicted to encode "hypothetical" proteins that lack homology to characterized proteins [7]. Furthermore, although the *T. vaginalis* genome does encode potential virulence factors of interest based on homology to established pathogenic factors such as the metalloprotease GP63-like and BspA leucine-rich repeat proteins, these are massively expanded gene families having at least 77 and 658 members, respectively. Together, these factors highlight the need to provide additional methods to screen potential proteins that contribute to *T. vaginalis* pathogenesis. A very fruitful approach, undertaken by de Miguel *et al.* was to identify proteins that are located at the cell surface of six different strains [1]. The cell surface proteome of three strains that have low attachment (T1, G3, and SD10) and three strains with high adherence (PA, B7268, SD7) was reported [1]. Eleven proteins that were more abundant in adherent versus non-adherent strains were identified [1]. However, ~1/3 of the

identified proteins were again annotated as hypothetical proteins, but at least we now have evidence of their putative cell surface localization [1].

In this chapter we report on the characterization of several proteins identified in the cell surface proteome, or proteins related to ones identified in the surface proteome. To help investigate the role of surface proteins contributing to pathogenesis it was also our goal to help develop additional tools to investigate proteins of interest and we also report some of those efforts in this chapter.

Currently, the most established molecular approach that has allowed the identification of two cell surface proteins that promote parasite attachment to host cells are gain of function experiments where a protein of interest is exogenously expressed in a *T. vaginalis* strain that displays low-to medium adherence and cytolytic properties and then the effect of producing more of the protein of interest on modulating these processes is assessed [1]. We were interested in adapting methods that would also allow us to perform the converse loss of function experiments in *T. vaginalis*.

Targeted gene deletion or targeted gene replacement are one of the most desirable ways to study a gene's function when it is not an essential gene [8]. In *T. vaginalis*, there have only been two published reports of successful gene knockouts of two different metabolic proteins, ferredoxin and a hydrogenosomal membrane protein (TvHMP23) [9, 10]. Extensive attempts targeting various genes have been made (our laboratory's unpublished results) but no successful knockout of other genes has been obtained.

An alternative to gene knockouts is performing knockdowns where the mRNA for a gene is bound by a complementary sequence, preventing expression of the protein [11]. Antisense oligos whose expression is driven from a plasmid have been used with limited success to target a

nuclear transcription factor called Myb3 [12] and three proteins that have been suggested to have roles in parasite attachment to host cells-glyceraldehyde 3-phosphate [13], AP33 [14], and AP65 [15]- although their putative function has been called into question [2]. During the course of our studies, Munoz *et al.* reported successfully delivering chemically synthesized phosphorothioate oligonucleotides into *T. vaginalis* targeting the protein phosphatase 1 gamma (TvPP1γ) [16]. The phosphorothioate modification involves replacing one of the non-bridging oxygens in the DNA phosphate backbone by a sulfur group (see Fig. 5-2 A) and this modification helps reduce endonuclease and exonuclease degradation of the oligos, increasing their stability in the cell [11].

This chapter presents our own efforts to develop knockdown technology using phosphorothioate antisense oligonucleotides that also contain locked nuclei acid bases (LNAs) also known as bridged nucleic acids [17, 18]. LNA bases are nucleotide analogues that have a methylene bridge between the 2'-oxygen and the 4'-carbon of the ribose ring (see Fig. 5-2 A). This chemical locking of the ribose ring causes reduced flexibility of the sugar, in turn leading to greater organization of the phosphate backbone and increased hybridization affinity to its complementary sequence. For example, each LNA base substitution in an oligo can increase the melting temperature (Tm) of an oligo by as much as 10°C [19, 20]. The LNA bases can be positioned throughout a DNA oligo to obtain LNA/DNA "mix-mers" or they can be placed at the ends of the oligo with DNA bases positioned in between to create LNA/DNA/LNA gap-mers [18]. In some studies, the LNA gap-mers have been found to be more efficient than mix-mers [20], and the successful use of gap-mers has been widely documented [18, 20-22].

Another very desirable feature of LNA-containing oligos is their potential to be used as therapeutics due to their high specificity, low or lack of *in vivo* toxicity, and the fact that they do not require special delivery vehicles [22]. There have been two LNA-oligo based therapies that

have reached Phase 2 clinical trials. One of these drugs (SPC2968 now called RG6061) targets the human transcription factor hypoxia-inducible factor-1 alpha, which is overexpressed in many cancers [23]. The other LNA-oligo drug is called miravirsen and it binds to a microRNA that is necessary for Hepatitis C virus replication in the liver [24]. Future studies will reveal the efficacy of LNA-oligo treatment modalities in humans.

In addition to technology targeting mRNA, we also sought to adapt a technology that has been successfully used in the Apicomplexan parasites *Toxoplasma gondii* and *Plasmodium falciparum* to regulate protein levels [25]. A system using a destabilization domain was first described by Banaszynski *et al.* in mammalian cells [26]. It involves fusion of a protein of interest to a mutant form of the rapamycin-binding protein (FKBP12)/destabilization domain which causes the fused protein to be targeted for proteosomal degradation [26] (see schematic in Fig. 5-1 A). The fusion protein can be stably expressed upon addition of a chemical ligand called Shield1, named for its ability to "shield" the protein from degradation [26]. The strength of this system relies on being able to achieve rapid, reversible, and tunable control of the protein of interest being studied [27].

We previously found that exogenous expression of the *T. vaginalis* rhomboid protease 1 (TvROM1) leads to an increased ability to lyse host ectocervical cells (Riestra *et al.* unpublished results; see Chapter 2). Therefore, we were interested in further investigating this phenotype and used this observation to explore the potential efficacy of LNA-oligos. In this chapter we also present the characterization of several proteins that we had identified as putative *T. vaginalis* TvROM1 substrates, which merited further study since they were identified in the *T. vaginalis* cell surface proteome and their roles in promoting attachment to host cells or cytolysis of host cells had not been previously investigated.

Results:

Regulatable expression of the *T. vaginalis* rhomboid 1 protein

The FKBP destabilization domain system was of great interest to us in part due to its successful application in other parasites. We previously found that exogenous expression of rhomboid 1 containing the catalytic residues Ser262 and His316 mutated to alanines led to about a 50% decrease in host cell lysis (data not shown). Rhomboid protease catalytic mutants have been previously hypothesized to function as dominant negative proteins, by their potential ability to bind their substrates and sequester them away from cleavage by the endogenous wildtype rhomboid in turn leading to a down modulation of functions they contribute to [28, 29]. It was discovered that a single mutation of the catalytic serine to alanine led to a decrease in thermodynamic stability, however, mutation of both catalytic residues rescued rhomboid stability and a catalytic histidine to alanine mutant was also stable [30]. Therefore, we initially tried to regulatably express both His316A and S262A H316A catalytic mutants. We could successfully regulate the expression of both TvROM1 mutants upon the addition of the Shield1 chemical ligand in two different strains, G3 and RU393 (representative of RU393 strain is shown in Fig. 5-1 B). However, expression of the double catalytic mutant was higher than the single mutant and therefore we focused on further functional characterization of the double mutant. For our purposes we also chose to focus on expression in the RU393 strain, since in this strain an18 hr incubation led to maximal protein expression and then an additional 4hrs was necessary to perform a cytolysis assay, and the total amount of time required was still within a window of time shown to lead to maximal protein expression (24 hrs) [26]. Regulatable expression of the rhomboid 1 catalytic mutant also caused a regulatable effect on host cell cytolysis, with expression of the potential dominant negative protein causing a 50% reduction of the parasite's

ability to lyse host cells (Fig. 5-1 C). Therefore, we have been able to successfully show a functional effect by regulation of a protein using the FKBP destabilization system in *T. vaginalis*.

Attempts to knockdown *T. vaginalis* rhomboid 1 using antisense LNA-oligos

Obtaining further evidence for a role of rhomboid 1 mediating effects on host cell cytolysis, we aimed to assess whether we could identify LNA-oligos (see Fig. 5-2) that could target rhomboid 1 and cause a decrease in cytolysis as proof of principle that this technology could be applied to *T. vaginalis*. During the course of this study 4 different LNA oligos that would bind to 4 different regions of rhomboid 1 mRNA were tested in total (shown in Fig. 5-2 B and C). We will describe different conditions that were tested below, but initially we wanted to examine if we could deliver the LNA-oligos into *T. vaginalis.*

LNA-oligos can be transfected into host cells and also uptaken from the media [22]. For example in a study by Zhang *et al.* they found that 26 out of 28 cell lines could uptake LNA oligos from the media causing at least a 20% reduction on HIF-1α mRNA [22]. Furthermore, the effect of LNA-oligos can be long-lasting as exemplified by Greenberger *et al.* who found that 24hrs after LNA-oligo transfection, there was a 24% reduction in HIF-1α protein levels and ~60% decreased protein levels after 5 days [31]. Therefore, in our beginning experiments we wanted to determine whether we could successfully deliver LNA-oligos into *T. vaginalis,* and whether we could still detect the presence and potential function of the oligos. We could successfully deliver FITC-labeled oligos both by transfection (Fig. 5-3 A and B) and by allowing the parasites to uptake the oligos (Fig. 5-3 C). We could detect the FITC-LNA oligo signal even after 54 hrs post-transfection (Fig. 5-3 B). While both methods of LNA-oligo delivery appeared to work, uptake of oligos required significantly higher amounts of the LNA-oligo and thus we focused on transfection of the LNA-oligos.

In the beginning of our study we did not have an anti-rhomboid 1 antibody therefore our initial experiments were performed using G3 cells exogenously expressing HA-tagged rhomboid 1. We observed a statistically significant decrease in host cell cytolysis by 50% and 70% (compared to the anti-TSP6 oligo control) in two independent experiments when we transfected 10 μM of the "anti-Rh1" oligo and tested cytolysis 20 and 30 hrs after transfection (Fig. 5-4 A). It must be noted that after transfection we transferred the parasites into a 50 ml volume, which gave a 60 nM final concentration of the oligo. Although more cost-prohibitive, we also tried transfecting with 100 uM of the anti-Rh1 oligo into *T. vaginalis* giving a final 600 nM oligo concentration in 50 ml with a longer incubation time of 54 hrs but we did not observe a statistically significant decrease in host cell cytolysis (Fig 5-4 B) and thus didn't place an emphasis on following up this concentration. We also observed a 30% decrease in host cell cytolysis compared to the negative control oligo when we allowed parasites to uptake the anti-Rh1 oligo (Fig. 5-4 C). Unfortunately, although we could detect an effect on host cell cytolysis with an oligo targeting rhomboid 1, and not when we targeted TSP6 which we haven't found to have a role in cytolysis (negative control), we could not observe an effect at knocking down rhomboid 1 at the protein level (Fig. 5-4 D, shows a representative).

We were hopeful that perhaps with other oligos we could observe an effect on host cell lysis and knockdown of rhomboid 1 at the protein level. For the first anti-Rh1 oligo, we had enlisted the help of the Exiqon company which synthesizes the oligos, so they inserted LNA bases at a proprietary locations. For the next 3 oligos we designed the insertion of the LNA bases and tested different negative controls.

To experiment with different time points, we allowed cytolysis assays with G3 parasites to proceed for 10.5 hrs, 12 hrs, and 14hrs. The assays were performed 16 hrs from the time of

transfection with the "anti-Rh1_A" oligo compared to a mismatch control that had 4 bases from the anti-Rh1_A sequence substituted by a different base (see Fig 5-2 B). We could not detect an inhibition on host cell cytolysis by LNA-oligo treatment (Fig 5-5 A). Nor could we detect an effect on endogenous rhomboid 1 levels using the anti-Rh1_A oligo (Fig. 5-5 B).

We then transitioned to using the RU393 strain since cytolysis assays with this strain only requires a 4 hr incubation with host cells, *vs.* 16-18 hrs required to assess cytolysis by the G3 strain, hoping that maybe we could see a more potent effect closer to the time of oligo-transfection. We tested the effect of the "anti-Rho1" oligo compared against a negative control that we generated by scrambling the anti-Rho1 sequence (see Fig 5-2 B), 18hrs after transfection. In 2 out of 4 experiments we found a statistically significant 30% decrease in host cell cytolysis when we targeted rhomboid 1 in *T. vaginalis* compared against the scrambled negative control (Fig. 5-6 A), however the vehicle control also caused a statistically significant 20% decrease in host cell lysis, thus we can not conclude with certainty about anti-Rho-1's observed effects. Furthermore, we could not observe a decrease of the rhomboid 1 protein either (Fig. 5-6 B).

For a last attempt, we switched over to using an anti-lacZ oligo that would target a sequence for mRNA of a protein that is not present in *T. vaginalis* as a negative control, since we had observed that the vehicle control was sometimes different than the oligo negative control and desired to eliminate such a difference. Transfecting *T. vaginalis* with 10 and 20 uM (60 and 120 nM final) concentrations of anti-ROM1 oligo caused a statistically significant increase (10% and 20%) in the parasite's ability to lyse host cells compared to the anti-lacZ negative control (Fig. 5-7).

Characterization of proteins identified in the *T. vaginalis* cell surface proteome

In parallel to the studies described above, we were also in the process of trying to identify putative substrates for rhomboid proteases in *T. vaginalis*. Fig. 5-8 provides a reference to where the proteins we tried to characterize below were identified, the approach used to identify the substrates listed from the 3,4-DCI mass spectrometry experiments and from searching the *T. vaginalis* surface proteome with a rhomboid parasite substrate search motif that we generated is described in Chapter 2. TVAG_166850 and TVAG_280090 were found to be cleaved *T. vaginalis* rhomboid 1. TVAG_166850 was previously studied by [1] and we present additional characterization in Chapter 2. We could not detect cleavage of the other putative substrates so we do not focus on their role as rhomboid substrates here, rather we hope to provide a reference about the possible role in contributing to pathogenesis. To study this role, we exogenously expressed some of the proteins with N-terminal GFP tags, localized them, and tested effects of exogenous expression on attachment and/or cytolysis of ectocervical cells. For some proteins we also tried to test if there was an effect caused by targeting the production of that protein using LNA-oligos as a means to help screen the function of the proteins.

TVAG_280090

TVAG_280090 was identified as a putative substrate for *T. vaginalis* rhomboid 1 by generating a motif that summarized common amino acid features in substrates cleaved by rhomboids in other parasites (see Chapter 2 Fig. 2-5). We first began the characterization of TVAG_280090 by trying to generate co-transfectants for another purpose in the G3 strain. We found that exogenous expression of TVAG_280090 in parasites co-transfected with an empty vector called EmptyPac had a 40% and 50% reduced ability to lyse host cells in 2 out of 4 experiments (Fig 5-9 A). This was puzzling to us, but as will become evident in the results below we have identified a couple of surface proteins that also lead to decreased host cell lysis.

We next tested whether this phenotype was also observed in three different single TVAG_280090 G3 transfectants and found that in 2 out 3 transfectants, exogenous expression of TVAG_280090 also led to decreased cytolysis of host cells (Fig. 5-9 B). In RU393 co-transfectants it also caused a decrease in host cell lysis (Fig. 5-10 A). Therefore, exogenous expression of TVAG_280090 causing decreased host cell lysis appears to be a true phenotype of this protein. Interestingly, exogenous expression of TVAG_280090 in G3 co-transfectants leads to an increase in host cell attachment (Fig. 5-9 C). TVAG_280090 was identified in the cell surface proteome (see Fig. 5-8) and we also determined the localization of GFP-TVAG_280090 to be on the cell surface and co-localized with the surface rhomboid 1 protein (Fig. 5-10 B). Fig. 5-10 C shows a representative of the protein expression pattern, in which we can observe a protein of the expected molecular weight and a higher migrating form likely due to glycosylation of the protein (3 predicted glycosylation sites by TOPO2).

TVAG_189150 and TVAG_321740:

We identified TVAG_189150 and TVAG_321740 as proteins of interest by searching the *T. vaginalis* surface proteome for proteins that had similar cleavage sites to the *T. gondii* microneme proteins MIC2 and MIC6 which are cleaved by rhomboid proteases [32-37]. TVAG_189150 also had our rhomboid substrate parasite search motif (see Chapter 2 Fig. 2-5). We confirmed the cell-surface localization of GFP-TVAG_189150 (Fig. 5-11 A) and GFP-TVAG_321740 (Fig. 5-12 A) and their expression (Fig. 5-11 C and Fig. 5-12 E), respectively. Exogenous expression of GFP-TVAG_189150 caused a very small 10% decrease in host cell cytolysis (Fig. 5-11 B), hence we did not proceed with its characterization. After our initial attempts to characterize TVAG_189150, Nackjang *et al.* re-annotated this protein as having an M60-like zinc metallopeptidase domain [38]. Therefore, that may be an interesting function to

investigate. Exogenous expression of GFP-TVAG_321740 led to a 60% and 30% decrease in host cell lysis by G3 co-transfectants (Fig. 5-12 B) and G3 single-transfectants (Fig 5-12 C), respectively. While exogenous expression did not cause an effect on attachment to host cells (Fig. 5-12 D).

TVAG_573910:

TVAG_573910 was one of the proteins identified in Chapter 2 Fig. 2-4, for being released less into the cell supernatant after *T. vaginalis* rhomboid 1 transfectants were incubated with the broad-spectrum 3,4-DCI serine protease inhibitor. TVAG_573910 could not be cleaved by *T. vaginalis* rhomboid 1 in the HEK293 heterologous cell cleavage assay, but it may be a substrate for another serine protease that normally causes release of this protein. To study this protein we incubated *T. vaginalis* with antisense LNA-oligos targeting TVAG_573910 as a quick way to assess a potential role in contributing to host cell lysis. In 2 out of 3 experiments, we could observe a 20% statistically significant decrease in host cell lysis in parasites treated with the anti-TVAG-573910 oligo compared to anti-lacZ negative control oligo treatment (Fig. 5-13). However, the vehicle control also had 20% reduced cytolysis compared to the anti-lacZ negative control, thus TVAG_573910 may contribute to cytolysis but future studies are necessary to confirm this.

TVAG_099730 and TVAG_394260:

TVAG_099730 and TVAG_394260 were identified in mass spectrometry experiments we performed to try to identify proteins that were differentially released into the cell supernatant when Empty vector, 3X-HA rhomboid 1 or 3X-HA rhomboid 1 double catalytic mutant transfectants were placed in contact with ectocervical cells (see Fig. 5-8). However, due to the large scale nature of the experiment, we observed differential lysis between the three different

conditions, thus we were careful about considering these proteins as putative rhomboid substrates. After trying to normalize for cell lysis, we identified two proteins that appeared to fit criteria of a potential rhomboid substrate. Their cleavage by *T. vaginalis* rhomboid 1 was assessed but they were not found to be substrates. We found that both GFP-TVAG_099730 and GFP-TVAG_394260 had cell surface-like localization (Fig. 5-14 A and 5-15 A) in agreement with both proteins also being identified in the *T. vaginalis* cell surface proteome [1]. Exogenous expression of TVAG_099730 led to both a 60% increase and a 70% decrease in host cell lysis in two independent G3 transfectants (Fig. 5-14 C). However, when we tried treatment with an anti-TVAG_099730 LNA oligo we observed a 40% decrease in host cell cytolysis in 3 out of 4 experiments compared to the negative control oligo (Fig. 5-14 D). Thus we hypothesize that TVAG_099730 may have a role in promoting host cell lysis. Fig. 5-14 B shows we could detect expression of the GFP-TVAG_099730 protein by western blot.

We could detect expression of GFP-TVAG_394260 by IFA, but we could not detect expression of the full-length protein by western blot (Fig. 5-15 B), this may be due to the very large size (~297 kDa including the GFP-tag) and proteolytic cleavage leading to the smaller molecular weight products we observed. Exogenous expression of TVAG_394260 did not cause an effect on host cell lysis (Fig. 5-15 C) or host cell attachment (Fig. 5-15 D) by trying to target this protein with antisense LNA-oligos.

Discussion:

Although we placed strong efforts on trying to further develop antisense LNA-oligo technology in *T. vaginalis*, we cannot conclude on its effective use at the moment. We could detect phenotypic changes compared to negative control oligos by 2 out of 4 different oligos we tested targeting rhomboid 1. However, the effect was not observed in every experiment in the

case of the anti-Rho1 oligo and we could not detect an effect at the rhomboid-1 protein level, thus due to the later we can not conclude that the decreased cytolysis that we observed is due to *T. vaginalis* rhomboid 1 protein knockdown. However, we did show successful delivery of FITC-labeled LNA oligos into *T. vaginalis* by both transfection and by allowing the parasite to uptake the oligos, and the fact that even after 54 hrs from transfection we could still detect their presence-highlights some of the attractive features of LNA oligos that may merit further optimization. Increasing the LNA-oligo concentrations may lead to more potent results. Due to the fact that rhomboid 1 is a multi-TM domain protein that is embedded in the plasma membrane, we needed larger numbers of parasites to have enough cells for the phenotypic assays and for western blot analysis since we needed to sonicate and solubilize the whole cell lysate samples for successful protein detection. Therefore, further optimization with a soluble protein may provide better results.

In regards to our characterization of surface proteome proteins, further characterization of TVAG_573910 and TVAG_099730 may be of interest due to decreased cytolysis observed with LNA-oligos that may potentially down-modulate these proteins compared to anti-lacZ negative control. However, an antibody against these proteins is necessary to confirm this finding. We have experimental evidence that TVAG_573910 is released into *T. vaginalis* cell supernatants based on our results presented in Chapter 2. Interestingly, even when this protein in expressed in mammalian HEK-293 cells it is also readily detected in cell supernatants (Chapter 2), providing further evidence of conserved features that lead to its release to the outside of the cell. TVAG_573910 has a concanavalin A-like lectin/glucanase domain however it is predicted to be located mostly in its small intracellular C-terminal tail, thus the role of this protein is still a mystery just like that of the many other conserved hypothetical proteins without identifiable

domains to further dissect. Our hope was that LNA-oligos could serve as a way to do initial screenings that then could be corroborated with transfectants. This was mostly the case with TVAG_099730 for which we observed a decrease of host cell cytolysis with LNA-oligo targeting and we observed an increase in host cell cytolysis when over-expressing GFP-TVAG_099730 in *T. vaginalis* with one transfectant. But it must be noted that another transfectant displayed decreased cytolysis when GFP-TVAG_099730 was overexpressed-highlighting part of the difficulty observed with *T. vaginalis* variability in cellular assays and the need to perform multiple transfections to determine an overall trend.

Exogenous expression of TVAG_280090, TVAG_321740, and TVAG_189150 caused a statistically significant decrease in host cell cytolysis. This was largely unexpected and we do not have a clear understanding of how this process is occurring. In the case of TVAG_280090, we may speculate that *T. vaginalis* rhomboid 1 may cleave it and the cleaved fragment may go on to bind ectocervical cells providing a cytoprotective effect. These results do highlight the complexity in understanding the connection between attachment and cytolysis of host cells, since for example although exogenous expression of GFP-TVAG_321740 does not affect attachment to host cells, but it does cause a reproducible decrease in host cell lysis. TVAG_189150 has now been identified to contain a domain found in metallopeptidases with potential mucin-degrading activity [38]. Thus although we didn't detect an effect on cytolysis in one experiment, further investigation of this protein other than cytolysis may be of interest, especially in testing its catalytic activity using host cell proteins as substrates.

We do report on the successful use of the FKBP-destabilization domain system leading to a functional effect in *T. vaginalis.* Screening proteins for their roles in cytolysis using this method may provide a clearer answer since the effect of a protein of interest is compared within

the same population of cells, helping to overcome some of the variability that can be observed even when transfecting the same protein into different transfectants. Furthermore, the tunability of the FKBP system may also allow the observation of a protein dose-dependent effect on the potential function of interest.

Materials and Methods:

Growth of *T. vaginalis.*

The *T. vaginalis* G3 (ATCC PRA98) or RU393 strain (ATCC 50142) was grown in TYM medium supplemented with 10% horse serum, penicillin and streptomycin (Invitrogen), and iron as described previously [39]. Parasites were incubated at 37°C and passaged daily for less than two weeks.

Growth of ectocervical cells.

The human ectocervical cell line Ect1 E6/E7 (ATCC CRL-2614) was grown as described [40] in Keratinocyte-serum free media (K-SFM, GIBCO) completed with recombinant protein supplements provided by the company (human recombinant epidermal growth factor and bovine pituitary extract), and 0.4 mM filter-sterilized calcium chloride. Cells were grown at 37°C in a 5% CO_2 incubator.

Cloning of surface proteome proteins with an N-terminal GFP tag and exogenous expression in *T. vaginalis.*

Putative surface proteome proteins were amplified from G3 genomic DNA with flanking SacII and BamH1 restriction sites encoded in the forward and reverse primers, respectively and without their initiating methionine (provided by fusion to GFP). PCR products were cloned into

Nt-eGFP-MasterNeo vector. The following primer pairs were used to amplify each indicated gene:

TVAG_280090Fwd: 5'-CCGCGGTTCGCTTTCTTAACTTATAATGTGC

TVAG_280090Rev: 5'-GGATCCTTAAACTGCAAGAGCTGCTTCATTATCC

TVAG_189150fwd: 5'-CCGCGGTTTCTCCTATTAGCTTTGGG

TVAG_189150Rev: 5'-GGATCCTTAAACTGCAAGAGCTGCTTCATTATCC

TVAG_321740Fwd: 5'-CCGCGGCTACTTGCATTAGAGCTCTTC

TVAG_321740Rev: 5'-GGATCCTTATTCTGTAGTAATGAGTGG

TVAG_573910fwd: 5'-CCGCGGGTAATCCTTACATCTGGCTCTAAAACAATTGAT

TVAG_573910rev: 5'-GGATCCTTAAGGTTTCTGACTTTCTTCGAATTCATCAGA

TVAG_099730fwd: 5'-CCGCGG CTGACCTTCTTCAGCGTGTTTTG

TVAG_099730rev: 5'-GGATCCTTAAACTGCTTCGGCTGGATG

TVAG_394260fwd: 5'-CCGCGG CATTGCTTTTTGTTTCTCAGCTTTGC

TVAG_394260rev: 5'-GGATCCTTATGGATTTTGTTCTTCAAATTCATCAGAG

Expression of the GFP-tagged proteins is driven from the strong alpha-succinyl CoA synthetase B (alpha-SCS) promoter [41]. Electroporation of the G3 and RU393 strain was performed as previously described [41] using 100 ug of circular plasmid DNA. Four hours after transfection, transfectants were selected with 100 μg/ml G418 (GIBCO) and maintained with drug selection. For co-transfectants, cells were transfected with the EmptyPac vector and selected with 60 μg/ml Puromycin Dihydrochloride (A.G. Scientific, Inc.) as described above, after parasites were stably expressing they were then transfected with the EpNeo or GFP-tagged protein constructs and selected with both G418 and Puromycin.

Western blot detection of tagged proteins:

$5X10^6$ cells of transfectants were spun down at 3,200 rpm for 10 minutes. Cell pellets were washed with 1 ml of PBS+5% sucrose+HALT protease inhibitors (SIGMA). Cells were spun for 5 minutes at 3,500 rpm and cell pellets were resuspended in 250 ul of 2%SDS/50 mM Tris pH 7.5 lysis buffer+HALT protease inhibitors. Sonication of samples was performed 3 times with 10 sec bursts at the 3.8 setting. Afterwards, cells were spun down at 13,000 rpm for 10 min to remove insoluble material, and the supernatant was transferred to a new tube. A BCA assay (Thermo Scientific) was performed to determine protein concentrations and equal protein concentration samples were used for western bot analysis. The following antibodies were used for western blots: anti-FKBP12 (Abcam), anti-HA (Covance), anti-GFP (Clontech), mouse anti-Rhomboid 1 produced against a synthetic peptide by Abcam, rabbit anti-hsp70, rabbit anti-ferredoxin, anti-mouse or anti-rabbit-HRP conjugated secondary antibodies (Jackson Laboratories). For all experiments an empty vector transfectant was carried along as a negative control.

RU393 FKBP-destabilization domain experiments:

$3.84X10^6$ transfectant cells were aliquoted, spun down at 3,200 rpm for 10 minutes, then resuspended in 32 ml of completed Diamonds media+G418. 14 ml of parasites were added to two 14-ml conical tubes. 1 uM final concentration of Shield1 was added to the experimental group. Parasites were incubated for 18 hrs, An aliquot of the parasites was taken for western blot analysis and the remainder used for a cytolysis assay. The cytolysis assay was performed as described above, except that for the "+Shield" samples, Shield1 was added to cKSFM media used for all of the steps including parasite washes and the final resuspension, thus Shield1 was present while the parasites were exposed to ectocervical cells. Shield1 was also added to ectocervical cells as a control, but no cell toxicity with Shield1 treatment was detected.

For all LNA-oligo experiments:

LNA-oligos were ordered from the Exiqon Company. Oligos were resuspended in Invitrogen Ultrapure DNase/RNase-Free water. This water was also used as the vehicle control. Volume used to transfect parasites with oligo or vehicle never exceeded 30 µl. All experiments were performed blinded.

Anti-Rh1 LNA-oligo transfection experiments with HA-Rhomboid 1 G3 transfectants:

$1.6X10^8$ transfectant cells were aliquoted, spun down at 3,200 rpm for 10 minutes, then resuspended in 2.4 ml of cold complete Diamonds media+G418. 300 µl of cells were aliquoted per transfection cuvette. Vehicle control or LNA-oligos were added to the cells and then cuvettes were placed on ice for 15 minutes. Samples were electroporated using our standard transfection settings using 350 volts and 975 µF capacitance [41]. Parasites were then transferred to 50 ml of warm complete Diamonds media+G418 and incubated for the indicated times in figure legends. Afterwards cells were used for 16-18 hr cytolysis assays (unless otherwise noted) and western blot analysis. For fluorescence detection of FITC-LNA oligos inside *T. vaginalis,* $2X10^6$ parasites were spun down at 3,200 rpm for 10 minutes, then resuspended in 2 ml of warm complete Diamonds media+G418. Glass coverslips were added to 24-well plates and 1 ml of parasite resuspension was added to two wells (duplicate samples). Parasites were allowed to adhere to coverslips for ~2 hrs, then fixed with 4% formaldehyde/1X PBS for 20 minutes. Afterwards coverslips were washed extensively (12Xs) with 1X PBS and then mounted onto a glass slide with ProLong Gold antifade reagent with 4'-6'-diamidino-2-phenylindole (DAPI) (Invitrogen).

Anti-Rh1 LNA-oligo uptake experiment with HA-Rhomboid 1 G3 transfectants

$2X10^6$ log-phase parasites were aliquoted, spun down at 3,200 rpm for 10 minutes, then resuspended in 4 ml of warm complete Diamond media (concentration was $5X10^5$ cells /ml). Parasites were incubated for 9 hrs. Detection of FITC-LNA oligo by fluorescence microscopy was performed as described above.

LNA-oligo transfection of the *T. vaginalis* RU393 strain

$2X10^7$ RU393 cells were aliquoted, spun down at 3,200 rpm for 10 minutes, then resuspended in 1.8 ml of cold complete Diamonds media. 300 µl of cells were aliquoted per transfection cuvette. Vehicle control or LNA-oligos were added to the cells and then cuvettes were placed on ice for 15 minutes. Samples were then electroporated as described above. Parasites were then transferred to 50 ml of warm complete Diamonds media and incubated for 18 hrs. A 3 hr incubation time was used for cytolysis assays. Anti-rhomboid 1 LNA oligo sequences are shown in Fig. 5-2. The following are the LNA-oligo sequences used for other genes tested (+indicates an LNA base and * indicates a phosphorothioate bond).

Anti-lacZ: +G*+G*+T*+T*T*A*T*G*C*A*G*C*A*A*C*G*+A*+G*+A*+C

Anti-TVAG_573910: +G*+T*+T*+G*T*G*A*T*C*A*C*A*A*A*C*A*+A*+A*+A*+A

Anti-TVAG_099730: +C*+T*+G*+A*G*T*G*T*T*C*G*C*T*A*T*A*+G*+A*+A*+G

Anti-TVAG_394260: +G*+A*+T*+G*A*A*C*A*A*A*A*A*G*A*T*A*+G*+C*+A*+A

Indirect Immunofluorescence Assays.

Transfectants were allowed to bind to glass coverslips and afterwards fixed with 4% formaldehyde/1X PBS for 20 minutes. Coverslips were washed three times with 1X PBS and then permeabilized for 15 min in PBS+0.2% TritonX-100. Samples were then blocked in 3% BSA/1X PBS for 30 minutes at room temperature. Coverslips were incubated for 1 hour in a 1:1,000 dilution of mouse anti-GFP (Clontech) diluted in the blocking solution. Co-transfectant

coverslips also had a 1:1,000 dilution of anti-HA (Covance) added. After three PBS washes, coverslips were incubated for 1 hour in a 1:5,000 goat anti-mouse Alexa Fluor®488-conjugated secondary antibody dilution (Molecular Probes) also prepared in blocking solution. Co-transfectant coverslips also had a 1:5,000 dilution of goat anti-rabbit-Alexa Fluor®-594 secondary antibodies (Molecular Probes) added. Three PBS washes were performed and coverslips were mounted onto glass microscope slides using ProLong Gold antifade reagent with 4'-6'-diamidino-2-phenylindole (DAPI) (Invitrogen). Images were taken using an Axio Imager Z1 microscope equipped with an AxioCamMR3 camera. Image processing was performed using the AxioVision 3.2 program (Zeiss).

Cytolysis and Attachment Assays.

T. vaginalis adherence and cytolysis of ectocervical cells was assayed as described in [42]. For G3 and RU393 attachment experiments, $5X10^4$ parasites were added per well and incubated with ectocervical cells for 30 minutes. For G3 and RU393 cytolysis experiments, $1X10^5$ parasites were added per well but the incubation times with ectocervical cells were adjusted as follows: 16-18 hrs for G3 and G3 transfectants and 3 hrs for RU393 cells.

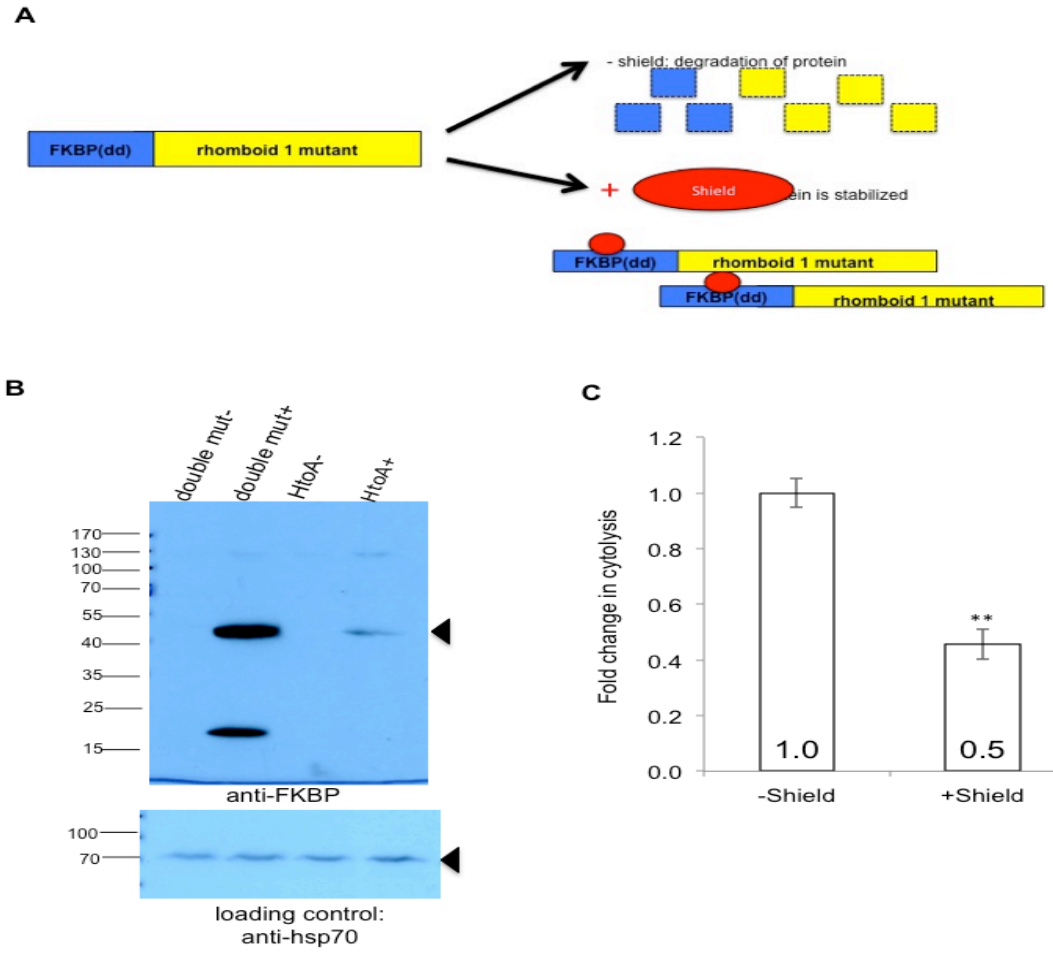

Figure 5-1: Regulatable expression of a *T. vaginalis* rhomboid 1 catalytic mutant using the FKBP destabilization domain.
(A) Schematic of the FKBP-destabilization domain system. The gene encoding for the FKBP destabilization domain (dd) was fused to a gene encoding a rhomboid 1 catalytic mutant. DD fusion causes the protein to be targeted for proteasomal degradation in the absence of the Shield1 chemical ligand. Upon addition of Shield1 the protein is stabilized and expressed [26]. **(B)** RU393 *T. vaginalis* cells were transfected with the dd fused to a rhomboid 1 double catalytic mutant (Ser262A and His316A-double mut) or a single catalytic mutant (H316A-HtoA). Cells were incubated in the absence or presence (+) of Shield1 for 18 hours and then whole cell lysates were prepared and analyzed by western blot. An anti-FKBP antibody was used to detect the fusion proteins, and an anti-hsp70 antibody was used as a loading control. Black triangles indicate the protein of the expected molecular weight. **(C)** The cells from **(B)** were analyzed for their ability to lyse ectocervical cells using the LDH release assay. Data show the average fold change in cytolysis compared to no Shield1 treatment for three experiments, each performed in triplicate, error bars denote the standard error.

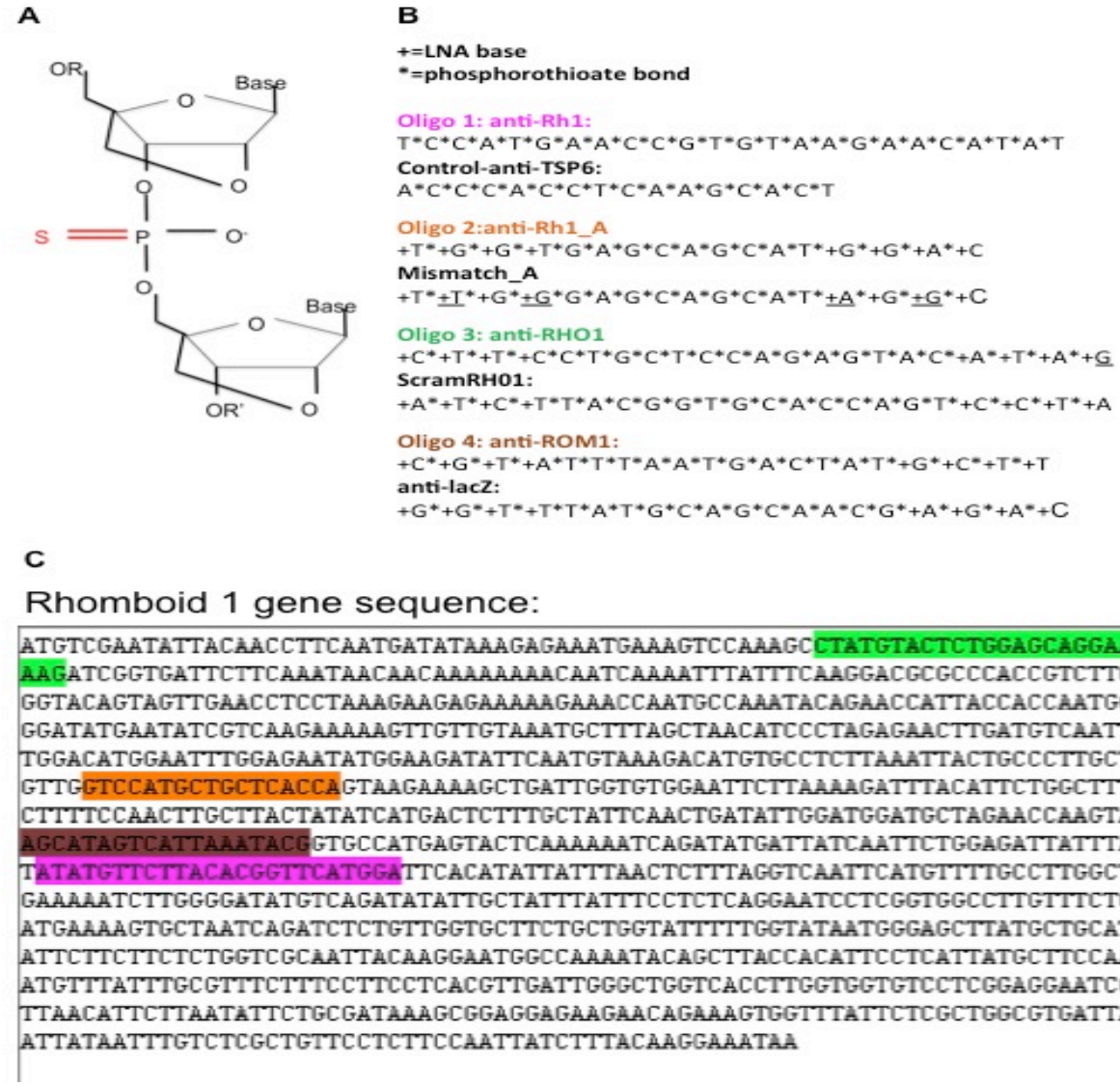

Figure 5-2: Summary of anti-sense LNA oligos and paired negative controls used to try to down-modulate *T. vaginalis* rhomboid 1 protein levels.
(A) Diagram of the chemical structure of two locked nucleic acid bases (LNA) connected by a phosphorothioate backbone. An LNA base is a nucleotide analog that contains a methylene bridge connecting the 2'-oxygen with the 4'-carbon of the ribose ring. This locked confirmation reduces the flexibility of the sugar and when included in an oligo leads to improved binding to its complementary sequence [19]. Inclusion of a phosphorothioate backbone in an oligo has been shown to increase its stability by preventing degradation of the oligo. A phosphorothioate bond has one of the non-bridging oxygens in the phosphate group of the DNA backbone replaced by a sulfur group (indicated in red). **(B)** Shows the sequences of the LNA oligos tested in this study and their respective negative controls. A "+" before the base indicates an LNA base in the oligo and "*" indicates a phosphorothioate backbone. For the "anti-Rh1" oligo, the Exiqon Company inserted LNA bases at proprietary locations. **(C)** Shows the DNA sequence of the rhomboid 1 gene. Colored highlighting indicates the region that would encode for mRNA predicted to be bound and targeted by the LNA-oligos shown in B.

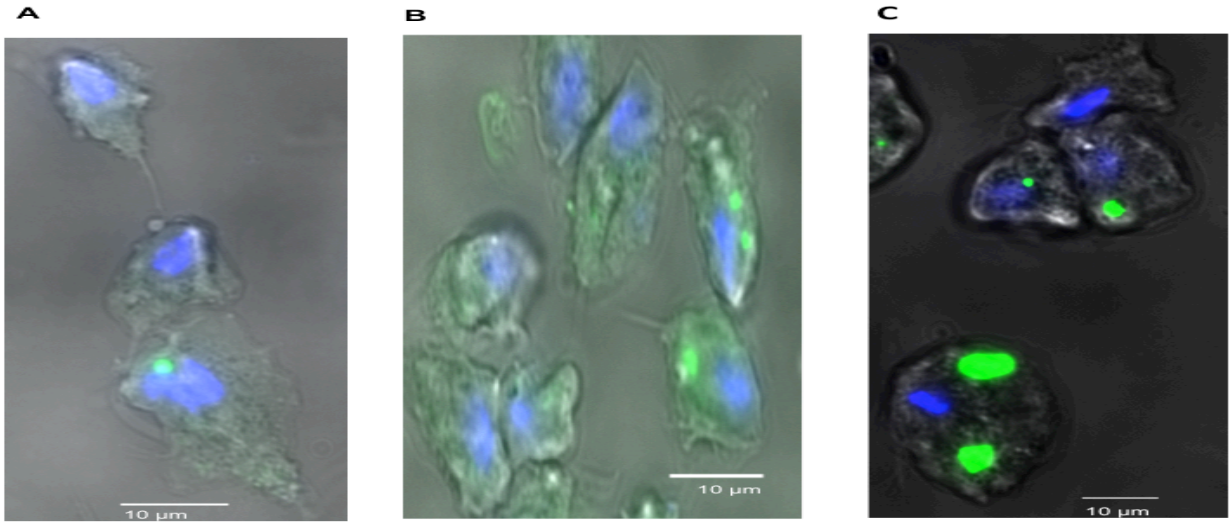

Figure 5-3: Successful delivery of fluorescein isothiocyanate (FITC)-labeled LNA oligos into *T. vaginalis* cells.
A-C show a merge of the green FITC-LNA oligo fluorescence, nuclear staining with 2-4-amidinophenyl)-1H -indole-6-carboxamidine (DAPI-blue), and a phase image. All experiments were performed with FITC-labeled "anti-Rh1" oligo targeting rhomboid 1 mRNA. Scale bar=10 µm. **(A)** 10 µM of oligo was transfected into HA-Rhomboid 1 G3 transfectants in a 300 µl volume and then brought up to 50 ml giving a final 60 nM concentration of LNA-oligo. Parasites were imaged 24 hrs after transfection. **(B)** 100 µM of oligo was transfected into HA-Rhomboid 1 G3 transfectants in a 300 µl volume and then brought up to 50 ml giving a final 600 nM concentration of LNA-oligo. Parasites were imaged 54 hrs after transfection. **(C)** HA-Rhomboid 1 G3 transfectants were incubated with 1 uM of oligo for 9hrs and then imaged. FITC-LNA oligo signal could be detected inside *T. vaginalis* 24 hrs **(A)** and 54 hrs **(B)** after oligo transfection and also when just allowed to be uptaken by the cells **(C)**.

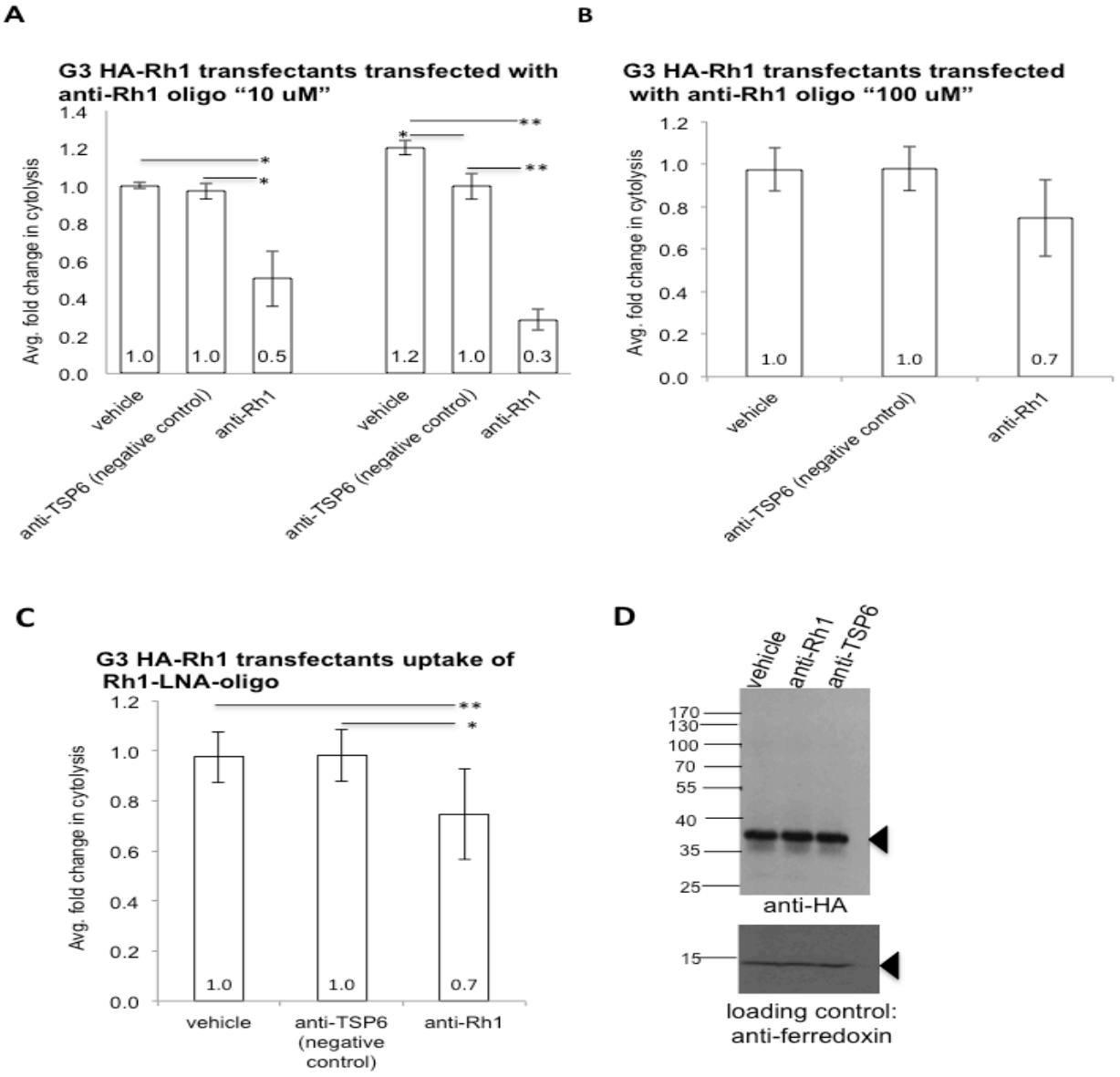

Figure 5-4: Transfection or uptake of the "anti-Rh1" LNA-oligo may cause a decrease in cytolysis of ectocervical cells in G3 HA-Rhomboid 1 transfectants.
For each experiment the effect of the "anti-Rh1" oligo or anti-TSP6 oligo (negative control) was tested. A vehicle (water) control was also included. The TSP6 protein has not been found to contribute to host cell cytolysis in our previous studies and thus the anti-TSP6 oligo served as a negative control. Different conditions were tested in A-C to introduce the oligos, and then the ability of the treated parasites to lyse ectocervical cells was assessed using the LDH release assay. Each sample was tested in triplicate. Results show the fold change in cytolysis compared to anti-TSP6 negative control, standard deviation of the population is shown as error bars. Bars above each graph indicate statistically significant changes between those groups, *$p<0.05$, **$p<0.01$. **(A)** $2X10^7$ parasites were transfected with 10 µM of the oligos in 300 µl, and then transferred to 50 ml giving a final LNA-oligo concentration of 60 nM. Cytolysis of ectocervical

cells was assessed 20 hrs (experiment on the left) or 30 hrs (experiment on the right) after oligo-transfection, both were independent experiments. **(B)** $2X10^7$ parasites were transfected with 100 μM of oligos in 300 μl, and then transferred to 50 ml giving a final LNA-oligo concentration of 600 nM. Cytolysis of ectocervical cells was tested 54 hrs after transfection. **(C)** $2X10^6$ parasites resuspended in 4 ml were incubated with 1 μM final concentration of the oligos for 9 hrs, and then cytolysis of ectocervical cells was tested. **(D)** Anti-Rh1 LNA-oligo treatment did not cause a down-modulation of HA-rhomboid 1 protein levels. A representative western blot of whole cell lysates from parasites transfected with 10 uM of LNA oligo is shown. Anti-HA was used to detect the HA-tagged rhomboid 1 protein, and an anti-ferredoxin antibody was used as a loading control. Black triangles denote the protein of the expected molecular weight.

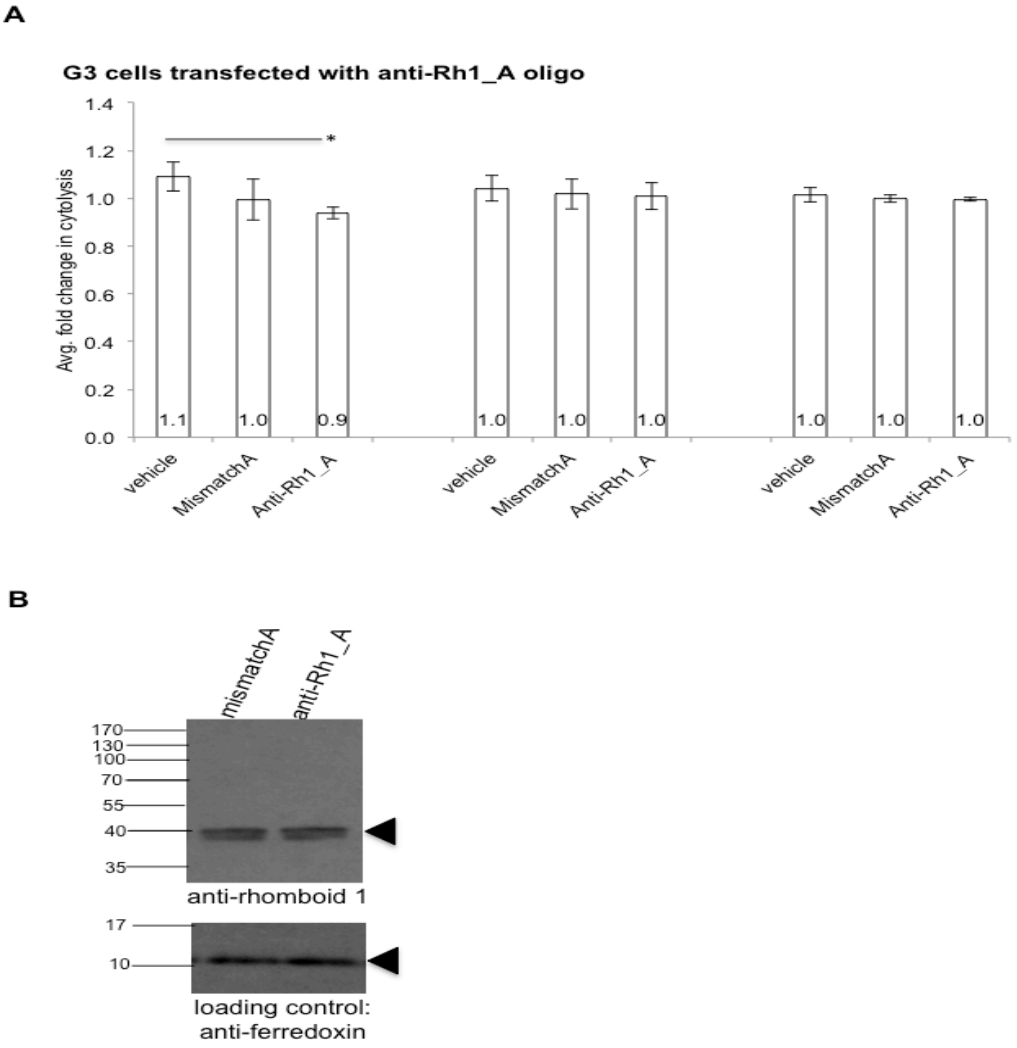

Figure 5-5: Transfection of the G3 *T. vaginalis* strain with the "anti-Rh1_A" LNA oligo does not have an effect on cytolytic ability or rhomboid 1 protein levels.
(A) $2X10^7$ G3 cells were transfected with 10 μM of "anti-Rh1_A" oligo or mismatchA negative control oligo (60 nM final concentration when brought up to 50 ml after transfection). A vehicle (water) control was also included. The ability of treated parasites to lyse ectocervical cells was tested 16hrs after oligo transfection in 10.5 hr (left), 12 hr (middle), and 14 hr (right) cytolysis assays. Cytolysis of host cells was tested using the LDH release assay. Fold change compared to mismatchA negative control is shown, standard deviation of the population is shown as error bars. Statistical significance between vehicle and anti-lacZ was found in the 10.5 hr assay, *$p<0.05$. Treatment with the anti-Rh1_A oligo did not have an effect on *T. vaginalis'* ability to lyse ectocervical cells. **(B)** Anti-Rh1_A LNA-oligo treatment did not cause a down-modulation of endogenous rhomboid 1 protein levels. Whole cell lysates prepared from parasites 16 hrs after LNA-oligo transfection were analyzed by western blot. An anti-rhomboid 1 antibody was used to detect the rhomboid 1 protein, and an anti-ferredoxin antibody was used as a loading control. Black triangles denote the protein of the expected molecular weight.

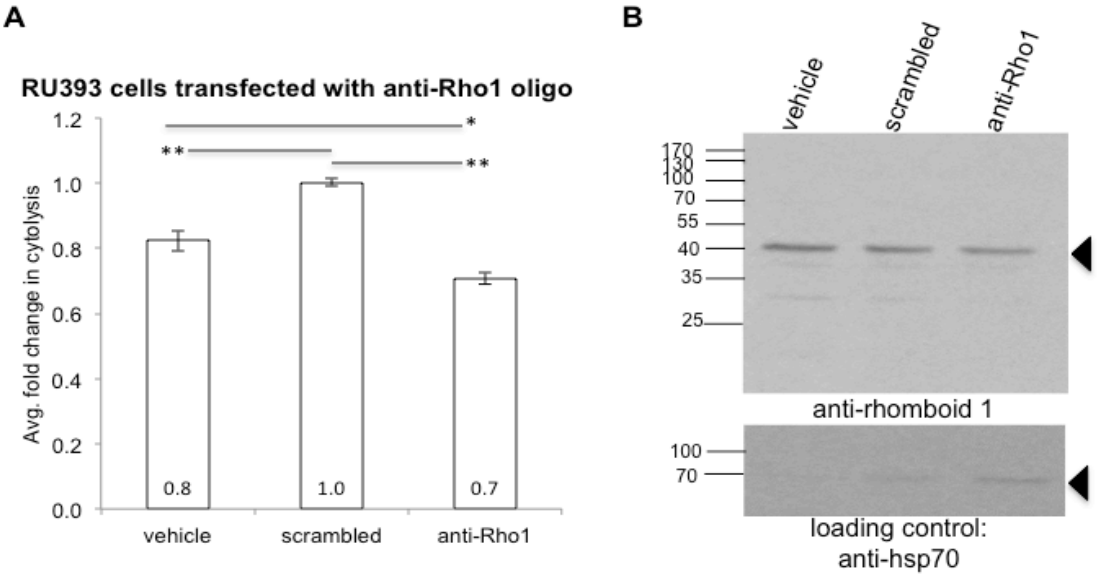

Figure 5-6: Transfection of the RU393 *T. vaginalis* strain with the "anti-Rho1" LNA-oligo shows a limited effect causing a decrease in cytolysis of ectocervical cells.
$2X10^7$ RU393 cells were transfected with 10 μM of the "anti-Rho1" oligo or a scrambled negative control oligo (60 nM final concentration when brought up to 50 ml after transfection). A vehicle (water) control was also included. The ability of treated cells to lyse ectocervical cells was tested 18 hrs after oligo transfection. Cytolysis of host cells was tested using the LDH release assay**. Results show a combined analysis of 2 experiments out of 4 where a statistically significant difference was observed.** Fold change compared to scrambled negative control is shown, error bars denote the standard error. Bars indicate statistical significance between those groups, *$p<0.05$, **$p<0.01$. Treatment with the anti-Rho1 oligo caused decreased parasite lysis of host cells compared to Empty vector and vehicle. **(B)** Anti-Rho1 LNA-oligo treatment did not cause significant down-modulation of endogenous rhomboid 1 protein levels. Whole cell lysates prepared from parasites 18 hrs after LNA-oligo transfection were analyzed by western blot. An anti-rhomboid 1 antibody was used to detect the rhomboid 1 protein, and an anti-hsp70 antibody was used as a loading control. Black triangles denote the protein of expected size.

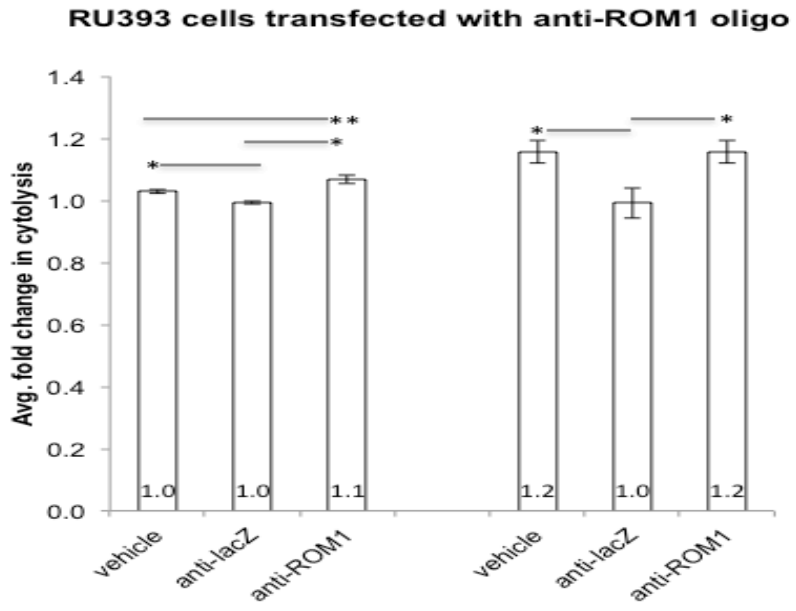

Figure 5-7: Transfection of the RU393 *T. vaginalis* strain with the "anti-ROM1" LNA-oligo shows a limited effect causing increased ectocervical cell cytolysis.
$2X10^7$ RU393 cells were transfected with 10 μM (experiment shown on the left) or 20 μM (experiment shown on the right) of "anti-ROM1" oligo or anti-lacZ negative control oligo (60 nM and 120 nM final concentrations when brought up to 50 ml after transfection). A vehicle (water) control was also included. The ability of treated cells to lyse ectocervical cells was tested 18 hrs after oligo transfection. Host cell lysis was assayed using the LDH release assay. Fold change compared to anti-lacZ negative control is shown, error bars denote the standard error of the population. Bars indicate statistical significance between those groups, *$p<0.05$, **$p<0.01$. A statistically significant increase in host cell lysis was observed between anti-ROM1 treated cells and the anti-lacZ negative control in the two independent experiments.

TrichDB ID:	Identified as protein of interest due to the following:	TrichDB annotation	TrichDB domain	InterPro domains	Identified in de Miguel *et al.* 2010 cell surface proteome? (strains)
TVAG_280090	putative rhomboid substrate identified in surface proteome screen with parasite search motif	conserved hypothetical protein	none	none	yes (2 adherent-B7268 and PA; 2 low-adherent G3 and SD10)
TVAG_189150	1) putative rhomboid substrate identified in surface proteome screen with parasite search moti 2) identified from screening *T. vaginalis* cell surface proteome for MIC2/MIC-6 like rhomboid cleavage site in TM domain	conserved hypothetical protein	Peptidase M60-like family domain	none	yes (G3-non-adherent strain)
TVAG_321740	identified from screening *T. vaginalis* cell surface proteome for MIC2/MIC-6 like rhomboid cleavage site in TM domain	conserved hypothetical protein	none	none	yes (PA-adherent strain)
TVAG_573910	putative substrate whose release into cell supernatant decreased after *T. vaginalis* treatment with 3,4-DCI serine protease inhibitor	conserved hypothetical protein	none	Concanavalin A-like lectin/glucanase domain	yes (found in all strains)
TVAG_099730	identified in mass spectrometry experiments of rhomboid 1 transfectants exposed to ectocervical cells	conserved hypothetical protein	none	none	yes (SD7 adherent strain)
TVAG_394260	identified in mass spectrometry experiments of rhomboid 1 transfectants exposed to ectocervical cells	conserved hypothetical protein	none	none	yes (2 adherent SD7 and B7268; 2 low- adherent G3 and T1)

Figure 5-8: Characteristics of *T. vaginalis* cell surface proteome proteins investigated.

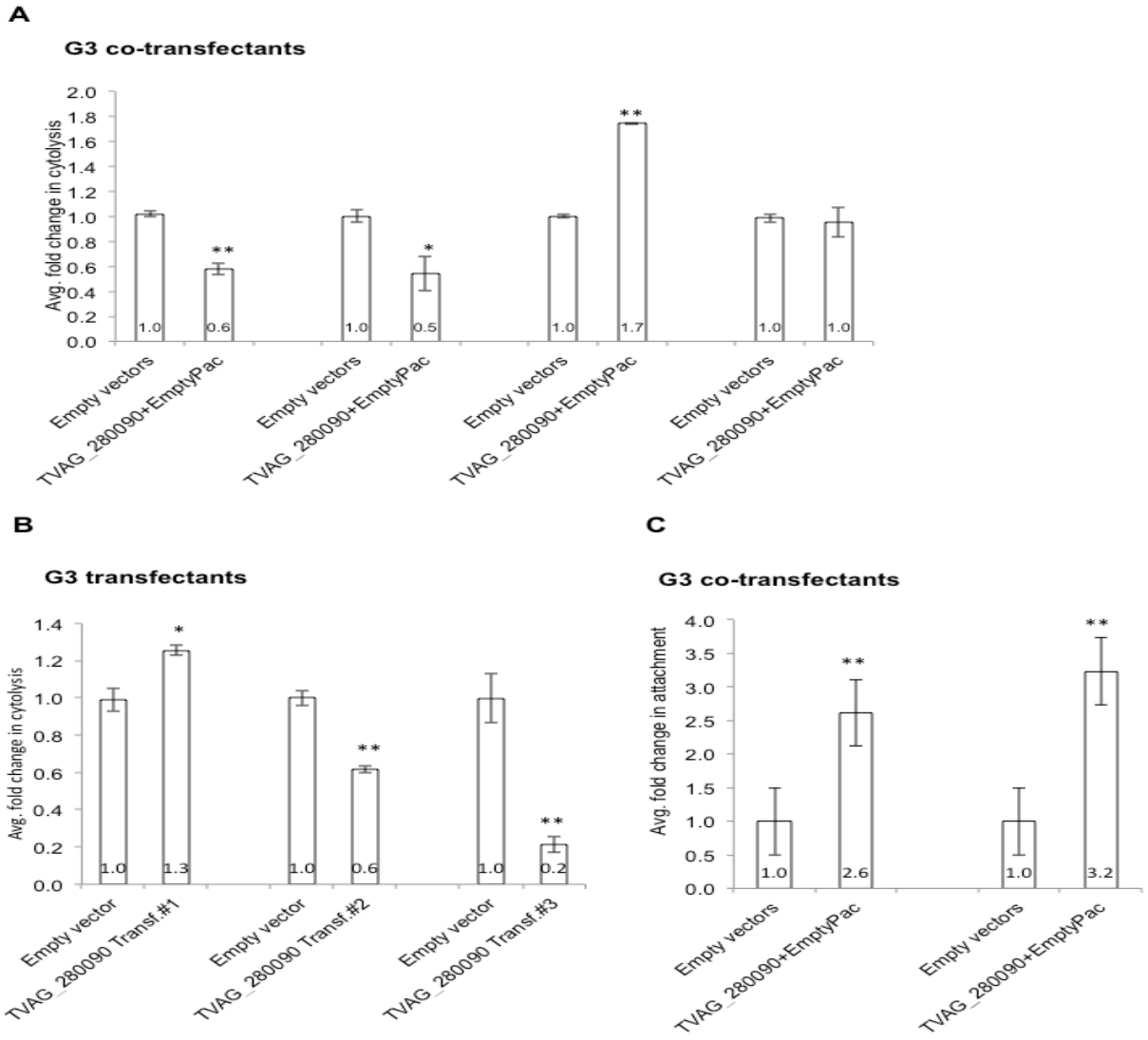

Figure 5-9: Exogenous expression of GFP-TVAG_280090 in the *T. vaginalis* G3 strain modulates parasite cytolysis and attachment to ectocervical cells.
The following transfectants were generated and their ability to lyse host cells or attach to host cells was assayed. Fold change in cytolysis and attachment to ectocervical cells compared to Empty vector/s controls is shown. Data from independent experiments is indicated by a space between bars. Each experiment was performed in triplicate, error bars denote the standard deviation of the population, and statistical significance is shown, *$p<0.05$, **$p<0.01$. **(A)** G3 was co-transfected with a plasmid encoding GFP-TVAG_280090 and the empty vector (EmptyPac) or two empty vectors (EmptyPac and EmptyNeo). Results of four cytolysis experiments are shown. **(B)** G3 was transfected with a plasmid encoding GFP-TVAG_280090 or empty vector control (EpNeo). Results from cytolysis experiments performed with three different transfectants (Transf#1-3) are shown. **(C)** The ability of G3 co-transfectants from **(A)** to attach to host ectocervical cells was tested in two independent experiments.

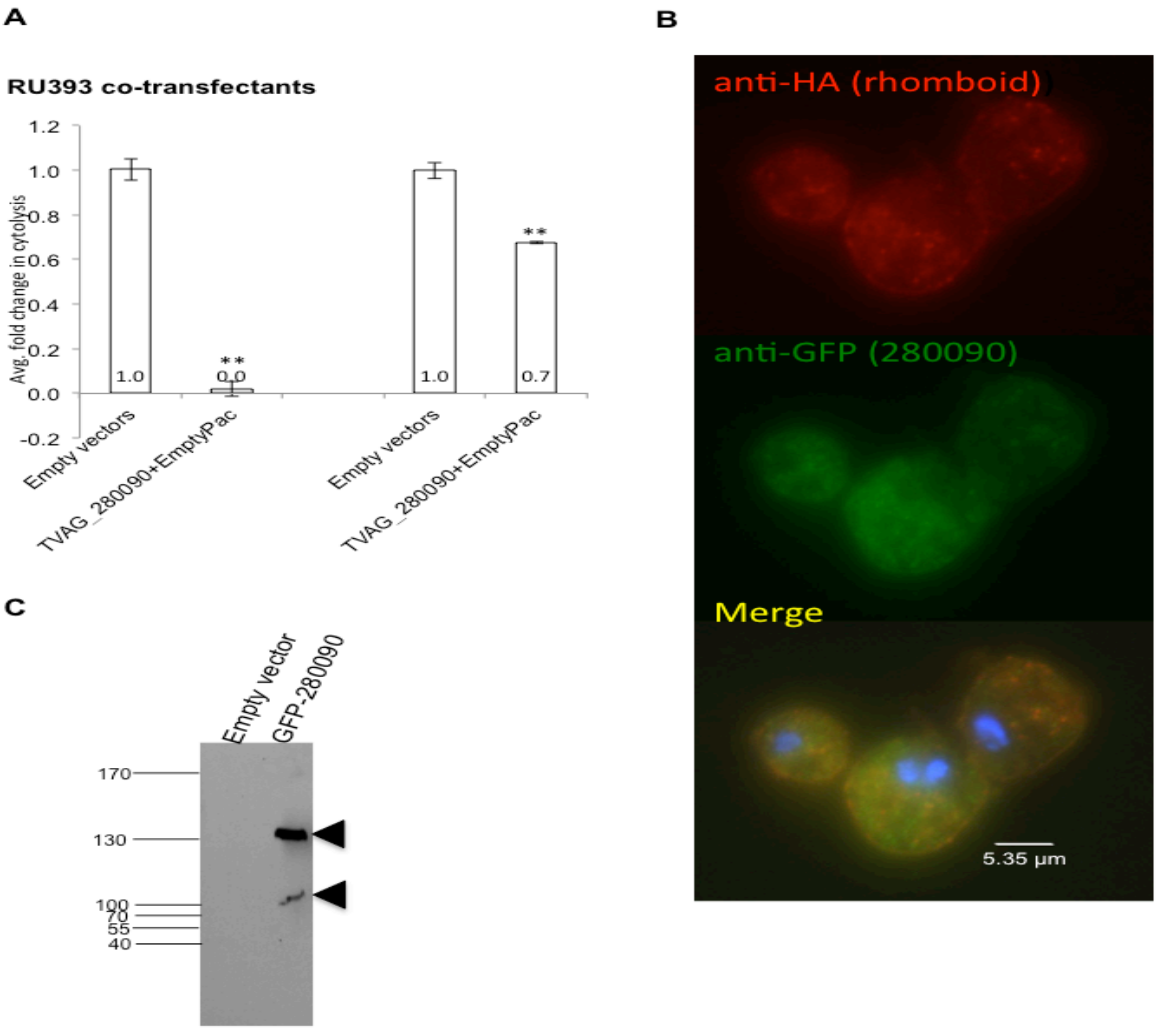

Figure 5-10: Further characterization of GFP-TVAG_280090 exogenous expression in the RU393 and G3 *T. vaginalis* strains.
(A) RU393 was co-transfected with a plasmid encoding GFP-TVAG_280090 and the empty vector EmptyPac or two empty vectors (EmptyPac and EmptyNeo). The ability to lyse ectocervical cells was tested using the LDH release assay. Fold change in cytolysis compared to empty vectors control is shown for two independent experiments. Each experiment was performed in triplicate, error bars denote the standard deviation of the population, and statistical significance is shown, **p<0.01. **(B)** Indirect immunofluorescence assay of G3 GFP-TVAG_280090 and HA-Rhomboid 1 co-transfectants was performed with an anti-HA antibody (red-top panel) or anti-GFP antibody (green-middle panel). Bottom panel shows a merge and nuclear staining with DAPI. **(C)** Representative western blot shows protein expression profile of GFP-TVAG_280090 in G3 transfectants. Western blot was performed with an anti-GFP antibody. Lower black triangle denotes detection the fusion protein of the expected molecular weight, and top triangle denotes a higher migrating band that likely corresponds to a glycosylated form of the tagged protein. Whole cell lysates of Empty vector transfectants were included as a negative control.

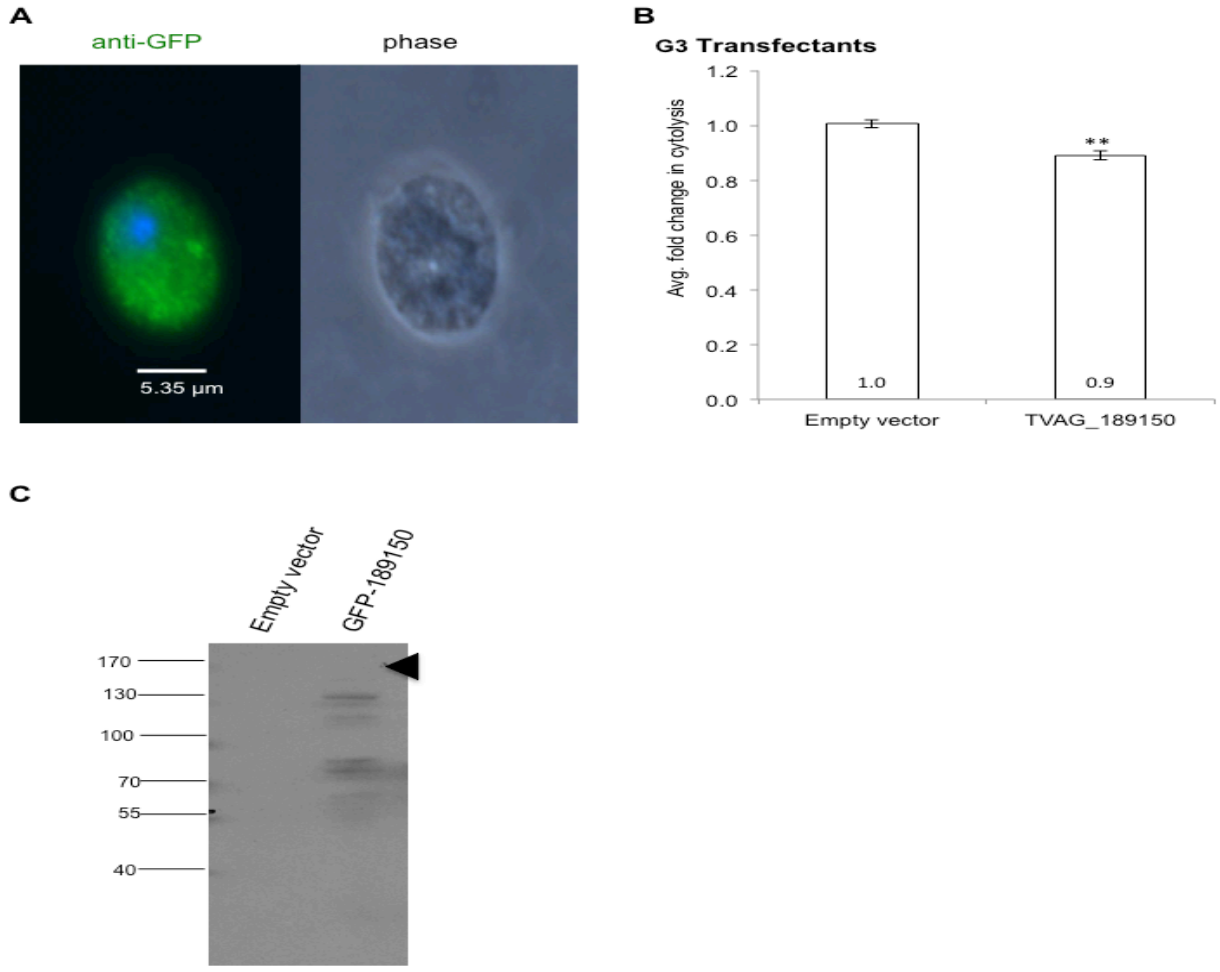

Figure 5-11: Subcellular localization of GFP-189150 in G3 transfectants and assessment of its overexpression effects on lysis of ectocervical cells.
GFP-TVAG_189150 was exogenously expressed in the G3 strain. **(A)** Indirect immunofluorescence assay of GFP-TVAG_189150 transfectants was performed using an anti-GFP antibody (green) and nuclear staining with DAPI (blue), phase image is shown on the right. **(B)** Cytolysis of ectocervical cells was tested using the LDH release assay. Cytolysis was tested in triplicate. Fold change compared to Empty vector transfectants is shown, error bars denote the standard deviation of the population. Statistical significance is indicated, **$p<0.01$. **(C)** Western blot analysis of GFP-TVAG_189150 transfectants using an anti-GFP antibody. Black triangle indicates faint expression of the full-length fusion protein of the expected molecular weight. Lower migrating species likely represent degradation products. Whole cell lysates of Empty vector transfectants were included as a negative control.

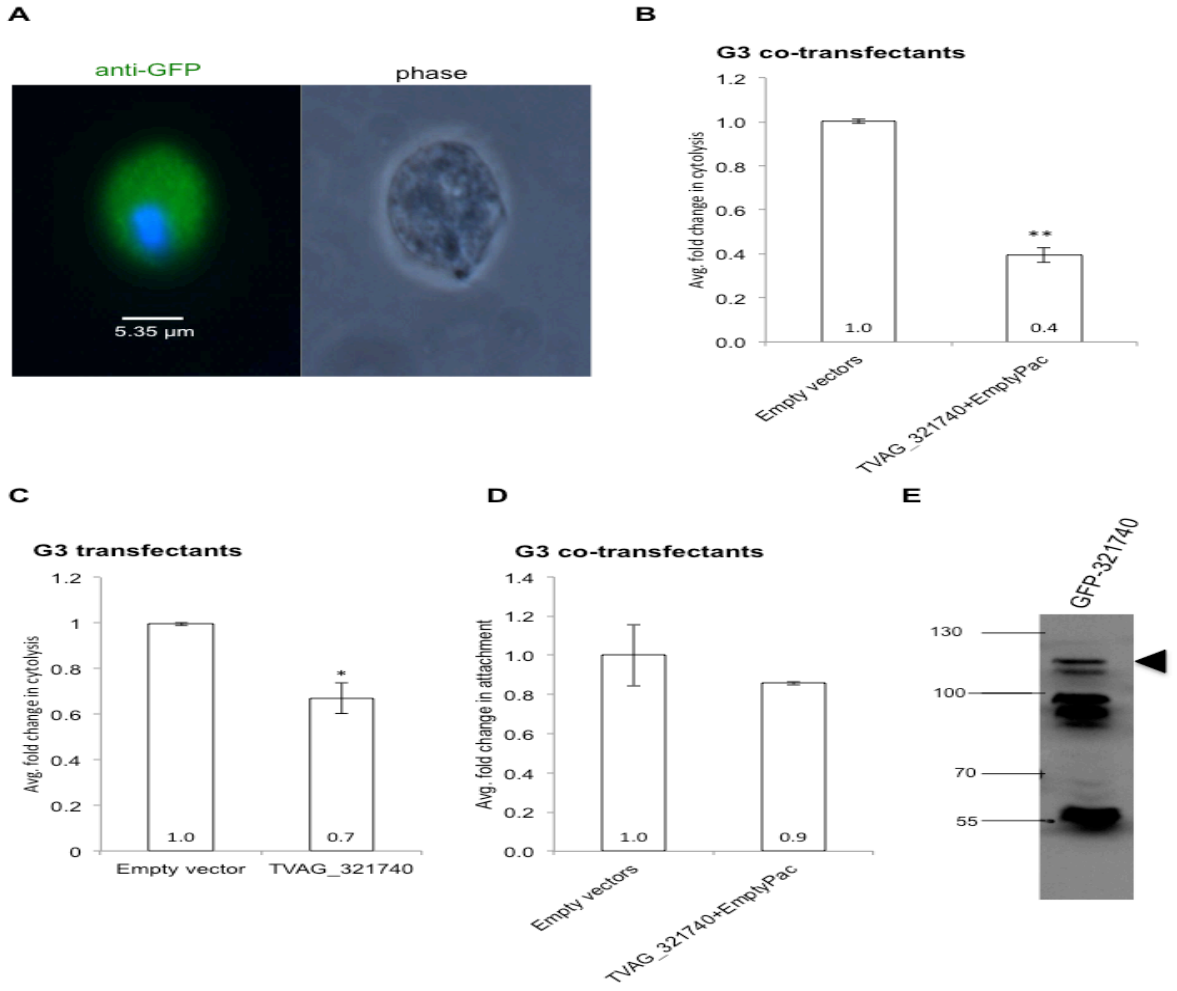

Figure 5-12: Subcellular localization of GFP-TVAG_321740 in G3 transfectants and assessment of its overexpression effects on cytolysis and attachment to ectocervical cells. G3 cells were co-transfected with a plasmid encoding GFP-TVAG_321740 and the empty vector EmptyPac or two empty vectors (EmptyPac and EmptyNeo). Single transfectants were also generated by transfecting G3 cells with a plasmid encoding for GFP-TVAG_321740 or an empty vector control plasmid (EpNeo). **(A)** Representative indirect immunofluorescence assay signal found in GFP-TVAG_321740 transfectants. IFA was performed using an anti-GFP antibody (green) and nuclear staining with DAPI (blue), phase image is shown on the right. **(B-D)** The ability of transfectants to lyse ectocervical cells or attach to them was assayed. Fold change in cytolysis or attachment to ectocervical cells compared to Empty vector/s transfectant controls is shown. **(B)** Shows a combined analysis of three experiments, error bars denote the standard error and statistical significance is shown, **$p<0.01$. **(C)** Shows the results of one experiment, error bars denote the standard deviation of the population, statistical significance is shown, *$p<0.05$. **(D)** Shows the results of one attachment assay, error bars denote the standard deviation of the population, no statistical difference was observed. **(E)** Representative western blot shows protein expression profile of GFP-TVAG_321740 in G3 transfectants. Black triangle indicates detection of the fusion protein at the expected molecular weight.

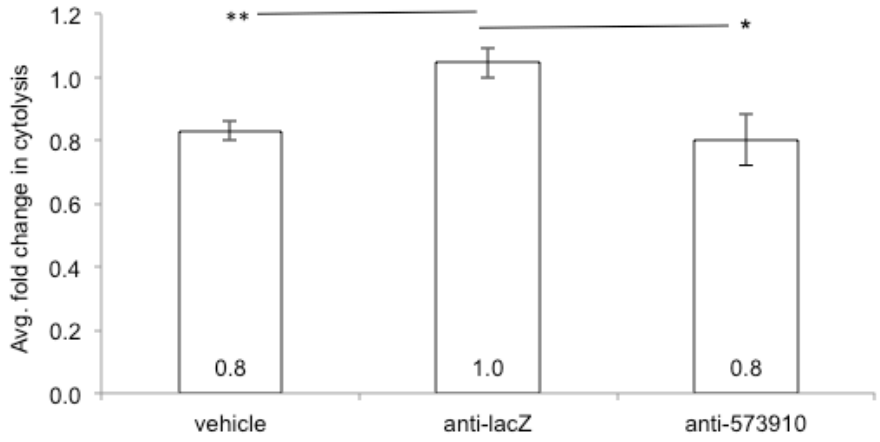

Figure 5-13: Transfection of the RU393 *T. vaginalis* strain with an anti-TVAG_573910 LNA-oligo shows a limited effect causing decreased ectocervical cell cytolysis.
$2X10^7$ RU393 cells were transfected with 10 µM of an LNA oligo targeting TVAG_573910 or the anti-lacZ negative control oligo in 300 µl, and then transferred to 50 ml giving a final LNA-oligo concentration of 60 nM. A vehicle (water) control was also included. Cytolysis of ectocervical cells by treated parasites was assessed 18 hrs after transfection. **Results are from a combined analysis of 2 out of 3 experiments where a statistical difference was observed**. Fold change compared to anti-lacZ negative control is shown, error bars denote the standard error of the population. Bars indicate statistical significance between those groups, *$p<0.05$, **$p<0.01$.

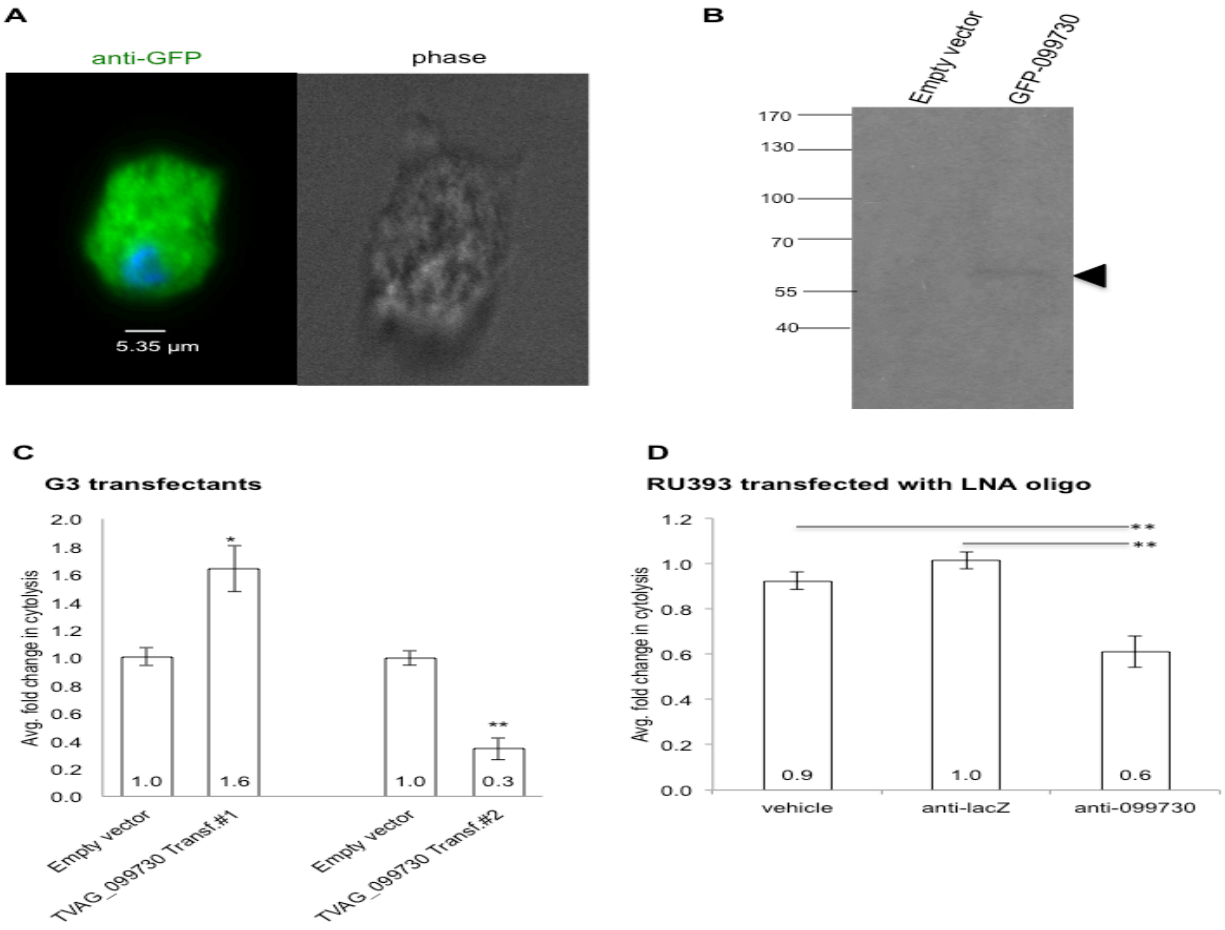

Figure 5-14: Subcellular localization of GFP-TVAG_099730 in RU393 transfectants and investigation of its role in cytolysis of ectocervical cells with LNA antisense-oligos. GFP-TVAG_099730 was exogenously expressed in the RU393 strain. **(A)** Indirect immunofluorescence assay of GFP-099730 transfectants was performed using an anti-GFP antibody (green) and nuclear staining with DAPI (blue), phase image is shown on the right. **(B)** Representative western blot shows the protein expression profile of GFP-099730 in transfectants. Black triangle indicates detection of the fusion protein at the expected molecular weight. Whole cell lysate of Empty vector transfectants was included as a negative control. **(C)** Cytolysis of ectocervical cells by two different transfectant sets (Transf#1-2) was tested using the LDH release assay. Cytolysis was tested in triplicate. A combined analysis of two assays for each transfectant set is shown as fold change compared to Empty vector transfectants, error bars denote the standard error. **(D)** $2X10^7$ RU393 cells were transfected with 10 µM of an LNA oligo targeting TVAG_099730 or the anti-lacZ negative control oligo in 300 µl, and then transferred to 50 ml giving a final LNA-oligo concentration of 60 nM. A vehicle (water) control was also included. Cytolysis of ectocervical cells by treated parasites was assessed 18 hrs after transfection. **Results are from a combined analysis of 3 out of 4 experiments were a statistical difference was observed.** Fold change compared to anti-lacZ negative control is shown, error bars denote the standard error. Bars indicate statistical significance between those groups **p<0.01.

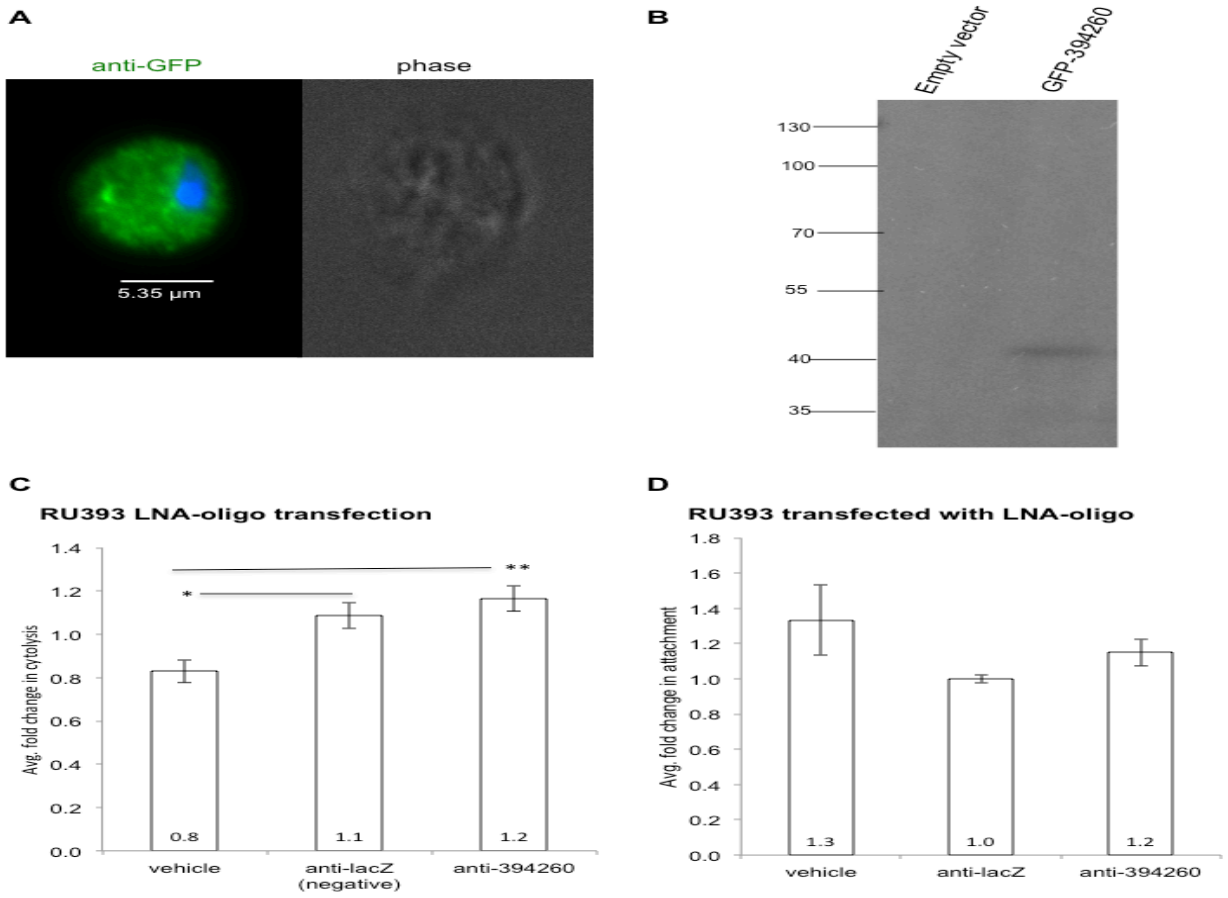

Figure 5-15: Subcellular localization of GFP-TVAG_394260 in RU393 transfectants and investigation of its role in cytolysis and attachment using an antisense LNA-oligo. GFP-TVAG_394260 was exogenously expressed in the RU393 strain. **(A)** Indirect immunofluorescence assay of GFP-394260 transfectants was performed using an anti-GFP antibody (green) and nuclear staining with DAPI (blue), phase image is shown on the right. **(B)** Western blot analysis of GFP-TVAG_394260 transfectants did not reveal detection of the full-length fusion protein of the expected molecular weight (297 kDa), however, smaller degradation products may indicate expression of the protein as they are not visible in whole cell lysates from Empty vector negative control transfectants. **(C)** $2X10^7$ RU393 cells were transfected with 10 µM of an LNA oligo targeting TVAG_394260 mRNA or the anti-lacZ negative control oligo in 300 µl, and then transferred to 50 ml giving a final LNA-oligo concentration of 60 nM. A vehicle (water) control was also included. Cytolysis of ectocervical cells by treated parasites was assessed 18 hrs after transfection. Results are from a combined analysis of 2 experiments. Fold change compared to anti-lacZ negative control is shown, error bars denote the standard error. Bars indicate statistical significance between those groups, *p<0.05, **p<0.01. **(D)** RU393 cells were transfected with LNA oligos as described in (C). The ability of treated parasites to attach to host cells was assessed in triplicate. No statistically significant changes were observed.

References:

1. de Miguel, N., et al., *Proteome analysis of the surface of Trichomonas vaginalis reveals novel proteins and strain-dependent differential expression.* Mol Cell Proteomics, 2010. **9**(7): p. 1554-66.

2. Ryan, C.M., N. de Miguel, and P.J. Johnson, *Trichomonas vaginalis: current understanding of host-parasite interactions.* Essays Biochem, 2011. **51**: p. 161-75.

3. Singh, B.N., et al., *Identification of the lipid moiety and further characterization of the novel lipophosphoglycan-like glycoconjugates of Trichomonas vaginalis and Trichomonas foetus.* Arch Biochem Biophys, 1994. **309**(2): p. 273-80.

4. Ryan, C.M., et al., *Chemical structure of Trichomonas vaginalis surface lipoglycan: a role for short galactose (beta1-4/3) N-acetylglucosamine repeats in host cell interaction.* J Biol Chem, 2011. **286**(47): p. 40494-508.

5. Singh, B.N., *Lipophosphoglycan-like glycoconjugate of Tritrichomonas foetus and Trichomonas vaginalis.* Mol Biochem Parasitol, 1993. **57**(2): p. 281-94.

6. Okumura, C.Y., L.G. Baum, and P.J. Johnson, *Galectin-1 on cervical epithelial cells is a receptor for the sexually transmitted human parasite Trichomonas vaginalis.* Cell Microbiol, 2008. **10**(10): p. 2078-90.

7. Conrad, M.D., et al., *Getting trichy: tools and approaches to interrogating Trichomonas vaginalis in a post-genome world.* Trends Parasitol, 2013. **29**(1): p. 17-25.

8. Cruz, A. and S.M. Beverley, *Gene replacement in parasitic protozoa.* Nature, 1990. **348**(6297): p. 171-3.

9. Land, K.M., et al., *Targeted gene replacement of a ferredoxin gene in Trichomonas vaginalis does not lead to metronidazole resistance.* Mol Microbiol, 2004. **51**(1): p. 115-22.

10. Bras, X.P., et al., *Knockout of the abundant Trichomonas vaginalis hydrogenosomal membrane protein TvHMP23 increases hydrogenosome size but induces no compensatory up-regulation of paralogous copies.* FEBS Lett, 2013. **587**(9): p. 1333-9.

11. Dias, N. and C.A. Stein, *Antisense oligonucleotides: basic concepts and mechanisms.* Mol Cancer Ther, 2002. **1**(5): p. 347-55.

12. Hsu, H.M., et al., *Transcriptional regulation of an iron-inducible gene by differential and alternate promoter entries of multiple Myb proteins in the protozoan parasite Trichomonas vaginalis.* Eukaryot Cell, 2009. **8**(3): p. 362-72.

13. Lama, A., et al., *Glyceraldehyde-3-phosphate dehydrogenase is a surface-associated, fibronectin-binding protein of Trichomonas vaginalis.* Infect Immun, 2009. **77**(7): p. 2703-11.

14. Mundodi, V., A.S. Kucknoor, and J.F. Alderete, *Antisense RNA decreases AP33 gene expression and cytoadherence by T. vaginalis.* BMC Microbiol, 2007. **7**: p. 64.

15. Mundodi, V., et al., *Silencing the ap65 gene reduces adherence to vaginal epithelial cells by Trichomonas vaginalis.* Mol Microbiol, 2004. **53**(4): p. 1099-108.

16. Munoz, C., et al., *A protein phosphatase 1 gamma (PP1gamma) of the human protozoan parasite Trichomonas vaginalis is involved in proliferation and cell attachment to the host cell.* Int J Parasitol, 2012. **42**(8): p. 715-27.

17. Obika, S., et al., *Inhibition of ICAM-I gene expression by antisense 2',4'-BNA oligonucleotides.* Nucleic Acids Symposium Series, 2001. **1**(1): p. 145-146.

18. Wahlestedt, C., et al., *Potent and nontoxic antisense oligonucleotides containing locked nucleic acids.* Proc Natl Acad Sci U S A, 2000. **97**(10): p. 5633-8.

19. Elayadi, A.N., D.A. Braasch, and D.R. Corey, *Implications of high-affinity hybridization by locked nucleic acid oligomers for inhibition of human telomerase.* Biochemistry, 2002. **41**(31): p. 9973-81.

20. Obika, S., et al., *Inhibition of ICAM-1 gene expression by antisense 2',4'-BNA oligonucleotides.* Nucleic Acids Res Suppl, 2001(1): p. 145-6.

21. Sun, Z., et al., *Inhibition of hepatitis B virus (HBV) by LNA-mediated nuclear interference with HBV DNA transcription.* Biochem Biophys Res Commun, 2011. **409**(3): p. 430-5.

22. Zhang, Y., et al., *Down-modulation of cancer targets using locked nucleic acid (LNA)-based antisense oligonucleotides without transfection.* Gene Ther, 2011. **18**(4): p. 326-33.

23. *Roche-Product Development Portfolio. Roche Selects First LNA Drug Candidate Following Santaris Acquisition.* http://www.roche.com/DE/research_and_development/who_we_are_how_we_work/pipeline.htm. 2015.

24. Janssen, H.L., et al., *Treatment of HCV infection by targeting microRNA.* N Engl J Med, 2013. **368**(18): p. 1685-94.

25. Striepen, B., *Switching parasite proteins on and off.* Nat Methods, 2007. **4**(12): p. 999-1000.

26. Banaszynski, L.A., et al., *A rapid, reversible, and tunable method to regulate protein function in living cells using synthetic small molecules.* Cell, 2006. **126**(5): p. 995-1004.

27. Sellmyer, M.A., et al., *A general method for conditional regulation of protein stability in living animals.* Cold Spring Harb Protoc, 2009. **2009**(3): p. pdb prot5173.

28. Rastew, E., L. Morf, and U. Singh, *Entamoeba histolytica rhomboid protease 1 has a role in migration and motility as validated by two independent genetic approaches.* Exp Parasitol, 2015. **154**: p. 33-42.

29. Santos, J.M., et al., *Intramembrane cleavage of AMA1 triggers Toxoplasma to switch from an invasive to a replicative mode.* Science, 2011. **331**(6016): p. 473-7.

30. Baker, R.P. and S. Urban, *Architectural and thermodynamic principles underlying intramembrane protease function.* Nat Chem Biol, 2012. **8**(9): p. 759-68.

31. Greenberger, L.M., et al., *A RNA antagonist of hypoxia-inducible factor-1alpha, EZN-2968, inhibits tumor cell growth.* Mol Cancer Ther, 2008. **7**(11): p. 3598-608.

32. Opitz, C., et al., *Intramembrane cleavage of microneme proteins at the surface of the apicomplexan parasite Toxoplasma gondii.* EMBO J, 2002. **21**(7): p. 1577-85.

33. Urban, S. and M. Freeman, *Substrate Specificity of Rhomboid Intramembrane Proteases Is Governed by Helix-Breaking Residues in the Substrate Transmembrane Domain.* Molecular Cell, 2003. **11**(6): p. 1425-1434.

34. Dowse, T.J., et al., *Apicomplexan rhomboids have a potential role in microneme protein cleavage during host cell invasion.* Int J Parasitol, 2005. **35**(7): p. 747-56.

35. Brossier, F., et al., *A spatially localized rhomboid protease cleaves cell surface adhesins essential for invasion by Toxoplasma.* Proc Natl Acad Sci U S A, 2005. **102**(11): p. 4146-51.

36. Zhou, X.W., et al., *Proteomic analysis of cleavage events reveals a dynamic two-step mechanism for proteolysis of a key parasite adhesive complex.* Mol Cell Proteomics, 2004. **3**(6): p. 565-76.

37. Sheiner, L., T.J. Dowse, and D. Soldati-Favre, *Identification of trafficking determinants for polytopic rhomboid proteases in Toxoplasma gondii.* Traffic, 2008. **9**(5): p. 665-77.

38. Nakjang, S., et al., *A novel extracellular metallopeptidase domain shared by animal host-associated mutualistic and pathogenic microbes.* PLoS One, 2012. **7**(1): p. e30287.

39. Clark, C.G. and L.S. Diamond, *Methods for cultivation of luminal parasitic protists of clinical importance.* Clin Microbiol Rev, 2002. **15**(3): p. 329-41.

40. Fichorova, R.N., J.G. Rheinwald, and D.J. Anderson, *Generation of papillomavirus-immortalized cell lines from normal human ectocervical, endocervical, and vaginal epithelium that maintain expression of tissue-specific differentiation proteins.* Biol Reprod, 1997. **57**(4): p. 847-55.

41. Delgadillo, M.G., et al., *Transient and selectable transformation of the parasitic protist Trichomonas vaginalis.* Proc Natl Acad Sci U S A, 1997. **94**(9): p. 4716-20.

42. Lustig, G., et al., *Trichomonas vaginalis contact-dependent cytolysis of epithelial cells.* Infect Immun, 2013. **81**(5): p. 1411-9.

Chapter 6:

Summary and Discussion

The characterization of the *Trichomonas vaginalis* cell surface and an understanding of mechanisms that may alter it will help us decipher important aspects of the parasite's cell biology and virulence factors. Furthermore, intramembrane proteolytic cleavage contributes to many biological functions and its possible role in *T. vaginalis* has not been previously investigated. The studies presented in this dissertation highlight the existence of active intramembrane proteases called rhomboids in *T. vaginalis* and their contribution to promoting parasite attachment and cytolysis of host cells (Chapter 2). This is an important finding as it highlights how regulation of the parasite's cell surface proteins may have implications on its interactions with host cells. The results presented in Chapter 3 illustrate the dynamic nature of *T. vaginalis* response to host cells by the identification of a tetraspanin protein that re-localizes from the flagella to the plasma membrane and dramatically back to the flagella upon contact with host cells. We also identified another *T. vaginalis* cell surface protein that may contribute to host-parasite interactions, as it promotes parasite attachment to and lysis of host ectocervical cells (Chapter 4). Propelled by these discoveries, we wanted to mechanistically interrogate our observed functions and sought to help develop molecular tools, our efforts towards this are presented in Chapter 5.

Active rhomboids in *T. vaginalis* and their site of action

Rhomboids are intramembrane serine proteases predicted to be one of the most conserved families of polytopic membrane proteins [1] and suggested to be one of the evolutionarily earliest regulatory enzymes [2]. Yet we are still in the initial phases of characterizing these proteases. Rhomboid proteases had not been previously studied in *T. vaginalis* prior to the results presented in this dissertation. Although their likely important role was hinted at due to their

contribution to pathogenesis in *Toxoplasma gondii*, *Plasmodium*, and *Entamoeba histolytica*-intracellular and extracellular protozoan parasites [3]. We started these studies with a clean slate, initially trying to find out whether *T. vaginalis* has active rhomboid proteases and to determine their site of action. To assess catalytic activity we could perform a heterologous cell cleavage assay and test a panel of substrates that are cleaved by rhomboid proteases from *Drosophila*, humans, bacteria, and other parasites [4-6]. We could detect cleavage of these model substrates by two out of four proteins that we hypothesized were active rhomboids, which we called TvROM1 and TvROM3 (Chapter 2). Interestingly, we found that TvROM1 and TvROM3 localize to different cell compartments. TvROM1 is located on the cell surface and vesicles, while TvROM3 and another predicted active rhomboid protease, TvROM2, localize to what appears to be the Golgi complex of *T. vaginalis*. Furthermore, while TvROM3 was able to cleave the *D. melanogaster* Spitz protein, TvROM1 could not. Vice versa, TvROM1 could cleave a variety of substrates that TvROM3 could not process. Similarly, we identified two putative endogenous *T. vaginalis* substrates that only TvROM1 could cleave. In *Drosophila*, one of the ways that rhomboid cleavage is regulated is by controlling when the Spitz substrate gets transported to the Golgi where Rhomboid-1 can then access it and cleave it [7]. Similarly, the differences in substrate specificities may allow TvROM1's substrates not to be cleaved prematurely by TvROM2 and TvROM3 as they pass through the secretory pathway.

Where TvROM4 functions is still a mystery. Although we made several attempts to exogenously express this protein, and multiple transfectant populations grew up, we could not detect expression of the protein by western blot or indirect immunofluorescence assays. Eukaryotic organisms are predicted to contain at least one rhomboid protease of the PARL-type in their mitochondria [8]. Since *T. vaginalis* does not contain mitochondria and instead contains

divergent mitochondrial-like organelles called hydrogenosomes for energy production [9], it is tempting to speculate that TvROM4 may localize there. However, TvROM4 has the same predicted topology as TvROMs1-3 whereas in PARL-type rhomboids the active site residues are not in TMs 4 and 6 but are located in TMs 5 and 7 and in the inverse topology. Thus, future studies trying to localize TvROM4 with different promoters or an antibody generated against it may aid the complete localization of all the predicted *T. vaginali*s active rhomboids.

TvROM2 and TvROM3's potential localization in the Golgi is also of interest to further characterize. In *Drosophila*, the EFGR ligands that are cleaved get released to the outside of the cell where they can initiate cell signaling in the cells that bind the cleavage fragments [4, 10, 11]. We identified 5 putative substrates that were differentially released by *T. vaginalis* TvROM1 transfectants into the cell media upon treatment of the parasites with the serine protease inhibitor 3,4-DCI which also has activity against rhomboids [12-15] and found that only one protein could be cleaved by TvROM1 (Chapter 2). The four remaining putative substrates are not cleaved by TvROM1 (Chapter 2). TvROM3 could not cleave any of the five putative substrates (Chapter 2). Testing whether these proteins can be cleaved by TvROM2 and TvROM4 is of merit, since it may help reveal whether TvROM2 and TvROM4 are catalytically active, as we did not identify a model substrate that could be cleaved by TvROM2 or TvROM4, and it may also reveal whether these rhomboid proteases also display a different flavor of substrate specificity.

Identifying a *T. vaginalis* Golgi-marker has also been an elusive task as proteins that are mainly predicted to reside in the Golgi that we have tried to tag and express localize to the endoplasmic reticulum (ER) and Golgi in *T. vaginalis*. Similarly, the ER protein BiP localizes to the ER and the Golgi (our laboratory's unpublished results). As a potential Golgi membrane-embedded protein that does not recycle between the ER and Golgi like many Rabs and Yip-

family members [16, 17], an anti-TvROM2 or TvROM3 antibody may serve as a good Golgi-marker. Little is known about the Golgi complex in *T. vaginalis* other than important and unique structural features [18]. It is known that a dictyosome of the Golgi attaches to striated roots called parabasal filaments, and this arrangement is unique amongst parabasalid flagellates [19, 20]. The 188 proteins identified in the cell supernatant of *T. vaginalis* as part of our studies in Chapter 2, highlights the high nature of released/secreted proteins including possible virulence factors. Therefore, the interesting localization of ER and Golgi proteins that we have observed and the unique Golgi structure of *T. vaginalis* may represent a druggable target with unique features that differ from its human host.

What substrates are cleaved by *T. vaginalis* rhomboid 1 and what is their potential contribution to pathogenesis?

An understanding of substrate features that contribute to cleavage by intramembrane cleaving proteases (I-CLiPs), including rhomboid proteases, is an area of heightened interest due to the contributions of I-CLiP's to several diseases such as Alzheimer's Disease and protozoan infections [3]. The hope of selectively targeting a protease of interest amongst the sea of proteases in a whole cell is a worthwhile endeavor for the development of therapeutics [21]. At the moment, the unifying feature present in substrates that get cleaved by I-CLiPs is the presence of helix-relaxing residues [22]. However, as the role of helix-relaxing residues is also influenced by surrounding residues and TM length [23], it can be difficult to develop a systematic approach to identify I-CLiP substrates.

We took a combinatorial approach that may aid in the identification of substrates cleaved by other intramembrane proteases at the cell surface. We reasoned that since TvROM1 is located at the cell surface, the substrates that are cleaved will be released to the outside of the

cell and thus upon serine protease inhibition should lead to decreased amounts of TvROM1's substrates. We had also noticed that substrates that have been shown to be cleaved by rhomboid proteases in other protozoan parasites had a high conservation of particularly small amino acids extending past the P1-P1' sites where rhomboid cleavage occurs [6, 15, 24-30]. Thus we generated a rhomboid substrate parasite search motif that encapsulated the small amino acid preference and together with our biochemical approach allowed our discovery of two TvROM1 *T. vaginalis* substrates (Chapter 2). While rhomboids do not recognize a strict set of particular amino acids like many other soluble serine proteases [31], the high conservation of particularly small amino acids in the predicted rhomboid cleavage site may contribute to a specific conformation that promotes rhomboid cleavage [25]. Some of these features are thus likely identifiable by sequence analysis, highlighted by the fact that two of our endogenous *T. vaginalis* substrates had our parasite search motif (Chapter 2). However, other putative *T. vaginalis* substrates that we identified by screening the cell surface proteome also had our parasite search motif but were not cleaved by TvROM1 or TvROM3. Closer inspection of the non-cleaved proteins may point to additional features that further help promote TvROM1 cleavage. For example, isoleucines are present at the predicted P2 and P3 sites in 6 of the 7 substrates that were not cleaved by TvROM1. This is of interest as it may reveal an additional level of heterogeneity amongst parasite rhomboid proteases that have been described as having "atypical substrate specificity" for their ability to cleave parasite adhesins and inability to cleave the *Drosophila* Spitz protein, like *E. histolytica* EhROM1 [29]. EhROM1 can cleave substrates that have isoleucine at the predicted P2 and P3 sites [29] and likely TvROM1 would not be able to cleave them.

Another common feature that appeared mainly amongst substrates that can be cleaved was the presence of small amino acids at the predicted P2' site (Chapter 2). Based on crystal structures of the *E. coli* rhomboid GlpG with different inhibitors it has been predicted that a cavity which likely accommodates the P2' residue of the substrate is important for proteolytic cleavage [32]. These results may indicate an important structural difference in substrate binding between the bacterial GlpG rhomboid, whose S2' pocket is likely to bind hydrophobic residues at the P2' site [33] versus TvROM1, and potentially other eukaryotic protozoan rhomboids, whose S2' pocket may bind smaller amino acids. If such a preference is not present in human rhomboids, it may allow for selective inhibition via modification of a substrate analog at the P2' site as has been successfully shown for a soluble serine protease [34]. It will also be interesting to determine whether substrate preferences at the P2 and P3 sites are linked to the potential P2' preference.

The two *T. vaginalis* proteins that we found to be potential substrates for TvROM1 (TVAG_166850 and TVAG_280090) belong to a family of potential adhesins [35, 36] (Chapter 2 and Chapter 5). Furthermore, TVAG_166850 has an annotated cadherin-like domain and TVAG_280090 also shows similarity to that portion of the protein. We have identified another protein, TVAG_393390, which has a predicted cadherin-like structure that spans through most of the protein (Chapter 4). Thus the potential role of cadherin-like proteins functioning as adhesins may be better initially investigated with TVAG_393390, and then important features can be studied in the other family members.

To cleave or not to cleave? An interesting theme that may be highlighted by the cleavage of TVAG_166850 by TvROM1 in Chapter 2 is the potential regulation of adhesion by proteolytic cleavage in *T. vaginalis*. A puzzling observation in the field has been the lack of a

correlation between attachment and host cell cytolysis in highly adherent strains [37]. We have also found that exogenous expression of some proteins promote attachment but they do not promote host cell lysis (ex. TVAG_166850 Chapter 2, TVAG_280090 Chapter 5). This may indicate that different factors may contribute to the processes of attachment and lysis of host cells, but the coordination of both is likely important. Furthermore, just as attachment is critical for *T. vaginalis* as an extracellular parasite, factors that also disengage these connections, like rhomboids or other intramembrane proteases, may also be necessary for productive host cell lysis. For example, when we overexpressed GFP-TVAG_166850 with a mutated rhomboid cleavage site in *T. vaginalis*, it led to greater attachment than exogenous expression of the wildtype GFP-TVAG_166850, but there was no statistically significant difference in host cell cytolysis. Johnson *et al.* found that alpha-1-defensin is released in response to the motile trypomastigote form of *T. cruzii* by colonic epithelial cells, and alpha-defensin 1 can damage the parasite flagella and immobilize the parasite. Interestingly, vaginal epithelial cells have also been reported to produce defensins [38]. Therefore, *in vivo* one can also envision why *T. vaginalis* needs to balance attachment to host cells and host cell lysis while regulating its movement in order to avoid remaining static for long periods of time and becoming vulnerable to released and damaging innate immune factors. It would be interesting to test whether immobilized *T. vaginalis* indeed become more susceptible to host innate immune factors and whether there is an overall decrease in host cell lysis. Furthermore, when we detect increases in host cell lysis-is this process mediated by the physical increased contact time between a parasite and a host cell, or is there an additive nature to cytolysis with multiple parasites each attaching and detaching that then leads to an overall increase in host cell lysis?

While cleavage of a protein is often thought of as an inactivation step, intramembrane cleavage may also lead to activation of a biological cell process. The phenotype of increased attachment to host cells and cytolysis of host cells by *T. vaginalis* TvROM1 transfectants may also be due to a TvROM1 signaling role analogous to regulated intramembrane proteolytic cleavage (RiP) mediated by I-CLiPs. In RiP, the extracellularly-released or the small intracellular C-terminal product can initiate cell signaling in another cell or in the same cell, respectively [39]. In the case of the Notch TM protein, its cleavage by γ-secretase causes the formation of a small intracellular domain (ITD) that can translocate to the nucleus and activate a transcriptional response [40]. RNA-Seq experiments comparing Empty vector and TvROM1 overexpressing transfectants in contact with host cells may help to reveal if TvROM1 has a cell signaling role and what pathways it may activate within the parasite. Cleavage and release of cell adhesion molecules by proteases, especially of the ADAM family, has been implicated in promoting inflammation and tumor metastasis in mammalian cells [41]. Therefore, another possibility is that the extracellular cleavage product produced by TvROM1 has a modulatory effect on the host cells, leading to changes in the host cell surface or its susceptibility to lysis by the parasite.

Characterization of additional proteins that may contribute to pathogenesis

The tetraspanin protein, TSP6, was also identified in the *T. vaginalis* cell surface proteome [42]. Exogenously expressed TSP6 localizes to the plasma membrane, flagella, and vesicles (Chapter 3). Interestingly, there appears to be a bimodal increase in expression of TSP6 upon contact with ectocervical cells. After contact with host cells there are two peaks of TSP6 expression at 30 minutes and 4 hrs, in which TSP6 mRNA increases by 14-fold and 19-fold, respectively. We interpret the initial peak to potentially contribute to *T. vaginalis* attachment to

host cells, as it has been found that maximal attachment of the B7RC2 strain occurs after 20 minutes [43]. A connection with promoting cell attachment is also mechanistically possible as tetraspanins have an established role in promoting adhesion strengthening and association with adhesive proteins such as integrins and immunoglobulin superfamily members [44]. Tetraspanins are predicted to function via their role in bringing together different transmembrane and intracellular proteins and maximizing their interactions and functions [45]. Since *T. vaginalis* does not have any proteins in the genome annotated as integrin-like, it is tempting to speculate that other cell adhesion molecules that are present in *T. vaginalis* such as cadherin-like (ex. TVAG_393390 and TVAG_166850) and immunoglobulin-like proteins may functionally compensate for integrins. We tried extensively to capture proteins interacting with TSP6 by co-immunoprecipitations, but unfortunately, other than TSP6 dimers which are known to exist [44], we could not identify any additional associated proteins (our unpublished results).

The peaks in TSP6 expression may also be indicative of temporal cell signaling functions. Mammalian tetraspanins can interact with signaling molecules such as protein kinase C [46] and phosphoinositide-4 kinase [47]. Therefore, the peaks of TSP6 expression observed likely reflect an active role in host cell sensing and initiation of cell signaling in the parasite. Visual observation of *T. vaginalis* in contact with host cells also shows periods of time of increased attachment, followed by high motility, then re-attachment. Therefore, the waves of TSP6 expression may reflect these phases of contact with host cells, but quantitative video microscopy and motility tracing would aid in confirming this observation. The 19-fold *vs.*14-fold increase in TSP6 may indicate the "primed" nature of the parasites in the second wave of expression, being able to sense and signal for even higher TSP6 production and promotion of its unknown function.

One of the other striking phenotypes of TSP6 was also its dramatic relocalization in *T. vaginalis* when the parasite was placed in contact with host cells (Chapter 3). At the beginning time points, TSP6 was predominantly located on the flagella and at lower levels in the plasma membrane and vesicle-like structures, and ~20% show flagella-only localization. After 30 min of contact with host cells the tagged protein is found mainly on the plasma membrane and flagella (~95%), and then the flagella-only signal starts to increase, and by 6 hrs greater than 50% of the cells have flagella-only targeting. On the other hand, when we remove the TSP6 C-terminal tail, there was no flagellar localization at all and no re-localization of the protein. This phenotype may be due to several explanations. One may be that ~30 min when there is initial maximal attachment, the newly synthesized or existing pool of TSP6 is post-translationally modified-for example by palmitoylation- to retain it at the cell surface where it can lead to a maximal role in adhesion at a greater surface-area location. As the contact time with host cells increases, the increased flagellar localization may be due to an increased sensory and cell signaling role through the flagella. For example, it has been proposed that the flagella is a strong signaling compartment where signaling proteins can he heavily concentrated such as in the case of sea urchin sperm cells having high amounts of resact receptors that bind the resact peptide which is a chemotactic signal produced by eggs [48]. Having the receptors concentrated on the flagella allows the strong response to a single peptide [48]. In the case of *T. vaginalis*, which has 5 flagella, there could be a great expansion of sensory signal reception and signal relay to initiate a maximal response in the presence of host cells. The C-terminal tail of TSP6 is likely the portion of the protein that is important for connecting TSP6 to signaling proteins that mediate the desired cellular response. This is very likely, since the C-terminal tail of TSP6 was sufficient for the relocalization of two other chimeric tetraspanins. Alternatively, the C-terminal tail may

simply act as a localization signal that allows co-localization of TSP6 and signaling proteins thus facilitating their interactions.

Interestingly, the GFP-tagged protein TVAG_393390, localized to the plasma membrane and what appears to be the recurrent flagellum/undulating membrane that is attached to the cell body of *T. vaginalis* (Chapter 4). We found that exogenous expression of TVAG_393390 led to an increase in both attachment to and lysis of ectocervical cells. Therefore, it is becoming clearer that proteins that may contribute to host-parasite interactions also coat the parasite's flagella, where again they may have a signaling role. Further characterization of this protein, such as investigating the role of Ca^{2+} binding for its predicted function are underway.

Characterization of proteins identified from the cell surface proteome, like those described in Chapter 5, reveal that at this point finding proteins that contribute to pathogenesis amongst hypothetical proteins is still a challenge. Our hope was that we could use antisense LNA-oligos to aid in the identification of proteins that may contribute to attachment and cytolysis. In part with this approach, we found two proteins that might have such functions (TVAG_573910 and TVAG_099730) but further analysis is necessary, especially given the variability observed in two different transfectant sets for TVAG_099730. While this type of variability presents an experimental challenge, it perhaps reflects an aspect of *T. vaginalis* inherent cell heterogeneity which may be important for its successful colonization of the host as has been predicted for other parasitic protists [49]. If so, it means that we are fighting an uphill battle with this parasite. For example, given that *T. vaginalis* is predicted to encode ~60,000 proteins, isn't it likely to use multiple cell adhesins and easily change its surface content? A more permanent gene ablation mechanism that may be possible through the use of the CRISPR/Cas9 system [50] may allow more rapid characterization of potential virulence factors

with lesser cell-cell variability. Furthermore, it may be necessary to target multiple family members at a time to observe more dramatic phenotypes. Lastly, one important and interesting question that remains to be investigated, is how does the *T. vaginalis* polysaccharide coat interplay with *T. vaginalis* adhesion and cytolytic factors? Does modulation of one affect the role of the other? For example, many of the proteins that we characterized from the cell surface proteome in Chapter 5 and Chapter 3, give a spotty cell surface-like localization. Perhaps, because they are not as abundant as other cell surface proteins (like TSP6) they present a less strong plasma membrane-like signal. Treatment of *T. vaginalis* with glycosidases may aid localization studies of predicted cell surface proteins, and may also help to observe more robust phenotypic effects. All these combined efforts may lead to the complete characterization of the parasite's adhesome together with how multiple proteins contribute to pathogenesis and help unravel the "trichy" nature of *T. vaginalis* [51, 52].

References:

1. Koonin, E.V., et al., *The rhomboids: a nearly ubiquitous family of intramembrane serine proteases that probably evolved by multiple ancient horizontal gene transfers.* Genome Biology, 2003. **4**(3): p. R19-R19.

2. Hooper, N.M. and U. Lendeckel, *Intramembrane-cleaving proteases (I-CLiPs)*, in *Proteases in biology and disease v 6*. 2007, Springer,: Dordrect, Netherlands. p. ix, 142 p.

3. Urban, S., *Making the cut: central roles of intramembrane proteolysis in pathogenic microorganisms.* Nat Rev Microbiol, 2009. **7**(6): p. 411-23.

4. Urban, S., J.R. Lee, and M. Freeman, *Drosophila rhomboid-1 defines a family of putative intramembrane serine proteases.* Cell, 2001. **107**(2): p. 173-82.

5. Stevenson, L.G., et al., *Rhomboid protease AarA mediates quorum-sensing in Providencia stuartii by activating TatA of the twin-arginine translocase.* Proc Natl Acad Sci U S A, 2007. **104**(3): p. 1003-8.

6. Baker, R.P., R. Wijetilaka, and S. Urban, *Two Plasmodium rhomboid proteases preferentially cleave different adhesins implicated in all invasive stages of malaria.* PLoS Pathog, 2006. **2**(10): p. e113.

7. Lee, J.R., et al., *Regulated intracellular ligand transport and proteolysis control EGF signal activation in Drosophila.* Cell, 2001. **107**(2): p. 161-71.

8. Lemberg, M.K. and M. Freeman, *Functional and evolutionary implications of enhanced genomic analysis of rhomboid intramembrane proteases.* Genome Res, 2007. **17**(11): p. 1634-46.

9. Schneider, R.E., et al., *The Trichomonas vaginalis hydrogenosome proteome is highly reduced relative to mitochondria, yet complex compared with mitosomes.* Int J Parasitol, 2011. **41**(13-14): p. 1421-34.

10. Wasserman, J.D., S. Urban, and M. Freeman, *A family of rhomboid-like genes: Drosophila rhomboid-1 and roughoid/rhomboid-3 cooperate to activate EGF receptor signaling.* Genes Dev, 2000. **14**(13): p. 1651-63.

11. Guichard, A., et al., *brother of rhomboid, a rhomboid-related gene expressed during early Drosophila oogenesis, promotes EGF-R/MAPK signaling.* Dev Biol, 2000. **226**(2): p. 255-66.

12. Urban, S. and M.S. Wolfe, *Reconstitution of intramembrane proteolysis in vitro reveals that pure rhomboid is sufficient for catalysis and specificity.* Proc Natl Acad Sci U S A, 2005. **102**(6): p. 1883-8.

13. Baxt, L.A., et al., *Downregulation of an Entamoeba histolytica rhomboid protease reveals roles in regulating parasite adhesion and phagocytosis.* Eukaryot Cell, 2010. **9**(8): p. 1283-93.

14. Ejigiri, I., et al., *Shedding of TRAP by a Rhomboid Protease from the Malaria Sporozoite Surface Is Essential for Gliding Motility and Sporozoite Infectivity.* PLoS Pathogens, 2012. **8**(7): p. e1002725.

15. Brossier, F., et al., *A spatially localized rhomboid protease cleaves cell surface adhesins essential for invasion by Toxoplasma.* Proc Natl Acad Sci U S A, 2005. **102**(11): p. 4146-51.

16. Klute, M.J., P. Melancon, and J.B. Dacks, *Evolution and diversity of the Golgi.* Cold Spring Harb Perspect Biol, 2011. **3**(8): p. a007849.

17. Tanimoto, K., et al., *Characterization of YIPF3 and YIPF4, cis-Golgi Localizing Yip domain family proteins.* Cell Struct Funct, 2011. **36**(2): p. 171-85.

18. Benchimol, M., et al., *Structure and division of the Golgi complex in Trichomonas vaginalis and Tritrichomonas foetus.* Eur J Cell Biol, 2001. **80**(9): p. 593-607.

19. Brugerolle, G. and E. Viscogliosi, *Organization and composition of the striated roots supporting the Golgi apparatus, the so-called parabasal apparatus, in parabasalid flagellates.* Biology of the Cell, 1994. **81**(3): p. 277-285.

20. Lee, K.E., et al., *Three-dimensional structure of the cytoskeleton in Trichomonas vaginalis revealed new features.* J Electron Microsc (Tokyo), 2009. **58**(5): p. 305-13.

21. Drag, M. and G.S. Salvesen, *Emerging principles in protease-based drug discovery.* Nat Rev Drug Discov, 2010. **9**(9): p. 690-701.

22. Beel, A.J. and C.R. Sanders, *Substrate specificity of gamma-secretase and other intramembrane proteases.* Cell Mol Life Sci, 2008. **65**(9): p. 1311-34.

23. Monne, M., et al., *Turns in transmembrane helices: determination of the minimal length of a "helical hairpin" and derivation of a fine-grained turn propensity scale.* J Mol Biol, 1999. **293**(4): p. 807-14.

24. Opitz, C., et al., *Intramembrane cleavage of microneme proteins at the surface of the apicomplexan parasite Toxoplasma gondii.* EMBO J, 2002. **21**(7): p. 1577-85.

25. Urban, S. and M. Freeman, *Substrate Specificity of Rhomboid Intramembrane Proteases Is Governed by Helix-Breaking Residues in the Substrate Transmembrane Domain.* Molecular Cell, 2003. **11**(6): p. 1425-1434.

26. Dowse, T.J. and D. Soldati, *Rhomboid-like proteins in Apicomplexa: phylogeny and nomenclature.* Trends Parasitol, 2005. **21**(6): p. 254-8.

27. Howell, S.A., et al., *Distinct mechanisms govern proteolytic shedding of a key invasion protein in apicomplexan pathogens.* Mol Microbiol, 2005. **57**(5): p. 1342-56.

28. O'Donnell, R.A., et al., *Intramembrane proteolysis mediates shedding of a key adhesin during erythrocyte invasion by the malaria parasite.* J Cell Biol, 2006. **174**(7): p. 1023-33.

29. Baxt, L.A., et al., *An Entamoeba histolytica rhomboid protease with atypical specificity cleaves a surface lectin involved in phagocytosis and immune evasion.* Genes Dev, 2008. **22**(12): p. 1636-46.

30. Zhou, X.W., et al., *Proteomic analysis of cleavage events reveals a dynamic two-step mechanism for proteolysis of a key parasite adhesive complex.* Mol Cell Proteomics, 2004. **3**(6): p. 565-76.

31. Dickey, S.W., et al., *Proteolysis inside the membrane is a rate-governed reaction not driven by substrate affinity.* Cell, 2013. **155**(6): p. 1270-81.

32. Vinothkumar, K.R., et al., *Structure of rhomboid protease in complex with beta-lactam inhibitors defines the S2' cavity.* Structure, 2013. **21**(6): p. 1051-8.

33. Strisovsky, K., H.J. Sharpe, and M. Freeman, *Sequence-specific intramembrane proteolysis: identification of a recognition motif in rhomboid substrates.* Mol Cell, 2009. **36**(6): p. 1048-59.

34. Bajaj, M.S., et al., *Engineering kunitz domain 1 (KD1) of human tissue factor pathway inhibitor-2 to selectively inhibit fibrinolysis: properties of KD1-L17R variant.* J Biol Chem, 2011. **286**(6): p. 4329-40.

35. de Miguel, N., et al., *Proteome analysis of the surface of Trichomonas vaginalis reveals novel proteins and strain-dependent differential expression.* Mol Cell Proteomics, 2010. **9**(7): p. 1554-66.

36. Hirt, R.P., et al., *Trichomonas vaginalis pathobiology new insights from the genome sequence.* Adv Parasitol, 2011. **77**: p. 87-140.

37. Lustig, G., et al., *Trichomonas vaginalis contact-dependent cytolysis of epithelial cells.* Infect Immun, 2013. **81**(5): p. 1411-9.

38. Han, J.H., et al., *Modulation of human beta-defensin-2 expression by 17beta-estradiol and progesterone in vaginal epithelial cells.* Cytokine, 2010. **49**(2): p. 209-14.

39. Lal, M. and M. Caplan, *Regulated intramembrane proteolysis: signaling pathways and biological functions.* Physiology (Bethesda), 2011. **26**(1): p. 34-44.

40. Nakayama, K., et al., *gamma-Secretase-regulated mechanisms similar to notch signaling may play a role in signaling events, including APP signaling, which leads to Alzheimer's disease.* Cell Mol Neurobiol, 2011. **31**(6): p. 887-900.

41. Reiss, K., A. Ludwig, and P. Saftig, *Breaking up the tie: disintegrin-like metalloproteinases as regulators of cell migration in inflammation and invasion.* Pharmacol Ther, 2006. **111**(3): p. 985-1006.

42. de Miguel, N., A. Riestra, and P.J. Johnson, *Reversible association of tetraspanin with Trichomonas vaginalis flagella upon adherence to host cells.* Cell Microbiol, 2012. **14**(12): p. 1797-807.

43. Okumura, C.Y., L.G. Baum, and P.J. Johnson, *Galectin-1 on cervical epithelial cells is a receptor for the sexually transmitted human parasite Trichomonas vaginalis.* Cell Microbiol, 2008. **10**(10): p. 2078-90.

44. Hemler, M.E., *Tetraspanin functions and associated microdomains.* Nat Rev Mol Cell Biol, 2005. **6**(10): p. 801-11.

45. Hemler, M.E., *Targeting of tetraspanin proteins--potential benefits and strategies.* Nat Rev Drug Discov, 2008. **7**(9): p. 747-58.

46. Zhang, X.A., A.L. Bontrager, and M.E. Hemler, *Transmembrane-4 superfamily proteins associate with activated protein kinase C (PKC) and link PKC to specific beta(1) integrins.* J Biol Chem, 2001. **276**(27): p. 25005-13.

47. Yauch, R.L. and M.E. Hemler, *Specific interactions among transmembrane 4 superfamily (TM4SF) proteins and phosphoinositide 4-kinase.* Biochem J, 2000. **351 Pt 3**: p. 629-37.

48. Nachury, M.V., *How do cilia organize signalling cascades?* Philos Trans R Soc Lond B Biol Sci, 2014. **369**(1650).

49. Seco-Hidalgo, V., A. Osuna, and L.M. Pablos, *To bet or not to bet: deciphering cell to cell variation in protozoan infections.* Trends Parasitol, 2015.

50. Sternberg, S.H. and J.A. Doudna, *Expanding the Biologist's Toolkit with CRISPR-Cas9.* Mol Cell, 2015. **58**(4): p. 568-574.

51. Winograd-Katz, S.E., et al., *The integrin adhesome: from genes and proteins to human disease.* Nat Rev Mol Cell Biol, 2014. **15**(4): p. 273-88.

52. Conrad, M.D., et al., *Getting trichy: tools and approaches to interrogating Trichomonas vaginalis in a post-genome world.* Trends Parasitol, 2013. **29**(1): p. 17-25.